UNIVERSITY OF SOUTHAMPTON

# Design and Implementation of Nonlinear and Robust Control for Hamiltonian Systems: The Passivity-Based Control Approach

by

Mutaz Muhammad Ryalat

A thesis submitted for the degree of Doctor of Philosophy

in the

Faculty of Engineering and the Environment

Engineering Sciences - Electromechanical Group

September 2015

*To the memory of my grandfather, who has always encouraged me to aim high.*

*To my parents, brothers, wife and children, for all the love and for always wanting me to succeed.*

# ABSTRACT

Recently, control techniques that adopt the geometrical structure and physical properties of dynamical systems have gained a lot of interest. In this thesis, we address nonlinear and robust control problems for systems represented by port-controlled Hami ltonian (PCH) models using the interconnection and damping assignment passivity-based control (IDA-PBC) methodology, which is the most notable technique facilitating the PCH framework.

In this thesis, a novel constructive framework to simplify and solve the partial differential equations (PDEs) associated with IDA-PBC for a class of underactuated mechanical systems is presented. Our approach focuses on simplifying the potential energy PDEs to shape the potential energy function which is the most important procedure in the stabilization of mechanical systems. The simplification is achieved by parametrizing the desired inertia matrix that shapes the kinetic energy function, thus achieving total energy shaping. The simplification removes some constraints (conditions and assumptions) that have been imposed in recently developed methods in literature, thus expanding the class of systems for which the methods can be applied including the separable PCH systems (systems with constant inertia matrix) and non-separable PCH systems (systems with non-constant inertia matrix). The results are illustrated through software simulations and hardware experiments on real engineering applications.

We also propose an integral control and adaptive control schemes to improve the robustness of the IDA-PBC method in presence of uncertainty. We first provide some results for the case of fully-actuated mechanical systems, and then extend those results to underactuated systems which are more complex. Integral action control on both the passive and non-passive outputs in the IDA-PBC construction, a strategy to ensure the robustness of the systems by preserving its stability in face of external disturbances, is introduced, establishing the input-to-state stability (ISS) property. The results are applied to both the separable and non-separable PCH systems and illustrated via several simulations. The extension to the non-separable case exhibits more complicated design as we need to take into account the derivative of the inertia matrix.

Finally, the IDA-PBC method is employed to solve an important nonlinear phenomenon called 'pull-in' instability associated with the electrostatically actuated microelectromechanical systems (MEMSs). The control construction is an output-feedback controller that ensures global asymptotic stability and avoids velocity measurement which may not be practically available. Furthermore, the integral, adaptive and ISS control schemes proposed in this thesis for mechanical systems are extended to facilitate the stabilization of electromechanical systems which exhibit strong coupling between different energy domains.

# Contents

# List of Figures

# List of Tables

# Declaration of Authorship

I, Mutaz Muhammad Ryalat, declare that the thesis entitled *Design and Implementation of Nonlinear and Robust Control for Hamiltonian Systems: The Passivity-Based Control Approach* and the work presented in the thesis are both my own, and have been generated by me as the result of my own original research. I confirm that:

- this work was done wholly or mainly while in candidature for a research degree at this University;
- where any part of this thesis has previously been submitted for a degree or any other qualification at this University or any other institution, this has been clearly stated;
- where I have consulted the published work of others, this is always clearly attributed;
- where I have quoted from the work of others, the source is always given. With the exception of such quotations, this thesis is entirely my own work;
- I have acknowledged all main sources of help;
- where the thesis is based on work done by myself jointly with others, I have made clear exactly what was done by others and what I have contributed myself;
- parts of this work have been published/submitted as: [84], [86], [85] and [87]

Signed:.....

Date:.....

# Acknowledgements

First and foremost I would like to express my sincere gratitude to my enthusiastic supervisor, Dr Dina Shona Laila. It has been an honour to be her first PhD student. She offered me every bit of guidance, assistance, and support I needed during my PhD. I appreciate all her efforts, patience and encouragement without which it would have been impossible for me to finish this work.

I would like to thank Dr Mohamed Torbati for his encouragement and hospitality.

Also many thanks to the staff and students at Electro-Mechanical Engineering Group for providing a very friendly and inspiring environment.

I am deeply grateful to my beloved parents and brothers for their never-ending love, continuous support and encouragement. My parents have always fueled my desire to learn and made big sacrifices so that I would reach higher education levels. I would also like to say a heartfelt thanks to my devoted wife, who has been with me all these years and been by my side during every challenging moment. My dear wife, thanks a lot for your invaluable love, patience, and understanding. To my beautiful children, Zaid and Sarah, for being wonderful kids and constant source of strength, happiness and hope. To every member of my family, thanks a lot for always believing in me and encouraging me for everything I do. This has been a very challenging journey, which I could not have done it without you. Thank you for everything.

Finally, I thank the German Jordanian University for their financial support. I hope I can give back to my country as generously as they offered me over the entire period of my PhD study.

# Chapter 1

# Introduction and Motivation

## 1.1 The Impact of Control on Technology

Technology plays a significant role in everyone's life. It makes life easier and more convenient and people are becoming increasingly dependent on technology in their daily lives, both for professional and social tasks. For example, smart phones and tablets have now become not just a means of communication between people, but with their advanced features and built-in applications, such as the Internet, GPS navigator, touch screen, and a multi-purpose personal digital assistant (note pad, calendar, address book, calculator, etc.), they help people to perform their daily work easily and quickly. Control system is an integral part of modern society and a main contributor to the advances and developments in technology. Control is a key enabling technology for numerous applications around us and control systems now play critical roles in many fields, including manufacturing, electronics, communications, transportation, computers and networks, and many others. Nowadays, manufacturing industries are equipped with fully automated machineries (Figure 1.1 shows cars being assembled by industrial robots); space shuttles and robots are used for space exploration like the Mars Rover shown in Figure 1.2. These are just a few examples of automatic control systems.

The increase in complexity of systems, the continuing need to improve product quality, the performance requirements, and demands for more effective, more accurate, more flexible, and more autonomy are just few drivers for the existence of the field of *control*. Furthermore, new developments in technology with emerging concepts and state-of-the-art devices make the control system design increasingly challenging to find enabled solutions, designs, tools and algorithms to ensure reliable, efficient and cost-effective operations [58]. The objective of control system design is that [95]: 'given a physical system to be controlled and the specifications of its desired behaviour, a feedback control law is constructed to make the closed-loop system displays the desired behaviour'. From this definition several key concepts have to be carefully considered when a control design

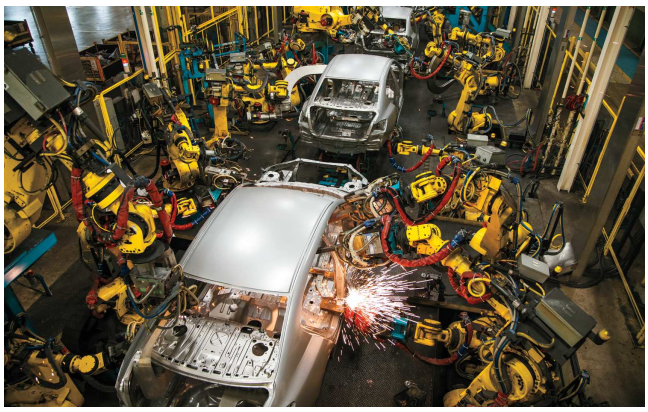

Figure 1.1: Automotive production lines [32].

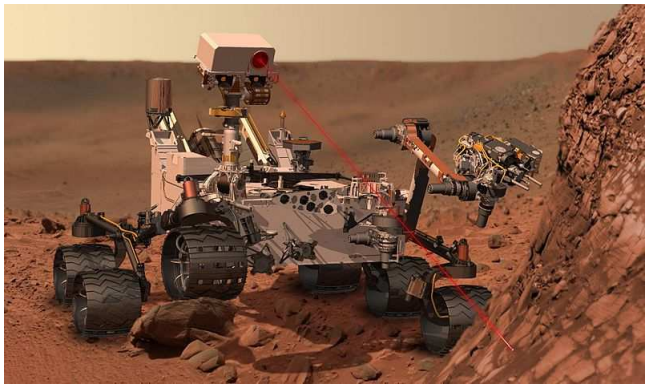

Figure 1.2: The rover landed on Mars in August 2012 [112].

is carried out. Firstly, a dynamical system must be clearly defined and, based on the definition, the system can then be modelled in mathematical terms. Secondly, a clear specifications for a system's desired behaviour should be given. Generally, the desired behaviour can be investigated for two types of tasks: stabilization (or set-point regulation) and tracking (time-varying trajectory tracking). Finally a controller is designed to achieve the desired behaviour while other criteria such as accuracy, cost and robustness should also be considered.

For many years, research and development in control system design have been devoted to the area of linear (classical) control, with a variety of powerful techniques developed in both frequency and time domains (see [30, 61, 62] and references therein), leading to extremely successful industrial applications. Linearization is a successful common practice in engineering, and whenever possible it should be used so that the powerful tools of classical control can be utilized.

While linearization would work in a large domain of applications, many systems have strong nonlinear dynamics that limits the application of the linear control approaches. Especially, with the increase in complexity of modern developed systems that requires

more accurate control to achieve stability and satisfactory performance. These factors have increased the interest in the field of *nonlinear control*. Another contributor to the application of nonlinear control is the advances in digital electronics which have led to a rapid development in computing and the availability of powerful low-cost microprocessors that makes it possible to solve complex nonlinear problems numerically. In recent years, nonlinear control has increasingly become more popular and extensive research has contributed to the development of both analysis and design of nonlinear control systems (see [95, 44, 51, 69, 109, 47, 7]).

In general, there are two main difficulties in controller design for real systems; nonlinearity and uncertainty. The research presented in this thesis aims at finding constructive solutions for both issues, and contributes to the development of the field of nonlinear control. This research focuses on a class of models that have a specific structure, the port-controlled Hamiltonian (PCH) framework. Among several nonlinear control approaches, passivity-based control (PBC), more specifically one of the PBC approaches known as the interconnection and damping assignment (IDA-PBC) is the most convenient approach to PCH framework. There are many advantages in adopting the PCH framework in the construction of PBC schemes including [31, 72]: **(i)** it provides a systematic approach for the modelling, analysis and control of complex dynamical systems stemming from various physical domains (electrical, mechanical, thermodynamics, etc.); **(ii)** this formalism invokes the *energy* of the system as a modelling tool which gives a clear physical interpretations such as conservation, dissipation and transformation of energy; **(iii)** it captures the energy-balancing property of the physical systems as PH systems are automatically passive (lossless). This property can be utilized to establish a link between the passivity of a system and Lyapunov stability; **(iv)** the system has a clear structural identification being the interconnection and damping matrices, i.e. the system has a clear distinct structure for internal interconnection from one side and the external interconnection between the system and the environment (the control action) from the other side. This means that the structural information about the system is available in the model description: the total energy of the system can be presented by the Hamiltonian (storage) function, which can usually be used as a Lyapunov function, while the interconnection property is contained in a structure matrix that is described by the interconnection and dissipative matrices; **(v)** the geometric structure of the PCH is a state space which provides a convenient and compact way to model and analyze (nonlinear) control systems.

The IDA-PBC is a feedback control design methodology that aims at stabilizing the dynamical system by rendering the closed-loop system passive with a desired storage function [74]. The main idea is to transform, via a state feedback, a nonlinear dynamical system, into a suitable closed-loop PCH form. This is achieved by modifying the energy (Hamiltonian) function and/or changing the interconnection structure of system and/or adding damping/dissipation controllers, thus the name (IDA). This method

has been successful in various engineering domains and applications including: electrical and power systems [77, 38], mechanical systems [37, 71], electromechanical systems [72, 81], discrete-time IDA-PBC design for underactuated Hamiltonian control systems [53], IDA-PBC design to general linear time-invariant systems [67, 49], a survey on IDA-PBC and its application can be found in [66]. In this thesis we are interested in two classes of systems; the mechanical systems, in particular the underactuted mechanical systems (UMSs); and the electromechanical systems, in particular microelectromechanical systems (MEMS).

One of the main contributions of this thesis is the control of underactuated mechanical systems (UMSs) using IDA-PBC method. UMSs have fewer control inputs than degrees of freedom. These systems are either naturally underactuated like in spacecrafts, wheeled mobile robots and underwater vehicles, or by design to reduce the cost and weight considering some practical issues like in satellites and flexible-link robots [63, 55]. The complex dynamics of the UMSs, restrictions on control authority and controllability, holonomic and non-holonomic constraints, and being not fully feedback linearizable are the main reasons for the complexity of the control design for these systems. A number of methods and tools have been recently developed for analysis and control of UMSs. Among these, it is worth citing the major research lines: methods that are based on partial feedback linearization [101], backstepping [64], immersion and invariance [89] and energy-based methods; controlled Lagrangian [16, 60] and IDA-PBC [71]. See [55] for an overview of some control design methods. From IDA-PBC design perspective, the control of UMSs is achieved via the solution of a set of partial differential equations (PDEs). Solving these PDEs is the main obstacle in the constitution of IDA-PBC. A lot of research effort has been devoted to the solution of the matching equations (see [39, 14, 2, 111]). In all proposed methods in literature, some conditions and assumptions have been imposed and also in many cases, linearization or partial linearization has been used to simplify the solution(s). These factors have restricted the proposed methods to certain systems and have also affected the possibility of achieving global stabilization of systems expected from applying the nonlinear control approaches. This motivates us to continue the investigation aimed at providing constructive method(s) to simplify and solve the PDEs associated with the IDA-PBC approach.

Another focus in this research is on nonlinear control design and analysis of electromechanical systems. This is triggered by the importance of electromechanical system as they are found in broad applications in industry such as electric drives, robotics, servomechanism. Electromechanical systems continue to increase in complexity. The multidisciplinary nature of such systems (they encompasses diverse domains), the higher demands in their performance and precision in various industrial applications and the fact that they exhibit complicated nonlinear phenomena such as saturation and deadzone, have brought new challenges to control analysis and design. Additional challenges have recently appeared in dealing with electromechanical systems on the micro scale,

with the so called MEMS. As a promising technology, MEMS have the ability to actuate, sense and control in miniaturized dimensional scale and have several applications. Control of MEMS devices is critical. Their size, fabrication process, interdisciplinary nature, working environment, and various applications and uses are issues that should be taken into account in the design of control systems. In this thesis, we will show a methodology to solve some stability issues related to the electrostatically actuated MEMS.

An important part of this research is the control of PCH systems with uncertainties. The behaviour of the control systems can be influenced by some externally acting signals (disturbances, noises, etc.) and model uncertainties which can be clearly noticed in the implementation phase. The control of nonlinear systems with uncertainties is traditionally approached as a robust or an adaptive control problem. Little is known about robust and adaptive control within PCH framework. Some major contributions toward the solution of robust and adaptive control problems have been recently appeared in works of [29, 26, 70, 82]. All these works have been dedicated to the case of fully-actuated mechanical systems whose control design is relatively simple since direct actuation is available on each degree of freedom. For underactuated mechanical systems, the control design is usually more complicated. This thesis provides the first contribution towards robust and adaptive control of underactuated mechanical systems within the PCH framework. In this thesis, we use the IDA-PBC method to (asymptotically) stabilize nonlinear systems formulated in PCH structure. However, little is known about the robustness of this method in response to the effects of uncertainty which could results from disturbances, noises, and modelling errors. This thesis explores the possibility of extending the IDA-PBC method by adopting a robustness perspective, with the aim of maintaining (asymptotic) stability of the system in the face of such perturbations which exist in any realistic problem. We propose constructive results on Robust IDA-PBC and PID-like controllers for a class of PCH systems. The results extend some existing methods and provide a new framework that allows the implementation of integral action control to underactuated PCH systems that are quite commonly found in practice. Furthermore, we provide a framework to add an integral action to robustly control the electromechanical systems, the MEMS in particular. This inclusion is quite complicated in the electromechanical systems applications due to the strong coupling in the dynamics of different domains, the electrical and mechanical.

## 1.2 Research Objectives

The general aim of this thesis is to develop constructive and systematic nonlinear and robust control design methods for PCH systems. In particular, the objectives of this research are summarized as:

- Providing constructive techniques for nonlinear PBC controller design for underactuated and electromechanical systems as alternatives to the classical ones. More specifically, the research goal is to develop a set of tools and techniques to control underactuated and electromechanical systems which constitute highly nonlinear and coupled dynamical systems.
- Improving and extending the scope of the IDA-PBC methodology for underactuated mechanical systems through simplification of the PDEs. The design construction enlarges the class of UMSs that can be stabilized, as well as, makes the application less cumbersome which is inherited in the nonlinear control designs and the PBC approaches in particular.
- Developing robust and adaptive control schemes for PCH systems to accommodate uncertainties, focusing on underactuated and electromechanical systems.
- Investigating the *pull-in* instability phenomenon which is associated with the electrostatically actuated MEMS, and providing a solution to this problem through a PBC design, to this instability issue.
- Applying the proposed controller design methods to some underactuated and electromechanical systems via realistic computer simulations and experimentally validating these proposed methods.

## 1.3 Outline of this Thesis and Contributions

Chapter 2 contains the mathematical preliminaries and some necessary theoretical backgrounds which will be used in the rest of this thesis. Stability is the most important issue in every control problem, therefore some basic tools that are used for stability analysis of nonlinear systems are presented. This includes Lyapunov stability and passivity theories. Input-to-state stability theory is also reviewed. In this research, the control design is based on the passivity-based control for systems in special structure, the port-controlled Hamiltonian systems. Thus, some background on PCH systems is given and the formulation of their structure are discussed in some detail. Finally, interconnection and damping assignment passivity-based control is explained, which is the methodology used to control a group of mechanical and electromechanical systems, namely, underactuated mechanical systems, and microelectromechanical systems.

In Chapter 3, we provide a constructive framework to solve the PDEs associated with the IDA-PBC for underactuated mechanical systems. We describe novel methods to simplify the matching PDEs for solving an IDA-PBC construction for separable and non-separable UMSs. This significantly simplifies the design computation and also yield a simpler form of the controller. Most importantly, it achieves 'almost' global stabilization which was unachievable in most previous designs in the literature. The results have been

applied to solve an almost global stabilization design of the inertia wheel pendulum which represents a class of underactuated mechanical systems with a constant inertia matrix.

In Chapter 4, we apply the results obtained in Chapter 3 to investigate a stabilization problem for the rotary inverted pendulum. First we derive the model of the system using the Newton-Euler formulation. Then we present a linear control design for this system, highlighting the limitations of this approach. Section 4.4 of this chapter, discusses the application of the proposed simplified IDA-PBC design to the inverted pendulum system. It is shown in this chapter, through both simulations and stability analysis, that this design results in 'almost' global asymptotic stability and a very effective closed-loop performance of this systems in its full nonlinear dynamics.

Chapter 5 considers the presence of uncertainties in the PCH framework and discusses both the simple case of a constant inertia matrix system, and the complex case of a non-constant inertia matrix that takes into account the derivative of the inertia matrix in the construction of the controller. We first propose a PID-like controller, a state feedback which imitates the concept of the proportional-integral-derivative (PID) controller. Then we investigate the addition of the integral action to the IDA-PBC controller in the PCH formulation for fully-actuated mechanical systems. Here, we show approaches for dealing with two cases of passive and non-passive outputs. Section 5.3.3 of this chapter establishes the main results, where the previous results are extended to the case of underactuated mechanical systems which has not been discussed in the literature before. We consider also in this chapter the development of a simplified robust controller, adopting the input-to-state stability (ISS) theory, to deal with PCH systems subject to external disturbances. Finally, parametric uncertainty in the PCH model is discussed in this chapter, and a novel adaptive controller is developed to counteract the effects of uncertainty in the model.

Chapter 6 provides an investigation on MEMS, particularly the pull-in instability that generally limits the operation of the electrostatically driven MEMS. We use two approaches to explain this instability problem, namely; the energy (Hamiltonian) approach, and the linearization approach. Next, we discuss a control design method based on the IDA-PBC to solve the pull-in instability. The main advantage of the proposed method is that it ensures achieving global asymptotic stability on one hand, while on the other hand it is an output-feedback controller that does not require the velocity measurement which is impossible in such applications. This chapter also discusses a new approach to include an integral control action for the MEMS applications. This approach uses the idea of coordinate transformations as proposed in the design of integral controllers for underactuated systems, but the idea is extended to deal with the complexity of the electromechanical systems arises from the strong coupling between different electrical and mechanical energy domains. The ISS property and the IDA-PBC method are combined to control the electrostatically actuated MEMS subject to external perturbations which has not been considered in existing works in the literature.

In Chapter 7 we present the validation of the controller design presented in Chapter 4 by applying it to a laboratory set-up rotary inverted pendulum. The application is modified to include a *friction compensator* which is excluded throughout the PCH modelling. The chapter demonstrates a successful experimental implementation of this approach to the rotary inverted pendulum hardware, demonstrating the effectiveness of the controller and its robustness with respect to disturbances.

Chapter 8 concludes the contributions of this research and provides directions for the future research work in this area.

## 1.4 Publications

- Ryalat, M. and Laila, D. S. (2013). IDA-PBC for a class of underactuated mechanical systems with application to a rotary inverted pendulum. In Proceedings of the 52nd IEEE Conference on Decision and Control, pages 5240-5245.
- Ryalat, M., Laila, D. S., and Torbati, M. (2015). Integral IDA-PBC and PID-like control for port-controlled Hamiltonian systems. *Accepted for publication in 2015 American Control Conference.*
- Ryalat, M., Laila, D. S., and Torbati, M. (2014). Robust IDA-PBC and PID-like control for port-controlled Hamiltonian systems. *Submitted to IEEE Transactions on Automatic Control.*
- Ryalat, M. and Laila, D. S. (2015). A simplified IDA-PBC design for underactuated mechanical systems with applications. *Submitted to European Journal of Control.*
- Ryalat, M. and Laila, D. S., (2015). Global stabilization of the rotary inverted pendulum via a simplified IDA-PBC design with experimental verification. *Submitted to IEEE Conference on Decision and Control.*
- Ryalat, M., Laila, D. S. (2015). Nonlinear and robust control of the electrostatically actuated microelectromechanical systems: The IDA-PBC approach. *In preparation.*

# Chapter 2

# Preliminaries

## 2.1 Definitions and Notation

The set of real and natural numbers (including 0) are denoted respectively by $\mathbb{R}$ and $\mathbb{N}$. Given an arbitrary matrix $G$, we denote the transpose and the pseudo inverse of $G$ by $G^\top$ and $G^+$, respectively. $G^\perp$ denotes the full rank left annihilator of $G$, i.e. $G^\perp G = 0$. We denote an $n \times n$ identity matrix with $I_n$. For any continuous function $H(i,j)$, we define $\nabla_i H(i,j) := \partial H(i,j)/\partial i$. $e_i, i \in \{1, \cdots, n\}$ are the Euclidean basis vectors.

## 2.2 Stability of Nonlinear Systems

The stability theory presented in this section plays a central role in constructing the nonlinear control design methods in this thesis. The fundamental stability theory for nonlinear systems and most fruitful ideas were introduced by A.M. Lyapunov when he published his PhD thesis in 1892, titled 'The General Problem of Motion Stability'. Lyapunov's key ideas are the basis for the analysis of stability of dynamical systems. Most nonlinear control theories revolve around Lyapunov's approaches. The principles of Lyapunov stability theory was originally used as a dynamical behaviour analysis tool and became a powerful method for nonlinear control system design. Here, Lyapunov stability theory is summarized for general nonlinear systems. The following paragraphs discuss the stability notion in the sense of Lyapunov and are based on [47], where the proofs of all theorems can be found.

Consider the autonomous system

$$\dot{x} = f(x), \tag{2.1}$$

where $f : \mathcal{D} \to \mathbb{R}^n$ is a locally Lipschitz map from a domain $\mathcal{D} \subset \mathbb{R}^n$ into $\mathbb{R}^n$. Suppose $\bar{x} \in \mathcal{D}$ is an equilibrium point for (2.1); that is $f(\bar{x}) = 0$. Without loss of generality, assume that $\bar{x} = 0$.

**Definition 2.1. (Stability of equilibrium point)** The equilibrium point $x = 0$ of (2.1) is

- **stable**, if for each $\epsilon > 0$ there is $\delta = \delta(\epsilon) > 0$ such that

$$\|x(0)\| < \delta \Rightarrow \|x(t)\| < \epsilon, \quad \forall\, t \geq 0 \tag{2.2}$$

- **unstable**, if not stable.
- **asymptotically stable**, if it is stable and $\delta$ can be chosen such that

$$\|x(0)\| < \delta \implies \lim_{t\to\infty} x(t) = 0.$$

■

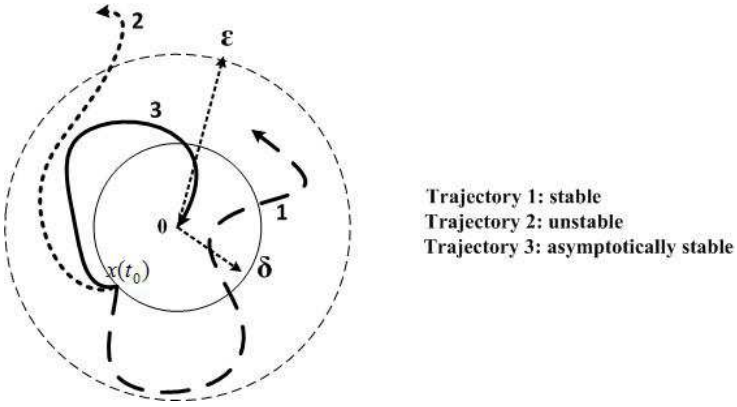


Figure 2.1: Illustration of the definition of stability

Figure 2.1 shows the concepts of stability. For nonautonomous systems, the stability properties of nonlinear systems can be characterized using the classes of scalar (comparison) functions defined below:

**Definition 2.2. (Class $\mathcal{K}$ and $\mathcal{K}_\infty$ functions)** A continuous function $\alpha : [0, a) \to \mathbb{R}_+$ is said to belong to class $\mathcal{K}$ if it is strictly increasing and $\alpha(0) = 0$, and it is said to belong to class $\mathcal{K}_\infty$ if $a = \infty$ and $\lim_{s\to\infty} \alpha(s) = \infty$. ■

**Definition 2.3. (Class $\mathcal{KL}$ function)** A continuous function $\beta : [0, a) \times \mathbb{R}_+ \to \mathbb{R}_+$ is said to belong to class $\mathcal{KL}$ if it is such that $\beta(\cdot, t) \in \mathcal{K}$ for each fixed $t \in \mathbb{R}_+$, and the function $\beta(s, \cdot)$ is decreasing and $\lim_{t\to\infty} \beta(s, t) = 0$ for each fixed $s \in [0, a)$. ■

Figure 2.2 shows a plot of $\mathcal{K}$ and $\mathcal{K}_\infty$ functions. The following definitions give equivalent definitions of stability and asymptotic stability using class $\mathcal{K}$ and $\mathcal{KL}$ functions.

Consider the system

$$\dot{x} = f(x, t), \tag{2.3}$$

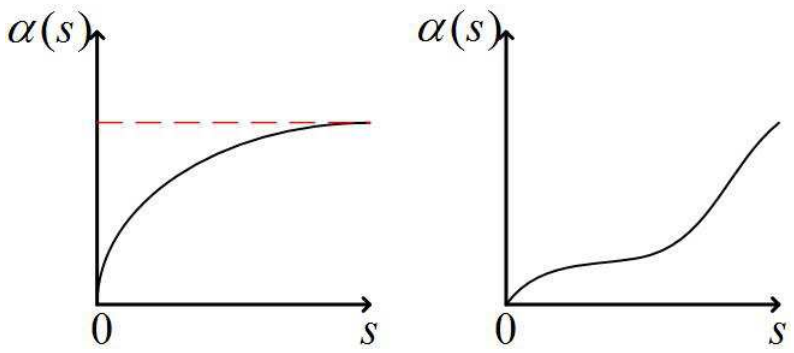


Figure 2.2: Class $\mathcal{K}$ (left) and class $\mathcal{K}_\infty$ (right) functions.

where $f : \mathcal{D} \times \mathbb{R}^+ \to \mathbb{R}^n$ is piecewise continuous in $t$ and locally Lipschitz in $x$ on $\mathcal{D} \times \mathbb{R}^+$, and $\mathcal{D} \subset \mathbb{R}^n$ is a domain that contains the origin $x = 0$. The origin is an equilibrium point for (2.1) at $t = 0$ if $f(0, t) = 0, \quad \forall\, t \geq 0$.

**Definition 2.4.** The equilibrium point $x = 0$ of (2.3) is said to be **stable** if there exist a class $\mathcal{K}$ function $\alpha(\cdot)$ and a positive constant $c$, independent of $t_0$, such that

$$||x(t)|| \leq \alpha(||x(t_0)||), \forall\, t \geq t_0 \geq 0, \forall\, ||x(t_0)|| < c, \tag{2.4}$$

and is **globally stable** if this condition is satisfied for any initial state. ■

Definition 2.4 suggests that we can keep the states in a ball of arbitrary small radius $c$ i.e. the solution is bounded and defined for all $t \geq t_0$ which implies stability.

**Definition 2.5.** The equilibrium point $x = 0$ of (2.3) is said to be **asymptotically stable** (AS) if there exist a class $\mathcal{KL}$ function $\beta(\cdot, \cdot)$ and a positive constant $c$, independent of $t_0$, such that

$$||x(t)|| \leq \beta(||x(t_0)||, t - t_0), \forall\, t \geq t_0 \geq 0, \forall\, ||x(t_0)|| < c, \tag{2.5}$$

and is **globally asymptotically stable** (GAS) if this condition is satisfied for any initial state. ■

Definition 2.5 suggests that satisfaction of the inequality (2.5) implies boundedness and hence stability. Moreover, for any initial condition $x(t_0)$ the trajectory of the solution $x(t)$ is asymptotically decaying to 0 as $t \to \infty$. Before discussing Lyapunov's stability theorems, some important definitions are first provided.

**Definition 2.6.** A scalar function $W(x)$ is called:

- **Positive definite**, if $W(0) = 0$ and $W(x) > 0\ \forall\ x \neq 0$.
- **Positive semi-definite**, if $W(0) = 0$ and $W(x) \geq 0\ \forall\ x \neq 0$.

- **Negative definite (Negative semi-definite)**, if $-W(x)$ is positive definite (positive semi-definite).
- **Radially unbounded**, if $W(x) \to \infty$ as $|x| \to \infty$. ■

**Lemma 2.7.** *Let $W : \mathbb{R}^n \to \mathbb{R}$ be a continuous positive-definite and radially unbounded function. Then there exist class $\mathcal{K}_\infty$ functions $\underline{\alpha}(\cdot)$ and $\overline{\alpha}(\cdot)$ such that*

$$\underline{\alpha}(|x|) \leq W(x) \leq \overline{\alpha}(|x|).$$

■

Lyapunov's stability theorems can now be given.

**Theorem 2.8.** ***(Lyapunov's first (indirect) method)*** *Let $x = 0$ be an equilibrium point for the system $\dot{x} = f(x)$, where $f : \mathcal{D} \to \mathbb{R}^n$ is continuously differentiable and $\mathcal{D}$ is a neighborhood of the origin. Let*

$$A = \left.\frac{\partial f}{\partial x}\right|_{x=0}. \tag{2.6}$$

*Then, the origin is*

- ***asymptotically stable**, if $\mathrm{Re}(\lambda_i) < 0$ for every eigenvalue $\lambda$ of $A$.*
- ***unstable**, if $\mathrm{Re}(\lambda_i) > 0$ for any eigenvalue $\lambda$ of $A$.* ■

**Theorem 2.9.** ***(Lyapunov's second (direct) method)*** *Let $x = 0$ be an equilibrium point for the system $\dot{x} = f(x)$ and $\mathcal{D} \subset \mathbb{R}^n$ be a domain containing $x = 0$. Let $W : \mathcal{D} \to \mathbb{R}$ be a continuously differentiable function such that*

$$W(0) = 0 \text{ and } W(x) > 0 \; \forall \; x \in \mathcal{D} - \{0\} \tag{2.7}$$

$$\dot{W}(x) \leq 0 \; \forall \; x \in \mathcal{D}. \tag{2.8}$$

*Then $x = 0$ is stable. Moreover, if*

$$\dot{W}(x) < 0 \; \forall \; x \in \mathcal{D} - \{0\}, \tag{2.9}$$

*then $x = 0$ is asymptotically stable.* ■

Lyapunov's second method can also be given by using the comparison functions:

**Theorem 2.10.** *Consider the system (2.1), where $x \in \mathbb{R}^n$ and $t \geq t_0$, with an equilibrium point $x = 0$, and suppose that there exists a continuously differentiable function $W(x, t)$ such that*

$$\underline{\alpha}(|x|) \leq W(x, t) \leq \overline{\alpha}(|x|), \tag{2.10}$$

$$\frac{\partial W}{\partial x} f(x,t) + \frac{\partial W}{\partial t} \leq -\mathcal{W}(|x|), \tag{2.11}$$

*where* $\underline{\alpha}(\cdot)$, $\overline{\alpha}(\cdot)$ *are class* $\mathcal{K}_\infty$ *functions and* $\mathcal{W}(\cdot)$ *is a continuous positive definite function. Then* $x = 0$ *is globally stable. Moreover, if in addition the function* $\mathcal{W}(\cdot)$ *is of class* $\mathcal{K}$*, then* $x = 0$ *is GAS.* ■

A continuously differentiable function $W(x)$ satisfying the conditions of Theorem 2.9 is called a **Lyapunov function**. Similarly, a function $W(x,t)$ satisfying the conditions of Theorem 2.10 is called a **Lyapunov function**.

The idea in the first theorem is to linearize the system around the origin and use the linearized model to investigate the stability of the nonlinear system. If the linearized model is asymptotically stable, then the nonlinear system is locally asymptotically stable around that equilibrium, in this case the origin. In the second theorem, stability can be analyzed without linearization of the nonlinear system i.e. it is applied directly to the nonlinear system, hence the name 'direct method'.

Some physical systems fail to satisfy the asymptotic stability conditions of Theorem 2.9, when $\mathcal{W}(\cdot)$ is only positive semi-definite. However, if in a domain about $x = 0$ a Lyapunov function can be found such that its derivative along the trajectories of the system is negative semi-definite, while no trajectory can stay identically at points where $\dot{W}(x) = 0$, except at $x = 0$, then $x = 0$ is *asymptotically* stable. This idea follows from LaSalle's invariance principle. To state LaSalle's invariance principle the definition of invariant set is needed.

**Definition 2.11.** A set $\mathcal{M}$ is said to be **invariant** with respect to (2.1) if

$$x(0) \in \mathcal{M} \Rightarrow x(t) \in \mathcal{M}, \quad \forall\, t \geq 0.$$

■

**Theorem 2.12.** ***(LaSalle's invariance principle)*** *Let* $\Omega \subset \mathcal{X}$ *be a compact set that is positively invariant with respect to (2.1). Let* $W(x) : \mathcal{D} \to \mathbb{R}$ *be a continuously differentiable function such that* $\dot{W}(x) \leq 0$ *in* $\Omega$*. Let* $\mathcal{E}$ *be the set of all points in* $\Omega$ *where* $\dot{W}(x) = 0$ *and let* $\mathcal{M}$ *be the largest invariant set contained in* $\mathcal{E}$*. Then every solution starting in* $\Omega$ *converges to* $\mathcal{M}$ *as* $t \to \infty$*.* ■

## 2.3 Input-to-State Stability

The theory of input-to-state stability (ISS) introduced in [96] is an extension of Lyapunov stability theory to deal with systems with inputs. ISS captures the Lyapunov stability notion and the *bounded-input-bounded-output (BIBO)* stability notion [97]. ISS

is a central tool in nonlinear systems analysis that studies the influence of input perturbations on the system and the robustness of the system with respect to such inputs. The concept of ISS and its variants is discussed in details in many textbooks and articles [96, 97, 98, 99, 47, 45, 51, 48, 6].

Consider a nonlinear system

$$\dot{x} = f(x, u, t) \tag{2.12}$$

with state $x(t) \in \mathbb{R}^n$ and input $u(t) \in \mathbb{R}^m$, where $f(x, u)$ is locally Lipschitz and $f(0, 0) = 0$. The input function $u : [0, \infty) \to \mathbb{R}^m$ can be any measurable essentially bounded function. The set of all such functions, endowed with the essential supremum norm $\|u\|_\infty = \text{ess sup}|u(t)|, t \geq 0$ is denoted by $\mathcal{L}_\infty^m$, where $|\cdot|$ denotes the usual Euclidean norm.

**Definition 2.13.** The system (2.12) is said to be input-to-state stable if there exist a class $\mathcal{KL}$ function $\beta$ and a class $\mathcal{K}_\infty$ function $\gamma$, called a gain function, such that, for all bounded input $u \in \mathcal{L}_\infty^m$ and all $x_0 \in \mathbb{R}^n$, the response $x(t)$ of (2.12) for the initial state $x(0) = x_0$ and the input $u$ satisfies

$$|x(t)| \leq \beta(|x_0|, t) + \gamma(\sup_{\tau \in [0,t]} |u|_\infty) \quad \text{for all } t \geq 0. \tag{2.13}$$

■

The following Lyapunov-like theorem gives a sufficient condition for ISS.

**Theorem 2.14.** *Let $W : \mathbb{R}^n \to \mathbb{R}$ be a continuous differentiable function such that*

$$\underline{\alpha}(|x|) \leq W(x) \leq \overline{\alpha}(|x|) \tag{2.14}$$

$$|x| \geq \rho(|u|) \Rightarrow \frac{\partial W}{\partial x} f(x, u) \leq -\alpha(|x|), \tag{2.15}$$

*for all $x \in \mathbb{R}^n$, and all $u \in \mathbb{R}^m$, where $\underline{\alpha}, \alpha, \overline{\alpha}$ are class $\mathcal{K}_\infty$ functions and $\rho$ is a class $\mathcal{K}$ function. Then, the system (2.12) is input-to-state stable, and $W$ is called an ISS Lyapunov function.* ■

The following theorem provides a generalization to ISS.

**Theorem 2.15.** *System (2.12) is input-to-state stable if and only if it admits a smooth ISS Lyapunov function.* ■

An alternative characterization of the ISS property can be established by replacing the inequality (2.15) in Theorem 2.14 with

$$\frac{\partial W}{\partial x} f(x, u) \leq -\alpha(|x|) + \rho(|u|), \text{ for all } x \in \mathbb{R}^n \text{ and all } u \in \mathbb{R}^m \tag{2.16}$$

where $\rho$ is a class $\mathcal{K}$ function [98]. Finally, As discussed in [97, Section 3.3] and [98, Remark 2.4], the definition of ISS can be restated as:

**Definition 2.16.** A smooth function $W$ is an ISS Lyapunov function for (2.12) if and only if there exist $\underline{\alpha}, \alpha, \overline{\alpha} \in \mathcal{K}_\infty$ such that (2.14) holds, and

$$\frac{\partial W}{\partial x} f(x,u) \leq -\alpha(|x|) + \sigma(|u|), \text{ for all } x \in \mathbb{R}^n \text{ and all } u \in \mathbb{R}^m \tag{2.17}$$

where $\sigma$ is a class $\mathcal{K}_\infty$ function. ■

## 2.4 Passivity

Dissipative systems are dynamical systems with states $x(t)$, inputs $u(t)$ and outputs $y(t)$, which satisfy the so-called *dissipation inequality*, which states that the increase in storage over a time interval cannot exceed the supply delivered to the system during this time-interval [115]. Passive systems are a class of dissipative systems in which the rate at which the energy flows into the system is not less than the increase in storage. This implies that a passive system cannot store more energy than what is supplied to it from the outside, with the difference being the dissipated energy. The idea originates from traditional circuit theory in which typical examples of dissipative systems can be found in electrical circuits (energy of the systems is dissipated in resistors). Dissipativity and passivity are of particular interest because of the connection between these properties and the stability [113]. The concept of passivity has evolved in various stages; a study of passive and dissipative systems, and investigation of their connections with the stability of feedback systems were introduced in [113, 114]. These works have been extended in [42, 43] to some classes of nonlinear systems. A technique to render a system passive by means of a state feedback was introduced in [19]. Some passivity based control techniques have been discussed in the text books [93, 69, 109].

Consider a general state space system

$$\Sigma \; : \; \begin{array}{ll} \dot{x} = f(x,u), & u \in U \\ y = h(x,u), & y \in Y \end{array} \tag{2.18}$$

with input $u \in \mathbb{R}^m$ output $y \in \mathbb{R}^p$ and $x = (x_1, \cdots, x_n)^\top$ being the local coordinates for an $n$-dimensional state space manifold $\mathcal{X}$, and $U$ and $Y$ are linear spaces, together with a scalar function $s(u(t), y(t))$ called the supply rate.

Now, recall the definitions of **dissipative** and **passive** systems [113, 109].

**Definition 2.17. (Dissipative system)** A system (2.18) is called *dissipative* with respect to the supply rate $s$ if there exists a function $S : \mathcal{X} \to \mathbb{R}_+$, called the storage

function, such that, for all $x_0 \in \mathcal{X}$, all $t_1 \geq t_0$, and all input functions $u$

$$S(x(t_1)) \leq S(x(t_0)) + \int_{t_0}^{t_1} s(u(t), y(t))dt, \tag{2.19}$$

where $x(t_0) = x_0$ and $x(t_1)$ is the state of (2.18) at time $t_1$ resulting from the initial condition $x_0$ and the input function $u(\cdot)$. If (2.19) hold with *equality* for all $x_0, t_1 \geq t_0$, and all $u(\cdot)$, then (2.18) is *lossless* with respect to $s$. ■

The inequality (2.19) is called a **dissipation inequality**. It shows that the maximum stored energy $S(x(t_1))$ is equal to the sum of the stored energy $S(x(t_0))$ and the total energy supplied by the external input $\int_{t_0}^{t_1} s(u(t), y(t))dt$ during the time interval $[t_0, t_1]$. Thus, internal creation of energy is impossible; only internal dissipation of energy is possible. To capture the dissipation effects, the inequality (2.19) can be written as

$$\underbrace{S(x(t_1)) - S(x(t_0))}_{\text{stored energy}} = \underbrace{\int_{t_0}^{t_1} s(u(t), y(t))dt}_{\text{energy supplied to the system}} - \underbrace{d(t)}_{\text{dissipated energy}}, \tag{2.20}$$

where the nonnegative function $d(t) \geq 0$ represents the dissipation. The following is an example of a dissipative system.

**Example 2.1.** Consider the mass-spring-damper system which is shown in Figure 2.3, where $x$ is the mass position, $v = \dot{x}$ is the mass velocity, and $u = F(t)$ is the input. $m$, $k$ and $b$ are the mass, spring constant, and the damping coefficient, respectively. The power of the system is the input force $u = F(t)$ times the output (velocity) $y = v$. Thus, the energy of the system, which is the integration of power, is

$$\begin{aligned}
\int_{t_0}^{t_1} F(s)v(s)ds &= \int_{t_0}^{t_1} (m\dot{v}(s) + kx(s) + bv(s))v(s)ds, \\
&= \int_{t_0}^{t_1} (m\dot{v}(s)v(s)(s)ds + kx(s)\dot{x}(s)ds + bv(s)^2 ds), \\
&= \left(\frac{1}{2}mv^2(s) + \frac{1}{2}kx^2(s)\right)\Big|_{t_0}^{t_1} + b\int_{t_0}^{t_1} v^2(s)ds, \\
&= S(x(t_1)) - S(x(t_0)) + b\int_0^t v^2(s)ds.
\end{aligned} \tag{2.21}$$

Rearranging the terms, we can write (2.21) as

$$S(x(t_1)) - S(x(t_0)) = \int_0^t F(s)v(s)ds - b\int_0^t v^2(s)ds, \tag{2.22}$$

which satisfies the inequality (2.20).

The concepts of dissipativity/passivity can similarly be illustrated by an electric circuit where energy is dissipated in the resistive elements, as depicted in Figure 2.4 [72].

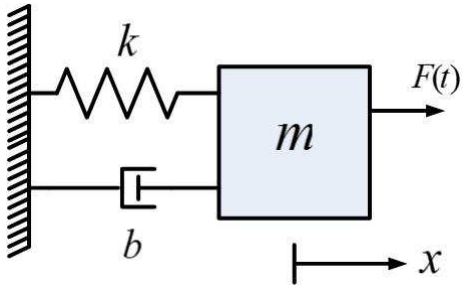


Figure 2.3: Mass-spring-damper system.

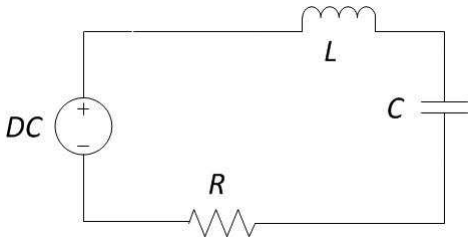


Figure 2.4: RLC circuit.

**Definition 2.18.** The system (2.18) with $U = Y = \mathbb{R}^m$ is **passive** if it is dissipative with respect to the supply rate $s(u, y) = u^\top y$. The system (2.18) is **input strictly passive (ISP)** if there exists a $\delta > 0$ such that (2.18) is dissipative with respect to $s(u, y) = u^\top y - \delta\|u\|^2$. The system (2.18) is **output strictly passive (OSP)** if there exists a $\epsilon$ such that (2.18) is dissipative with respect to $s(u, y) = u^\top y - \epsilon\|y\|^2$. ■

There are useful relationships between passivity and Lyapunov stability [47]:

**Lemma 2.19.** *If the system (2.18) is* ***passive*** *with a positive definite storage function $S(x) = W(x)$, then the origin of $f(x, 0)$ is* ***stable.*** ■

To show asymptotically stability of the origin of $\dot{x} = f(x, 0)$, an additional condition of observability must be satisfied.

**Definition 2.20. (Zero-state observability & detectability)** The system (2.18) is zero-state observable if $u(t) = y(t) = 0$, $\forall t \geq 0$, implies $x(t) = 0$, and is zero-state detectable if $u(t) = y(t) = 0$, $\forall t \geq 0$, implies $\lim_{t\to\infty} x(t) = 0$. ■

**Lemma 2.21.** *Consider the system (2.18). The origin of $\dot{x} = f(x, 0)$ is* ***asymptotically stable*** *if the system is* ***output strictly passive*** *and* ***zero-state observable.*** ■

**Example 2.2.** Consider the system

$$\begin{aligned} \dot{x}_1 &= x_2, \\ \dot{x}_2 &= -k_1 x_1^3 - k_2 x_2 + u, \quad k_1, k_2 > 0 \\ y &= x_2, \end{aligned}$$

with the Lyapunov function candidate

$$V(x) = \frac{1}{4}k_1 x_1^4 + \frac{1}{2}x_2^2.$$

The derivative of $V(x)$ is

$$\begin{aligned}\dot{V}(x) &= k_1 x_1^3 x_2 + x_2(-k_1 x_1^3 - k_2 x_2 + u) \\ &= uy - k_2 y^2.\end{aligned}$$

Hence, the system is output strictly passive. The system is also zero-state observable because

$$u(t) = y(t) \equiv 0 \implies x_2(t) \equiv 0 \implies -k_1 x_1^3(t) \equiv 0 \implies x_1(t) = 0.$$

Thus, the origin of the unforced system is asymptotically stable.

## 2.5 The Port-Controlled Hamiltonian Framework

Hamiltonian systems are an important class of nonlinear systems that are used to model mechanical, electrical and electromechanical systems, e.g. robotics systems, electrical networks, vehicles. The Hamiltonian function usually represents the total energy of the system. For example, for many mechanical systems, the Hamiltonian function represents the sum of the kinetic and the potential energies. Hamiltonian systems are conservative, i.e. the total energy function remains constant along trajectories. For example, a simple pendulum (assuming no friction and air drag) is a conservative Hamiltonian system, in the sense that if no external force is applied to it, its total energy is conserved (the summation of its kinetic energy and potential energy is a constant value). The passivity of a Hamiltonian system is associated with the existence of passive elements such as dampers in mechanical systems, and resistors, inductors and capacitors in electrical networks. Passive elements dissipate energy from the system, and hence stability or asymptotic stability can be achieved.

Port-based network modelling of lumped parameter physical systems naturally leads to a geometrically defined class of systems which is referred to as port-Hamiltonian systems [109]. The Hamiltonian approach has its roots in analytical mechanics as a generalization of the classical Hamiltonian equations of motion while the network modelling described by a Dirac structure arises from electrical engineering concept [109]. The Hamiltonian dynamics are then described by their interconnection structure (Dirac structure) and the Hamiltonian function which represents the total energy stored in the system. The port-Hamiltonian system is controlled by interconnecting it to dissipation components, energy shaping components, or by assigning its structure, or via energy transfer between subsystems, or the combination of any of them [31]. This leads to a control *paradigm*

known as the *port-controlled Hamiltonian systems*. The advantage of adopting the port-controlled Hamiltonian framework from control perspective is that it describes a large class of (nonlinear) systems including mechanical, electrical and electromechanical systems. The following shows the formulation of port-controlled Hamiltonian systems, and gives more mathematical overview of the conservative and passive features of these systems. Most of the material is based on [109].

Port-controlled Hamiltonian systems originate from the classical framework of Lagrangian and Hamiltonian differential equations. The standard Euler-Lagrange equations for mechanical systems are given as

$$\frac{d}{dt}\left(\frac{\partial L}{\partial \dot{q}}(q,\dot{q})\right) - \frac{\partial L}{\partial q}(q,\dot{q}) = \tau, \tag{2.23}$$

where $q = (q_1, \ldots, q_k)^\top$ are the generalized configuration coordinates for the system with $k$ degrees of freedom, the Lagrangian $L$ equals the difference $K - V$ between the kinetic energy $K$ and the potential energy $V$, and $\tau = (\tau_1, \ldots, \tau_k)^\top$ is the vector of generalized forces acting on the system. Furthermore, $\frac{\partial L}{\partial \dot{q}}$ denotes the column-vector of partial derivatives of $L(q,\dot{q})$ with respect to the generalized velocities $\dot{q}_1, \cdots, \dot{q}_k$, and similarly for $\frac{\partial L}{\partial q}$.

In standard mechanical systems the kinetic energy $K$ is of the form

$$K(q,\dot{q}) = \frac{1}{2}\dot{q}^\top M(q)\dot{q}, \tag{2.24}$$

where $M(q)$ is the $k \times k$ inertia (generalized mass) matrix, which is symmetric and positive definite for all $q$. In this case the vector of generalized momenta $p = (p_1, \ldots, p_k)^\top$, defined as $p = \frac{\partial L}{\partial \dot{q}}$, is simply given by

$$p = M(q)\dot{q}. \tag{2.25}$$

Define the state vector $(q_1, \ldots, q_k, p_1, \ldots, p_k)^\top$, then the $k$ second-order equations (2.23) are transformed into $2k$ first-order equations

$$\begin{aligned} \dot{q} &= \frac{\partial H}{\partial p}(q,p) \quad (= M^{-1}(q)p) \\ \dot{p} &= -\frac{\partial H}{\partial q}(q,p) + \tau, \end{aligned} \tag{2.26}$$

where

$$H(q,p) = \frac{1}{2}p^\top M^{-1}(q)p + V(q) \quad \left(= \frac{1}{2}\dot{q}^\top M(q)\dot{q} + V(q)\right), \tag{2.27}$$

is the total energy of the system. The system of equations (2.26) is called the **Hamiltonian equations** of motion, and $H$ is called the **Hamiltonian** (function). The following

energy balance condition immediately follows from (2.26):

$$\begin{aligned}\frac{d}{dt}H &= \left(\frac{\partial H}{\partial q}(q,p)\right)^\top \dot{q} + \left(\frac{\partial H}{\partial p}(q,p)\right)^\top \dot{p} \\ &= \frac{\partial H}{\partial q}^\top(q,p)\frac{\partial H}{\partial p}(q,p) + \frac{\partial H}{\partial p}^\top(q,p)\left(-\frac{\partial H}{\partial q}(q,p)+\tau\right) \\ &= \frac{\partial H}{\partial q}^\top(q,p)\frac{\partial H}{\partial p}(q,p) - \frac{\partial H}{\partial p}^\top(q,p)\frac{\partial H}{\partial q}(q,p) + \frac{\partial H}{\partial p}^\top(q,p)\tau \\ &= \frac{\partial H}{\partial p}^\top(q,p)\tau \\ &= \dot{q}^\top\tau,\end{aligned} \tag{2.28}$$

expressing that the increase in energy of the system is equal to the supplied work $\dot{q}^\top\tau$ (conservation of energy).

If the Hamiltonian $H(q,p)$ is assumed to be the sum of a positive kinetic energy and a potential energy which is bounded from below, it means that for (2.27) we have

$$M(q) = M^\top(q) > 0,\ \exists\, C > -\infty\ \ s.t.\ V(q) \geq C. \tag{2.29}$$

Then it follows that (2.26) with inputs $u = \tau$ and outputs $y = \dot{q}$ is a passive (in fact, lossless) state space system with storage function $H(q,p) - C \geq 0$. Since the energy is only defined up to a constant, one may also take as potential energy the function $V(q,p) - C \geq 0$, in which case the total energy $H(q,p)$ becomes nonnegative and thus itself is a storage function.

System (2.26) is an example of a **Hamiltonian system**, which more generally is given in the following form

$$\begin{aligned}\dot{q} &= \frac{\partial H}{\partial p}(q,p) \\ \dot{p} &= -\frac{\partial H}{\partial q}(q,p) + G(q)u, \quad u \in \mathbb{R}^m \\ y &= G^\top(q)\frac{\partial H}{\partial p}(q,p), \quad (= G^\top(q)\dot{q}) \quad y \in \mathbb{R}^m\end{aligned} \tag{2.30}$$

where $G(q)$ is the input force matrix, with $G(q)u$ denoting the generalized forces resulting from the control input $u$.

Because of the form of the output equations $y = G^\top(q)\dot{q}$, we again obtain the energy balance

$$\frac{d}{dt}H(q(t),p(t)) = u^\top(t)y(t), \tag{2.31}$$

hence if $H$ is non-negative (or bounded from below), any Hamiltonian system (2.30) is lossless. A major generalization of the class of Hamiltonian systems (2.30) is to consider systems which are described in local coordinates as

$$\begin{aligned} \dot{x} &= \mathcal{J}(x)\frac{\partial H}{\partial x}(x) + g(x)u, \\ y &= G^\top(x)\frac{\partial H}{\partial x}(x), \end{aligned} \tag{2.32}$$

where $\mathcal{J}(x)$ is a $n \times n$ matrix with entries depending smoothly on $x$, which is assumed to be skew-symmetric, i.e.

$$\mathcal{J}(x) = -\mathcal{J}^\top(x), \tag{2.33}$$

and $x = (x_1, \ldots, x_n)^\top$ are local coordinates for an $n$-dimensional state space manifold $\mathcal{X}$. Because $\mathcal{J}(x)$ is skew symmetric, we easily recover the energy-balance

$$\frac{d}{dt}H(x(t)) = u^\top(t)y(t), \tag{2.34}$$

showing that (2.32) is lossless if $H \geq 0$. We call (2.32) with $\mathcal{J}(x)$ satisfying (2.33) a **port-controlled Hamiltonian system (PCH)** with structure matrix $\mathcal{J}(x)$ and Hamiltonian $H$. Energy dissipation is also included in the framework of PCH systems. System (2.32) is then written as

$$\begin{aligned} \dot{x} &= (\mathcal{J}(x) - \mathcal{R}(x))\frac{\partial H}{\partial x}(x) + g(x)u, \\ y &= G^\top(x)\frac{\partial H}{\partial x}(x). \end{aligned} \tag{2.35}$$

where $\mathcal{R}(x)$ is a positive definite symmetric matrix, also called the damping matrix. In this case the energy balance property takes the form

$$\frac{dH}{dt}(x(t)) = u^\top(t)y(t) - \left(\frac{dH}{dt}(x(t))\right)^\top \mathcal{R}(x(t))\frac{dH}{dt}(x(t)), \tag{2.36}$$

showing that a port-controlled Hamiltonian system is passive if the Hamiltonian $H$ is bounded from below. We call (2.35) a **port-controlled Hamiltonian system with dissipation (PCHD)**. Note that in this case two geometric structures play a role: the internal interconnection structure given by $\mathcal{J}$ and an additional resistive structure given by $\mathcal{R}$ which represents the internal energy dissipation (e.g. friction).

**Example 2.3.** *Consider a magnetic levitation system [72]. It consists of an iron ball with mass $m$, in a vertical magnetic field created by a single electromagnet (see Figure 2.5). The state variables of the system are the ball position $q$, its momentum $p$ and the flux in the inductance $\phi$. The system is controlled via an input voltage $u$ applied to the electromagnet. The equations of motion for this system are:*

$$\begin{aligned} m\ddot{q} - \frac{1}{2k}\phi^2 + mg &= 0 \\ \dot{\phi} + \frac{1}{Rk}(a - q)\phi - u &= 0. \end{aligned} \tag{2.37}$$

*Then the dynamic of the system is described by a port-controlled Hamiltonian system*

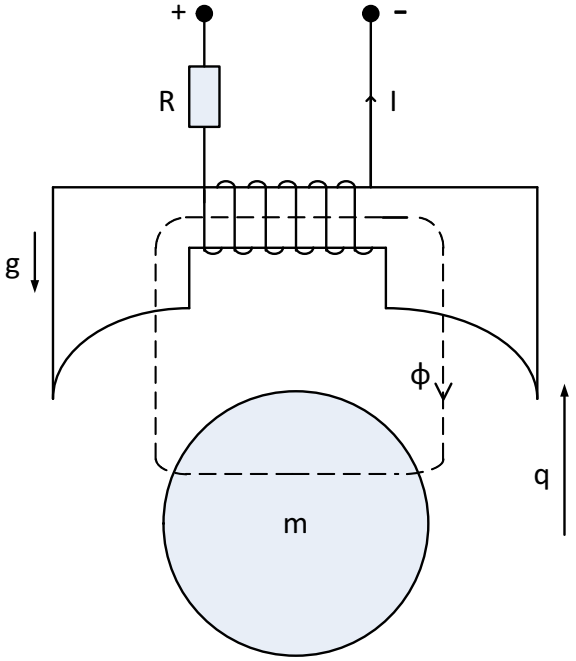


Figure 2.5: The magnetic levitation system.

*of the form (2.35)*

$$\begin{bmatrix} \dot{q} \\ \dot{p} \\ \dot{\phi} \end{bmatrix} = \begin{bmatrix} 0 & 1 & 0 \\ -1 & 0 & 0 \\ 0 & 0 & -\frac{1}{R} \end{bmatrix} \begin{bmatrix} \frac{\partial H}{\partial q}(q,p,\phi) \\ \frac{\partial H}{\partial p}(q,p,\phi) \\ \frac{\partial H}{\partial \phi}(q,p,\phi) \end{bmatrix} + \begin{bmatrix} 0 \\ 0 \\ 1 \end{bmatrix} u, \tag{2.38}$$

*with* $x = [q, p, \phi]^\top$ *and*

$$\mathcal{J} = \begin{bmatrix} 0 & 1 & 0 \\ -1 & 0 & 0 \\ 0 & 0 & 0 \end{bmatrix}, \quad \mathcal{R} = \begin{bmatrix} 0 & 0 & 0 \\ 0 & 0 & 0 \\ 0 & 0 & \frac{1}{R} \end{bmatrix}, \quad G = \begin{bmatrix} 0 \\ 0 \\ 1 \end{bmatrix}.$$

*The Hamiltonian is composed of the sum of the potential, kinetic and electromagnetic energies*

$$H(q,p,\phi) = mgq + \frac{1}{2m}p^2 + \frac{1}{2k}(a-q)\phi^2, \tag{2.39}$$

*where* $g$ *is the gravitational acceleration,* $R$ *is the coils resistance,* $a$ *is the nominal gap and the constant* $k > 0$ *depends on the number of coil turns. This electromechanical system shows the coupling between the electrical and mechanical elements via their energy, the Hamiltonian* $H(q,p,\phi)$.

## 2.6 Interconnection and Damping Assignment Passivity-Based Control

Passivity-based control (PBC) is a control methodology which achieves stabilization by passivation of the closed-loop dynamics and was first introduced in [105]. The objective of PBC is to render the closed-loop system passive with a desired storage function which usually qualifies as a Lyapunov function that has a minimum at the desired equilibrium point. Asymptotic stability is ensured if detectability of the passive output is ensured [74].

In general, there are two large divisions of PBC. The first is called classical PBC, where a storage function is first selected and a controller is designed to render the storage function non-increasing [66]. This type is applied to systems described by Euler-Lagrange equations of motion and the control design is called controlled Lagrangian method [69, 16]. In the second class, the control action is split into two tasks; energy-shaping where the desired energy function to the passive map is assigned, and damping injection where damping is applied to ensure asymptotic stability. This approach is known as interconnection and damping assignment passivity-based control (IDA-PBC) [74]. IDA-PBC has proven to be successful for a wide range of applications: mechanical systems [71], electromechanical systems [81], and discrete-time IDA-PBC design for underactuated Hamiltonian control systems [53], to mention a few. A survey on IDA-PBC and its applications can be found in [66]. The standard formulation of IDA-PBC was introduced in [73, 74], to control port-controlled Hamiltonian systems of the form (2.35).

Consider the general nonlinear system

$$\dot{x} = f(x) + g(x)u, \tag{2.40}$$

with $x \in \mathbb{R}^n$, $u \in \mathbb{R}^p$. IDA-PBC concerns finding a smooth state feedback law $u = \beta(x)$ in order to render the closed-loop system a PCH system of the form

$$\begin{aligned} \dot{x} &= (\mathcal{J}_d(x) - \mathcal{R}_d(x))\frac{\partial H_d}{\partial x}(x) \\ y &= G^\top(x)\frac{\partial H_d}{\partial x}(x), \quad y \in \mathbb{R}^m \end{aligned} \tag{2.41}$$

where $H_d$ is the desired new Hamiltonian (storage function) of the closed loop, which has to have a strict minimum at the desired equilibrium point $x = x_d$ to guarantee stability, and $\mathcal{J}_d(x)$, and $\mathcal{R}_d(x)$ are the desired interconnection and damping matrices, respectively. $\mathcal{J}_d(x)$ and $\mathcal{R}_d(x)$ should satisfy

$$\mathcal{J}_d(x) = -\mathcal{J}_d^\top(x), \quad \mathcal{R}_d(x) = \mathcal{R}_d^\top(x) \geq 0.$$

To render (2.40) with $u = \beta(x)$ equal to (2.41), we need to find a solution to the equation

$$f(x) + g(x)u = (\mathcal{J}_d(x) - \mathcal{R}_d(x))\frac{\partial H_d}{\partial x}(x). \tag{2.42}$$

which is called the matching equation. The strategy for solving this matching equation is realized by the following Lemma [66].

**Lemma 2.22.** *Consider the system (2.40). Assume there exist matrices*

$$G^{\perp}(x), \quad \mathcal{J}_d(x) = -\mathcal{J}_d^{\top}(x), \quad \mathcal{R}_d(x) = \mathcal{R}_d^{\top}(x) \geq 0,$$

*and a smooth function $H_d(x)$ such that the partial differential equation*

$$G^{\perp}(x)f(x) = G^{\perp}(x)(\mathcal{J}_d(x) - \mathcal{R}_d(x))\frac{\partial H_d}{\partial x}(x), \tag{2.43}$$

*where $G^{\perp}(x)$ is a full rank left annihilator of $G(x)$ , i.e. $G^{\perp}(x)g(x) = 0$ holds (which eliminates the input functions from the matching equation), and $H_d(x)$ is such that*

$$x_d = \arg\min H_d(x), \tag{2.44}$$

*where $x_d$ is the desired equilibrium point to be stabilized. Then the closed loop system (2.40) with $u = \beta(x)$, where*

$$\beta(x) = (G^{\top}(x)G(x))^{-1}G^{\top}(x)\left([\mathcal{J}_d(x) - \mathcal{R}_d(x)]\nabla H_d - f(x)\right), \tag{2.45}$$

*with the pseudo inverse $G^{+} = (G^{\top}G)^{-1}G^{\top}$ is used to obtain control law, can be presented as the following PCH form*

$$\dot{x} = (\mathcal{J}_d(x) - \mathcal{R}_d(x))\frac{\partial H_d}{\partial x}(x) \tag{2.46}$$

*with $x_d$ being a local stable equilibrium.* ■

Lemma 2.22 can only guarantee stability of the equilibrium point $x_d$. Asymptotic stability is guaranteed if $x_d$ is an isolated minimum of $H_d(x)$, and by invoking LaSalle's invariance principle (Theorem 2.12) as follows.

If the largest invariant set for the closed-loop system contained in

$$\{x \in \mathbb{R}^n \mid (\nabla H_d^{\top} R_d(x)\nabla H_d = 0)\},$$

equals $x_d$, then the closed loop system is asymptotically stable.

The basic idea of IDA-PBC is to transform, via static state-feedback, the system (2.40) into a PCH system with some desired energy function. This is done in two stages. First, the control signal is decomposed into two parts $u = u_{es} + u_{di}$, where $u_{es}$ is responsible

for energy-shaping and $u_{di}$ is to inject damping into the system. Second, solving the matching equation (2.42), a set of partial differential equations (PDEs) for the desired closed-loop Hamiltonian, which is the main challenge in IDA-PBC design. There are several ways to solve the matching equation, including [66]:

**a. Non-Parameterized IDA**: the interconnection $\mathcal{J}_d$ and damping $\mathcal{R}_d$ matrices are fixed, then the matching equation is pre-multiplied by a left annihilator $g^{\perp}$ such that it becomes a pure PDE in $H_d$ , which can then be solved.

**b. Algebraic IDA**: the desired Hamiltonian function $H_d$ is fixed, and then the resulting algebraic equations are solved for $\mathcal{J}_d$, $\mathcal{R}_d$, and $g^{\perp}$.

**c. Parameterized IDA**: for some physical systems, mainly mechanical systems, the knowledge of a priori structure of the desired Hamiltonian is used to simplify the PDE, giving constraints on $\mathcal{J}_d$, $\mathcal{R}_d$, and $g^{\perp}$.

There is no preferable method to solve the matching equation. One method may be applicable to certain classes of systems while others are pertinent for other classes of systems. Hence, the strategy to solve the matching equation depends mainly on the systems (mechanical, electrical, etc.), energy considerations and one may use physical insight to simplify and solve the PDEs.

# Chapter 3

# IDA-PBC of a Class for Underactuated Mechanical Systems

## 3.1 Introduction

Control of underactuated mechanical systems (UMSs) has been a central and challenging topic that has attracted the attention of control researchers [55]. UMSs, defined as systems that have fewer control inputs than degrees of freedom to be controlled, can model many important applications including robotics, spacecraft, and satellites as well as a benchmark to study complex nonlinear control systems. While the absence of actuation in some degrees of freedom imposes a challenging task to achieve the desired control objectives with a lower number of actuators, underactuation control has the advantages of reducing the cost and complexity of the control system, and ensuring the functionality of a system in the case of actuation failure [63]. However, the fact that UMSs have complex internal dynamics and in many cases are not fully feedback linearizable complicates the control design, because the nonlinear control methods proposed for general mechanical systems often cannot be applied directly to this class of systems.

Various nonlinear control techniques have been developed for stabilization of UMSs (see [55] for a survey). Among the most popular techniques, passivity-based control methods, such as controlled Lagrangian [16] and the interconnection and damping assignment passivity-based control (IDA-PBC) [74], have proven to be powerful due to their structure preserving and systematic approach, and the fact that they capture the essential physical property of energy conservation (passivity) [14, 74]. A constructive stabilization method for a class of UMSs based on a newly developed immersion and invariance (I&I) technique has been proposed in [89], and a comparison between the IDA-PBC and I&I methods for UMSs has been presented in [50].

IDA-PBC is a control design method formulated for systems described by port-controlled Hamiltonian models. The main idea of this method is to assign a new (desired) closed-loop PCH model that has certain features, utilizing the physically-inspired principles of energy shaping, interconnection structure and damping assignment (dissipation) [2]. The stabilization of an UMS via IDA-PBC is usually achieved by shaping the kinetic and potential energy functions and obtained through a state feedback law. The existence of such law constitutes the matching conditions of the IDA-PBC method which are a set of partial differential equations (PDEs) [71].

Solving these PDEs, which identify the desired potential and kinetic energy functions, is the main obstacle in the applicability of the IDA-PBC method. A number of constructive approaches to solve or simplify these PDEs for different classes of UMSs have been recently proposed in [2, 14, 39, 56, 71, 111] and references therein. Also, IDA-PBC has been applied to various underactuated systems, such as pendulum on a cart [107], inertia wheel and ball and beam systems [71], Pendubot [88] and Acrobot [56]. However, the existing results still leave open problems on solving a large class of PCH systems, either too complicated or inapplicable.

In this chapter we develop a novel constructive strategy to simplify and solve the PDEs in IDA-PBC design method for a class of UMSs with underactuation degree one. The key idea is to parametrize the desired inertia matrix that shapes the kinetic energy, and use it to simplify the potential energy PDEs, and solve them to shape the potential energy function, thus achieving total energy shaping. That is, with suitable choice of the desired inertia matrix that must be positive definite and taking into account some physical considerations, the potential energy PDEs are simplified and the final solution, the energy function must have a minimum at the desired equilibrium point. Furthermore, asymptotic stability is achieved by means of damping injection. This strategy expands the class of UMSs that can be dealt with compared to those in [2]. That is, we have proposed some design methods to deal with two groups of underactuated PCH systems, namely, the *separable* PCH systems (systems with constant inertia matrix) and *non-separable* PCH systems (systems with non-constant inertia matrix). We apply our results to the stabilization, as well as the swing up, of an inertia wheel pendulum and a rotary inverted pendulum, also known as *Furuta pendulum*, systems. The latter has more complex dynamics than most other commonly studied benchmark systems [63].

The main contributions of this and the next chapter are

- A constructive method to solve the potential energy PDEs for mechanical systems with underactuation degree one. The motivation for this is that most position stabilization problems can be solved by shaping the potential energy function [2]. For underactuated mechanical systems, the kinetic energy function also needs to be shaped. We have assigned the inertia matrix that shapes the kinetic energy,

and used it to simplify the potential energy PDE, and solve them to shape the potential energy function, thus reshaping the total energy function.

- While most works in the literature use either normalized, linearized, or partial feedback linearized model of the UMSs to simplify the problem, we have employed a full nonlinear model of the system.

- The proof that our proposed controller design method ensures an 'almost' global asymptotic stabilization for the rotary inverted pendulum in its full nonlinear dynamics. To the best of our knowledge, this is the first work that achieves stabilization of this system over the entire domain of attraction using the IDA-PBC technique. Also, it shows an 'almost' global stabilization of the inertia wheel pendulum using *realistic* model parameters.

## 3.2 Problem Formulation

We review the general procedure of the IDA-PBC design as has been proposed for instance in [74, 66]. Some existing methods to solve the matching equations associated with the IDA-PBC are also reviewed, highlighting some limitations of those methods. Consider a PCH system the dynamics of which can be written as

$$\begin{aligned} \begin{bmatrix} \dot{q} \\ \dot{p} \end{bmatrix} &= \begin{bmatrix} 0 & I_n \\ -I_n & 0 \end{bmatrix} \begin{bmatrix} \nabla_q H \\ \nabla_p H \end{bmatrix} + \begin{bmatrix} 0 \\ G(q) \end{bmatrix} u, \\ y &= G^\top(q) \nabla_p H, \end{aligned} \tag{3.1}$$

where $q \in \mathbb{R}^n$, $p \in \mathbb{R}^n$ are the states and $u, y \in \mathbb{R}^m$, $m \leq n$, are the control input and the output, respectively. The matrix $G \in \mathbb{R}^{n \times m}$ is determined by the manner in which the control $u \in \mathbb{R}^m$ enters into the system. If $m = n$ the system is called fully-actuated, while if $m < n$ it is called underactuated. The Hamiltonian function, which is the total energy of the system, is defined as the sum of the kinetic energy and the potential energy, namely

$$H(q,p) = K(q,p) + V(q) = \frac{1}{2} p^T M^{-1}(q) p + V(q), \tag{3.2}$$

where $M(q) > 0$ is the symmetric inertia matrix and $V(q)$ is the potential energy function. The IDA-PBC control law

$$u = u_{es} + u_{di}, \tag{3.3}$$

consists of two parts, which correspond to its design steps; the *energy shaping* and the *damping injection*.

**Energy shaping**

The main objective of IDA-PBC is to stabilize the underactuated mechanical system by

a state-feedback controller. This is achieved by replacing the interconnection matrix and the energy function (Hamiltonian) of the system with a *desired* ones while preserving the PCH structure of the total system in closed-loop. This can be mathematically expressed as

$$\begin{bmatrix} 0 & I_n \\ -I_n & 0 \end{bmatrix} \begin{bmatrix} \nabla_q H \\ \nabla_p H \end{bmatrix} + \begin{bmatrix} 0 \\ G(q) \end{bmatrix} u_{es} = \begin{bmatrix} 0 & M^{-1}M_d \\ -M_d M^{-1} & J_2(q,p) \end{bmatrix} \begin{bmatrix} \nabla_q H_d \\ \nabla_p H_d \end{bmatrix}. \tag{3.4}$$

The desired total energy in closed-loop is assigned to be

$$H_d(q,p) = K_d(q,p) + V_d(q) = \frac{1}{2} p^T M_d^{-1}(q) p + V_d(q), \tag{3.5}$$

with $M_d = M_d^T > 0$ the desired inertia matrix and $V_d(q)$ the desired potential energy, such that $H_d$ has an isolated minimum at the desired equilibrium point $q_e$, i.e.

$$q_e = \arg\min H_d(q) = \arg\min V_d(q). \tag{3.6}$$

The following conditions are required so that (3.6) hold.

**Condition 3.1.** Necessary extremum assignment: $\nabla_q V_d(q_e) = 0$.

**Condition 3.2.** Sufficient minimum assignment: $\nabla_q^2 V_d(q_e) > 0$, i.e. the Hessian of the function at the equilibrium point is positive [71].

Equation (3.4) constitutes the matching conditions of the IDA-PBC method [74], which is a set of PDEs in the form of

$$G^{\perp}\{\nabla_q H - M_d M^{-1} \nabla_q H_d + J_2 M_d^{-1} p\} = 0, \tag{3.7}$$

with $J_2 = -J_2^T$ a free parameter. The PDE (3.7) can be equivalently written as the kinetic energy PDE (dependent on $p$)

$$G^{\perp}\{\nabla_q (p^T M^{-1} p) - M_d M^{-1} \nabla_q (p^T M_d^{-1} p) + 2 J_2 M_d^{-1} p\} = 0 \tag{3.8}$$

and the potential energy PDE (independent of $p$)

$$G^{\perp}\{\nabla_q V - M_d M^{-1} \nabla_q V_d\} = 0. \tag{3.9}$$

If these sets of PDEs (3.8) and (3.9) are solved, or in other words $M_d$, $V_d$ and $J_2$ are obtained, then $u_{es}$ is given by

$$\begin{aligned} u_{es} &= (G^{\top} G)^{-1} G^{\top} \left( \nabla_q H - M_d M^{-1} \nabla_q H_d + J_2 M_d^{-1} p \right) \\ &= G^{+} \left( \nabla_q H - M_d M^{-1} \nabla_q H_d + J_2 M_d^{-1} p \right). \end{aligned} \tag{3.10}$$

**Damping injection**

The next task after finding $u_{es}$ is to find the damping injection (dissipation) controller,

$u_{di}$ which is

$$u_{di} = -K_v G^T \nabla_p H_d, \qquad K_v > 0 \tag{3.11}$$

to add damping to the closed-loop system that ensures asymptotic stabilization to the desired equilibrium. $u_{di}$ is applied via a negative feedback of the passive output to achieve asymptotic stability, provided that the system is zero-state detectable (see Definition 2.20). Given a PCH system (3.1), by applying the IDA-PBC design we obtain the desired PCH dynamics

$$\begin{aligned} \begin{bmatrix} \dot{q} \\ \dot{p} \end{bmatrix} &= \begin{bmatrix} 0 & M^{-1}M_d \\ -M_d M^{-1} & J_2 - R_d \end{bmatrix} \begin{bmatrix} \nabla_q H_d \\ \nabla_p H_d \end{bmatrix} \\ y_d &= G^\top(q) \nabla_p H_d, \end{aligned} \tag{3.12}$$

where $R_d = G K_v G^\top \geq 0$ is the dissipation matrix.

### 3.2.1 Total energy shaping

From the passivity-based control perspective the natural way to stabilize a mechanical system is by modifying/shaping its energy function, which comprises the kinetic and the potential energy functions. The most important procedure in this stabilization is to shape its potential energy function. This is due to several reasons; first, the stability of the system at its equilibria is achieved through the potential energy shaping [54, 108]. The energy of the mechanical system in its equilibria is represented by the potential energy at the position coordinates $q$ [101]. Secondly, the qualitative behavior of the system can be concluded from the features of the potential energy function. Thirdly, most approaches that rely on kinetic energy shaping only have resulted in unsatisfactory stability and closed-loop performance of the system, in the sense that the stability is limited to reduced domain of attraction. In [15, 16] where the method of controlled Lagrangian restricted to kinetic energy shaping has been used, only local asymptotic stability has been achieved (for instance in the inverted pendulum applications, the pendulum can be stabilized at the upward position if it starts from a nearly horizontal position i.e. small domain of attraction).

As for the PCH framework, where the IDA-PBC is the most popular method being used, the focus in most approaches has been on solving the kinetic energy PDE, by modifying the interconnection matrix $M_d$ and using it to produce the closed-loop potential energy function $V_d$. As discussed in [2, Remark 7], the restriction on $M_d$ in solving the kinetic energy PDE limits achieving global stability. This is evident by the reduced DoA obtained in the cart pendulum system and the Furuta pendulum system applications in [2] and [111]. While the potential energy shaping is sufficient in most regulation problems for mechanical systems, for underactuated systems it is necessary also to shape the

kinetic energy function, thus achieving total energy shaping that enlarges the class of systems that can be stabilized [71].

### 3.2.2 The matching equations

Some constructive techniques have been proposed in the literature, for instance in [2, 14, 39, 111], to solve the matching equations for various subclasses of PCH systems, imposing particular conditions to satisfy. In [39], a method to reduce the kinetic energy PDE (3.8) to a simpler nonlinear ODE has been proposed. This method has been developed for a class of UMSs whose open-loop inertia matrix $M$ depends only on the non-actuated coordinate. The idea is then to parametrize the closed-loop inertia matrix $M_d$ to follow the structure of $M$ and to use the free parameter matrix $J_2$ to force these equations to satisfy certain mathematical properties and hence reducing these PDE to a simpler nonlinear ODE. This procedure contributes to kinetic energy shaping. The assigned $M_d$ which must be symmetric and positive definite is then substituted into (3.9) to solve for $V_d$, i.e. potential energy shaping.

Another technique to simplify the kinetic energy PDEs has been proposed in [14]. A notation of $\lambda - Equations$ originally proposed in [12] to simplify a nonlinear system of PDEs into a set of linear PDEs has been adopted to generate one quadratic PDE in $\lambda$ and subsequently a linear PDE in $M_d$. This PDE has been solved and the resulting $M_d$ is used in (3.9) to solve for $V_d$.

In [2] a constructive technique to solve the PDEs has been suggested. In the method therein several conditions have been imposed on $M$, $G$ and $V$ to simplify these PDEs. First, the system has underactuation degree one and $M$ does not depend on the unactuated coordinate. This condition eliminates the first term (also called the forcing term) in (3.8) which transforms these equations from inhomogeneous to homogeneous PDEs. If the first condition is not satisfied, a partial feedback linearization can be used. Then, parametrizing $M_d$ and partially parametrizing $J_2$, in such a way so that the PDEs (3.8) are transformed into a set of algebraic equations in the (partially) unknown $J_2$ for a fixed $M_d$, solve the kinetic energy shaping problem (see Proposition 3 of [2]). The potential energy shaping is then achieved by using the fixed $M_d$ and by imposing that $M_d$ and $V_d$ are both functions of *one* and *the same* actuated subspace. Inspired by the work of [2], several IDA-PBC controllers have been proposed in [56], [88], [107] and [111], for various UMSs.

The aforementioned results have imposed conditions and assumptions, restricting their applicability to small classes of UMSs.

### 3.2.3 Simplifying the PDEs via change of coordinates

A common practice to simplify the PDEs is to employ a change of coordinates (see for instance [2], [71], [111] and references therein). In [71], a change of coordinates is used to obtain a simplified description of the dynamics of the inertia wheel pendulum which belongs to separable PCH systems.

In [111], a simplification to the kinetic energy PDEs, which are nonlinear and inhomogeneous, is obtained via a certain change of coordinates that eliminates the forcing term in this set of PDEs, making them homogeneous. This change of coordinates involves replacing the momentum vector $p$ by its corresponding quasi-velocities. The method is known as *quasi-linearization* as it involves elimination of the quadratic terms of velocity (resembles the linearization). As a result, the inertia matrix becomes constant in the energy function (i.e., the system is only affected by the potential field) [111]. In [21] and [110], some necessary and sufficient conditions (such as, Riemannian curvature, constant inertia matrix, skew-symmetry, and zero Christoffel symbols) on the inertia matrix $M$ have been given, which need to be verified for the existence of such transformation. Although these methods simplify the control problem, the applicability is limited to the class of systems that admits quasi-linearization. For example, the method in [111] can not be applied directly to the rotary inverted pendulum.

Inspired by the discussion above, we propose a novel approach to address this problem, concentrating on simplifying and solving the potential energy PDEs which implies modifying the inertia matrix (note that in (3.9), $M_d$ is the only term that can be modified). By parametrizing $M_d$, which shapes the kinetic energy function it can be used to solve the potential energy PDE rather than focusing on finding the solution for the kinetic energy PDE itself.

## 3.3 Main Results: Simplifying the Potential Energy PDEs

In this section we propose a novel approach for IDA-PBC design, focusing on solving (3.9), the set of PDEs associated with the potential energy. In [2], it was shown that the potential energy PDEs can be explicitly solved, provided that the inertia matrix $M$ and the potential energy $V$ depend only on the *actuated* coordinates. This method is applicable only to a subclass of UMSs that satisfy the following conditions:

**Condition 3.3.** The inertia matrix $M$ and the potential energy function $V$ do not depend on the **unactuated** coordinates.

**Condition 3.4.** The system has underactuation degree one, i.e. $m = n - 1$.

Violating Condition 3.3, the forcing term $G^{\perp}\nabla_q(p^T M^{-1} p)$ in (3.8) is not eliminated and hence does not simplify the process of solving the PDEs. In this work, we propose a new

procedure to relax Condition 3.3 (while Condition 3.4 is kept), with the implication to also extend the class of underactuated systems that can be treated using this method.

In the sequel, for the sake of the clarity of the constructive presentation, we focus our attention to systems with two degrees of freedom (and underactuation degree one), i.e $n = 2$, $m = 1$. This is motivated by the fact that the majority of classical problems in underactuated control such as all examples mentioned in Chapter 1 (see also the survey paper [55] for most common examples of UMSs) share this property. However, extending the results to more general classes of systems with underactuation degree 1 is possible, although the formulation is more complicated. The following condition identifies the class of PCH systems considered in this work.

**Condition 3.5.** The inertia matrix $M$ and the potential energy function $V$ depend only on one coordinate, not necessarily the actuated coordinate.

Condition 3.5 is a relaxation of Condition 3.3, in the sense that this method can be applied to all cases; either **1)** $M$ is constant, or **2)** $M$ depends only on one coordinate either actuated or unactuated. Without loss of generality, we assume that the unactuated coordinate is $q_1$ and hence $G = e_2$ ($G^\perp = e_1^\top$), otherwise we may reorder the coordinates to yield this structure.

Clearly, one source of difficulty in solving (3.9) arises from the complex structure and, for many dynamical systems, the dependencies on $q$ of the inertia matrix, and hence its inverse. Recognizing that (3.9) contains a coupling term ($M_d M^{-1}$), we can simplify this PDE by choosing the structure of $M_d$ in a certain way that eliminates some terms as follows.

Let the inertia matrix be
$$M(q) = \begin{bmatrix} k_1(q_1) & k_2(q_1) \\ k_2(q_1) & k_3(q_1) \end{bmatrix}. \tag{3.13}$$

Denote its determinant as $\Delta := \det(M) = k_1(q_1)k_3(q_1) - k_2^2(q_1)$. By the inclusion of $\Delta$ in the *desired* inertia matrix, or in other words by choosing

$$M_d(q) = \begin{bmatrix} m_1(q) & m_2(q) \\ m_2(q) & m_3(q) \end{bmatrix} = \Delta \begin{bmatrix} \bar{m}_1(q) & \bar{m}_2(q) \\ \bar{m}_2(q) & \bar{m}_3(q) \end{bmatrix}, \tag{3.14}$$

and suppose that Conditions 3.4 and 3.5 hold, (3.9) can then be written as

$$\begin{bmatrix} 1 & 0 \end{bmatrix} \left\{ \begin{bmatrix} \nabla_{q_1} V(q_1) \\ 0 \end{bmatrix} - \begin{bmatrix} \bar{m}_1\Delta & \bar{m}_2\Delta \\ \bar{m}_2\Delta & \bar{m}_3\Delta \end{bmatrix} \begin{bmatrix} \frac{k_3}{\Delta} & \frac{-k_2}{\Delta} \\ \frac{-k_2}{\Delta} & \frac{k_1}{\Delta} \end{bmatrix} \begin{bmatrix} \nabla_{q_1} V_d(q) \\ \nabla_{q_2} V_d(q) \end{bmatrix} \right\} = 0, \tag{3.15}$$

which further gives

$$(\bar{m}_1 k_3 - \bar{m}_2 k_2)\nabla_{q_1} V_d(q) + (-\bar{m}_1 k_2 + \bar{m}_2 k_1)\nabla_{q_2} V_d(q) = \nabla_{q_1} V(q_1). \tag{3.16}$$

Notice that with this parametrization of $M_d$, $\Delta$ is eliminated from the potential energy PDE, which gives the first step of the simplification.

In general, based on the forms of the inertia matrix, PCH systems, or in our case the UMSs, can be classified into two groups [52]: **i)** separable UMSs, if the inertia matrix is constant i.e. $M$ is independent of the states $(q, p)$, **ii)** non-separable UMSs, if otherwise. Now, we deal with each group separately.

### 3.3.1 Separable UMSs

An example of separable UMSs is the inertia wheel pendulum (IWP) [103]. In some cases, a non-separable UMS model can be transformed into a separable one via partial feedback linearization [100] or a change of coordinates [63, 110].

Because $M$ is constant, we can choose $M_d$ to be also constant. Hence, we can write (3.13) and (3.14) as

$$M = \begin{bmatrix} k_1 & k_2 \\ k_2 & k_3 \end{bmatrix}, \tag{3.17}$$

$$M_d = \begin{bmatrix} m_1 & m_2 \\ m_2 & m_3 \end{bmatrix} = \Delta \begin{bmatrix} \bar{m}_1 & \bar{m}_2 \\ \bar{m}_2 & \bar{m}_3 \end{bmatrix}. \tag{3.18}$$

Further simplification to (3.16) is achieved by choosing

$$\bar{m}_2 = \frac{k_2}{k_1}\bar{m}_1 + \varepsilon, \quad \varepsilon > 0 \tag{3.19}$$

yielding

$$\begin{aligned} (\bar{m}_1 k_3 - \bar{m}_2 k_2)\nabla_{q_1} V_d(q) + \varepsilon k_1 \nabla_{q_2} V_d(q) &= \nabla_{q_1} V(q_1), \\ \left(\bar{m}_1 \left(k_3 - \frac{k_2^2}{k_1}\right) - \varepsilon k_2\right) \nabla_{q_1} V_d(q) + \varepsilon k_1 \nabla_{q_2} V_d(q) &= \nabla_{q_1} V(q_1). \end{aligned} \tag{3.20}$$

The general solution of this PDE is of the form

$$V_d(q) = V_d(q_1) + \Psi(q_2 + \pi_1 q_1), \tag{3.21}$$

where $\Psi$ is an arbitrary differentiable function that we must choose to satisfy the condition (3.6) for $q_e$, and $\pi_1$ is constant. The procedure can now be summarized in the following proposition.

**Proposition 3.6.** *Consider the separable underactuated PCH system (3.1) satisfying Conditions 3.4 and 3.5. Let the inertia matrix $M > 0$ and the parametrized desired inertia matrix $M_d > 0$ take the form (3.17) and (3.18), respectively. Then the potential energy PDE (3.9) can be written in its simplified form (3.20) by choosing $\bar{m}_2 = \frac{k_2}{k_1}\bar{m}_1 + \varepsilon$, with a constant $\varepsilon > 0$. Furthermore, the solution of the potential energy PDE is given by (3.21).* ■

**Remark 3.7.** The choice of $\bar{m}_2 = \frac{k_2}{k_1}\bar{m}_1 + \varepsilon$ in the separable case is critical to make the potential energy PDE as simple as possible. The fact that $M$ is constant gives more freedom in parametrizing the matrix $M_d$ to assign $\bar{m}_i$, $i = 1, 2, 3$, where again the parametrization is such that $M_d > 0$ is symmetric and $V_d$ admits a minimum at the desired equilibrium point $q_e$. Furthermore, since $M$ and $M_d$ are constant, we can choose $J_2 = 0$.

### 3.3.2 Non-separable UMSs

Non-separable UMSs are more complex. This class of systems contains the majority of UMSs that frequently appear in applications. We proceed with our simplification by choosing

$$\bar{m}_2(q) = \frac{k_2(q_1)}{k_1(q_1)}\bar{m}_1(q), \tag{3.22}$$

which simplifies (3.16) into

$$\begin{aligned}(\bar{m}_1(q)k_3(q_1) - \bar{m}_2(q)k_2(q_1))\nabla_{q_1}V_d(q) &= \nabla_{q_1}V(q_1)\\ \bar{m}_1(q)\left(k_3(q_1) - \frac{k_2^2(q_1)}{k_1(q_1)}\right)\nabla_{q_1}V_d(q) &= \nabla_{q_1}V(q_1),\end{aligned} \tag{3.23}$$

which is then rewritten as

$$\nabla_{q_1}V_d(q) = \frac{\nabla_{q_1}V(q_1)}{\bar{m}_1(q)\pi(q_1)}, \quad \pi(q_1) = \left(k_3 - \frac{k_2^2}{k_1}\right). \tag{3.24}$$

Notice that $\nabla_{q_1}V(q_1)$ and $\pi(q_1)$ are known. The obvious next step is to find $\bar{m}_1(q)$ in (3.24) such that the solution of this potential energy PDE guarantees that $V_d$ has an isolated minimum. As $M$ is a function of $q_1$ only, we can simply take $M_d$ as also a function of $q_1$ only. Then (3.24) can be solved as either ODE or PDE. However, we chose to solve it as PDE for two reasons; first, to satisfy Conditions 3.1 and 3.2, and second, to keep track on the coordinate $q_2$. The solution of (3.24) is given by

$$V_d(q) = \int_0^{q_1} \frac{\nabla_x V(x)}{\bar{m}_1(x)\pi(x)}dx + \Psi(q_2), \tag{3.25}$$

where the function $\Psi(\cdot)$ is an arbitrary differentiable function that must be chosen such that (3.6) is satisfied. This whole procedure can now be summarized in the following proposition.

**Proposition 3.8.** *Consider the non-separable underactuated PCH system (3.1) satisfying Conditions 3.4 and 3.5. Let the inertia matrix $M(q) > 0$ and the parametrized desired inertia matrix $M_d(q) > 0$ take the form (3.13) and (3.14), respectively. The potential energy PDE (3.9) can then be written in its simplified form (3.24) by choosing $\bar{m}_2 = \frac{k_2}{k_1}\bar{m}_1$. Furthermore, the solution of the potential energy PDE is given by (3.25)* ■

**Remark 3.9.** Using Propositions 3.6 and 3.8, the PDE (3.8) and (3.9) are simplified and their general solutions depend on the dynamics of the underactuated system. Clearly, the inclusion of the determinant $\Delta$ is essential in the parametrization of $M_d$. It simplifies the PDEs by canceling out the term $\Delta$ from the denominator of each element of $M^{-1}$.

**Remark 3.10.** The elimination of the second term on the left hand side of (3.16) by choosing $\bar{m}_2 = \frac{k_2}{k_1}\bar{m}_1$ in the non-separable case is critical to make the potential energy PDE as simple as possible. The parametrization of $M_d$ to assign $\bar{m}_i$, $i = 1, 2, 3$ depends mainly on the dynamics of the system. They must be chosen to ensure that $M_d$ is symmetric and positive definite (i.e. $\bar{m}_1 > 0$, and $\bar{m}_3 > \frac{\bar{m}_2^2}{\bar{m}_1}$ ), and then from the set of symmetric and positive definite $M_d$, we can choose one that shapes the potential energy function satisfying Conditions 3.1 and 3.2. Once all of the above are satisfied, then the free skew-symmetric matrix $J_2(q, p)$ is brought into play. Since we have fixed $M_d$, the kinetic energy (3.8) is no longer a nonlinear and inhomogeneous PDE but is an algebraic equation in the unknown $J_2$ for a given $M_d$.

Now, using Proposition 3.8, we have established the existence of a solution for the potential energy PDE. It remains to verify the existence of solution(s) to the kinetic energy PDEs (3.8). Solving (3.8) is essential for the completion of the kinetic energy shaping, as well as to find $J_2$ which contributes to the last term on the right hand side of (3.10). Since we have fixed $M_d$, the kinetic energy (3.8) becomes an algebraic equation and can be written as

$$G^{\perp}\{2J_2M_d^{-1}p\} = G^{\perp}\{M_dM^{-1}\nabla_q H_d - \nabla_q H\}, \tag{3.26}$$

and thus can be solved to obtain $J_2$.

**Remark 3.11.** The application of the result in [2] to a pendulum on a cart, which is a non-separable system, requires partial feedback linearization to satisfy Condition 3.3. Using Proposition 3.8, we can solve it directly without linearization. Furthermore, our proposed method is the first that guarantee an 'almost' global asymptotic stability of the cart pendulum system using IDA-PBC. In Chapter 4 we show as an application example a rotary inverted pendulum that has a similar but more complicated structure than a pendulum on a cart.

Equations (3.20) and (3.24) represent simplified PDEs which are applicable to a wide range of UMSs such as the inertia wheel pendulum, the pendulum on a cart, and the rotary pendulum. In Section 3.4 and Chapter 4, we apply our results to an inertia wheel pendulum system and a rotary inverted pendulum to illustrate the cases of separable and non-separable Hamiltonian systems, respectively.

## 3.4 Separable Hamiltonian Systems: The Inertia Wheel Pendulum Example

In this section we apply the proposed design method to stabilize at the upright position, an inertia wheel pendulum (IWP), also known as a reaction wheel pendulum. IWP was first introduced in [103], where a control design based on a partial feedback linearization was proposed. Another approach based on a global change of coordinates to transform the dynamics of the system into strict feedback form and then applying the standard backstepping procedure was presented in [63]. Energy-based approach was shown in [33]. IDA-PBC of IWP has been recently reported in [71], where a change of coordinates and scaling have been used. Here, we apply our design method to the system *without* any change of coordinates or scaling, simulating a practical set-up using parameters from a real system.

### 3.4.1 Inertia wheel pendulum model

We use the model of the Quanser IWP module [17], as shown in Figure 3.1 together with the simplified free body diagram of its mechanical part. The system comprises an unactuated planar inverted pendulum with actuated symmetric wheel attached to the end of the pendulum and is free to rotate about an axis parallel to the axis of rotation of the pendulum. The system has two degrees-of-freedom; the angular position of the pendulum $q_1$ and the angular position of the wheel $q_2$. As only the wheel is actuated, the system is underactuated. The Euler-Lagrange's equations of motion for the IWP

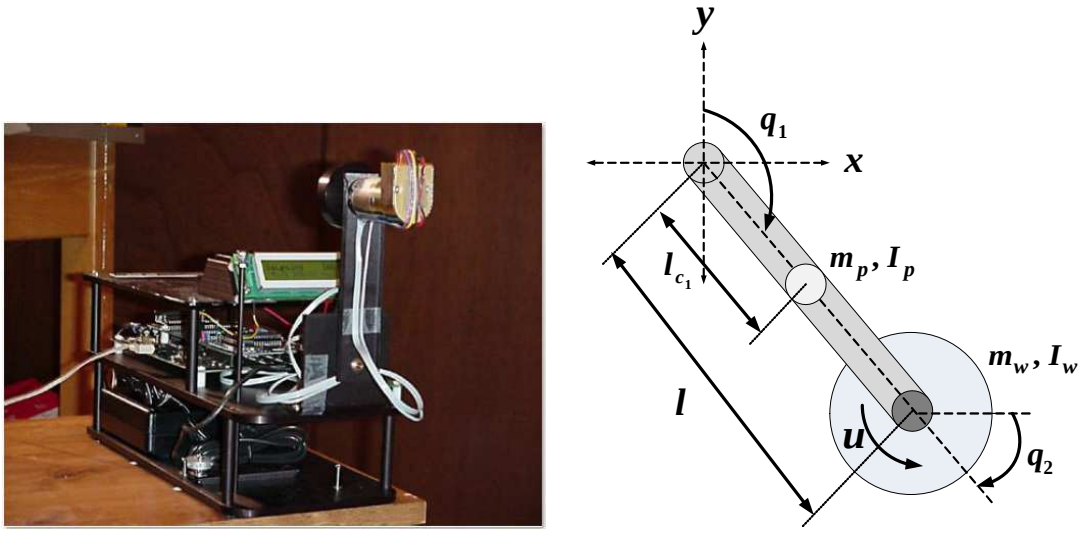


Figure 3.1: The inertia wheel pendulum system and its free body diagram.

are [71] :

$$\begin{bmatrix} a_1 + a_2 & a_2 \\ a_2 & a_2 \end{bmatrix} \begin{bmatrix} \ddot{q}_1 \\ \ddot{q}_2 \end{bmatrix} + \begin{bmatrix} -a_3 \sin(q_1) \\ 0 \end{bmatrix} = \begin{bmatrix} 0 \\ 1 \end{bmatrix} \tau, \tag{3.27}$$

where the control input $u = \tau$ is the motor torque, $a_1 = m_p l_{c_1}^2 + m_w l^2 + I_p + I_w$, $a_2 = I_w$ and $a_3 = g(m_p l_{c_1} + m_w l)$. The remaining parameters are listed in Table 3.1. The

Table 3.1: The parameters of the inertia wheel pendulum

| **Parameter** | **Description** | **Value** | **Unit** |
|---|---|---|---|
| $m_p$ | Mass of the pendulum | 0.2164 | $kg$ |
| $l$ | Total length of the pendulum | 0.2346 | $m$ |
| $l_{c_1}$ | length to the pendulum center of mass | 0.1173 | $m$ |
| $I_p$ | Moment of inertia of the pendulum | $2.233 \times 10^{-4}$ | $kg.m^2$ |
| $m_w$ | Mass of the wheel | 0.0850 | $kg$ |
| $I_w$ | Moment of inertia of the wheel | $2.495 \times 10^{-5}$ | $kg.m^2$ |
| $g$ | Gravitational acceleration | 9.81 | $m/s^2$ |

dynamic equations of the IWP can be written in PCH form (3.1) with $n = 2$, $m = 1$ and

$$M = \begin{bmatrix} a_1 + a_2 & a_2 \\ a_2 & a_2 \end{bmatrix}, \quad G = e_2 = \begin{bmatrix} 0 \\ 1 \end{bmatrix},$$
$$V(q_1) = a_3(\cos(q_1) + 1).$$

### 3.4.2 Controller design

We apply the procedure given in Section 3.3, Proposition 3.6 in particular, to design the controller for the IWP. The main objective is to provide a continuous-time control law to swing up the pendulum by spinning the wheel and to asymptotically stabilize the pendulum at its upward position $q_e = (0, q_2)$ for any $q_2 \in [0,\ 2\pi]$. First we design the energy shaping controller $u_{es}$ and then adding the damping to the closed-loop system by designing the damping injection controller $u_{di}$.

**Reshaping the total energy**

Following the procedures in Proposition 3.6, we fix $M_d$ in the form of

$$M_d = \Delta \begin{bmatrix} m_1 & m_2 \\ m_2 & m_3 \end{bmatrix} = \Delta \begin{bmatrix} m_1 & \frac{m_1 a_2}{a_1 + a_2} + \varepsilon \\ \frac{m_1 a_2}{a_1 + a_2} + \varepsilon & m_3 \end{bmatrix}, \tag{3.28}$$

where $\Delta = \det(M) = a_1 a_2$. With this choice of $M_d$, and having $G^\perp = [1\ 0]$, the PDE (3.9) becomes

$$\begin{bmatrix} 1 & 0 \end{bmatrix} \left\{ \begin{bmatrix} -a_3 \sin(q_1) \\ 0 \end{bmatrix} - \Delta \begin{bmatrix} m_1 & \frac{m_1 a_2}{a_1 + a_2} + \varepsilon \\ \frac{m_1 a_2}{a_1 + a_2} + \varepsilon & m_3 \end{bmatrix} \begin{bmatrix} \frac{a_2}{\Delta} & \frac{-a_2}{\Delta} \\ \frac{-a_2}{\Delta} & \frac{a_1 + a_2}{\Delta} \end{bmatrix} \begin{bmatrix} \nabla_{q_1} V_d \\ \nabla_{q_2} V_d \end{bmatrix} \right\} = 0,$$

which further gives

$$\left( m_1 a_2 - \frac{m_1 a_2^2}{a_1 + a_2} - \varepsilon a_2 \right) \nabla_{q_1} V_d + \varepsilon (a_1 + a_2) \nabla_{q_2} V_d = -a_3 \sin(q_1).$$

Solving this PDE produces the desired potential energy

$$V_d(q) = -a_3\gamma_1 \cos(q_1) + \Psi(x(q)), \tag{3.29}$$

$$x(q) = q_2 + \gamma_1\varepsilon(a_1 + a_2)q_1, \tag{3.30}$$

with $\gamma_1 = \frac{a_1+a_2}{a_2(\varepsilon(a_1+a_2)-a_1m_1)} > 0$. The function $\Psi(\cdot)$ in (3.29) is an arbitrary differentiable function that must be chosen to satisfy condition (3.6). This condition, along with the conditions $m_1 > 0$ and $m_1m_3 > m_2^2$ are satisfied by choosing $\Psi(x(q)) = \frac{1}{2}K_p(x(q))^2$, where $K_p > 0$ is the gain of the energy shaping controller. Note that $\Psi$ is a quadratic function such that the desired energy function is positive definite (see the proof of Corollary 4.2).

Substituting all the terms into (3.10), we obtain the energy shaping controller

$$u_{es} = \gamma_2 \sin(q_1) + K_p\gamma_3(q_2 + \gamma_1\varepsilon(a_1 + a_2)q_1), \tag{3.31}$$

with $\gamma_2 = -m_0\gamma_1a_2(m_2 - m_3)$ and $\gamma_3 = m_2a_2(\gamma_1 - 1) + m_3(a_1 + a_2)(1 - \gamma_1a_2)$.

**Damping assignment**

The damping injection controller follows the construction (3.11). From (3.5) and given $M_d$ that has been obtained when reshaping the total energy, we have

$$\begin{aligned}\nabla_p H_d = M_d^{-1}p &= \frac{\Delta}{\Delta_d}\begin{bmatrix} m_3 & -\frac{m_1a_2}{a_1+a_2} - \varepsilon \\ -\frac{m_1a_2}{a_1+a_2} - \varepsilon & m_1 \end{bmatrix}\begin{bmatrix} p_1 \\ p_2 \end{bmatrix} \\ &= \frac{\Delta}{\Delta_d}\begin{bmatrix} m_3p_1 - \left(\frac{m_1a_2}{a_1+a_2} + \varepsilon\right)p_2 \\ -\left(\frac{m_1a_2}{a_1+a_2} + \varepsilon\right)p_1 + m_1p_2 \end{bmatrix}\end{aligned} \tag{3.32}$$

with $\Delta_d = \det(M_d) = \Delta^2(m_1m_3 - m_2^2)$. Substituting (3.32) into (3.11), the damping injection controller is then

$$u_{di} = -K_v\frac{\Delta}{\Delta_d}\left(-\left(\frac{m_1a_2}{a_1 + a_2} + \varepsilon\right)p_1 + m_1p_2\right). \tag{3.33}$$

We can conclude the IDA-PBC design for the IWP by the following corollary.

**Corollary 3.12.** *The state feedback controller (3.31), (3.33) with $K_p > 0$, $K_v > 0$ and $m_3 > \frac{m_2^2}{m_1}$, is an asymptotically stabilizing controller for the IWP (3.27) at its unstable equilibrium point $q_e = 0$.* ■

**Proof of Corollary 3.12:** The proof can be established by verifying that $V_d$ satisfies the Conditions 3.1 and 3.2, and $M_d$ is positive definite and symmetric, thus, $H_d$ qualifies as a Lyapunov function. Moreover, asymptotic stability is proved invoking LaSalle's invariance principle (see the proof of Corollary 4.2). ■

### 3.4.3 Simulation results

Some simulation results are obtained by applying the controller (3.31), (3.33) to the inertia wheel pendulum model. In all simulations, the initial condition $[q_0,\ p_0] = [\pi, 0, 0, 0.05]$, i.e. the pendulum vertical downward position, is used. The parameters and gains for the stabilizing IDA-PBC controller are $m_1 = 0.7$, $m_3 = 3.48$ and $\epsilon = 1$.

Figure 3.2 shows the response of the system for different values of $K_p$ (with $K_v = 2 \times 10^{-5}$). Their corresponding control inputs are shown in Figure 3.3. As shown, the pendulum asymptotically converges toward its upward position, from a point close to its downward position, i.e. 'almost' global stabilization. Observe that the states converge faster for small $K_p$, while high-gain controller causes more oscillations.

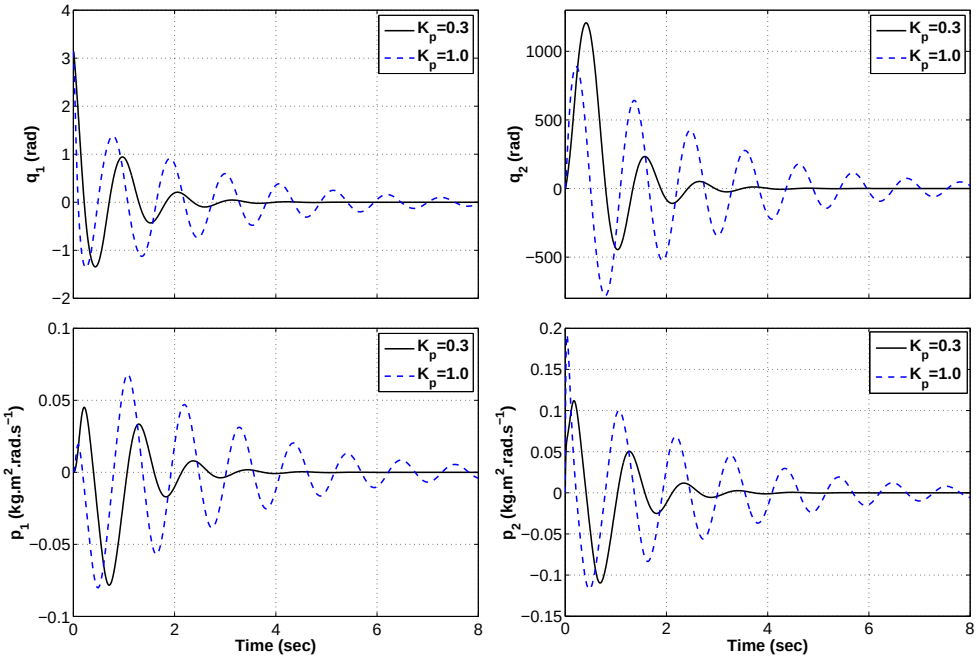


Figure 3.2: State histories of the IWP for different values of $K_p$.

Figures 3.4 and 3.5 illustrate the effect of varying the damping gain $K_v$ for a constant $K_p = 0.3$. As expected, increasing this damping gain leads to achieving faster convergence with less oscillations.

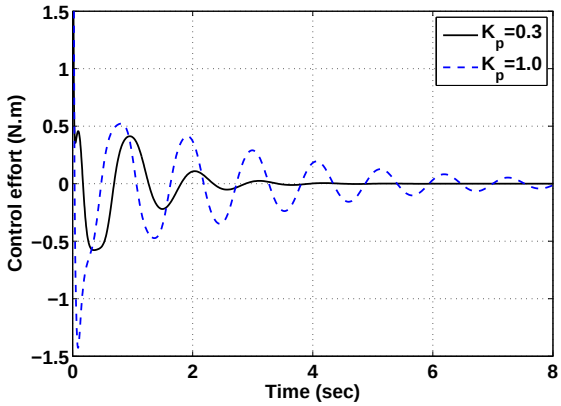


Figure 3.3: Control torque of the IWP for different values of $K_p$.

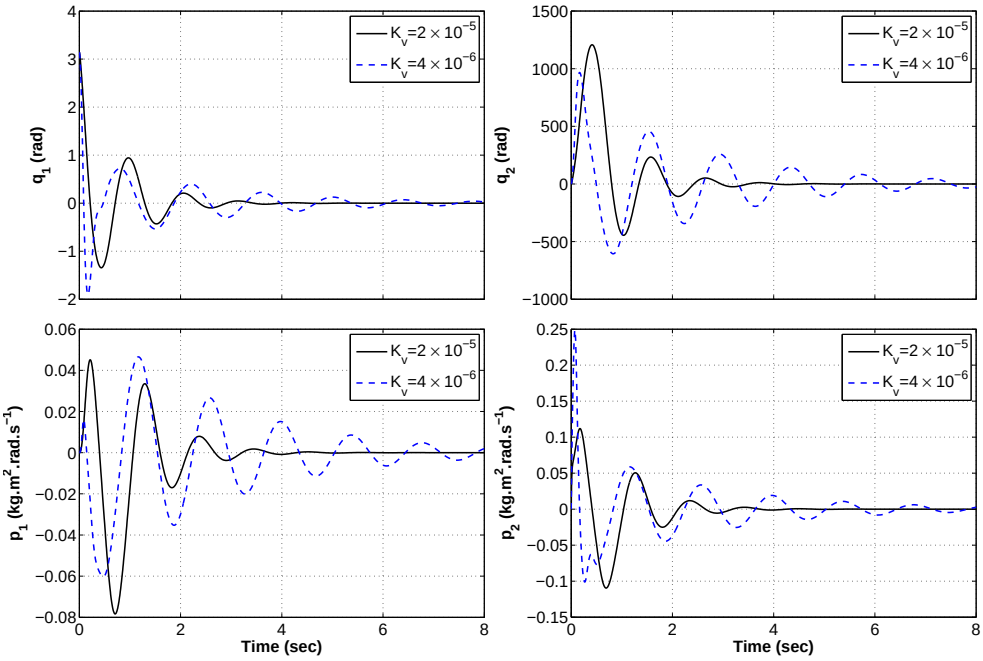


Figure 3.4: State histories of the IWP for different values of $K_v$.

## 3.5 Conclusion

In this chapter we have developed a method to simplify the partial differential equations associated with the potential energy for interconnection and damping assignment passivity based control for a class of underactuated mechanical systems. Solving the PDEs, also called the matching equations, is the main difficulty in the construction and application of the IDA-PBC. The proposed methods in the literature have so far focused on using the (partially) linearized models, and/or imposing some conditions to simplify and solve these PDEs, limiting their applicability. We have proposed a simplification to the potential energy PDEs through a particular parametrization of the closed-loop inertia matrix that appears as a coupling term with the inverse of the original inertia

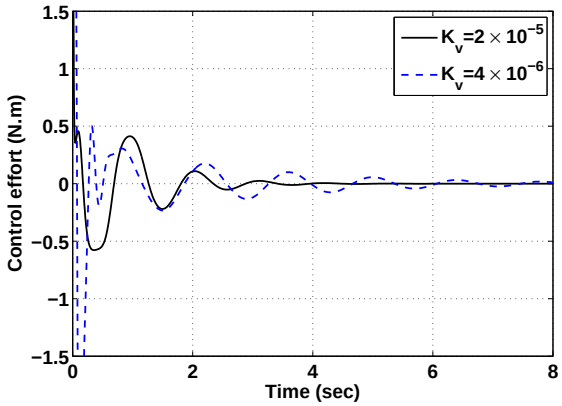


Figure 3.5: Control torque of the IWP for different values of $K_v$.

matrix. This parametrization accounts for kinetic energy shaping, which is then used to simplify the potential energy PDEs the solution of which accounts for potential energy shaping. Thus, leading to a new underactuated mechanical system with a totally modified energy function. This approach avoids the cancellation of nonlinearities, and extends the applicability of this method to a larger class of systems, including separable and non-separable PCH systems. The proposed scheme has been tested via simulations on the inertia wheel pendulum which belongs to the family of separable PCH systems. The simulation results have shown the effectiveness of the proposed approach.

In Chapter 4 we apply this approach to more complicated systems: non-separable PCH systems, the rotary inverted pendulum. The stability and performance of this system using the proposed approach are demonstrated through stability analysis and numerical simulations. Moreover, experimental validation of this scheme is presented in Chapter 7.

# Chapter 4

# IDA-PBC of the Rotary Inverted Pendulum

## 4.1 Introduction

In this chapter we show the effectiveness of our proposed method applied to a more complex structure of UMSs, the non-separable systems, using a rotary inverted pendulum as an illustrative example. We show that this technique reduces the design complexity, while at the same time preserves the effectiveness of the IDA-PBC design to asymptotically stabilize this pendulum at its upright position.

The control problem of a rotary inverted pendulum has been classically solved via switching between two controllers. The first controller swings the pendulum up, close to its upright position from its downward position, and is usually designed using energy based techniques [11]. At this point, the second, a balancing controller often a linear control is applied to stabilize the pendulum at the desired upright position. Some energy based methods to control this system have been proposed in the literature such as a swing-up control law for general pendulum-like systems [11], energy-based controller involving passivity to enforce the system to converge to its homoclinic orbit [34], and a strategy based on the controlled Lagrangian framework [60].

Two works have been reported for the control of this system within the PCH structure: in [10], a method which incorporates shaping the 'normalized' Hamiltonian function of the system and energy damping/pumping has been developed. In [111], the IDA-PBC method is adopted, and the simplification of the kinetic energy PDEs has been achieved using quasi-linearization. In this example, we apply Proposition 3.8, exploiting the full nonlinear dynamics of the rotary inverted pendulum.

## 4.2 Rotary Inverted Pendulum Model

We use the Quanser QUBE-Servo inverted pendulum module as shown in Figure 4.1. This system consists of an inverted pendulum which is attached at the end of a motor-driven horizontally-rotating arm. The pendulum is also free to rotate in a vertical plane. Thus, the system has 2-DOF: the angular position of the arm ($\alpha$) and the angular position of the pendulum ($\theta$). This system is underactuated because only the arm is subjected to an input torque (applied by a DC motor), and hence the system is 2-DOF with only one control input.


Figure 4.1: The QUBE-Servo inverted pendulum [79].

The simplified free body diagram of the mechanical part of the rotary pendulum is shown in Figure 4.2. The servo-system is used to apply a torque $\tau$ to the arm which has mass $m_r$, length $L_r$ and moment of inertia about its center of mass $J_r$. The reference frame $(x, y, z)$ is defined for the arm at point $A$ and the arm rotates positively in the counter-clock wise direction in the horizontal plane $(x_1, y_1)$ only . The pendulum attached to the arm has mass $m_p$, length $L_p$ and moment of inertia about its center of mass $J_p$. As shown in Figure 4.2, the center of mass is $\frac{L_p}{2}$. The pendulum motion is restricted in the $(x_2, y_2)$ plane only and its angle, $\alpha$, increases positively when it rotates counter-clock wise. The parameters of the rotary pendulum and the servo-system along with their physical values are listed in Tables 4.1 and 4.2, respectively.

### 4.2.1 Modeling using classical mechanics

In general, there are two methods to derive the equations of motion for mechanical systems. The first is the Lagrangian formulation where the dynamic model of the system is obtained starting from its energy. The second is the Newton-Euler formulation which is based on a balance of all forces (and torques) acting on the system. Here, we have

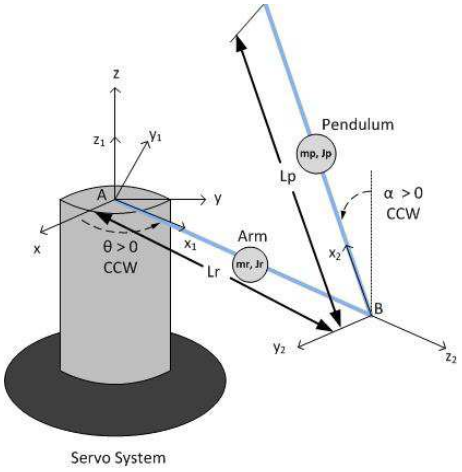


Figure 4.2: The free body diagram of the rotary pendulum system.

Table 4.1: The parameters of the rotary inverted pendulum

| **Parameter** | **Description** | **Value** | **Unit** |
|---|---|---|---|
| $m_p$ | Mass of pendulum | 0.024 | $kg$ |
| $L_p$ | Total length of pendulum | 0.129 | $m$ |
| $J_p$ | Moment of inertia of pendulum | $3.33 \times 10^{-5}$ | $kg.m^2$ |
| $m_r$ | Mass of arm | 0.095 | $kg$ |
| $L_r$ | Total length of arm | 0.085 | $m$ |
| $J_r$ | Moment of inertia of arm | $5.72 \times 10^{-5}$ | $kg.m^2$ |
| $v$ | Output Voltage range | $\pm 10$ | $volt$ |

Table 4.2: The parameters of the Servo-sytem

| **Parameter** | **Description** | **Value** | **Unit** |
|---|---|---|---|
| $\eta_g$ | Gearbox efficiency | 0.9 | - |
| $\eta_m$ | Motor efficiency | 0.69 | - |
| $K_g$ | Hign-gear total gear ration | 70 | - |
| | Low-gear total gear ration | 14 | - |
| $k_t$ | Motor current-torque constant | $7.68 \times 10^{-3}$ | N.m/A |
| $k_m$ | Motor back-emf constant | $7.68 \times 10^{-3}$ | V/(rad/s) |

adopted the *recursive*, also known as *iterative*, Newton-Euler formulation which gives some alternatives for modeling of the Furuta pendulum and to give better insight into the structure of the equations. This approach has been described in some robotics textbooks (see [22] and [94]), and has been recently presented for underactuated mechanical systems in [20].

In the recursive Newton-Euler method, a set of equations is obtained via a recursive type of solution; a *forward computation* of the positions, velocities and accelerations of the arm and pendulum, followed by a *backward computation* of the forces and moments

acting on them. We proceed with this method, by defining the geometric framework using a tensor notation.

First we define the *rotation matrix* which is used to perform a rotation in Euclidean space, and describes the position of a frame relative to another one. The rotation matrix for the arm is

$$ {}^{r}\mathbf{R}_0 = \begin{bmatrix} \cos(\theta) & -\sin(\theta) & 0 \\ \sin(\theta) & \cos(\theta) & 0 \\ 0 & 0 & 1 \end{bmatrix}, \tag{4.1} $$

and for the pendulum is the rotation matrix from the arm to the pendulum multiplied by another matrix represents the rotation of a pendulum of $(\pi/2)$ about its $z$-axis, that is

$$ \begin{aligned} {}^{p}\mathbf{R}_r &= \begin{bmatrix} \cos(\alpha) & -\sin(\alpha) & 0 \\ -\sin(\alpha) & -\cos(\alpha) & 0 \\ 0 & 0 & 1 \end{bmatrix} \begin{bmatrix} \cos(\pi/2) & 0 & \sin(\pi/2) \\ 0 & 1 & 0 \\ -\sin(\pi/2) & 0 & \cos(\pi/2) \end{bmatrix} \\ &= \begin{bmatrix} \cos(\alpha) & -\sin(\alpha) & 0 \\ -\sin(\alpha) & -\cos(\alpha) & 0 \\ 0 & 0 & 1 \end{bmatrix} \begin{bmatrix} 0 & 0 & 1 \\ 0 & 1 & 0 \\ -1 & 0 & 0 \end{bmatrix} = \begin{bmatrix} 0 & -\sin(\alpha) & \cos(\alpha) \\ 0 & -\cos(\alpha) & -\sin(\alpha) \\ -1 & 0 & 0 \end{bmatrix}, \end{aligned} \tag{4.2} $$

where the indices 0, $r$ and $p$ refer to the origin of the reference, arm and pendulum frames respectively.

**A) Forward computation**

We first compute the angular velocity $(w)$, angular acceleration $(\dot{w})$, linear velocity $(v)$, and linear acceleration $(\dot{v})$ of each link in terms of the proceeding link. Let the initial conditions for the reference (base) frame be $w_0 = \dot{w}_0 = 0$ and $v_0 = \dot{v}_0 = 0$.

*Angular velocity*

The "propagation" of angular velocity from link $i$ to link $i-1$ is given by

$$ {}^{i}w_i = {}^{i}\mathbf{R}_{i-1}({}^{i-1}w_{i-1}) + {}^{i-1}z_{i-1}\dot{\vartheta}_i, \tag{4.3} $$

where ${}^{i-1}z_{i-1}\dot{\vartheta}_i$ is the angular velocity of link $i$ relative to link $i-1$, ${}^{i-1}z_{i-1}$ is a unit vector pointing along the $i$th joint axis, and $\vartheta$ is the angle of rotation ($\alpha$ or $\theta$ in our case). Hence, the angular velocity of the arm is

$$ w_r = \begin{bmatrix} \cos(\theta) & -\sin(\theta) & 0 \\ \sin(\theta) & \cos(\theta) & 0 \\ 0 & 0 & 1 \end{bmatrix} \begin{bmatrix} 0 \\ 0 \\ 0 \end{bmatrix} + \begin{bmatrix} 0 \\ 0 \\ 1 \end{bmatrix} \dot{\theta} = \begin{bmatrix} 0 \\ 0 \\ \dot{\theta} \end{bmatrix}, \tag{4.4} $$

and of the pendulum is

$$w_p = \begin{bmatrix} 0 & -\sin(\alpha) & \cos(\alpha) \\ 0 & -\cos(\alpha) & -\sin(\alpha) \\ -1 & 0 & 0 \end{bmatrix} \begin{bmatrix} 0 \\ 0 \\ \dot{\theta} \end{bmatrix} + \begin{bmatrix} 0 \\ 0 \\ 1 \end{bmatrix} \dot{\alpha} = \begin{bmatrix} \cos(\alpha)\dot{\theta} \\ -\sin(\alpha)\dot{\theta} \\ \dot{\alpha} \end{bmatrix}. \tag{4.5}$$

*Angular acceleration*

The angular acceleration is obtained by differentiating (4.3) with respect to time

$${}^{i}\dot{w}_i = {}^{i}\mathbf{R}_{i-1}({}^{i-1}\dot{w}_{i-1}) + {}^{i}\mathbf{R}_{i-1}({}^{i-1}w_{i-1}) \times {}^{i-1}z_{i-1}\dot{\vartheta}_i + {}^{i-1}z_{i-1}\ddot{\vartheta}_i, \tag{4.6}$$

where $(\times)$ denotes the cross product. Hence, the angular velocity of the arm is

$$\dot{w}_r = \begin{bmatrix} \cos(\theta) & -\sin(\theta) & 0 \\ \sin(\theta) & \cos(\theta) & 0 \\ 0 & 0 & 1 \end{bmatrix} \begin{bmatrix} 0 \\ 0 \\ 0 \end{bmatrix} + \begin{bmatrix} \cos(\theta) & -\sin(\theta) & 0 \\ \sin(\theta) & \cos(\theta) & 0 \\ 0 & 0 & 1 \end{bmatrix} \begin{bmatrix} 0 \\ 0 \\ 0 \end{bmatrix} \times \begin{bmatrix} 0 \\ 0 \\ \dot{\theta} \end{bmatrix} + \begin{bmatrix} 0 \\ 0 \\ \ddot{\theta} \end{bmatrix} = \begin{bmatrix} 0 \\ 0 \\ \ddot{\theta} \end{bmatrix}, \tag{4.7}$$

and of the pendulum is

$$\begin{aligned} \dot{w}_p &= \begin{bmatrix} 0 & -\sin(\alpha) & \cos(\alpha) \\ 0 & -\cos(\alpha) & -\sin(\alpha) \\ -1 & 0 & 0 \end{bmatrix} \begin{bmatrix} 0 \\ 0 \\ \ddot{\theta} \end{bmatrix} + \begin{bmatrix} 0 & -\sin(\alpha) & \cos(\alpha) \\ 0 & -\cos(\alpha) & -\sin(\alpha) \\ -1 & 0 & 0 \end{bmatrix} \begin{bmatrix} 0 \\ 0 \\ \dot{\theta} \end{bmatrix} \times \begin{bmatrix} 0 \\ 0 \\ \dot{\alpha} \end{bmatrix} + \begin{bmatrix} 0 \\ 0 \\ \ddot{\alpha} \end{bmatrix} \\ &= \begin{bmatrix} \cos(\alpha)\ddot{\theta} - \sin(\alpha)\dot{\theta}\dot{\alpha} \\ -\sin(\alpha)\ddot{\theta} - \cos(\alpha)\dot{\theta}\dot{\alpha} \\ \ddot{\alpha} \end{bmatrix}. \end{aligned} \tag{4.8}$$

*Linear velocity*

The linear velocity of each link is obtained by

$${}^{i}v_i = {}^{i}\mathbf{R}_{i-1}({}^{i-1}v_{i-1} + {}^{i-1}w_{i-1} \times {}^{i}r_i), \tag{4.9}$$

where ${}^{i}r_i$ is the position vector of the origin of the $i$-th link frame with respect to the $(i-1)$-th link frame. Then, the linear velocity of the arm is

$$v_r = \begin{bmatrix} \cos(\theta) & -\sin(\theta) & 0 \\ \sin(\theta) & \cos(\theta) & 0 \\ 0 & 0 & 1 \end{bmatrix} \begin{bmatrix} 0 \\ 0 \\ 0 \end{bmatrix} + \begin{bmatrix} 0 \\ 0 \\ 0 \end{bmatrix} \times \begin{bmatrix} 0 \\ 0 \\ 0 \end{bmatrix} = \begin{bmatrix} 0 \\ 0 \\ 0 \end{bmatrix}, \tag{4.10}$$

and of the pendulum is

$$v_p = \begin{bmatrix} 0 & -\sin(\alpha) & \cos(\alpha) \\ 0 & -\cos(\alpha) & -\sin(\alpha) \\ -1 & 0 & 0 \end{bmatrix} \left( \begin{bmatrix} 0 \\ 0 \\ 0 \end{bmatrix} + \begin{bmatrix} 0 \\ 0 \\ \dot{\theta} \end{bmatrix} \times \begin{bmatrix} L_r \\ 0 \\ 0 \end{bmatrix} \right) = \begin{bmatrix} -L_r \sin(\alpha)\dot{\theta} \\ -L_r \cos(\alpha)\dot{\theta} \\ 0 \end{bmatrix}. \tag{4.11}$$

*Linear acceleration*

The linear acceleration is obtained by differentiating (4.9) with respect to time

$$ {}^{i}\dot{v}_i = {}^{i}\mathbf{R}_{i-1}({}^{i-1}\dot{v}_{i-1} + {}^{i-1}\dot{w}_{i-1} \times {}^{i}r_i + {}^{i-1}w_{i-1} \times ({}^{i-1}w_{i-1} \times {}^{i}r_i)), \tag{4.12} $$

where the first term is the acceleration exerted on a link by its neighbours, the second term is the centripetal acceleration and the last term is the rotational acceleration. The linear acceleration of the arm is (note that $v_r = 0$)

$$ \dot{v}_r = \begin{bmatrix} 0 & 0 & 0 \end{bmatrix}^\top, \tag{4.13} $$

and for the pendulum is

$$ \begin{aligned} \dot{v}_p &= \begin{bmatrix} 0 & -\sin(\alpha) & \cos(\alpha) \\ 0 & -\cos(\alpha) & -\sin(\alpha) \\ -1 & 0 & 0 \end{bmatrix} \left( \begin{bmatrix} 0 \\ 0 \\ 0 \end{bmatrix} + \begin{bmatrix} 0 \\ 0 \\ \ddot{\theta} \end{bmatrix} \times \begin{bmatrix} L_r \\ 0 \\ 0 \end{bmatrix} + \begin{bmatrix} 0 \\ 0 \\ \dot{\theta} \end{bmatrix} \times \left( \begin{bmatrix} 0 \\ 0 \\ \dot{\theta} \end{bmatrix} \times \begin{bmatrix} L_r \\ 0 \\ 0 \end{bmatrix} \right) \right) \\ &= \begin{bmatrix} -L_r \sin(\alpha)\ddot{\theta} \\ -L_r \cos(\alpha)\ddot{\theta} \\ L_r \dot{\theta}^2 \end{bmatrix}. \end{aligned} \tag{4.14} $$

*Acceleration of gravity*

The linear acceleration acting on a link due to gravity is given by

$$ {}^{i}g = {}^{i}\mathbf{R}_{i-1}({}^{i-1}g), \tag{4.15} $$

and computed for the arm as

$$ g_r = \begin{bmatrix} \cos(\theta) & -\sin(\theta) & 0 \\ \sin(\theta) & \cos(\theta) & 0 \\ 0 & 0 & 1 \end{bmatrix} \begin{bmatrix} 0 \\ 0 \\ g \end{bmatrix} = \begin{bmatrix} 0 \\ 0 \\ g \end{bmatrix} \tag{4.16} $$

and for the pendulum as

$$ g_p = \begin{bmatrix} 0 & -\sin(\alpha) & \cos(\alpha) \\ 0 & -\cos(\alpha) & -\sin(\alpha) \\ -1 & 0 & 0 \end{bmatrix} \begin{bmatrix} 0 \\ 0 \\ g \end{bmatrix} = \begin{bmatrix} g\cos(\alpha) \\ -g\sin(\alpha) \\ 0 \end{bmatrix}. \tag{4.17} $$

*Linear acceleration of the centre of mass*

The linear acceleration of the centre of mass for each link is computed by applying

$$ {}^{i}\dot{v}_{ci} = {}^{i}\dot{v}_i + {}^{i}\dot{w}_i \times {}^{i}r_{ci} + {}^{i}w_i \times ({}^{i}w_i \times {}^{i}r_{ci}) + {}^{i}g, \tag{4.18} $$

which can be written for the arm as

$$\dot{v}_{cr} = \begin{bmatrix}0\\0\\0\end{bmatrix} + \begin{bmatrix}0\\0\\\ddot{\theta}\end{bmatrix} \times \begin{bmatrix}\frac{1}{2}L_r\\0\\0\end{bmatrix} + \begin{bmatrix}0\\0\\\dot{\theta}\end{bmatrix} \times \left( \begin{bmatrix}0\\0\\\dot{\theta}\end{bmatrix} \times \begin{bmatrix}\frac{1}{2}L_r\\0\\0\end{bmatrix} \right) + \begin{bmatrix}0\\0\\g\end{bmatrix} = \begin{bmatrix}-\frac{1}{2}L_r\dot{\theta}^2\\\frac{1}{2}L_r\ddot{\theta}\\g\end{bmatrix}, \quad (4.19)$$

and for the pendulum as

$$\begin{aligned}\dot{v}_{cp} &= \begin{bmatrix}-L_r\sin(\alpha)\ddot{\theta}\\-L_r\cos(\alpha)\ddot{\theta}\\L_r\dot{\theta}^2\end{bmatrix} + \begin{bmatrix}\cos(\alpha)\ddot{\theta} - \sin(\alpha)\dot{\theta}\dot{\alpha}\\-\sin(\alpha)\ddot{\theta} - \cos(\alpha)\dot{\theta}\dot{\alpha}\\\ddot{\alpha}\end{bmatrix} \times \begin{bmatrix}\frac{1}{2}L_p\\0\\0\end{bmatrix} \\ &\quad + \begin{bmatrix}\cos(\alpha)\dot{\theta}\\-\sin(\alpha)\dot{\theta}\\\dot{\alpha}\end{bmatrix} \times \left( \begin{bmatrix}\cos(\alpha)\dot{\theta}\\-\sin(\alpha)\dot{\theta}\\\dot{\alpha}\end{bmatrix} \times \begin{bmatrix}\frac{1}{2}L_p\\0\\0\end{bmatrix} \right) + \begin{bmatrix}g\cos(\alpha)\\-g\sin(\alpha)\\0\end{bmatrix} \\ &= \begin{bmatrix}-L_r\sin(\alpha)\ddot{\theta} - \frac{1}{2}L_p\sin^2(\alpha)\dot{\theta}^2 - \frac{1}{2}L_p\dot{\alpha}^2 + g\cos(\alpha)\\-L_r\cos(\alpha)\ddot{\theta} + \frac{1}{2}L_p\ddot{\alpha} - \frac{1}{2}L_p\sin(\alpha)\cos(\alpha)\dot{\theta}^2 - g\sin(\alpha)\\L_r\dot{\theta}^2 + \frac{1}{2}L_p\sin(\alpha)\ddot{\theta} + L_p\cos(\alpha)\dot{\theta}\dot{\alpha}\end{bmatrix}. \end{aligned} \quad (4.20)$$

The index $c$ refers to the center of mass, i.e. ${}^{i}r_{ci}$ is the position with respect to the center of mass, ${}^{i}v_{ci}$ is the linear velocity with respect to the center of mass, and so on.

**B) Backward computation**

Having found the velocities and accelerations of the arm and pendulum, we can apply the following Newton-Euler equations

$${}^{i}f_i = m_i{}^{i}\dot{v}_{ci}, \quad (4.21)$$

$${}^{i}n_i = {}^{i}J_i{}^{i}\dot{w}_i + {}^{i}w_i \times ({}^{i}J_i{}^{i}w_i), \quad (4.22)$$

to compute the internal force ($f$) and moment ($n$) acting at the centre of mass of each link, where ${}^{i}J_i$ is the diagonal inertia tensor

$${}^{i}J_i = \begin{bmatrix}J_{ixx} & 0 & 0\\0 & J_{iyy} & 0\\0 & 0 & J_{izz}\end{bmatrix}. \quad (4.23)$$

In most rotary pendulums, the arm and pendulum have rotational symmetries and a relatively small cross-sectional areas, thus the inertia tensor can be approximated to

$${}^{i}J_i = \begin{bmatrix}0 & 0 & 0\\0 & J_i & 0\\0 & 0 & J_i\end{bmatrix}. \quad (4.24)$$

Next, the forces ($F$) and moments ($N$) that each link exerts on the other are computed in a backward manner and then the net forces and moments are computed by applying

$$^{i-1}F_{i,i-1} = {}^{i}f_i + {}^{i}\mathbf{R}_{i+1}\,{}^{i}F_{i+1,i}, \tag{4.25}$$

$$^{i-1}N_{i,i-1} = {}^{i}n_i + {}^{i-1}\mathbf{R}_i\,{}^{i}N_{i+1,i} + {}^{i}r_i \times ({}^{i-1}\mathbf{R}_i\,{}^{i}F_{i+1,i}) + {}^{i}r_{ci} \times {}^{i}f_{i,i-1}. \tag{4.26}$$

*Backward computation for the pendulum*

Applying equations (4.21)-(4.26) to the pendulum, we obtain the internal forces as

$$f_p = m_p\dot{v}_{cp} = m_p \begin{bmatrix} -L_r\sin(\alpha)\ddot{\theta} - \frac{1}{2}L_p\sin^2(\alpha)\dot{\theta}^2 - \frac{1}{2}L_p\dot{\alpha}^2 + g\cos(\alpha) \\ -L_r\cos(\alpha)\ddot{\theta} + \frac{1}{2}L_p\ddot{\alpha} - \frac{1}{2}L_p\sin(\alpha)\cos(\alpha)\dot{\theta}^2 - g\sin(\alpha) \\ L_r\dot{\theta}^2 + \frac{L_p}{2}\sin(\alpha)\ddot{\theta} + L_p\cos(\alpha)\dot{\theta}\dot{\alpha} \end{bmatrix}, \tag{4.27}$$

and the internal moments as

$$\begin{aligned} n_p = {} & \begin{bmatrix} 0 & 0 & 0 \\ 0 & Jp & 0 \\ 0 & 0 & Jp \end{bmatrix} \begin{bmatrix} \cos(\alpha)\ddot{\theta} - \sin(\alpha)\dot{\theta}\dot{\alpha} \\ -\sin(\alpha)\ddot{\theta} - \cos(\alpha)\dot{\theta}\dot{\alpha} \\ \ddot{\alpha} \end{bmatrix} + \begin{bmatrix} \cos(\alpha)\dot{\theta} \\ -\sin(\alpha)\dot{\theta} \\ \dot{\alpha} \end{bmatrix} \\ & \times \left( \begin{bmatrix} 0 & 0 & 0 \\ 0 & Jp & 0 \\ 0 & 0 & Jp \end{bmatrix} \begin{bmatrix} \cos(\alpha)\dot{\theta} \\ -\sin(\alpha)\dot{\theta} \\ \dot{\alpha} \end{bmatrix} \right) = \begin{bmatrix} 0 \\ -J_p\sin(\alpha)\ddot{\theta} - J_p\cos(\alpha)\dot{\theta}\dot{\alpha} \\ J_p\ddot{\alpha} - J_p\sin(\alpha)\cos(\alpha)\dot{\theta}^2 \end{bmatrix}. \end{aligned} \tag{4.28}$$

The net forces (including internal and external) are

$$^{r}F_{p,r} = f_p + {}^{p}\mathbf{R}_3(0) = f_p, \tag{4.29}$$

where ${}^{i}F_{i+1,i} = 0$ as the pendulum is the last link. The net moments acting on the pendulum are

$$\begin{aligned} {}^{r}N_p(x,y,z) &= n_p + {}^{r}\mathbf{R}_p(0) + \begin{bmatrix} \frac{1}{2}L_p \\ 0 \\ 0 \end{bmatrix} \times {}^{r}\mathbf{R}_p(0) + \begin{bmatrix} \frac{1}{2}L_p \\ 0 \\ 0 \end{bmatrix} \times f_p \\ &= \begin{bmatrix} 0 \\ -J_p\sin(\alpha)\ddot{\theta} - 2J_p\cos(\alpha)\dot{\theta}\dot{\alpha} \\ J_p\ddot{\alpha} - J_p\sin(\alpha)\cos(\alpha)\dot{\theta}^2 \end{bmatrix} \\ &\quad + \begin{bmatrix} 0 \\ -\frac{1}{2}mpL_pL_r\dot{\theta}^2 - \frac{1}{4}mpL_p^2\sin(\alpha)\ddot{\theta} - \frac{1}{2}mpL_p^2\cos(\alpha)\dot{\theta}\dot{\alpha} \\ \frac{1}{2}mpL_p\left(-L_r\cos(\alpha)\ddot{\theta} + \frac{1}{2}L_p\ddot{\alpha} - \frac{1}{2}L_p\sin(\alpha)\cos(\alpha)\dot{\theta}^2 - g\sin(\alpha)\right) \end{bmatrix}. \end{aligned} \tag{4.30}$$

As the expressions become too long and complicated, we write them separately as

$$
\begin{aligned}
{}^{r}N_p(x) &= 0,\\
{}^{r}N_p(y) &= -\big(J_p\sin(\alpha)+\frac{1}{4}mpL_p^2\big)\ddot{\theta}-\big(2J_p\cos(\alpha)+\frac{1}{2}mpL_p^2\cos(\alpha)\big)\dot{\theta}\dot{\alpha}-\frac{1}{2}mpL_pL_r\dot{\theta}^2,\\
{}^{r}N_p(z) &= \left(J_p+\frac{1}{4}m_pL_p^2\right)\ddot{\alpha}-\left(\frac{1}{2}mpL_pL_r\cos(\alpha)\right)\ddot{\theta}-\frac{1}{2}mpL_pg\sin(\alpha)\\
&\quad-\left(J_p\sin(\alpha)\cos\alpha+\frac{1}{4}m_pL_p^2\sin(\alpha)\cos(\alpha)\right)\dot{\theta}^2.
\end{aligned}
$$

*Backward computation for the arm*

We also apply equations (4.21)-(4.26) to the arm, thus obtaining the internal forces and moments as

$$
f_r = m_r\dot{v}_{cr} = \begin{bmatrix} -\frac{1}{2}m_rL_r\dot{\theta}^2 \\ \frac{1}{2}m_rL_r\ddot{\theta} \\ m_rg \end{bmatrix}, \tag{4.31}
$$

$$
n_r = \begin{bmatrix} 0 & 0 & 0 \\ 0 & Jr & 0 \\ 0 & 0 & Jr \end{bmatrix}\begin{bmatrix} 0 \\ 0 \\ \ddot{\theta} \end{bmatrix} + \begin{bmatrix} 0 \\ 0 \\ \dot{\theta} \end{bmatrix} \times \left( \begin{bmatrix} 0 & 0 & 0 \\ 0 & Jr & 0 \\ 0 & 0 & Jr \end{bmatrix}\begin{bmatrix} 0 \\ 0 \\ \dot{\theta} \end{bmatrix} \right) = \begin{bmatrix} 0 \\ 0 \\ J_r\ddot{\theta} \end{bmatrix}. \tag{4.32}
$$

The net forces and moments are computed as

$$
\begin{aligned}
{}^{0}F_{r,0} &= f_r + {}^{r}\mathbf{R}_p\,{}^{r}F_{p,r}\\
&= \begin{bmatrix} -\frac{1}{2}m_rL_r\dot{\theta}^2 \\ \frac{1}{2}m_rL_r\ddot{\theta} \\ m_rg \end{bmatrix} + \left( \begin{bmatrix} 0 & 0 & -1 \\ -\sin(\alpha) & -\cos(\alpha) & 0 \\ \cos(\alpha) & -\sin(\alpha) & 0 \end{bmatrix} \times \right.\\
&\quad \left. \begin{bmatrix} -m_pL_r\sin(\alpha)\ddot{\theta}-\frac{1}{2}m_pL_p\sin^2(\alpha)\dot{\theta}^2-\frac{1}{2}m_pL_p\dot{\alpha}^2+m_pg\cos(\alpha) \\ -m_pL_r\cos(\alpha)\ddot{\theta}+\frac{1}{2}m_pL_p\ddot{\alpha}-\frac{1}{2}m_pL_p\sin(\alpha)\cos(\alpha)\dot{\theta}^2-m_pg\sin(\alpha) \\ m_pL_r\dot{\theta}^2+\frac{1}{2}m_pL_p\sin(\alpha)\ddot{\theta}+m_pL_p\cos(\alpha)\dot{\theta}\dot{\alpha} \end{bmatrix} \right)\\
&= \begin{bmatrix} -\frac{1}{2}m_rL_r\dot{\theta}^2-m_pL_r\dot{\theta}^2-\frac{1}{2}m_pL_p\sin(\alpha)\ddot{\theta}-m_pL_p\cos(\alpha)\dot{\theta}\dot{\alpha} \\ \frac{m_rL_r}{2}\ddot{\theta}+m_pL_r\ddot{\theta}+\frac{m_pL_p}{2}(\sin^3(\alpha)\dot{\theta}^2+\sin(\alpha)\dot{\alpha}^2-\cos(\alpha)\ddot{\alpha}+\sin(\alpha)\cos^2(\alpha)\dot{\theta}^2) \\ m_rg-\frac{1}{2}m_pL_p\cos(\alpha)\dot{\alpha}^2-\frac{1}{2}m_pL_p\sin(\alpha)\ddot{\alpha}+m_pg \end{bmatrix},
\end{aligned} \tag{4.33}
$$

$$
\begin{aligned}
{}^0N_r &= n_r + \begin{bmatrix} \frac{L_r}{2} \\ 0 \\ 0 \end{bmatrix} \times f_r + {}^r\mathbf{R}_p\, {}^rN_{p,r} + \begin{bmatrix} L_r \\ 0 \\ 0 \end{bmatrix} \times {}^r\mathbf{R}_p\, {}^rF_{p,r} \\
&= \begin{bmatrix} 0 \\ 0 \\ J_r\ddot{\theta} \end{bmatrix} + \begin{bmatrix} \frac{L_r}{2} \\ 0 \\ 0 \end{bmatrix} \times \begin{bmatrix} -\frac{1}{2}m_rL_r\dot{\theta}^2 \\ \frac{1}{2}m_rL_r\ddot{\theta} \\ m_rg \end{bmatrix} + \left( \begin{bmatrix} 0 & 0 & -1 \\ -\sin(\alpha) & -\cos(\alpha) & 0 \\ \cos(\alpha) & -\sin(\alpha) & 0 \end{bmatrix} \times \right. \\
&\quad \left. \begin{bmatrix} 0 \\ -J_p\sin(\alpha)\ddot{\theta} - 2J_p\cos(\alpha)\dot{\theta}\dot{\alpha} + \frac{1}{2}mpL_p(-L_r\dot{\theta}^2 - \frac{1}{2}L_p\sin(\alpha)\ddot{\theta} - L_p\cos(\alpha)\dot{\theta}\dot{\alpha}) \\ J_p(\ddot{\alpha} - \sin(\alpha)\cos\alpha\dot{\theta}^2) + \frac{mpL_p}{2}(\frac{L_p}{2}\ddot{\alpha} - L_r\cos(\alpha)\ddot{\theta} - \frac{L_p}{2}\sin(\alpha)\cos(\alpha)\dot{\theta}^2 - g\sin(\alpha)) \end{bmatrix} \right) \\
&\quad + \begin{bmatrix} L_r \\ 0 \\ 0 \end{bmatrix} \times \left( \begin{bmatrix} 0 & 0 & -1 \\ -\sin(\alpha) & -\cos(\alpha) & 0 \\ \cos(\alpha) & -\sin(\alpha) & 0 \end{bmatrix} \right. \\
&\quad \left. \begin{bmatrix} -m_pL_r\sin(\alpha)\ddot{\theta} - \frac{1}{2}m_pL_p\sin^2(\alpha)\dot{\theta}^2 - \frac{1}{2}m_pL_p\dot{\alpha}^2 + m_pg\cos(\alpha) \\ -m_pL_r\cos(\alpha)\ddot{\theta} + \frac{1}{2}m_pL_p\ddot{\alpha} - \frac{1}{2}m_pL_p\sin(\alpha)\cos(\alpha)\dot{\theta}^2 - m_pg\sin(\alpha) \\ m_pL_r\dot{\theta}^2 + \frac{1}{2}m_pL_p\sin(\alpha)\ddot{\theta} + m_pL_p\cos(\alpha)\dot{\theta}\dot{\alpha} \end{bmatrix} \right). \quad (4.34)
\end{aligned}
$$

Here we write the elements of net moment separately (due to long expressions) as

$$
\begin{aligned}
{}^0N_r(x) &= -\left(J_p + \frac{1}{4}mpL_p^2\right)\ddot{\alpha} + \left(\frac{1}{2}mpL_pL_r\cos(\alpha)\right)\ddot{\theta} - g\sin(\alpha) \\
&\quad + \left(J_p\sin(\alpha)\cos\alpha - \frac{1}{2}L_p\sin(\alpha)\cos(\alpha)\right)\dot{\theta}^2, \\
{}^0N_r(y) &= \left(\frac{1}{2}m_pL_pL_r\sin(\alpha)\right)\ddot{\alpha} + \left(J_p\sin(\alpha)\cos(\alpha) + \frac{1}{4}m_pL_p^2\sin(\alpha)\cos(\alpha)\right)\ddot{\theta} \\
&\quad + \left(2J_p\cos^2(\alpha) + \frac{1}{4}m_pL_p^2\cos^2(\alpha)\right)\dot{\theta}\dot{\alpha} + \left(\frac{1}{2}mpL_pL_r\cos(\alpha)\right)\dot{\theta}^2 \\
&\quad + \left(\frac{1}{2}m_pL_pL_r\cos(\alpha)\right)\dot{\alpha}^2 - m_pL_rg - \frac{1}{2}m_rL_rg, \\
{}^0N_r(z) &= \left(-\frac{1}{2}m_pL_pL_r\cos(\alpha)\right)\ddot{\alpha} + \left(J_r + \frac{1}{4}m_rL_r^2 + J_p\sin^2(\alpha) + \frac{1}{4}m_pL_p^2\sin^2(\alpha) + m_pL_r^2\right)\ddot{\theta} \\
&\quad + \left(2J_p\sin(\alpha)\cos(\alpha) + \frac{1}{4}m_pL_p^2\sin(\alpha)\cos(\alpha)\right)\dot{\theta}\dot{\alpha} + (mpL_pL_r\sin(\alpha))\,\dot{\theta}^2 \\
&\quad + \left(\frac{1}{2}m_pL_pL_r\sin(\alpha)\right)\dot{\alpha}^2.
\end{aligned}
$$

**C) The equations of motion**

To obtain the equations of motion, the generalized moments at the pendulum and arm are computed by projecting the moments $({}^0N_r)$ and $({}^rN_p)$ along the joint axis. This can be expressed as

$$\tau_i = {}^{i-1}N_{i,i-1} \cdot \hat{z}_i + B_i\dot{\vartheta}_i, \quad (4.35)$$

where $(\cdot)$ denotes the dot product, and the second term of (4.35) represents the viscous force(s). By applying (4.35), we obtain the two dynamical equations as

$$
\begin{aligned}
&-\frac{1}{2}m_pL_pL_r\cos(\alpha)\ddot{\theta}+\left(J_p+\frac{1}{4}m_pL_p^2\right)\ddot{\alpha}-\frac{1}{2}m_pL_pg\sin(\alpha)\\
&-\frac{1}{4}m_pL_p^2\cos(\alpha)\sin(\alpha)\dot{\theta}^2=-B_p\dot{\alpha} \qquad (4.36)\\
&\left(J_r+m_pL_r^2+\frac{1}{4}m_rL_r^2+(J_p+\frac{1}{4}m_pL_p^2)\sin^2(\alpha)\right)\ddot{\theta}-\frac{1}{2}m_pL_pL_r\cos(\alpha)\ddot{\alpha}\\
&+\frac{1}{2}m_pL_pL_r\sin(\alpha)\dot{\alpha}^2+\frac{1}{2}m_pL_p^2\cos(\alpha)\sin(\alpha)\dot{\theta}\dot{\alpha}=\tau_r-B_r\dot{\theta}. \qquad (4.37)
\end{aligned}
$$

Note that $\tau_p = 0$ (the system is underactuated). These equations demonstrate various dynamical effects, including Centrifugal forces ($\frac{1}{2}m_pL_pL_r\sin(\alpha)\dot{\alpha}^2$), Coriolis forces ($\frac{1}{2}m_pL_p^2\cos(\alpha)\sin(\alpha)\dot{\theta}\dot{\alpha}$), Gravitational forces ($-\frac{1}{2}m_pL_pg\sin(\alpha)$), and coupling between different forces.

### 4.2.2 Port-controlled Hamiltonian model

To apply the IDA-PBC design, we need to obtain the PCH representation of the system. We define the generalized coordinate $q$ to be

$$q = \begin{bmatrix} q_1 \\ q_2 \end{bmatrix} = \begin{bmatrix} \alpha \\ \theta \end{bmatrix}, \tag{4.38}$$

and introduce the new constants (to simplify the notations)

$$\gamma = J_p + \frac{1}{4} m_p L_p^2, \quad \rho = J_r + m_p L_r^2 + \frac{1}{4} m_r L_r^2, \quad \sigma = \frac{1}{2} m_p L_p L_r, \quad \kappa = \frac{1}{2} m_p g L_p. \tag{4.39}$$

Applying Newton's Second Law for rotational motion, and by ignoring the effect of friction, from (4.36)-(4.37) we can extract the inertia matrix

$$M(q) = \begin{bmatrix} \gamma & -\sigma \cos(q_1) \\ -\sigma \cos(q_1) & \rho + \gamma \sin^2(q_1) \end{bmatrix}, \tag{4.40}$$

and also the potential energy of the system

$$V(q) = \kappa \left(1 + \cos(q_1)\right). \tag{4.41}$$

The Hamiltonian function of the system can then be obtained using (3.2). Moreover, the PCH model of the rotary pendulum can be described by (3.1) with $u = \tau$, and the input matrix

$$G = e_2 = \begin{bmatrix} 0 \\ 1 \end{bmatrix}. \tag{4.42}$$

The Hamiltonian model for general mechanical systems is

$$\dot{q} = \frac{\partial H}{\partial p}(q, p) \tag{4.43}$$

$$\dot{p} = -\frac{\partial H}{\partial q}(q, p) + \tau, \tag{4.44}$$

and hence for the rotary pendulum it is

$$\begin{aligned}
\dot{q}_1 &= \frac{1}{\Delta} \left[ (\rho + \gamma \sin^2(q_1)) p_1 + (\sigma \cos(q_1)) p_2 \right], \\
\dot{q}_2 &= \frac{1}{\Delta} \left[ (\sigma \cos(q_1)) p_1 + \gamma p_2 \right], \\
\dot{p}_1 &= \frac{1}{2\Delta^2} \left[ \left(\rho + \gamma \sin^2(q_1)\right) p_1^2 + \gamma p_2^2 + 2\sigma \cos(q_1) p_1 p_2 \right] \left( (\gamma^2 + \sigma^2) \sin(2q_1) \right) \\
&\quad + \frac{1}{2\Delta} \left[ 2\sigma \sin(q_1) p_1 p_2 - \gamma \sin(2q_1) p_1^2 \right] + \kappa \sin(q_1), \\
\dot{p}_2 &= Gu.
\end{aligned} \tag{4.45}$$

where $\Delta = \gamma\rho + \gamma^2 \sin^2(q_1) - \sigma^2 \cos^2(q_1)$ is the determinant of the matrix $M$.

### 4.2.3 Passivity of the rotary inverted pendulum

The total energy of the system is

$$H = K(q,p) + V(q) = \frac{1}{2}p^\top M^{-1}(q)p + \kappa(1+\cos(q_1)). \tag{4.46}$$

Therefore, from (4.43) and (4.44), we obtain

$$\dot{H} = \frac{\partial^\top H}{\partial q}(q,p)\dot{q} + \frac{\partial^\top H}{\partial p}(q,p)\dot{p} = \frac{\partial^\top H}{\partial p}\tau = \dot{q}^\top\tau. \tag{4.47}$$

Equation (4.47) shows the fact that the increase in energy of the system is equal to the supplied work (conservation of energy). Integrating both sides of (4.47), we obtain

$$\int_0^\top \dot{q}^\top\tau = H(t) - H(0) \geq \kappa(1+\cos(\pi)) - H(0) \geq 0 - H(0). \tag{4.48}$$

Where $\kappa$ is given in (4.39). Thus, the system is passive with the input $\tau$ and output $\dot{q}$. From equations of motion (4.36)-(4.37), notice that there are also the non-conservative forces (viscous friction) attached to the output (the velocity of the arm and pendulum) which are $B_r\dot{\theta}$ and $B_p\dot{\alpha}$. Thus, we can conclude, following Definition 2.18, that the system is output strictly passive. Note that in case of unforced system i.e. $(u = 0)$ and $q_1 \in [0, 2\pi]$, the system (4.45) has two equilibrium points; $(q_1 = \pi, \dot{q_1} = 0, q_2 = q_2^*, \dot{q_2} = 0)$, corresponds to the pendulum in downward position which is stable, while $(q_1 = 0, \dot{q_1} = 0, q_2 = q_2^*, \dot{q_2} = 0)$, corresponds to its upright position which is unstable. The total energy $H(q,\dot{q})$ of the rotary pendulum has the minimum $(H = 0)$ at the stable equilibrium point and the maximum $(H = 2\kappa)$ at the unstable equilibrium. Figure 4.3 shows the total energy of the system over the range of $q_1 \in [-\pi, \pi]$. It shows that the system has minimum energy corresponding to the stable equilibrium, and maximum energy corresponding to the unstable equilibrium. In Subsection 4.4, we will show how we can reshape the total energy function of the system such that its minimum occurs at the upright position, thus this equilibrium point is stabilized.

## 4.3 Preliminary Observations with Linear Control

One possible way to stabilize the upward equilibrium position of the rotary pendulum is to linearize the model and then apply linear control. However, by linearization, the dynamics of the system is approximated around a certain operating point and hence cannot guarantee a stable behaviour in a large region of operation. This limitation can be overcome by switching between different controllers; a swing-up controller (usually designed using energy methods) that brings the pendulum from the downward position to close to the upright position, then it switches to a balancing (stabilization) controller. In this section, we discuss a design of a linear controller for the stabilization of the

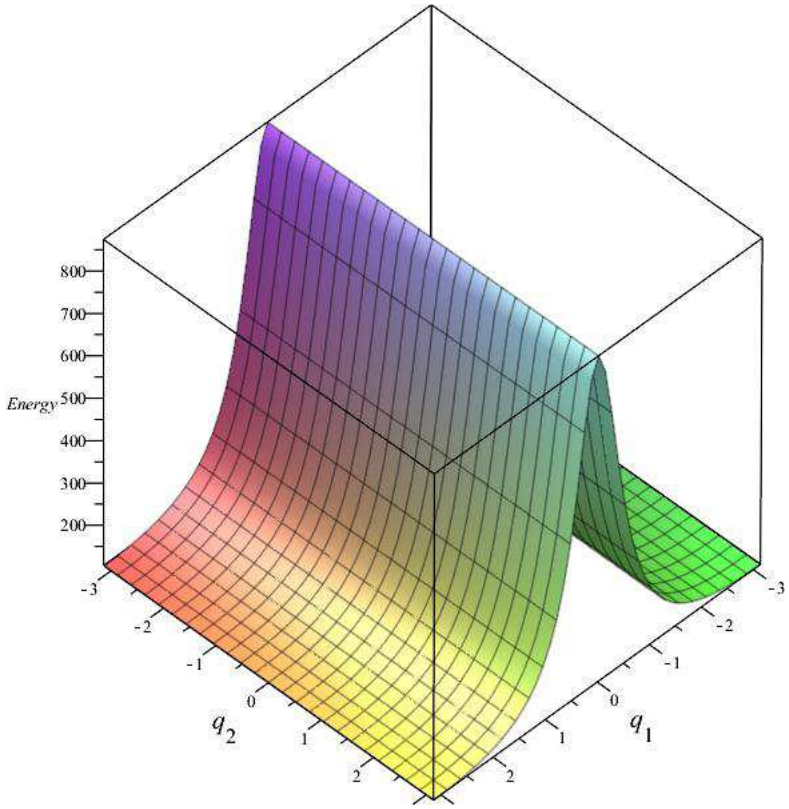


Figure 4.3: The energy of the uncontrolled inverted pendulum system.

rotary inverted pendulum, and will show the limitation of such type of controllers that motivates the design of a nonlinear controller.

### 4.3.1 Linearization

Linearizing (4.36)-(4.37) about the upright position ($\alpha = \theta = \dot{\alpha} = \dot{\theta} = 0$) using the Taylor series expansion

$$f(z) \approx f(z_0) + \left(\frac{\partial f(z)}{\partial z}\right)|_{z=z_0}\,(z - z_0),$$

the following linear equations are obtained

$$(m_p L_r^2 + J_r)\ddot{\theta} - \frac{1}{2}m_p L_r L_p \ddot{\alpha} = \tau - B_r\dot{\theta} \tag{4.49}$$

$$-\frac{1}{2}m_p L_r L_p \ddot{\theta} - \left(J_p + \frac{1}{4}m_p L_p^2\right)\ddot{\alpha} - \frac{1}{2}m_p g L_p \alpha = -B_r\dot{\alpha}. \tag{4.50}$$

Defining the state and output as

$$\mathbf{x} = \begin{bmatrix}\theta & \alpha & \dot{\theta} & \dot{\alpha}\end{bmatrix}^\top \tag{4.51}$$

$$\mathbf{y} = \begin{bmatrix}x_1 & x_2\end{bmatrix}^\top. \tag{4.52}$$

Then, the state-space representation of the complete system is obtained as

$$\begin{aligned}\dot{\mathbf{x}} &= \mathbf{A}\mathbf{x} + \mathbf{B}\mathbf{u} \\ \mathbf{y} &= \mathbf{C}\mathbf{x} + \mathbf{D}\mathbf{u},\end{aligned} \tag{4.53}$$

where

$$\mathbf{A} = \frac{1}{J_T}\begin{bmatrix} 0 & 0 & 1 & 0 \\ 0 & 0 & 0 & 1 \\ 0 & \frac{1}{4}m_p^2 L_p^2 L_r g & -\left(J_p + \frac{1}{4}m_p L_p^2\right) B_r & -\frac{1}{2}m_p L_p L_r B_p \\ 0 & \frac{1}{2}m_p L_p g(J_r + m_p L_r^2) & -\frac{1}{2}m_p L_p L_r B_r & -(J_r + m_p L_r^2)B_p \end{bmatrix} \tag{4.54}$$

$$\mathbf{B} = \frac{1}{J_T}\begin{bmatrix} 0 \\ 0 \\ J_p + \frac{1}{4}m_p L_p^2 \\ \frac{1}{2}m_p L_p L_r \end{bmatrix} \quad (J_T = J_p m_p L_r^2 + J_r J_p + \frac{1}{4}J_r m_p L_p^2) \tag{4.55}$$

$$\mathbf{C} = \begin{bmatrix} 1 & 0 & 0 & 0 \\ 0 & 1 & 0 & 0 \end{bmatrix} \tag{4.56}$$

$$\mathbf{D} = \begin{bmatrix} 0 \\ 0 \end{bmatrix}. \tag{4.57}$$

### 4.3.2 Stability analysis of the linearized model

The stability of a system can be determined by examining the location of the eigenvalues values of the transfer function (i.e. the roots of the system's characteristic equation). This characteristic equation can be expressed by $\det(\lambda\mathbf{I} - \mathbf{A}) = 0$ where $\lambda_i$ $(i = 1, \ldots, n)$ are the eigenvalues of $\mathbf{A} \in \mathbb{R}^{n\times n}$, which are also the open-loop poles, and $\mathbf{I}_n$ is the identity matrix. By substituting the values of the parameters from Tables 4.1 and 4.2 into (4.55) and (4.56), and considering the actuator dynamics, we obtain

$$\mathbf{A} = \begin{bmatrix} 0 & 0 & 1 & 0 \\ 0 & 0 & 0 & 1 \\ 0 & 81.4 & -10.25 & -0.93 \\ 0 & 122.1 & -10.33 & -1.4 \end{bmatrix} \tag{4.58}$$

$$\mathbf{B} = \begin{bmatrix} 0 & 0 & 83.47 & 80.32 \end{bmatrix}^\top. \tag{4.59}$$

Using MATLAB command eig($\mathbf{A}$), we find that the open-loop poles of the system, which are $\lambda_1 = -17.1, \lambda_2 = -2.88, \lambda_3 = 0$ and $\lambda_4 = 8.34$ shows the system unstable. Moreover, based on the state space equations of the system, the following two transfer functions corresponding to two outputs ($\theta$ and $\alpha$) can be derived as

$$\frac{\theta}{U} = \frac{83.5s^2 + 42.2s - 3654}{s^4 + 11.65s^3 - 117.4s^2 - 410.7s} \tag{4.60}$$

$$\frac{\alpha}{U} = \frac{80.3s^2 - 39s}{s^4 + 11.65s^3 - 117.4s^2 - 410.7s}, \tag{4.61}$$

and their corresponding root-locus plots are shown in Figure 4.4.

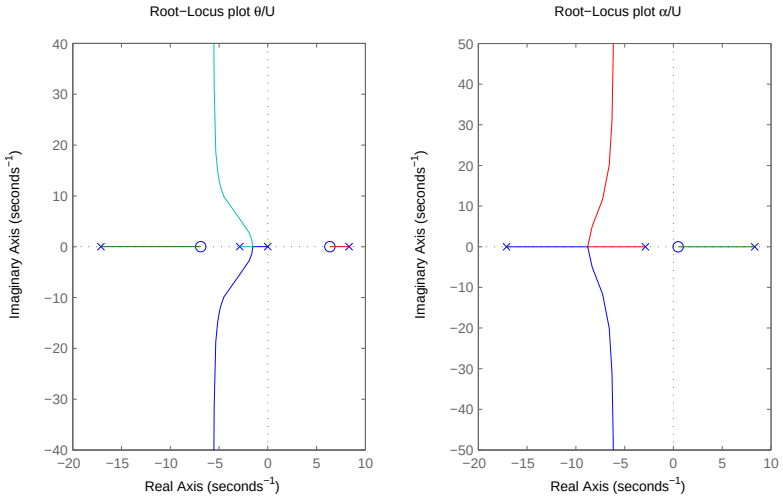


Figure 4.4: The root-locus of the open-loop system.

The analysis and root-locus plots show that there is one pole in the right-half of the s-plane, thus we can conclude that the system is unstable. In the following subsection we show how the linear control technique, namely the pole placement, is used to locally stabilize the system.

### 4.3.3 Balancing control using pole-placement

As mentioned before, when the pendulum is in a neighborhood of its unstable equilibrium point, a balancing controller is activated through a switching mechanism. The balancing controller catches the pendulum and stabilizes the system at the equilibrium position and keeps it at that position. In [4] a comparative study between some balancing controllers has been presented. Here, we discuss the design of a full state feedback regulator, also known as pole-placement. This method is based on the state model of the system and its idea is to place the poles of the closed-loop system in any desirable locations, characterizing stability and performance of the system. By placing the closed-loop poles of the plant in pre-determined locations, we can control the characteristics of the response of the system. To implement a full state feedback controller, the linearized system must be considered controllable. Thus, the first step is to check if the following

controllability condition is satisfied. A linear system is controllable if the rank of its controllability matrix

$$\mathbf{C_M} = \begin{bmatrix} \mathbf{B} & \mathbf{AB} & \mathbf{A^2B} & \cdots & \mathbf{A}^n\mathbf{B} \end{bmatrix}$$

equals the number of states $n$ [62]. The controllability matrix $\mathbf{C_M}$ for the rotary pendulum model is

$$\mathbf{C_M} = \begin{bmatrix} 0 & 83.5 & -930.7 & 16989 \\ 0 & 80.3 & -974.6 & 20780 \\ 83.5 & -930.7 & 16989 & -272898 \\ 80.3 & -974.6 & 20780 & -323519 \end{bmatrix},$$

and its rank is found, using the MATLAB command rank($\mathbf{C_M}$), equal to the number of states ($rank(\mathbf{C_M}) = n = 4$), thus the matrix is full rank, and the system is controllable.

In Subsection 4.3.2 it has been shown that the open-loop system is unstable due to the presence of one pole on the right half side of the s-plane. By placing all the closed-loop poles on the left half side of the s-plane, stability can be guaranteed. Pole-placement is an effective technique to deal with this. The aim of pole placement control is to construct a state feedback law $u = -\mathbf{Kx}$ by finding the state feedback gain matrix $\mathbf{K}$ so that all closed-loop poles are placed on the left half side of the complex plane.

Given that the system is completely controllable, the next step is to locate the desired closed-loop poles. One way of doing this is by using the root-locus design approach. The **"dominant second-order poles method"** is used to place the dominant pair which are the roots of the characteristic equation for a second order system

$$s^2 + 2\zeta\omega_n s + \omega_n^2 = 0$$

so they are expressed as

$$s_1 = -\zeta\omega_n + j\omega_n\sqrt{1-\zeta^2} \quad \text{and} \quad s_2 = -\zeta\omega_n - j\omega_n\sqrt{1-\zeta^2}.$$

These equations show the relation between the dominant poles and the natural frequency, $\omega_n$, and the damping ratio, $\zeta$. Consequently, defining the natural frequency and damping ratio of the system determine the values of the two dominant poles. The values of $\zeta$ and $\omega_n$ are defined to meet some transient-response specifications such as rise time ($t_r$), peak time ($t_p$), maximum overshoot ($M_p$) and settling time ($t_s$) which specifies the performance characteristics of a control system. The control design and time-response requirements are.

**Specification 1:** The maximum overshoot in the unit step response is 4.6%.
**Specification 2:** The settling time within 2% allowable tolerance in the unit step response is 1.43 sec.

The maximum overshoot $M_p$ is given by

$$M_p = e^{-(\zeta/\sqrt{1-\zeta^2})\pi}. \tag{4.62}$$

This value must be 4.6%. Thus,

$$0.046 = e^{-(\zeta/\sqrt{1-\zeta^2})\pi} \text{ or } 3.079 = \frac{\zeta\pi}{\sqrt{1-\zeta^2}}$$

which yields $\zeta = 0.7$. The settling time $t_s$, for the 2% allowable tolerance is given by

$$t_s = \frac{4}{\zeta\omega_n}, \tag{4.63}$$

and is specified as 1.43 sec. Thus, $\omega_n = \frac{4}{t_s\zeta} = 4 \quad \text{rad/sec}$.

Substituting $\zeta$ and $\omega_n$ into the characteristic equation and solving for the roots, we obtain the dominant pairs as $s_{1,2} = -2.8 \pm 2.8566\text{i}$. The rest of the poles are placed such that they are far to the left of the dominant closed-loop poles, i.e. can be arbitrarily chosen as long as the complex pairs dominates the response [62], and hence are chosen as $s_3 = -30$ and $s_4 = -40$.

The final step it to compute the values of the gain matrix $\mathbf{K}$. The most commonly used approach is to find these values using Ackermann's formula

$$\mathbf{K} = \begin{bmatrix} 0 & 0 & \cdots & 0 & 1 \end{bmatrix} {\mathbf{C_M}}^{-1} \phi(\mathbf{A}), \tag{4.64}$$

where $\phi(\cdot)$ is the desired characteristic equation of the closed-loop system. The controller gain for this system with the desired poles $-2.8 \pm 2.86\text{i}$, $-30$ and $-40$ is

$$\mathbf{K} = \begin{bmatrix} -5.28 & 30.14 & -2.65 & 3.55 \end{bmatrix}.$$

Hence, using the state feedback control

$$u = -\mathbf{K}\mathbf{x}, \tag{4.65}$$

we can derive two transfer functions for the closed-loop system corresponding to two outputs ($\theta$ and $\alpha$) as

$$\frac{\theta}{U} = \frac{s^4 + 77s^3 + 1684s^2 + 9887s + 27262}{s^4 + 76s^3 + 1608s^2 + 7840s + 19200} \tag{4.66}$$

$$\frac{\alpha}{U} = \frac{422s - 205}{s^4 + 76s^3 + 1608s^2 + 7840s + 19200}, \tag{4.67}$$

and their corresponding root-locus plots along with those for the open-loop system are shown in Figure 4.5. As expected, all the closed-loop poles are on the left-half side of the s-plane and the system is asymptotically stable around the equilibrium point with the

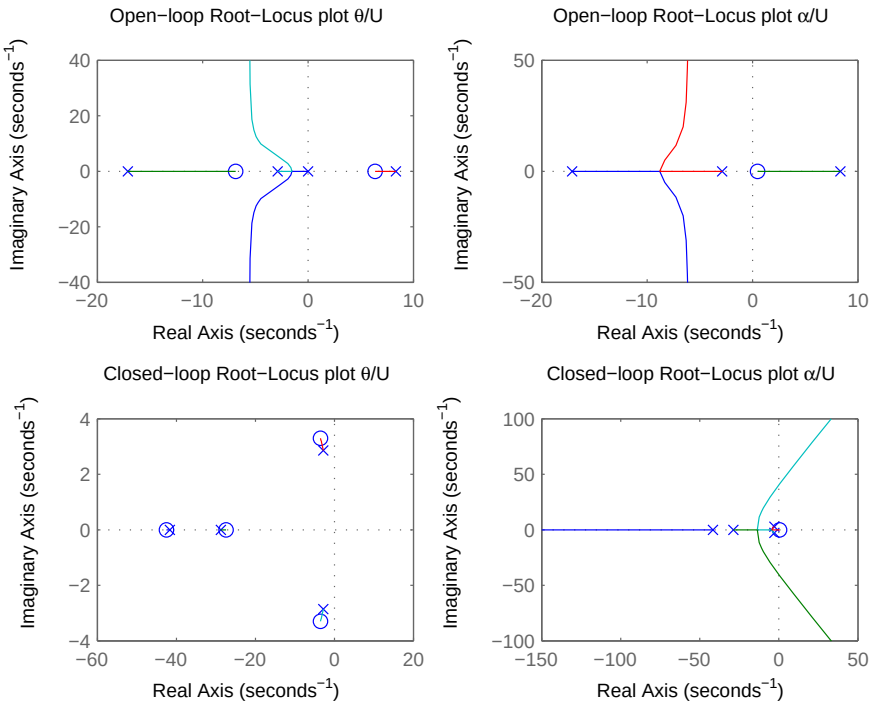


Figure 4.5: The root-locus of the open-loop and closed-loop systems.

proposed controller. Figure 4.6 shows the time response for the closed-loop system with the initial conditions $\mathbf{x}_0 = \begin{bmatrix} 0 & 0.1 & 0 & 0 \end{bmatrix}^\top$, corresponding to a starting position of the pendulum ($\approx 5.7°$) away from the upright position. It shows that the proposed balancing controller asymptotically stabilizes the rotary pendulum around it's equilibrium point with all design specifications satisfied.

### 4.3.4 Applying a linear controller on the nonlinear model

To show the range where the linear controller can be applied, we define the states as

$$\begin{bmatrix} x_1 \\ x_2 \\ x_3 \\ x_4 \end{bmatrix} = \begin{bmatrix} \theta \\ \alpha \\ \dot{\theta} \\ \dot{\alpha} \end{bmatrix}. \tag{4.68}$$

For a generalized coordinate vector $x$, the rotary inverted pendulum model can be written in the matrix form

$$D(x)\ddot{x} + C(x, \dot{x})\dot{x} + g(x) = \tau, \tag{4.69}$$

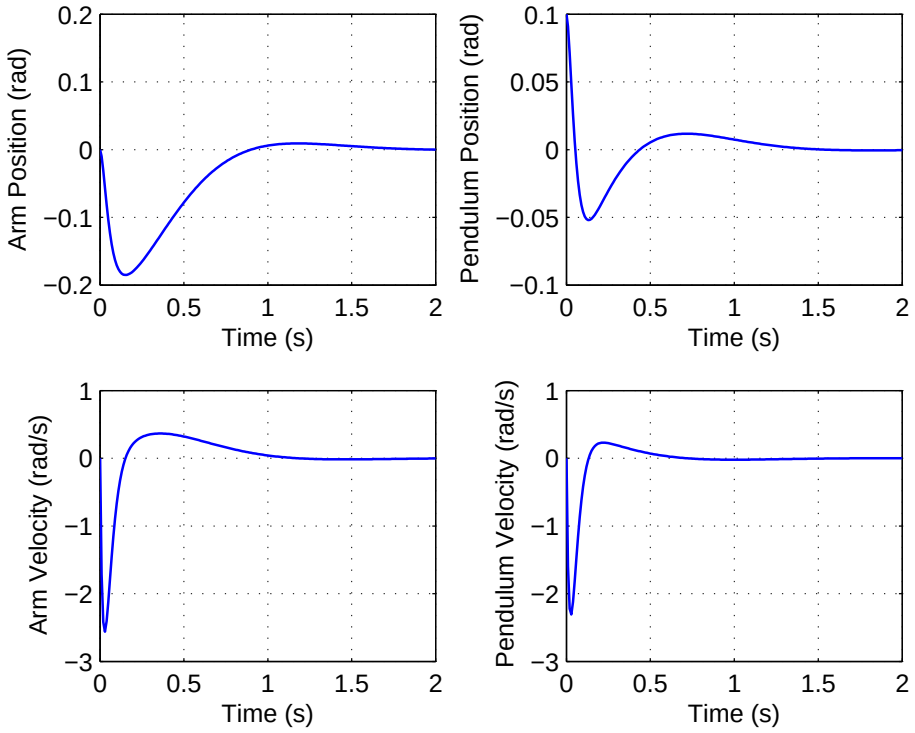


Figure 4.6: State histories of the closed-loop system with $x_0 = [0, 0.1, 0, 0]$.

where $D$ is the inertia matrix, $C$ is the damping matrix, $g$ is the gravitational vector, and $\tau$ is the applied torque vector, as

$$\begin{bmatrix} \rho + \gamma \sin^2(x_2) & -\sigma \cos(x_2) \\ -\sigma \cos(x_2) & \gamma \end{bmatrix} \begin{bmatrix} \ddot{x}_1 \\ \ddot{x}_2 \end{bmatrix} + \begin{bmatrix} \gamma \sin 2(x_2)\dot{x}_2 + B_r & \sigma \sin(x_2)\dot{x}_2 \\ -\frac{1}{2}\gamma \sin 2(x_2)\dot{x}_1 & B_p \end{bmatrix} \begin{bmatrix} \dot{x}_1 \\ \dot{x}_2 \end{bmatrix} + \begin{bmatrix} -\kappa \sin(x_2) \\ 0 \end{bmatrix} = \begin{bmatrix} 0 \\ \tau \end{bmatrix}.$$

Solving for the acceleration terms in the equations of motion, yields:

$$\begin{bmatrix} \ddot{x}_1 \\ \ddot{x}_2 \end{bmatrix} = \begin{bmatrix} \rho + \gamma \sin^2(x_2) & -\sigma \cos(x_2) \\ -\sigma \cos(x_2) & \gamma \end{bmatrix}^{-1} \left( \begin{bmatrix} \gamma \sin 2(x_2)\dot{x}_2 + B_r & \sigma \sin(x_2)\dot{x}_2 \\ -\frac{1}{2}\gamma \sin 2(x_2)\dot{x}_1 & B_p \end{bmatrix} \begin{bmatrix} \dot{x}_1 \\ \dot{x}_2 \end{bmatrix} + \begin{bmatrix} -\kappa \sin(x_2) \\ 0 \end{bmatrix} - \begin{bmatrix} 0 \\ \tau \end{bmatrix} \right). \tag{4.70}$$

by carrying out the matrix multiplication in (4.70), the first and second equations (after expanding the equations and collecting common terms) become

$$\ddot{x}_1 = \frac{1}{\Delta_D} \left( -\frac{1}{2}\gamma\sigma \cos(x_2) \sin 2(x_2)\dot{x}_1^2 + \gamma\sigma \sin(x_2)\dot{x}_2^2 + \gamma^2 \sin 2(x_2)\dot{x}_1\dot{x}_2 + \gamma B_r \dot{x}_1 + B_p\sigma \cos(x_2)\dot{x}_2 - \gamma\kappa \sin(x_2) - \tau\sigma \cos(x_2) \right),$$

$$\ddot{x}_2 = \frac{1}{\Delta_D}\Big(-\frac{1}{2}\gamma \sin 2(x_2)\left(\rho + \gamma \sin^2(x_2)\right)\dot{x}_1^2 + \sigma^2 \cos(x_2)\sin(x_2)\dot{x}_2^2 + B_r\sigma\cos(x_2)\dot{x}_1 \\ +\gamma\sigma\cos(x_2)\sin 2(x_2)\dot{x}_1\dot{x}_2 + B_p\left(\rho + \gamma\sin^2(x_2)\right)\dot{x}_2 \\ -\sigma\kappa\cos(x_2)\sin(x_2) - \tau\left(\rho + \gamma\sin^2(x_2)\right)\Big),$$

where $\Delta_D = \gamma\rho + \gamma^2\sin^2(q_1) - \sigma^2\cos^2(q_1)$ is the determinant of the matrix $D$. From (4.68), it is given that $\dot{x}_1 = x_3$ and $\dot{x}_2 = x_4$. Thus, the equations of motion is obtained as

$$\begin{aligned}
\dot{x}_1 &= x_3 \\
\dot{x}_2 &= x_4 \\
\dot{x}_3 &= \frac{1}{\Delta_D}\Big(-\frac{1}{2}\gamma\sigma\cos(x_2)\sin 2(x_2)x_3^2 + \gamma\sigma\sin(x_2)x_4^2 + \gamma^2\sin 2(x_2)x_3x_4 + \gamma B_r x_3 \\
&\quad + B_p\sigma\cos(x_2)x_4 - \gamma\kappa\sin(x_2) - \tau\sigma\cos(x_2)\Big) \qquad (4.71) \\
\dot{x}_4 &= \frac{1}{\Delta_D}\Big(-\frac{1}{2}\gamma\sin 2(x_2)\left(\rho + \gamma\sin^2(x_2)\right)x_3^2 + \sigma^2\cos(x_2)\sin(x_2)x_4^2 + B_r\sigma\cos(x_2)x_3 \\
&\quad + \gamma\sigma\cos(x_2)\sin 2(x_2)x_3x_4 + B_p\left(\rho + \gamma\sin^2(x_2)\right)x_4 - \sigma\kappa\cos(x_2)\sin(x_2) \\
&\quad - \tau\left(\rho + \gamma\sin^2(x_2)\right)\Big).
\end{aligned}$$

Figure 4.7 shows the response of the actual system to the pole placement controller. It shows that this controller can stabilize the equilibrium of system starting very close to the upright position (up to 20 degrees away from that position). It also shows that starting from a slightly distanced point (25 degrees) the system becomes unstable, this means that the proposed linear controller can only guarantee a local stability. This motivates us to design a nonlinear controller to expand the domain of attraction and so the pendulum can swing up from any position in the plane, achieving 'almost' global stability.

## 4.4 IDA-PBC Control Design

Moving back to the IDA-BPC design, we apply the procedure given in Section 3.3, in particular Proposition 3.8, to design the controller for the system. The main objective is to asymptotically stabilize the rotary inverted pendulum at its unstable equilibrium point $q_e = (0, q_2)$ for any $q_2 \in [0, 2\pi]$. First we design the energy shaping controller $u_{es}$ and then adding the damping to the closed-loop system by designing the damping injection controller $u_{di}$.

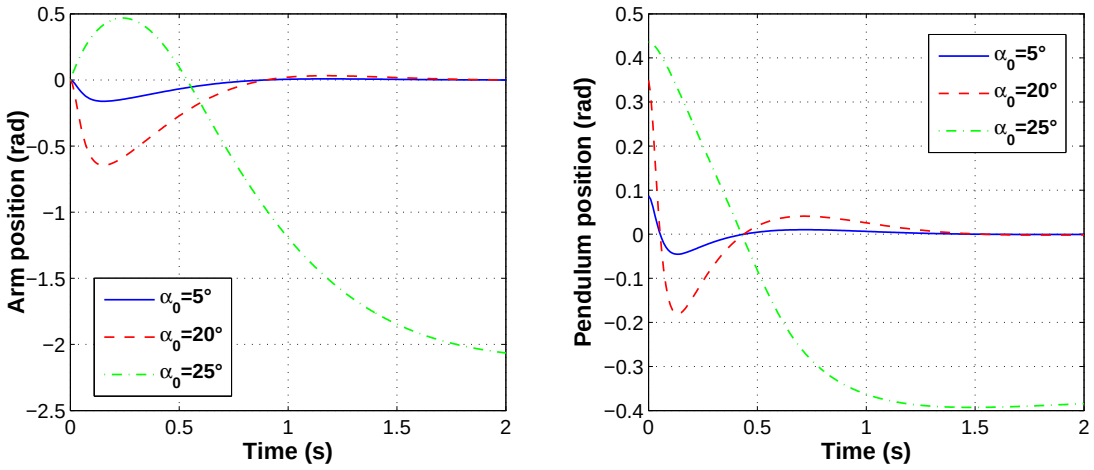


Figure 4.7: State histories of the closed-loop system with various initial conditions.

### 4.4.1 Reshaping the total energy

We start with parametrizing the inertia matrix $M_d$, then solve the PDE of the potential energy. From (4.40), we obtain the inverse inertia matrix

$$M^{-1}(q) = \frac{1}{\Delta}\begin{bmatrix} \rho + \gamma \sin^2(q_1) & \sigma \cos(q_1) \\ \sigma \cos(q_1) & \gamma \end{bmatrix}, \tag{4.72}$$

where $\Delta = \det(M) = \gamma\rho + \gamma^2 \sin^2(q_1) - \sigma^2 \cos^2(q_1)$. Because $M$ depends on $q_1$, it is clear that $M^{-1}$ does not have a simple structure. Solving directly the PDEs (3.8)-(3.9) incurs a high computational load, that leads to an unreasonable form of the controller.

Applying Proposition 3.8, with $G^\perp = [1\ 0]$, the potential energy PDE (3.9) is

$$\begin{bmatrix} 1 & 0 \end{bmatrix} \left\{ \begin{bmatrix} -\kappa \sin(q_1) \\ 0 \end{bmatrix} - \begin{bmatrix} \Delta m_1(q_1) & \Delta m_2(q_1) \\ \Delta m_2(q_1) & \Delta m_3(q_1) \end{bmatrix} \begin{bmatrix} \frac{\rho+\gamma \sin^2(q_1)}{\Delta} & \frac{\sigma \cos(q_1)}{\Delta} \\ \frac{\sigma \cos(q_1)}{\Delta} & \frac{\gamma}{\Delta} \end{bmatrix} \begin{bmatrix} \nabla_{q_1} V_d \\ \nabla_{q_2} V_d \end{bmatrix} \right\} = 0,$$

which further gives

$$\left( \rho + \gamma \sin^2(q_1) - \frac{\sigma^2 \cos^2(q_1)}{\gamma} \right) \nabla_{q_1} V_d = \frac{-\kappa \sin(q_1)}{m_1},$$

that can be written in its simplest form

$$\nabla_{q_1} V_d = -\frac{\gamma \kappa \sin(q_1)}{m_1 \Delta}, \tag{4.73}$$

by choosing $m_2 = \frac{k_2}{k_1} m_1$, and including $\Delta$ in the expression of $M_d$. The solution for the PDE (4.73) is given by

$$V_d(q) = -\gamma\kappa \int_0^{q_1} \frac{\sin(x)}{m_1(x)\Delta(x)} dx + \Psi(q_2), \tag{4.74}$$

where the function $\Psi(\cdot)$ is an arbitrary differentiable function that must be chosen to satisfy condition (3.6). This condition, along with the conditions $m_1 > 0$ and $m_1 m_3 > m_2^2$ are satisfied by choosing $\Psi(q_2) = \frac{1}{2} K_p q_2^2$ (positive definite function), where $K_p > 0$ is the gain of the energy shaping controller. Note that the $\Psi(\cdot)$ term contributes for the (2,2) term of the Hessian matrix (4.83), which must be positive to guarantee the positive definiteness of the Hessian. The second step is to fix $m_1$ in (4.73) such that the solution of this PDE satisfies Conditions 3.1 and 3.2. Notice that $M$ is a function of $q_1$ only, hence, we can simply take $M_d$ as also a function of $q_1$ only. Among the different possible choices, we have fixed the desired inertia matrix as

$$M_d(q) = \Delta \begin{bmatrix} m_1 & m_2 \\ m_2 & m_3 \end{bmatrix} = \Delta \begin{bmatrix} (\cos(q_1) + \epsilon) & \frac{-\sigma\cos(q_1)(\cos(q_1)+\epsilon)}{\gamma} \\ \frac{-\sigma\cos(q_1)(\cos(q_1)+\epsilon)}{\gamma} & m_3 \end{bmatrix}. \tag{4.75}$$

Choosing $\epsilon > 1$ is to guarantee $m_1 > 0$ and hence $M_d > 0 \ \forall \ q_1 \in [0, 2\pi]$. Then, the closed-loop potential function $V_d$ is computed (using Maple software) as

$$V_d(q) = \lambda_1 \Big( - \lambda_2 \tanh^{-1}\big(\lambda_2 \cos(q_1)\big) + \ln\big(\cos(q_1) + \epsilon\big)\Big) + \Psi(q_2), \tag{4.76}$$

with

$$\lambda_1 = \frac{\kappa\gamma}{\gamma\rho + \gamma^2 - \sigma^2\epsilon^2 - \gamma^2\epsilon^2} > 0, \quad \lambda_2 = \sqrt{\frac{\gamma^2 + \sigma^2}{\gamma(\rho + \gamma)}},$$

where $0 < \lambda_2 < 1$ is such that $\tanh^{-1}(\cdot)$ is bounded.

**Remark 4.1.** For this particular design we have fixed $m_1 = \cos(q_1) + \epsilon$. The term $\cos(q_1)$ ensures that $V_d$ is minimum at $q_e$, and $\epsilon$ is added to guarantee the positivity of $M_d$ in the whole DoA.

Now, using (3.26) we can compute $J_2$, which after lengthy but straightforward calculations is obtained as

$$J_2 = \begin{bmatrix} 0 & j_2 \\ -j_2 & 0 \end{bmatrix}, \tag{4.77}$$

where

$$j_2 = \frac{K_j \gamma \Delta_d}{2\Delta} \frac{\Big((\varphi\mathcal{B}_1 - \mathcal{A}_1)p_1^2 + 2(\varphi\mathcal{B}_2 - \mathcal{A}_2)p_1 p_2 + (\varphi\mathcal{B}_3 - \mathcal{A}_3)p_2^2\Big)}{(\cos(q_1) + \epsilon)\,(\sigma\cos(q_1)p_1 + \gamma p_2)} \tag{4.78}$$

with $K_j > 0$, and

$$\mathcal{A}_1 = \frac{\sin(2q_1)}{\Delta^2}\left(\gamma\Delta - \left(\rho + \gamma\sin^2(q_1)\right)\left(\gamma^2+\sigma^2\right)\right),$$
$$\mathcal{A}_2 = -\frac{\sigma\sin(q_1)}{\Delta^2}\left(\Delta + 2\cos^2(q_1)(\gamma^2+\sigma^2)\right),$$
$$\mathcal{A}_3 = -\frac{\gamma(\gamma^2+\sigma^2)\sin(2q_1)}{\Delta^2},$$
$$\mathcal{B}_1 = \frac{m_3\sin(q_1)}{(\gamma\Delta_d)^2}\Big(-2\gamma^2\Delta_d\cos(q_1)(\gamma^2+\sigma^2)+\Delta^3\big(m_3\gamma^2-\epsilon\sigma^2\cos^2(q_1)-\sigma^2\cos^3(q_1)\big)$$
$$-\sigma^2\Delta^3\cos(q_1)\big(\epsilon+\cos(q_1)\big)\big(2\epsilon+3\cos(q_1)\big)\Big),$$
$$\mathcal{B}_2 = -\frac{\sigma\sin(q_1)\big(\epsilon+\cos(q_1)\big)}{\gamma\Delta_d\big(m_3\gamma^2-\epsilon\sigma^2\cos^2(q_1)-\sigma^2\cos^3(q_1)\big)}\Big(\sigma^2\Delta\cos^2(q_1)\big(2\epsilon+3\cos(q_1)\big)$$
$$+\big(2\cos^2(q_1)(\gamma^2+\sigma^2)+\Delta\big)\big(m_3\gamma^2-\epsilon\sigma^2\cos^2(q_1)-\sigma^2\cos^3(q_1)\big)\Big),$$
$$\mathcal{B}_3 = -\frac{\sin(q_1)\cos(q_1)\big(\epsilon+\cos(q_1)\big)}{\Delta_d\big(m_3\gamma^2-\epsilon\sigma^2\cos^2(q_1)-\sigma^2\cos^3(q_1)\big)}\times$$
$$\Big(2(\gamma^2+\sigma^2)\big(m_3\gamma^2-\epsilon\sigma^2\cos^2(q_1)-\sigma^2\cos^3(q_1)\big)+\sigma^2\Delta\big(2\epsilon+3\cos(q_1)\big)\Big),$$
$$\varphi = \big(\cos(q_1)+\epsilon\big)\left(\rho+\gamma\sin^2(q_1)-\frac{\sigma^2\cos^2(q_1)}{\gamma}\right),$$

and $\Delta_d = \det(M_d) = \frac{\Delta^2}{\gamma^2}\big(\cos(q_1)+\epsilon\big)\Big(m_3\gamma^2-\sigma^2\cos^2(q_1)\big(\cos(q_1)+\epsilon\big)\Big)$.

Now, we substitute all the terms into (3.10) to obtain the energy shaping controller

$$u_{es} = -\frac{\sigma\cos(q_1)}{\gamma}\Big(\gamma m_3-\big(\rho+\gamma\sin^2(q_1)\big)\big(\epsilon+\cos(q_1)\big)\Big)\left(\frac{\mathcal{B}_1}{2}p_1^2+\mathcal{B}_2p_1p_2+\frac{\mathcal{B}_3}{2}p_2^2\right.$$
$$\left.+\frac{\epsilon\lambda_1\lambda_2^2\sin(q_1)}{1-\lambda_2^2\cos^2(q_1)}-\frac{\lambda_1\sin(q_1)}{\epsilon+\cos(q_1)}\right)-\Big(\gamma m_3-\frac{\sigma^2\cos^2(q_1)(\cos(q_1)+\epsilon)}{\gamma}\Big)K_pq_2$$
$$-j_2\frac{\Delta}{\gamma\Delta_d}\Big(\gamma m_3p_1+\sigma\cos(q_1)\big(\cos(q_1)+\epsilon\big)p_2\Big). \tag{4.79}$$

### 4.4.2 Damping assignment

The damping injection controller follows the construction (3.11). Given $M_d$ that has been obtained when reshaping the total energy, we have

$$\nabla_pH_d = M_d^{-1}p = \frac{\Delta}{\Delta_d}\begin{bmatrix} m_3 & \frac{\sigma\cos(q_1)(\cos(q_1)+\epsilon)}{\gamma} \\ \frac{\sigma\cos(q_1)(\cos(q_1)+\epsilon)}{\gamma} & \epsilon+\cos(q_1)\end{bmatrix}\begin{bmatrix}p_1\\p_2\end{bmatrix}$$
$$= \frac{\Delta}{\Delta_d}\begin{bmatrix} m_3p_1+\frac{\sigma\cos(q_1)(\cos(q_1)+\epsilon)}{\gamma}p_2 \\ \frac{\sigma\cos(q_1)(\cos(q_1)+\epsilon)}{\gamma}p_1+(\cos(q_1)+\epsilon)p_2\end{bmatrix}. \tag{4.80}$$

Substituting (4.80) into (3.11), the damping injection controller is obtained as

$$u_{di} = -\frac{K_v \Delta\big(\cos(q_1)+\epsilon\big)}{\gamma \Delta_d}\big(\sigma \cos(q_1) p_1 + \gamma p_2\big). \tag{4.81}$$

Now, we can conclude the IDA-PBC controller design for our rotary inverted pendulum by stating the following corollary.

**Corollary 4.2.** *The state feedback controller (4.79), (4.81), with* $m_3 > (\cos(q_1)+\epsilon)\frac{\sigma^2\cos^2(q_1)}{\gamma^2}$, $\epsilon > 1$ *and* $K_p, K_v, K_j > 0$ *is an asymptotically stabilizing controller for the rotary pendulum system (4.36)-(4.37) at its unstable equilibrium point* $q = (0, q_2)$ *for any* $q_2 \in [0,\ 2\pi]$. ■

**Proof of Corollary 4.2:** The proof of Corollary 4.2 is discussed in Section 4.5. ■

## 4.5 Stability Analysis

As mentioned earlier (see also Proposition 1 in [2]), one important property of the IDA-PBC method is that the closed-loop energy function $H_d(q,p)$ qualifies as a Lyapunov function candidate $W(q,p)$, thus has a stable equilibrium point at $(q_e, 0)$. For this to apply, $H_d(q,p)$ itself must satisfy two conditions: **1)** $M_d$ is positive definite and symmetric, and **2)** the closed-loop potential energy function $V_d$ must have an isolated minimum at this equilibrium point. Furthermore, this equilibrium point is asymptotically stable provided that the closed-loop system satisfies the detectability condition from the output $y_d = G^\top \nabla_p H_d$.

As explained through the design procedures, a sufficient condition to guarantee the positive definiteness of $M_d$ in (4.75) is that $m_1 > 0$ and $m_1 m_3 > m_2^2$. The former is achieved by assigning $m_1 = (\cos(q_1)+\epsilon)$ with $\epsilon > 1$. By choosing $m_3$ such that it satisfies the condition $m_3 > \big(\epsilon + \cos(q_1)\big)\frac{\sigma^2\cos^2(q_1)}{\gamma^2}$, for instance $m_3 := (\cos(q_1)+\epsilon)\frac{\sigma^2\cos^2(q_1)}{\gamma^2} + \mu$ with a constant $\mu > 0$, the latter condition is also achieved. Finally, it is clear that $M_d$ is symmetric since the elements $m_{12} = m_{21} := m_2$.

To prove the assignment of the minimum of the potential energy $q_e = \arg\min V_d(q)$, we show that Conditions 3.1 and 3.2 are satisfied. The gradient of $V_d$ is computed as

$$\nabla_q V_d = \lambda_1 \sin(q_1) \begin{bmatrix} \frac{\epsilon(\sigma^2+\gamma^2)}{\gamma(\rho+\gamma)-(\sigma^2+\gamma^2)\cos^2(q_1)} - \frac{1}{(\epsilon+\cos(q_1))} \\ K_p q_2 \end{bmatrix}.$$

Solving at the equilibrium point $q_e = (0,0)$, yields $\nabla_q V_d|_{q_e} = \begin{bmatrix} 0 & 0 \end{bmatrix}^\top$. Hence, Condition 3.1 is satisfied. To verify that the Hessian of $V_d$ is positive definite, we evaluate

$$\nabla_q^2 V_d = \begin{bmatrix} (\nabla_q^2 V_d)_{11} & 0 \\ 0 & K_p \end{bmatrix}, \tag{4.82}$$

where

$$(\nabla_q^2 V_d)_{11} = \left( \frac{\lambda_1 \cos(q_1)\epsilon(\sigma^2+\gamma^2)}{\gamma(\rho+\gamma) - (\sigma^2+\gamma^2)\cos^2(q_1)} - \frac{\lambda_1 \cos(q_1)}{\big(\epsilon + \cos(q_1)\big)} \right) - \left( \frac{2\epsilon \cos(q_1)(\sigma^2+\gamma^2)^2 \lambda_1 \sin^2(q_1)}{\big(\gamma(\rho+\gamma) - (\sigma^2+\gamma^2)\cos^2(q_1)\big)^2} + \frac{\lambda_1 \sin^2(q_1)}{\big(\epsilon + \cos(q_1)\big)^2} \right),$$

at $q_e$, thus we obtain

$$\nabla_q^2 V_d|_{q_e} = \begin{bmatrix} \lambda_1 \left( \frac{\epsilon(\sigma^2+\gamma^2)}{\gamma\rho - \sigma^2} - \frac{1}{\big(\epsilon+1\big)} \right) & 0 \\ 0 & K_p \end{bmatrix}, \tag{4.83}$$

which is positive definite for $K_p, \lambda_1 > 0$ and $\epsilon > 1$. Notice that $\epsilon > 1$ in (4.83) guarantees that $\frac{\epsilon(\sigma^2+\gamma^2)}{\gamma\rho-\sigma^2} > \frac{1}{\big(\epsilon+1\big)}$. Hence Condition 3.2 also holds. Since all conditions are satisfied, we can conclude that $H_d$ qualifies as a Lyapunov function, i.e.

$$H_d(q,p) = W(q,p) = \frac{1}{2} p^\top M_d^{-1}(q) p + V_d(q), \tag{4.84}$$

and so that the rotary inverted pendulum system (4.36)-(4.37) is stabilized at its unstable equilibrium point $q = (0, q_2)$ by the proposed IDA-PBC design. To prove that the system is asymptotically stable, either detectability condition should be guaranteed, or, since the closed-loop energy function of the system qualifies as a Lyapunov function candidate, we can invoke LaSalle's invariance principle as follows.

The derivative of (4.84) along the trajectories of the closed-loop system is

$$\begin{aligned} \dot{W}(q,p) &= (\nabla_q H_d)^\top \dot{q} + (\nabla_p H_d)^\top \dot{p} = -p^\top M_d^{-1} G K_v G^\top M_d^{-1} p \\ &= -K_v (G^\top \nabla_p H_d)^2 \leq 0, \end{aligned} \tag{4.85}$$

where $K_v > 0$. Thus, $\dot{W}$ is negative semidefinite. Using LaSalle's invariance principle [47], we define the set $\Omega$ as

$$\Omega = \{(q,p) : \dot{W}(q,p) = G^\top \nabla_p H_d = G^\top M_d^{-1}(q) p = 0\}. \tag{4.86}$$

Using

$$M_d^{-1} = \frac{\Delta}{\Delta_d} \begin{bmatrix} m_3 & \frac{\sigma \cos(q_1)(\cos(q_1)+\epsilon)}{\gamma} \\ \frac{\sigma \cos(q_1)(\cos(q_1)+\epsilon)}{\gamma} & \epsilon + \cos(q_1) \end{bmatrix}, \tag{4.87}$$

we obtain

$$\begin{aligned} G^\top M_d^{-1}(q) p &= \begin{bmatrix} 0 & 1 \end{bmatrix} \left( \frac{\Delta}{\Delta_d} \begin{bmatrix} m_3 & \frac{\sigma \cos(q_1)(\cos(q_1)+\epsilon)}{\gamma} \\ \frac{\sigma \cos(q_1)(\cos(q_1)+\epsilon)}{\gamma} & \epsilon + \cos(q_1) \end{bmatrix} \right) \begin{bmatrix} p_1 \\ p_2 \end{bmatrix} = 0 \\ &= \frac{\Delta\big(\cos(q_1)+\epsilon\big)}{\gamma \Delta_d} \big(\sigma \cos(q_1) p_1 + \gamma p_2\big) = 0, \end{aligned} \tag{4.88}$$

which implies

$$\sigma\cos(q_1)p_1 + \gamma p_2 = 0, \tag{4.89}$$

as the term $\frac{\Delta\big(\cos(q_1)+\epsilon\big)}{\gamma\Delta_d} > 0$ due to $\epsilon > 1$. From (4.89), there are two cases to satisfy $\dot{H}_d = 0$:
Case 1: $\cos(q_1) = \frac{k\pi}{2}$ with $k$ odd and $p_2 = 0$, or
Case 2: $p_1 = p_2 = 0$.

We will now show that Case 1 is not feasible. Note that $p_2 = 0 \implies \dot{p}_2 = 0$, and from the system dynamics (4.45), $\dot{p}_2$ is the control input (4.79), (4.81). That is

$$\begin{aligned}\dot{p}_2 = &-\frac{\sigma\cos(q_1)}{\gamma}\Big(\gamma m_3 - \big(\rho + \gamma\sin^2(q_1)\big)\big(\epsilon + \cos(q_1)\big)\Big)\left(\frac{\mathcal{B}_1}{2}p_1^2 + \mathcal{B}_2 p_1 p_2 + \frac{\mathcal{B}_3}{2}p_2^2\right.\\
&\left.+ \frac{\epsilon\lambda_1\lambda_2^2\sin(q_1)}{1-\lambda_2^2\cos^2(q_1)} - \frac{\lambda_1\sin(q_1)}{\epsilon+\cos(q_1)}\right) - \Big(\gamma m_3 - \frac{\sigma^2\cos^2(q_1)(\cos(q_1)+\epsilon)}{\gamma}\Big)K_p q_2\\
&- j_2\frac{\Delta}{\gamma\Delta_d}\Big(\gamma m_3 p_1 + \sigma\cos(q_1)\big(\cos(q_1)+\epsilon\big)p_2\Big)\\
&- \frac{K_v\Delta\big(\cos(q_1)+\epsilon\big)}{\gamma\Delta_d}\big(\sigma\cos(q_1)p_1 + \gamma p_2\big) = 0.\end{aligned}$$

Substituting $\cos(q_1) = \frac{k\pi}{2}$ (with $k$ odd) and $p_2 = 0$ yields

$$j_2\frac{\Delta}{\gamma\Delta_d}\gamma m_3 p_1 = 0, \tag{4.90}$$

which implies that $p_1 = 0 \implies \dot{p}_1 = 0$. Now, from the system dynamics,

$$\begin{aligned}\dot{p}_1 = &\frac{1}{2\Delta^2}\left[\big(\rho + \gamma\sin^2(q_1)\big)p_1^2 + \gamma p_2^2 + 2\sigma\cos(q_1)p_1p_2\right]\big((\gamma^2+\sigma^2)\sin(2q_1)\big)\\
&+ \frac{1}{2\Delta}\left[2\sigma\sin(q_1)p_1p_2 - \gamma\sin(2q_1)p_1^2\right] + \kappa\sin(q_1) = 0.\end{aligned} \tag{4.91}$$

Note that because of the last term $(\kappa\sin(q_1))$ in (4.91), $\dot{p}_1 = 0$ is only satisfied if $q_1 \neq \frac{k\pi}{2}$ with $k$ odd. It is indeed satisfied if $q_1 = 0$. Thus, Case 1 cannot happen, and only Case 2 is true. Hence, the system can maintain the $\dot{H}_d = 0$ condition only at the equilibrium point $(q_e, 0)$, which proves that this equilibrium is *'almost' globally asymptotically stable*.

**Remark 4.3.** Note that for these type of systems, a global asymptotic stabilization cannot be achieved as the systems evolve on manifolds which are not diffeomorphic to the euclidean space. Thus, the best it can be achieved is *'almost'* globally asymptotically stable [5].

Figure 4.8 depicts the energy evolution for the rotary pendulum for an initial pendulum angle of 180°. It shows that the system converges to its stable manifold corresponding to its isolated minimum energy. It also illustrates the fact that for the closed-loop system, the total energy function $H_d$ and the potential energy function $V_d$ satisfy the relation $V_d(t) < H_d(t) < H_d(0)$, $\forall t$.

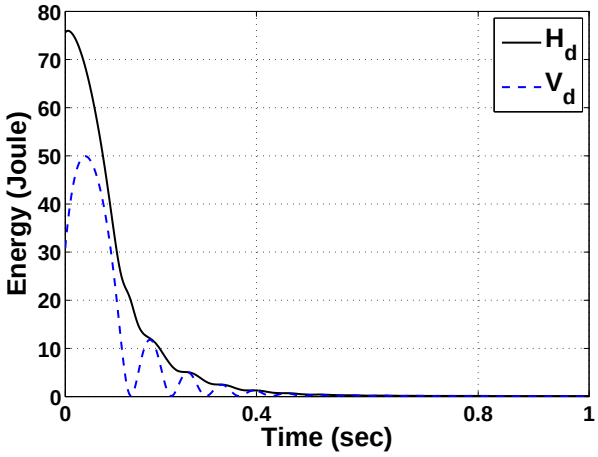


Figure 4.8: The total energy of the rotary inverted pendulum.

## 4.6 Simulation Results

We present some simulation results obtained for the model of Quanser QUBE-Servo rotary pendulum shown in Figure 4.1 with the IDA-PBC controller (4.79), (4.81). The closed-loop performance is evaluated with two sets of simulations. In the first set, the pendulum starts at ($q_{1_0} = \frac{\pi}{4}$) and the controller parameters $K_p = 0.01$, $K_v = 1.7 \times 10^{-5}$, $K_j = 2 \times 10^{-5}$, $m_3 = 50$, $\epsilon = 1.1$. This $q_{1_0}$ is more than twice the initial angular position of the pendulum that is recommended for the balancing experiment of this rotary pendulum hardware using a linear state feedback controller obtained via a pole placement design shown in Subsection 4.3.3. The results are depicted in Figures 4.9 and 4.10. As can be observed, the pendulum can easily be stabilized at its upright position using the proposed controller with very little effort as shown by the low value of the control input. To show the global behaviour of the closed-loop system, simulations have been carried out with the pendulum swings up from the hanging position ($q_{1_0} = \pi$), and having the parameters $K_p = 6$, $K_v = 2.1 \times 10^{-4}$, $K_j = 1 \times 10^{-5}$, $m_3 = 54$, $\epsilon = 1.3$. It is apparent from Figure 4.11 that the proposed controller yields an almost global asymptotic stabilization of the rotary inverted pendulum pendulum. However, it can be observed from Figure 4.12 that the control effort significantly increases with the increased initial angular position of the pendulum. More simulations on a different type of rotary inverted pendulum hardware can be found in [84].

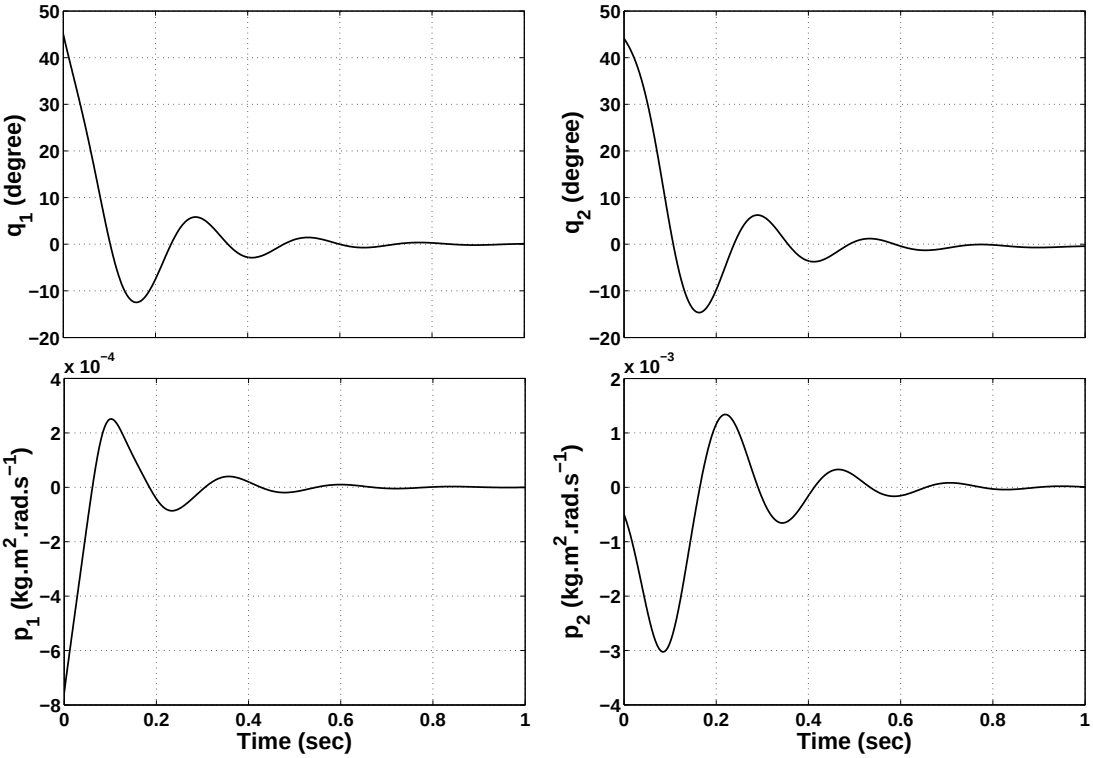


Figure 4.9: State histories with $[q_0, p_0] = [\frac{\pi}{4}, 0.8, -0.7 \times 10^{-3}, -0.5 \times 10^{-3}]$.

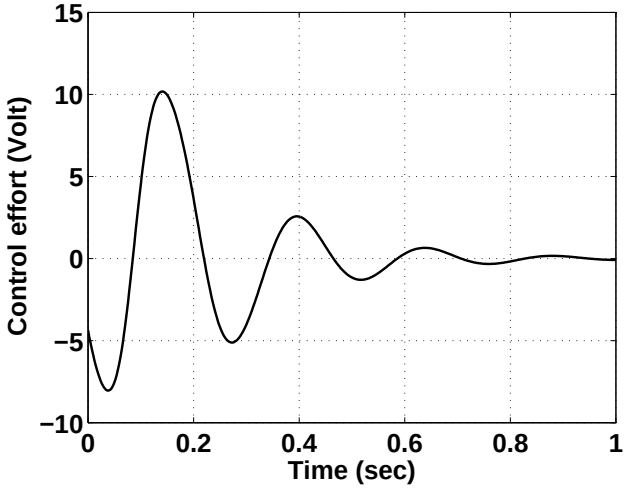


Figure 4.10: Control input with $[q_0, p_0] = [\frac{\pi}{4}, 0.8, -0.7 \times 10^{-3}, -0.5 \times 10^{-3}]$.

## 4.7 Conclusion

In Chapter 3 a constructive methodology to simplify the partial differential equations associated with the design of IDA-PBC for two groups of underactuaded mechanical systems has been presented. Also in that chapter, the methodology has been successfully applied to one of these groups: separable underactuated mechanical systems, with the inertia wheel pendulum system as an example. In this chapter, we have shown the

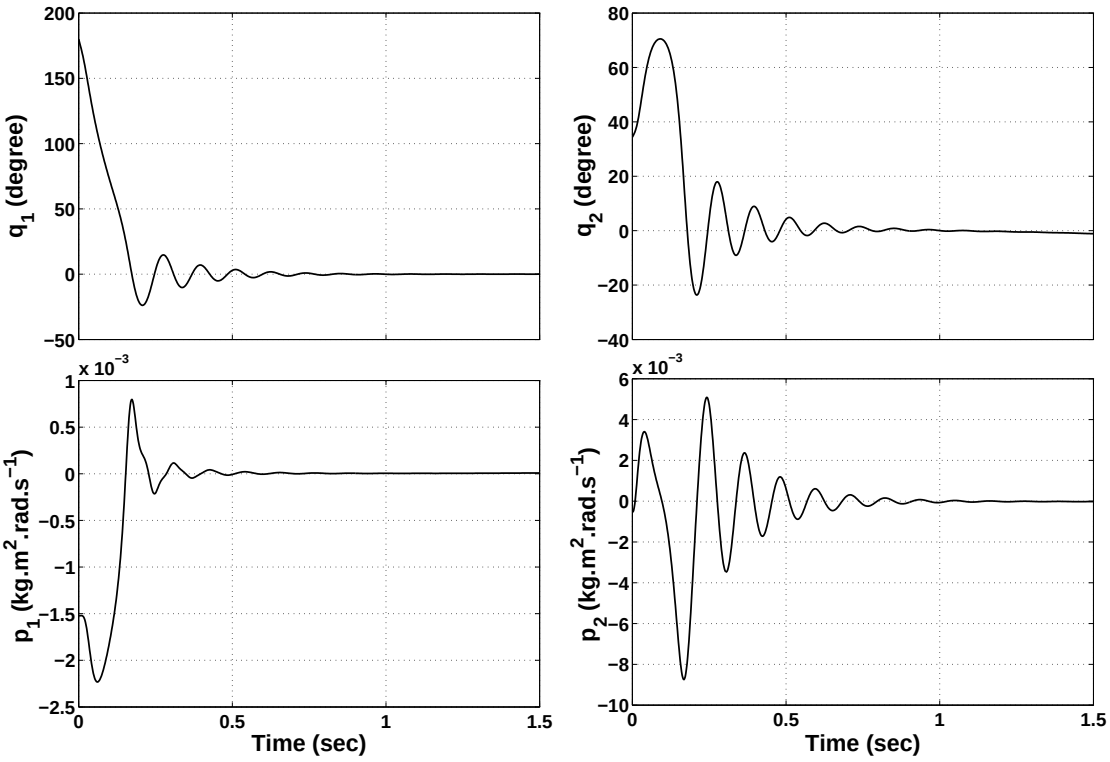


Figure 4.11: State histories with $[q_0, p_0] = [\pi, 0.6, -1.5 \times 10^{-3}, -0.5 \times 10^{-3}]$.

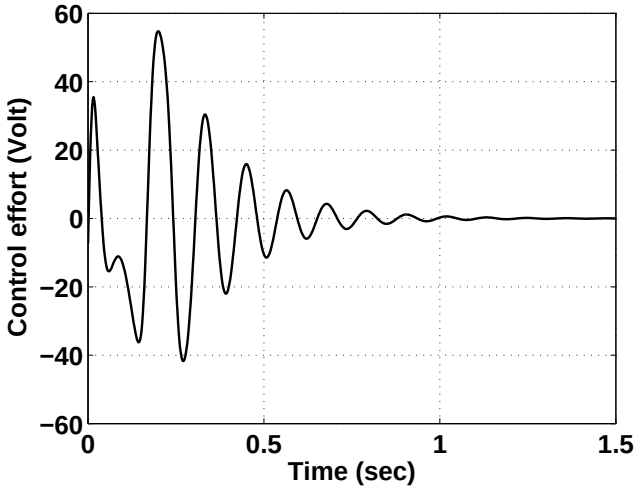


Figure 4.12: Control input with $[q_0, p_0] = [\pi, 0.6, -1.5 \times 10^{-3}, -0.5 \times 10^{-3}]$.

effectiveness of this methodology applied to a more complex structure of underactuated mechanical systems, the non-separable systems, with the rotary inverted pendulum as an illustrative example.

First we have provided a complete derivation of the equations of motion using a recursive Newton-Euler method to obtain a PCH model of the rotary inverted pendulum system. Then a linear control design using pole-placement has been discussed, highlighting the limitation of applying this approach. The design of nonlinear IDA-PBC controller for the

system is thoroughly discussed in this chapter. The almost global asymptotic stability has been proved as discussed in the stability analysis section. To the best of our knowledge, this is the first method that achieves almost GAS of this system using IDA-PBC. Finally, simulations using real parameters have been carried out to verify the stability and performance of the closed-loop system using the proposed scheme. Experimental validation of this approach is discussed in Chapter 7.

# Chapter 5

# Robust IDA-PBC and PID-like Control for PCH Systems

## 5.1 Introduction

In Chapters 3 and 4, we have proposed some control design methods for the stabilization problem of mechanical systems within the PCH framework using the IDA-PBC methodology. These methods assume accurate modelling of the system as well as ignore the external effects such as noises and disturbances. Though these methods have shown good simulation results, the real time implementation of such controllers may be highly affected by model uncertainties.

One major factor that influences the performance of dynamical systems is uncertainty. Uncertainties in dynamical system may result from modeling errors where some aspects of the physical system are approximated or neglected, or environmental influences such as disturbances or noises. The complexity of systems and demand for accurate control systems have made control design problems more challenging. This motivates the establishment of the robust control paradigm, with the integral and adaptive control among the main approaches. In the context of linear control design, the integral action control is the most popular approach, and PI, PID controllers still dominate in practice, to improve the robustness of systems by eliminating the steady-state errors. PI controller is also one of the most popular tools in nonlinear control design [7, 82].

Control design methods for systems described by PCH model have recently been investigated in several works (see [66] for a survey). Adopting the PCH structure that geometrically describes a large class of nonlinear models gives a number of advantages such as the obvious relation between the dynamics and the energy of the system, the energy conservative property that makes the model marginally stable to start with, and

the coupling between the non-damping and the damping elements. However, this modeling approach results in exclusion of important ingredients of the system's dynamics such as friction. Hence, relying only on the pure PCH model, often results in a controller that works very well in simulation, but needs further adjustment in implementation [66, 47]. The IDA-PBC, introduced in [74], is a physically inspired control design method that invokes the principles of *energy shaping* and *dissipation* and formulated for systems described by PCH models. The main objective of this method is to stabilize the dynamical system by rendering the closed-loop system *passive* (by shaping its energy) with a desired storage function (which is a proper Lyapunov function) [72]. Furthermore, the system can be asymptotically stabilized if it can be rendered strictly (output) passive by means of damping injection [109]. While IDA-PBC controller is theoretically proven to asymptotically stabilize classes of PCH systems, in real applications, the effect of disturbances, uncertainties or reference signal may deteriorate the performance of the control system [29], and the closed-loop system is more likely to suffer from steady-state errors or even instability. Moreover, when it comes to parametric uncertainties, the real-time implementation of control system requires a real-time and reasonably accurate estimate of these uncertainties.

There have been relatively few works that discuss the robustness issues in the context of the PCH framework. A general method to add integral action that depends on the passive outputs has been proposed in [66]. In [29], a framework that includes state transformation to add the integral action on the non-passive outputs have been developed. Integral control has been also introduced to PCH systems to deal with unmatched disturbances in [70]. The robustness of fully actuated mechanical systems subject to external disturbances has been recently discussed in [82]. This method which incorporates a change of coordinates and adopts the ISS and integral ISS (iISS) theories has improved the robustness of these systems by rejecting matched and unmatched disturbances. Using a power-based modelling framework of PCH and using a canonical change of coordinates, integral and adaptive control schemes have been presented in [27]. For parametric uncertainty in the control input where uncertainties can be linearly parametrized as errors in the control input, an adaptive stabilization and tracking control methods for fully-actuated mechanical systems have been proposed in [28].

In this chapter extension of results from [29, 82] for fully-actuated PCH mechanical systems are proposed. In Subsection 5.3.1, we extend the robust PI controller of mechanical system proposed in [82] to the robust PID-like controller that provides a more general framework. In Subsection 5.3.2, inspired by the work of [29] and using the idea of coordinates transformation [82], we show that the integral action control can be incorporated to improve the robustness of IDA-PBC controller for PCH mechanical systems. Subsection 5.3.3 provides the most important contribution of the work reported in this chapter, i.e. a novel integral control scheme for underactuated mechanical systems within PCH structure which has not previously been investigated in the literature. As we will discuss

later, the system being underactuated significantly complicates the inclusion of the integral control. For this, we first introduce a technique to modify the structure of the model of the underactuated system, which then allows the implementation of the integral IDA controllers on the *separable* underactuated PCH systems.

The robustness of the separable PCH mechanical systems under the presence of matched and unmatched time-varying disturbances is discussed in Subsection 5.3.4. We show that using a certain change of coordinates a new method to characterize the property of system with disturbances such that the well-known input-to-state stability (ISS) property is satisfied. This method provides a simpler controller design than the one proposed in [82]. Furthermore, it provides a framework to apply this method to underactuated PCH systems. We also show that in some conditions asymptotic stability property of the closed-loop system can be achieved. Subsection 5.3.5 describes the design of a novel adaptive controller for uncertain PCH systems. Extension of the results to the case of non-separable inertia matrix is presented in Section 5.4. The results are validated in Section 5.5 where we apply our various proposed methods to robustly control an inertia wheel pendulum (IWP) system. Finally, concluding remarks are made in the last section.

## 5.2 Preliminaries

### Review on integral control within PCH framework

In PCH framework, the states $p$ and $q$ are known as the **passive outputs** and the **non-passive outputs**, respectively [29].

To improve control performance, particularly with respect to steady-state error and reference inputs, the idea of applying integral action on the *passive* outputs of PCH systems has been proposed in [66]. In this method the integral control (IC)

$$v = -K_i \int y_d dt = -K_i G^\top \int \nabla_p H_d dt, \tag{5.1}$$

with the integral gain $K_i = K_i^\top > 0$, is added to the IDA-PBC stabilized PCH system (3.12) to form an extended dynamical system

$$\begin{bmatrix} \dot{q} \\ \dot{p} \end{bmatrix} = \begin{bmatrix} 0 & M^{-1}M_d \\ -M_d M^{-1} & J_2 - R_d \end{bmatrix} \begin{bmatrix} \nabla_q H_d \\ \nabla_p H_d \end{bmatrix} + \begin{bmatrix} 0 \\ G \end{bmatrix} v \tag{5.2}$$

which can be written into an extended PCH form as

$$\begin{bmatrix} \dot{q} \\ \dot{p} \\ \dot{v} \end{bmatrix} = \begin{bmatrix} 0 & M^{-1}M_d & 0 \\ -M_d M^{-1} & J_2 - R_d & GK_i \\ 0 & -K_i G^\top & 0 \end{bmatrix} \begin{bmatrix} \nabla_q H_{dv} \\ \nabla_p H_{dv} \\ \nabla_v H_{dv} \end{bmatrix} \tag{5.3}$$

where

$$H_{dv} = H_d + \frac{1}{2} v^\top K_i^{-1} v. \tag{5.4}$$

In reality, applying the IC only to the states which are the *passive* outputs is often insufficient. In Section 5.3, we present the extension of this approach to more general classes of PCH systems allowing the IC input on the states which are the non-passive outputs.

## 5.3 Robust Control of Separable Hamiltonian Systems

Subsections 5.3.1 and 5.3.2 present extensions to the results in [29] and [82] which deal with the fully-actuated mechanical systems. Then, Subsection 5.3.3 extends the integral IDA-PBC results to deal with underactuated mechanical systems. In Subsection 5.3.4 an ISS controller is proposed for general PCH mechanical systems subject to external matched and unmatched disturbances. It shows also an extension to the case of underactuated systems. An adaptive control design method is also proposed in Subsection 5.3.5.

### 5.3.1 PID-like control for separable PCH systems

In [82], a PI controller has been proposed to reject constant disturbance(s) for the case of a separable PCH system which is assumed to have natural damping. On the contrary, here we start with assuming that the system *does not* have natural damping and we introduce the damping to the system (3.1) by means of a derivative controller, thus, we obtain a PID-like controller. This assumption of no damping is *consistent* with the PCH model that we consider in this thesis.

**Remark 5.1.** Note that we call the controller as PID-like controller because it consists of the P, I and D terms. However, this controller is a state feedback controller and not exactly the same as the conventional PID controller which sits on the feed-forward path of the system. This type of control has been used for instance in [82].

Given the separable PCH system (3.1) with the PID-like controller

$$\begin{aligned} u &= -M\dot{x}_v - K_d x_v - K_d M^{-1} p \\ &= -\underbrace{M K_i G^\top \nabla_{x_q} V(x_q)}_{Proportional} - \underbrace{K_d K_i G^\top \int \nabla_{x_q} V(x_q) dt}_{Integral} - \underbrace{K_d M^{-1} p}_{Derivative}, \qquad (p = M\dot{q}) \end{aligned} \tag{5.5}$$

where $K_i = K_i^\top > 0$, $K_d = K_d^\top > 0$ and introducing $x_v$ such that

$$\dot{x}_v = K_i G^\top \nabla_{x_q} \tilde{H} = K_i G^\top \nabla_{x_q} V.$$

Using the coordinate transformation

$$x_q = q; \qquad x_p = p + MGx_v \tag{5.6}$$

the closed-loop system in the new variables $x := [x_q\ x_p\ x_v]$ takes the form

$$\begin{bmatrix} \dot{x}_q \\ \dot{x}_p \\ \dot{x}_v \end{bmatrix} = \begin{bmatrix} 0 & I_n & -GK_i \\ -I_n & -K_d & 0 \\ K_i G^\top & 0 & 0 \end{bmatrix} \begin{bmatrix} \nabla_{x_q}\tilde{H} \\ \nabla_{x_p}\tilde{H} \\ \nabla_{x_v}\tilde{H} \end{bmatrix}, \tag{5.7}$$

with the total energy function

$$\tilde{H} = \frac{1}{2}x_p^\top M^{-1}x_p + \frac{1}{2}x_v^\top K_i^{-1}x_v + V(x_q). \tag{5.8}$$

The procedure can now be summarized in the following proposition.

**Proposition 5.2.** *Consider the separable PCH system (3.1). Define the state transformation (5.6) to realize the augmented closed-loop PCH system (5.7) with the Hamiltonian function (5.8). Then, the PID-like controller (5.5) is an asymptotically stabilizing controller for the system.* ■

**Proof of Proposition 5.2:** Consider the Hamiltonian function (5.8) as a candidate Lyapunov function for the system (5.7). Because $M$ is constant, then $\nabla_{x_q}\tilde{H} = \nabla_{x_q}V$. Its derivative along the trajectories of the system is

$$\begin{aligned} \dot{\tilde{H}} &= x_p^\top M^{-1}\dot{x}_p + x_v^\top K_i^{-1}\dot{x}_v + \nabla_{x_q}V^\top(x_q)\dot{x}_q \\ &= x_p^\top M^{-1}(-\nabla_{x_q}V - K_dM^{-1}x_p) + x_v^\top K_i^{-1}(K_iG^\top\nabla_{x_q}V) + \nabla_{x_q}V^\top(x_p^\top M^{-1} - Gx_v) \\ &= -x_p^\top M^{-1}K_dM^{-1}x_p, \end{aligned}$$

which is negative semi-definite. By invoking LaSalle's invariance principle [47], one can prove that the largest invariant set contained in

$$\Omega = \{x_{\{q,p,v\}} : \dot{\tilde{H}} = -x_p^\top M^{-1}K_dM^{-1}x_p = 0 \,|\, x_p = 0\}$$

is the equilibrium point $x_e = (x_{qe}, 0, 0) = (q_e, 0, 0)$, thus it is asymptotically stable (see the proof of Proposition 5.4). The PID-like controller (5.5) is found by equating (3.1) and (5.7) and applying the coordinate transformation (5.6), that is

$$\begin{aligned} \dot{p} &\equiv \dot{x}_p - M\dot{x}_v \\ -\nabla_q H + Gu &= -\nabla_{x_q}\tilde{H} - K_d\nabla_{x_p}\tilde{H} - M\dot{x}_v. \end{aligned}$$

Notice that with (5.6) we have $\nabla_q H = \nabla_{x_q}\tilde{H}$ and $\nabla_{x_p}\tilde{H} = M^{-1}(p + Mx_v)$, thus, we obtain (5.5). ■

**Remark 5.3.** The PCH structure of the original model (3.1) has been preserved in the augmented system (5.7). This can be shown from i) the coincidence of the state equations of both models (they are matched) ii) the preservation of the Hamiltonian and the Poisson structure [82] of the model, i.e. the positive definiteness of the interconnection matrix. This preservation in the closed-loop system ensures asymptotic stability of the system as shown in the Proof of Proposition 5.2, and robustness property is provided through the introduction of the integral action.

### 5.3.2 Integral IDA-PBC (IIDA) for separable PCH systems

In Subsection 5.3.1, a PID-like controller has been proposed for both asymptotically stabilizing and robustifying the fully-actuated PCH system. In this section, we assume that the stabilization problem has been solved using IDA-PBC method and we need to introduce an integral action to solve the robustness issue. As discussed in Subsection 5.2, a method to include the IC for passive outputs has existed. However for non-passive outputs, it is difficult to add the IC action while preserving the PCH structure and stability properties simultaneously.

In [36] a method that involves canonical transformation of coordinates and solving a set of PDEs was proposed. Coordinate transformation was also used in [70] to deal with the robust control of non-passive outputs with unmatched disturbances. An initial result towards applying IC on non-passive outputs of PCH systems has been recently proposed in [29]. In this method the IC is added to the PCH model that has already been stabilized using a PBC method, exploiting a state transformation that preserves the Poisson structure of the open-loop system. However, this method requires solving a set of algebraic equations that account for defining the state transformation which makes it quite complicated.

Inspired by the work of [29, 70, 82], we present a simpler method to include the IC for non-passive outputs of PCH system assuming a stabilizing IDA-PBC controller has already been obtained and we are dealing with steady-state error. The main idea is to use the change of coordinates as in Subsection 5.3.1 and [82] to obtain the IC, while preserving the structure and stability properties of the original PCH model.

Consider the closed-loop PCH system (5.2) with equilibrium satisfying (3.6) when $v = 0$. Since throughout the IDA-PBC design procedures, $J_2$ is set to 0 as both $M$ and $M_d$ are constants [71], the system can be rewritten as

$$\begin{bmatrix} \dot{q} \\ \dot{p} \end{bmatrix} = \begin{bmatrix} 0 & M^{-1}M_d \\ -M_dM^{-1} & -R_d \end{bmatrix} \begin{bmatrix} \nabla_q H_d \\ \nabla_p H_d \end{bmatrix} + \begin{bmatrix} 0 \\ G \end{bmatrix} v. \tag{5.9}$$

Applying the same coordinate transformation (5.6), with the integral control

$$\begin{aligned} v &= -R_d M_d^{-1} M G x_v \\ \dot{x}_v &= K_i G^\top \nabla_{x_q} \tilde{H}, \end{aligned} \tag{5.10}$$

the closed-loop system can be written in the augmented PCH form

$$\begin{bmatrix} \dot{x}_q \\ \dot{x}_p \\ \dot{x}_v \end{bmatrix} = \begin{bmatrix} 0 & M^{-1}M_d & -GK_i \\ -M_d M^{-1} & -R_d & 0 \\ K_i G^\top & 0 & 0 \end{bmatrix} \begin{bmatrix} \nabla_{x_q} \tilde{H} \\ \nabla_{x_p} \tilde{H} \\ \nabla_{x_v} \tilde{H} \end{bmatrix} \tag{5.11}$$

with the total energy function

$$\tilde{H} = \frac{1}{2} x_p^\top M_d^{-1} x_p + \frac{1}{2} x_v^\top K_i^{-1} x_v + V(x_q). \tag{5.12}$$

The total control input is then

$$u = u_{IDA} + v + u_p \tag{5.13}$$

where $u_p = -MK_iG^\top \nabla_{x_q} V(x_q)$ is an additional control term that appears through the procedure of finding the closed-loop controller.

**Proposition 5.4.** *Consider the separable PCH system (3.1). Assume a stabilizing IDA-PBC controller (3.3) has already been obtained with the desired (closed-loop) energy function (3.5) and the desired PCH dynamics take the form (5.9). Defining the state transformation (5.6) to realize the augmented closed-loop PCH system (5.11) with the Hamiltonian function (5.12), asymptotic stability of the equilibrium point $x_e = (x_{qe}, 0, 0) = (q_e, 0, 0)$ is preserved with the integral control (5.10). Furthermore, the total control input with integral action takes the form (5.13).* ■

**Proof of Proposition 5.4:** The proof can be established following the same procedures as in the proof of Proposition 5.2. Furthermore, in view of (3.6), (5.6) and (5.12), we obtain $\dot{\tilde{H}} = -x_p^\top M_d^{-1} R_d M_d^{-1} x_p \leq 0$, i.e the system is stable. LaSalle's invariance principle is then used to prove that the largest invariant set contained in

$$\Omega = \{x_{\{q,p,v\}} : \dot{\tilde{H}} = -x_p^\top M_d^{-1} R_d M_d^{-1} x_p = 0 \,|\, x_p = 0\},$$

is the equilibrium point $x_e = (q_e, 0, 0)$, thus it is asymptotically stable. Notice that for the system to maintain $\dot{\tilde{H}} = 0$ condition, the trajectory must be confined to $x_p = 0$. Using the system closed-loop dynamics (5.11) we show that

$$x_p \equiv 0 \implies \dot{x}_p \equiv 0 \implies -M_d M^{-1} \nabla_{x_q} \tilde{H} - R_d \nabla_{x_p} \tilde{H} = 0 \implies \nabla_{x_q} \tilde{H} = 0,$$

as $M_d M^{-1} > 0$ by definition. For PCH systems, the gradient of the potential energy function vanishes ($\nabla_{x_q} \tilde{H} = \nabla_{x_q} V(x_q) = 0$) if the system converges to its equilibrium

point $q_e$ (see (3.6), Section IV in [2] and Lemma 4.2. in [40]). Thus,

$$\nabla_{x_q}\tilde{H} \equiv 0 \implies x_q = q_e \text{ and } x_v = 0.$$

Hence, the system can maintain $\dot{\tilde{H}} = 0$ only at the equilibrium point $x_e = (q_e, 0, 0)$, which proves that this equilibrium is *asymptotically* stable. The controller is obtained by matching the momenta of (5.9) and (5.11), that is

$$\begin{aligned}\dot{p} &= -M_d M^{-1}\nabla_q H_d - R_d \nabla_p H_d + v \\ &\equiv \dot{x}_p - MG\dot{x}_v \\ &= -M_d M^{-1}\nabla_{x_q}\tilde{H} - R_d\nabla_{x_p}\tilde{H} - MG\dot{x}_v.\end{aligned} \tag{5.14}$$

Solving (5.14), we get (5.10) and the controller extra term $u_p = -MK_iG^\top\nabla V(x_q)$. ■

**Remark 5.5.** The integral control laws (5.5) and (5.10) obtained in the PID-like and IIDA methods, respectively, are very similar, except that there is the term $M_d^{-1}M$ in the one constructed using IDA-PBC method. This is due to the different interconnection matrices used for the design; the original interconnection matrix is used in the case of PID-like and the desired one in the case of IIDA. Also, the total control input $u$ of IIDA includes an additional proportional control term $u_p$.

### 5.3.3 Integral control for underactuated PCH mechanical systems

In Subsections 5.3.1 and 5.3.2, we have discussed the construction of controllers for separable PCH systems, requiring the input matrix $G$ to be full rank. This condition makes the application to underactuated systems in which $G$ is non full rank, not straightforward, whereas these systems are often found in practice, either by design or due to faults. In this section, a more general result, the design of integral control action for *underactuated* mechanical systems is proposed.

While PCH models allow some extensions in the system coordinates, such as adding integral action, two main properties must be ensured when these extensions are added to the model:

a. Preserving the PCH Poisson structure matrix (consult [90] for detailed formulation). The extension must not break the skew-symmetry of the interconnection matrix and the positive definiteness of the dissipation matrix.

b. Preserving the passivity and (asymptotic) stability of the closed-loop system.

Due to these constraints, all existing integral control schemes within PCH framework were limited to fully-actuated mechanical systems, imposing the following conditions:

(i) The input matrix $G$ is full rank.

(ii) $G = G^\top$, or sometimes $K_i = K_i^\top$ is used instead.

In fact, Condition (i) can be relaxed because the PCH structure can still be preserved even if the system is underactuated. This can be proved for instance using the Schur's complement [117], by showing the positive definiteness of the interconnection and dissipation matrices even if $rank(G){=}m < n$. Moreover, the formalism of IDA-PBC for underactuated mechanical systems also shows that the PCH structure is preserved even when $G$ is not invertible [71].

Unfortunately, stability cannot be easily verified if the integral action is added to the underactuated PCH mechanical systems, because Condition (ii) is not satisfied. This can be illustrated in the following case. A simple calculation of the derivative of the Hamiltonian function (5.12) along the trajectories of the system gives

$$\dot{\tilde{H}} = -x_p^\top M_d^{-1} R_d M_d^{-1} x_p - M_d^{-1} x_p G x_v + M_d^{-1} x_p G^\top x_v.$$

If $G = G^\top$ like in the case of fully-actuated PCH system, the last two terms are equal except with opposite signs, thus cancel out each other. Hence,

$$\dot{\tilde{H}} = -x_p^\top M_d^{-1} R_d M_d^{-1} x_p \leq 0,$$

which proves the stability of the equilibrium point. For underactuated mechanical systems, since $G \in \mathbb{R}^{n\times m} \neq G^\top \in \mathbb{R}^{m\times n}$, we cannot draw any conclusion about the stability of the system. A similar illustration can also be shown for the integral control presented in Subsection 5.2. Therefore, a modification is needed to deal with underactuated systems, as discussed next.

**A) Integral control on passive outputs**

Here we present results for underactuated PCH systems with $n = 2,\ m = 1$. Recall the desired closed-loop PCH system (5.3). For underactuated systems, the matrix $G$ can be defined as

$$G = \begin{bmatrix} g_1 \\ g_2 \end{bmatrix} \quad \left(G^\top = \begin{bmatrix} g_1 & g_2 \end{bmatrix}\right). \tag{5.15}$$

Depending on how the input acts on the states, we may have either

$$G_1 = \begin{bmatrix} g_1 \\ 0 \end{bmatrix} \quad \left(G_1^\top = \begin{bmatrix} g_1 & 0 \end{bmatrix}\right),$$

if the first passive output receives the direct action from the input, or

$$G_2 = \begin{bmatrix} 0 \\ g_2 \end{bmatrix} \quad \left(G_2^\top = \begin{bmatrix} 0 & g_2 \end{bmatrix}\right),$$

if the second passive output receives the direct action from the input. Without loss of generality, for the augmented system we define a new matrix $\mathcal{G}$ as

$$\mathcal{G} = \begin{bmatrix} g_1 & 0 \\ 0 & g_2 \end{bmatrix}, \left( \mathcal{G}^\top = \begin{bmatrix} g_1 & 0 \\ 0 & g_2 \end{bmatrix} \right) \tag{5.16}$$

thus, we obtain either

$$\mathcal{G}_1 = \begin{bmatrix} g_1 & 0 \\ 0 & 0 \end{bmatrix}, \left( \mathcal{G}_1^\top = \begin{bmatrix} g_1 & 0 \\ 0 & 0 \end{bmatrix} \right)$$

corresponding to $G_1$, or

$$\mathcal{G}_2 = \begin{bmatrix} 0 & 0 \\ 0 & g_2 \end{bmatrix}, \left( \mathcal{G}_2^\top = \begin{bmatrix} 0 & 0 \\ 0 & g_2 \end{bmatrix} \right)$$

corresponding to $G_2$.

**Remark 5.6.** Notice that $\mathcal{G} = \mathcal{G}^\top$. When either $g_1$ or $g_2$ is zero, exclusively, replacing $G$ with $\mathcal{G}$ in (5.3) neither breaks the PCH structure (the dynamics) nor changes the contribution of the augmented state to the system. This is due to the fact that $rank(G) = rank(\mathcal{G})$. For example, using $G_1$ in the extended state equation, we have

$$\dot{v} = -K_i G^\top \nabla_p H_{dv} = -K_i \begin{bmatrix} g_1 & 0 \end{bmatrix} \begin{bmatrix} \nabla_{p_1} H_{dv} \\ \nabla_{p_2} H_{dv} \end{bmatrix} = -K_i g_1 \nabla_{p_1} H_{dv},$$

and using $\mathcal{G}_1$, we obtain

$$\dot{v} = -K_i \mathcal{G}_1^\top \nabla_p H_{dv} = -K_i \begin{bmatrix} g_1 & 0 \\ 0 & 0 \end{bmatrix} \begin{bmatrix} \nabla_{p_1} H_{dv} \\ \nabla_{p_2} H_{dv} \end{bmatrix} = \begin{bmatrix} -K_i g_1 \nabla_{p_1} H_{dv} \\ 0 \end{bmatrix}.$$

As the last column is zero, it can be excluded. Thus, the same result is obtained in both cases, and the PCH dynamics are preserved. The same case also applies to $(G_2, \mathcal{G}_2)$. Hence, with this substitution we obtain

$$\dot{H}_{dv} = -p^\top M_d^{-1} R_d M_d^{-1} p \leq 0,$$

which proves the stability of the system.

**Remark 5.7.** Note that the replacement of $G$ with $\mathcal{G}$, is not meant to change the input matrix of the original PCH system, but it is applied to the augmented system to proceed with the design procedure.

**Proposition 5.8.** *Replacing the $G$ in the PCH model (5.3) with $\mathcal{G}$ to obtain*

$$\begin{bmatrix} \dot{q} \\ \dot{p} \\ \dot{v} \end{bmatrix} = \begin{bmatrix} 0 & M^{-1} M_d & 0 \\ -M_d M^{-1} & J_2 - R_d & \mathcal{G} K_i \\ 0 & -K_i \mathcal{G}^\top & 0 \end{bmatrix} \begin{bmatrix} \nabla_q H_{dv} \\ \nabla_p H_{dv} \\ \nabla_v H_{dv} \end{bmatrix}, \tag{5.17}$$

*allows for the integral action to be applied to underactuated mechanical systems.* ■

**Proof of Proposition 5.8** is established in Remark 5.6. ■

**B) Integral control on non-passive outputs**

In Subsection 5.3.3 we have considered integral control on passive outputs. However in the context of PCH mechanical systems, non-passive outputs, usually being the states representing displacement or positions, are often the outputs of interest. In this subsection we will present the method of introducing the integral action on non-passive outputs for underactuated systems. The construction of this integral control for non-passive outputs follows closely the procedures as in Subsection 5.3.2, with the replacement of matrix $G$ by $\mathcal{G}$.

Introducing the integral control action to the non-passive outputs, in the same way as how it was done to the passive outputs, yields the closed-loop PCH system (note: compare this with (5.17)):

$$\begin{bmatrix} \dot{q} \\ \dot{p} \\ \dot{v} \end{bmatrix} = \begin{bmatrix} 0 & M^{-1}M_d & 0 \\ -M_dM^{-1} & J_2 - R_d & \mathcal{G}K_i \\ -K_i\mathcal{G}^\top & 0 & 0 \end{bmatrix} \begin{bmatrix} \nabla_q H_{dv} \\ \nabla_p H_{dv} \\ \nabla_v H_{dv} \end{bmatrix}. \tag{5.18}$$

However, this way destroys the PCH structure of the system (the system is no more Hamiltonian), which is obvious from the unsymmetrical interconnection matrix.

Another option is to write the augmented system as

$$\begin{bmatrix} \dot{q} \\ \dot{p} \\ \dot{v} \end{bmatrix} = \begin{bmatrix} 0 & M^{-1}M_d & \mathcal{G}K_i \\ -M_dM^{-1} & J_2 - R_d & 0 \\ -K_i\mathcal{G}^\top & 0 & 0 \end{bmatrix} \begin{bmatrix} \nabla_q H_{dv} \\ \nabla_p H_{dv} \\ \nabla_v H_{dv} \end{bmatrix}, \tag{5.19}$$

which preserves the PCH structure. However, with this form, the integral control action is not included in the control law, i.e. the integral control term is not attainable from the augmented system. To solve this, some methods have recently been reported in literature where the integral action is admitted by means of coordinates transformation such as using canonical transformation in [36, 26] or other methods as in [29, 82, 70].

**C) Integral IDA-PBC**

To complete our results in this chapter, we present the extension of the integral IDA-PCB from Subsection 5.3.2 to apply to underactuated PCH systems. The following result is a direct extension of Proposition 5.4.

**Proposition 5.9.** *Consider the separable PCH system (3.1) with $G$ non-full rank. Assume a stabilizing IDA-PBC controller (3.3) is already obtained with the desired (closed-loop) energy function (3.5) and the desired PCH dynamics take the form (5.9). We*

*employ the state transformation (5.6) to realize the augmented closed-loop PCH system*

$$\begin{bmatrix} \dot{x}_q \\ \dot{x}_p \\ \dot{x}_v \end{bmatrix} = \begin{bmatrix} 0 & M^{-1}M_d & -\mathcal{G}K_i \\ -M_dM^{-1} & -R_d & 0 \\ K_i\mathcal{G}^\top & 0 & 0 \end{bmatrix} \begin{bmatrix} \nabla_{x_q}\tilde{H} \\ \nabla_{x_p}\tilde{H} \\ \nabla_{x_v}\tilde{H} \end{bmatrix}, \tag{5.20}$$

*with the Hamiltonian function (5.12) and replacing $G$ with $\mathcal{G}$. Then, asymptotic stability of the equilibrium point $x_e = (q_e, 0, 0)$ is preserved with the integral control*

$$\begin{aligned} v &= -G^+R_dM_d^{-1}M\mathcal{G}x_v \\ \dot{x}_v &= K_i\mathcal{G}^\top\nabla_{x_q}\tilde{H}. \end{aligned} \tag{5.21}$$

*Furthermore, the total control input takes the form*

$$u = u_{IDA} + v + u_p \tag{5.22}$$

*where $u_p = -G^+MK_i\mathcal{G}\dot{x}_v$ is an additional control term which appears through the procedure of finding the feedback controller.* ■

**Proof of Proposition 5.9** is established following the same procedures as in the proof of Proposition 5.4 and involving Remark 5.6. ■

Later in Section 5.5, we will illustrate by example, how this integral control action eliminates the steady-state error.

### 5.3.4 Input-to-State Stability for separable PCH systems using IDA-PBC method

We present our results for the Input-to-State Stability (ISS) control for separable PCH mechanical systems with time-varying disturbances employing IDA-PBC method to obtain the stabilizing controller. First, we present our results for the fully-actuated mechanical systems, and then we present some extensions to deal with the underactuation case.

Consider the PCH system

$$\begin{bmatrix} \dot{q} \\ \dot{p} \end{bmatrix} = \begin{bmatrix} 0 & I_n \\ -I_n & 0 \end{bmatrix} \begin{bmatrix} \nabla_q H \\ \nabla_p H \end{bmatrix} + \begin{bmatrix} 0 \\ G \end{bmatrix} u + \begin{bmatrix} d_1 \\ d_2 \end{bmatrix}. \tag{5.23}$$

The objective is to provide a control method to deal with systems subject to matched, $d_2$, and unmatched, $d_1$, time-varying bounded disturbances. We first discuss the case of matched disturbances where we adopt the integral Input-to-State Stability (iISS) approach, and then we give a general method based on ISS approach to deal with both types of disturbances.

**A) iISS for time-varying matched disturbance**

Interestingly, the system (5.23) subject to matched disturbance $d_2$ ($d_1 = 0$) is *naturally* iISS using the integral control proposed in Proposition 5.4 with the PCH form (5.11) rewritten (to include the disturbance) as:

$$\begin{bmatrix} \dot{x}_q \\ \dot{x}_p \\ \dot{x}_v \end{bmatrix} = \begin{bmatrix} 0 & M^{-1}M_d & -GK_i \\ -M_dM^{-1} & -R_d & 0 \\ K_iG^\top & 0 & 0 \end{bmatrix} \begin{bmatrix} \nabla_{x_q}\tilde{H} \\ \nabla_{x_p}\tilde{H} \\ \nabla_{x_v}\tilde{H} \end{bmatrix} + \begin{bmatrix} 0 \\ d_2 \\ 0 \end{bmatrix}. \tag{5.24}$$

This can be proven by taking

$$\tilde{H} = \frac{1}{2}x_p^\top M_d^{-1}x_p + \frac{1}{2}x_v^\top K_i^{-1}x_v + V(x_q) \tag{5.25}$$

as a candidate iISS-Lyapunov function. The Lyapunov derivative along the trajectories of (5.24) is computed as

$$\begin{aligned} \dot{\tilde{H}} &= x_p^\top M_d^{-1}\dot{x}_p + x_v^\top K_i^{-1}\dot{x}_v + \nabla V^\top(x_q)\dot{x}_q \\ &= -x_p^\top M_d^{-1}R_dM_d^{-1}x_p + x_p^\top M_d^{-1}d_2 \\ &\leq -\lambda_{min}(R_d)|M_d^{-1}x_p|^2 + x_p^\top M_d^{-1}d_2 \end{aligned} \tag{5.26}$$

where $\lambda_{min}(R_d)$ is the smallest non-zero eigenvalue of $R_d$. Using the Young's inequality [82], rewritten as $-\zeta|y|^2 + \eta|y||z| \leq -\frac{\zeta}{2}|y|^2 + \frac{\eta^2}{2\zeta}|z|^2$, this yields

$$\begin{aligned} \dot{\tilde{H}} &\leq -\frac{\lambda_{min}(R_d)}{2}|M_d^{-1}x_p|^2 + \frac{1}{2\lambda_{min}(R_d)}|d_2|^2 \\ &\leq -\alpha(|x_p|) + \sigma(|d_2|), \end{aligned} \tag{5.27}$$

with $\alpha,\ \sigma \in \mathcal{K}_\infty$. The inequality (5.27) proves that the system is smoothly dissipative. Furthermore, the system is zero-state detectable from the output $M_d^{-1}x_p$. This can be shown as follows, from (5.24) and (5.26)

$$d_2 \equiv 0,\ M_d^{-1}x_p \equiv 0 \implies x_p = x_q = x_v = 0.$$

Thus, all conditions of the iISS property [6] are satisfied, which proves that the closed-loop PCH system is iISS w.r.t the matched disturbances.

**B) ISS for time-varying matched and unmatched disturbances**

Here we show the general case when both matched and unmatched disturbances are present. A method to deal with this situation has been recently reported in [82]. However, this method results in a complicated closed-loop system, due to the complex augmented PCH structure and the complex controller. The following proposition shows our new approach, providing a simpler ISS control design method. This approach requires

a change of coordinates on both the positions and momenta states to establish the ISS property.

**Proposition 5.10.** *Consider the separable PCH system (5.23) with time-varying bounded disturbances $d_1(t), d_2(t)$. Define the state transformation*

$$x_q = q - x_v; \qquad x_p = \frac{1}{2}p + x_v \tag{5.28}$$

*to realize the closed-loop system in the new variables $x := [x_q\ x_p\ x_v]$ as*

$$\begin{bmatrix} \dot{x}_q \\ \dot{x}_p \\ \dot{x}_v \end{bmatrix} = \begin{bmatrix} -M^{-1} & M^{-1}M_d & -M^{-1} \\ -M_dM^{-1} & -R_d & -M_dM^{-1} \\ M^{-1} & M^{-1}M_d & -M^{-1} \end{bmatrix} \begin{bmatrix} \nabla_{x_q}\tilde{H} \\ \nabla_{x_p}\tilde{H} \\ \nabla_{x_v}\tilde{H} \end{bmatrix} + \begin{bmatrix} d_1 \\ \frac{1}{2}d_2 \\ 0 \end{bmatrix}, \tag{5.29}$$

*with the desired Hamiltonian function*

$$\tilde{H} = \frac{1}{2}x_p^\top M_d^{-1}x_p + \frac{1}{2}x_v^\top x_v + V(x_q), \tag{5.30}$$

*then the closed-loop system is ISS with respect to the disturbances $d_1$ and $d_2$ and the function (5.25) is the ISS-Lyapunov function for the system (5.29). Furthermore, the control law is obtained as*

$$\begin{aligned} Gu = {} & \nabla_q H - 2(M^{-1} + M_dM^{-1})\nabla_{x_q}\tilde{H} - M^{-1}p - R_dM_d^{-1}p \\ & - 2(R_dM_d^{-1} + M_dM^{-1})x_v \\ \dot{x}_v = {} & M^{-1}\nabla_{x_q}\tilde{H} + \frac{1}{2}M^{-1}p. \end{aligned} \tag{5.31}$$

■

**Proof of Proposition 5.10:** First, we show the coincidence of the positions and momenta states of system (5.23) with their corresponding states in (5.29). For the position states $q$, from (5.28) we have

$$\begin{aligned} \dot{q} &\equiv \dot{x}_q + \dot{x}_v \\ M^{-1}p + d_1 &\equiv -M^{-1}\nabla_{x_q}\tilde{H} + M^{-1}x_p - M^{-1}x_v + d_1 + M^{-1}\nabla_{x_q}\tilde{H} + M^{-1}x_p - M^{-1}x_v \\ &= \frac{1}{2}M^{-1}p + M^{-1}x_v - M^{-1}x_v + d_1 + \frac{1}{2}M^{-1}p + M^{-1}x_v - M^{-1}x_v, \end{aligned}$$

and for the momenta $p$,

$$\begin{aligned} \dot{p} &\equiv 2\dot{x}_p - 2\dot{x}_v \\ Gu - \nabla_q H + d_2 &\equiv -2M_dM^{-1}\nabla_{x_q}\tilde{H} - 2R_d\nabla_{x_p}\tilde{H} - 2M_dM^{-1}\nabla_{x_v}\tilde{H} \\ &\quad - 2M^{-1}\nabla_{x_q}\tilde{H} - 2M^{-1}M_d\nabla_{x_p}\tilde{H} + 2M^{-1}\nabla_{x_v}\tilde{H} + d_2. \end{aligned}$$

Substituting (5.28) and cancelling equal terms but with opposite signs, and rearranging we obtain the control law (5.31). Consider (5.30) as a candidate ISS-Lyapunov function.

Its time-derivative along the trajectories of (5.29) along with (5.28) is given by

$$\begin{aligned}
\dot{\tilde{H}} &= \nabla_{x_p}\tilde{H}^\top \dot{x}_p + x_v^\top \dot{x}_v + \nabla_{x_q}\tilde{H}(x_q)^\top \dot{x}_q \\
&= \nabla_{x_p}\tilde{H}^\top(-M_d M^{-1}\nabla_{x_q}\tilde{H} - R_d\nabla_{x_p}\tilde{H} - M_d M^{-1}\nabla_{x_v}\tilde{H} + d_2) \\
&\quad + \nabla_{x_v}\tilde{H}^\top(M^{-1}\nabla_{x_q}\tilde{H} + M^{-1}M_d\nabla_{x_p}\tilde{H} - M^{-1}\nabla_{x_v}\tilde{H}) \\
&\quad + \nabla_{x_q}\tilde{H}^\top(-M^{-1}\nabla_{x_q}\tilde{H} + M^{-1}M_d\nabla_{x_p}\tilde{H} - M^{-1}\nabla_{x_v}\tilde{H} + d_1) \\
&= -\nabla_{x_p}\tilde{H}^\top R_d\nabla_{x_p}\tilde{H} - \nabla_{x_v}\tilde{H}^\top M^{-1}\nabla_{x_v}\tilde{H} - \nabla_{x_q}\tilde{H}^\top M^{-1}\nabla_{x_q}\tilde{H} + \nabla_{x_p}\tilde{H}^\top d_2 \\
&\quad + \nabla_{x_q}\tilde{H}^\top d_1 \\
&= -x_p^\top M_d^{-1}R_d M_d^{-1}x_p - M^{-1}|\nabla_{x_q}\tilde{H}|^2 - M^{-1}|\nabla_{x_v}\tilde{H}|^2 + x_p^\top M_d^{-1}d_2 + \nabla_{x_q}\tilde{H}^\top d_1 \\
&\leq -\lambda_{min}(R_d)|M_d^{-1}x_p|^2 - \rho|\nabla_{x_q}\tilde{H}|^2 - \rho|\nabla_{x_v}\tilde{H}|^2 + x_p^\top M_d^{-1}d_2 + \nabla_{x_q}V^\top d_1,
\end{aligned}$$

where the constant $\rho$ is such that $\rho I_n \leq M^{-1}(q)$. Applying the Young's inequality, gives

$$\begin{aligned}
\dot{\tilde{H}} &\leq -\frac{\lambda_{min}(R_d)}{2}|M_d^{-1}x_p|^2 + \frac{1}{2\lambda_{min}(R_d)}|d_2|^2 - \frac{\rho}{2}|\nabla_{x_q}\tilde{H}|^2 + \frac{1}{2\rho}|d_1|^2 \\
&\quad - \frac{\rho}{2}|\nabla_{x_v}\tilde{H}|^2 \\
&\leq -\alpha(|x_q, x_p, x_v|) + \sigma(|d|),
\end{aligned} \tag{5.32}$$

Now, from (5.32) and the fact that $\tilde{H}$ function is positive definite, proper and has an isolated minimum (3.6) as a consequence of using IDA-PBC method, all conditions of the ISS property from Theorem 2.14 and Definition 2.16 are satisfied, which proves that the closed-loop PCH system is ISS with respect to the matched and unmatched disturbances.

**Remark 5.11.** Proposition 5.10 can be extended to apply to underactuated PCH mechanical systems by replacing the matrix $G$ in (5.29) with $\mathcal{G}$ as in (5.16), in a similar way as the results in Section 5.3.3.

### 5.3.5 Adaptive IDA-PBC control for separable PCH systems

The implementation of the IDA-PBC controller (3.3) requires the exact knowledge of the system's parameters, essentially the inertia matrix $M$ and the potential energy function $V$. Neglecting parameter uncertainties may cause inaccuracy or instability for the control systems [95]. This motivates the establishment of an adaptive scheme to estimates the uncertainties.

A commonly occurring uncertainties in PCH models is the uncertainty in the potential energy function, thus in the gradient of this function. The linearly parameterized gradient of the potential energy function can then be written as

$$\nabla_q V(q,\theta) = F(q)\theta, \tag{5.33}$$

where the matrix function $F(q)$ is known and the constant vector $\theta$ contains the unknown parameters. Notice that in the IDA-PBC method the *desired* potential energy function $V_d(q)$ (the second term in (3.5)) contains $V(q)$ in its terms. Therefore, the gradient of this function can be written as

$$\nabla_q V_d(q,\theta) = \nabla_q V(q,\theta) + S(q) = F(q)\theta + S(q), \tag{5.34}$$

where $S(q)$ is known as $V_d$ is chosen by design through solving the matching equations. To deal with the class of PCH systems with this type of uncertainty, we propose two adaptive-IDA-PBC control methods. In the first method, the integral action is applied on the passive outputs, while in the second method it is applied on the non-passive outputs and includes a change of coordinates. First we introduce the following assumption.

**Assumption 5.1.** The matrix $F(q)$ is symmetric, i.e. $F(q) = F(q)^\top$.

Assumption 5.1 essentially imposes that the potential energy function $V(q)$ is on the form $V(q) = \sum_{i=1}^{n} V(q_i)$.

**Remark 5.12.** Although we focus here on the uncertainty of the potential energy function $V(q)$, the parameters of this function are also the parameters of the inertia matrix $M$ which forms the kinetic energy function $K = \frac{1}{2}pM^{-1}p$. Thus, there could be uncertainty in the kinetic energy function, which we do not take into account in this case.

### A) Integral control on passive outputs

**Proposition 5.13.** *Consider the separable PCH system (3.1) which can be written on the form* $\dot{x} = f^*(x(t))$, *where* $f^*(x(t))$ *represents the ideal system,* $x = \begin{bmatrix} q \\ p \end{bmatrix}$, *and* $x_e = (q_e, 0)$ *is the equilibrium of the ideal system. Assume that the potential energy function* $V(q,\theta)$ *of the system contains uncertainties, hence its gradient can be represented as in (5.33). Define the augmented closed-loop PCH system as*

$$\begin{bmatrix} \dot{q} \\ \dot{p} \\ \dot{\hat{\theta}} \end{bmatrix} = \begin{bmatrix} 0 & M^{-1}M_d & 0 \\ -M_dM^{-1} & -R_d & QF(q) \\ 0 & -(QF(q))^\top & 0 \end{bmatrix} \begin{bmatrix} \nabla_q H_d \\ \nabla_p H_d \\ \nabla_{\tilde{\theta}} H_d \end{bmatrix}, \tag{5.35}$$

*where* $\hat{\theta}$ *is the estimate of* $\theta$, $\tilde{\theta} = \hat{\theta} - \theta$ *is the estimation error,* $Q = (I_n - M_dM^{-1})$ *and*

$$H_d(q,p,\tilde{\theta}) = \frac{1}{2}p^\top M_d^{-1}p + \frac{1}{2}|\tilde{\theta}|^2 + V_d(q,\theta) \tag{5.36}$$

*is the desired Hamiltonian function. Then, the controller*

$$Gu = F\hat{\theta} - M_dM^{-1}F\hat{\theta} - M_dM^{-1}S - R_dM_d^{-1}p, \tag{5.37}$$

*with the update law*

$$\dot{\hat{\theta}} = -(QF)^\top \nabla_p H_d, \tag{5.38}$$

*stabilizes the system at the equilibrium* $(q_e, 0, \theta)$. ■

**Proof of Proposition 5.13:** Consider the desired Hamiltonian function (5.36) as a candidate Lyapunov function. Its time derivative along the trajectories of (5.35) satisfies

$$\begin{aligned}
\dot{H}_d &= p^\top M_d^{-1}\dot{p} + \tilde{\theta}^\top \dot{\tilde{\theta}} + \nabla_q V_d^\top \dot{q} \\
&= p^\top M_d^{-1}(-M_d M^{-1}\nabla_q V_d - R_d \nabla_p H_d + QF\nabla_{\tilde{\theta}} H_d) - \tilde{\theta}^\top (F^\top Q^\top \nabla_p H_d) \\
&\quad + \nabla_q V_d^\top (M^{-1} M_d \nabla_p H_d) \\
&= -p^\top M^{-1}\nabla_q V_d - p^\top M_d^{-1} R_d M_d^{-1} p + p^\top M_d^{-1} QF\tilde{\theta} - \tilde{\theta}^\top F^\top Q^\top M_d^{-1} p \\
&\quad + \nabla_q V_d^\top M^{-1} p \\
&= -p^\top M^{-1}\nabla_q V_d + (p^\top M^{-1}\nabla_q V_d)^\top + p^\top M_d^{-1} QF\tilde{\theta} - (p^\top M_d^{-1} QF\tilde{\theta})^\top \\
&\quad - p^\top M_d^{-1} R_d M_d^{-1} p \\
&= -p^\top M_d^{-1} R_d M_d^{-1} p \leq -|M_d^{-1} p|^2_{R_d} \leq 0
\end{aligned} \tag{5.39}$$

with $\frac{\partial H_d}{\partial x} f^*(x(t)) \leq 0$. If $\frac{\partial H_d}{\partial x} f^*(x(t)) < 0$, for all $x \neq x_e$, then LaSalle's invariance principle is sufficient to conclude the convergence of the states to their equilibrium. Otherwise, it is necessary to add the following detectability assumption to complete the stability proof [7].

**Assumption 5.2.** *(Detectability)* The trajectories of the system (5.35) are such that $\frac{\partial H_d}{\partial x} f^*(x(t)) \equiv 0$ implies $\lim_{t\to\infty} x(t) = x_e$.

Note that from (5.39), we have $\dot{H}_d = 0 \implies p = 0$. Furthermore, $p \equiv 0 \implies \dot{p} \equiv 0$. Thus, under the dynamics (5.35) yields:

$$\begin{aligned}
\dot{p} &= -M_d M^{-1}\nabla_q V_d - R_d \nabla_p H_d + QF(q)\nabla_{\hat{\theta}} H_d \\
&= -M_d M^{-1}(F\theta + S(q)) - \underbrace{R_d M_d^{-1} p}_{=0} + QF\tilde{\theta} \\
&= -M_d M^{-1}(F\theta + S) + (I_n - M_d M^{-1})F(\hat{\theta} - \theta) \\
&= -M_d M^{-1} F\theta + M_d M^{-1} F\theta - M_d M^{-1} S - M_d M^{-1} F\hat{\theta} + F\hat{\theta} - F\theta \\
&= -M_d M^{-1}(S + F\hat{\theta}) + F(\hat{\theta} - \theta) = 0.
\end{aligned} \tag{5.40}$$

From (5.36) and (5.39), $p \in \mathcal{L}_2 \cap \mathcal{L}_\infty$ and $q, \tilde{\theta} \in \mathcal{L}_\infty$. Therefore, the zero momentum (velocity) may guarantee boundedness of $\tilde{\theta}$ and consequently the convergence of the position states $(q)$ to their desired values, although this could involve steady-state errors. If $\tilde{\theta}$ is very small, which means $\hat{\theta} \approx \theta$, then the term $F(\hat{\theta} - \theta)$ in (5.40) $\approx 0$ which implies that $F\hat{\theta} + S \approx 0$. Since $F\hat{\theta} + S = \nabla_q H_d = 0$, using similar arguments as in the proof of Proposition 5.4, we have

$$\nabla_q H_d \equiv 0 \implies q = q_e.$$

This shows that some asymptotic properties of the proposed design method can be concluded. The adaptive controller (5.37) is obtained by matching the momenta of (3.1) and (5.35), that is

$$\begin{aligned}
-\nabla_q V + Gu &\equiv -M_d M^{-1}\nabla_q V_d - R_d\nabla_p H_d + QF(q)\nabla_{\hat{\theta}} H_d \\
-F\theta + Gu &\equiv -M_d M^{-1}\left(F\theta + S(q)\right) - R_d M_d^{-1} p + (I_n - M_d M^{-1})F(\hat{\theta} - \theta) \\
Gu &\equiv -M_d M^{-1} F\theta - M_d M^{-1} S - R_d M_d^{-1} p + M_d M^{-1} F\theta - M_d M^{-1} F\hat{\theta} \\
&\quad + F\hat{\theta} - F\theta + F\theta \\
Gu &\equiv F\hat{\theta} - M_d M^{-1} F\hat{\theta} - M_d M^{-1} S - R_d M_d^{-1} p.
\end{aligned}$$

Hence, it completes the proof. ■

**B) Integral control on non-passive outputs**

Another method to design an adaptive controller is by applying the integral action on the non-passive outputs. The motivation for this approach is that the IC on passive output cannot guarantee the convergence of the states towards an equilibrium.

Consider the following closed-loop PCH model

$$\begin{bmatrix} \dot{q} \\ \dot{p} \\ \dot{\hat{\theta}} \end{bmatrix} = \begin{bmatrix} 0 & M^{-1}M_d & \mathcal{U} \\ -M_d M^{-1} & -R_d & 0 \\ -\mathcal{U}^\top & 0 & 0 \end{bmatrix} \begin{bmatrix} \nabla_q H_d \\ \nabla_p H_d \\ \nabla_{\tilde{\theta}} H_d \end{bmatrix}. \tag{5.41}$$

Where $\mathcal{U}$ is a symmetric matrix to be defined later. Two problems arise from this method; 1) the update law $\dot{\hat{\theta}} = -\mathcal{U}^\top \nabla_q H_d = -\mathcal{U}^\top(F(q)\theta + S(q))$, is a function of the unknown $\theta$, and 2) the integral action is unattainable from the closed-loop system. To solve these problems we propose a change of coordinates similar to those proposed in the previous sections, aiming at asymptotically stabilizing the uncertain system (3.1) at the equilibrium point $(q_e, 0, \theta)$.

**Proposition 5.14.** *Consider the separable PCH system (3.1). Assume that the potential energy function $V(q,\theta)$ of the system contains uncertainties, hence its gradient can be represented as in (5.33). Define the state transformation*

$$\begin{aligned}
x_q &= q \\
x_p &= p - \mathcal{U}\tilde{\theta} \\
x_{\tilde{\theta}} &= \tilde{\theta},
\end{aligned} \tag{5.42}$$

*to realize the augmented closed-loop PCH system*

$$\begin{bmatrix} \dot{x}_q \\ \dot{x}_p \\ \dot{x}_{\hat{\theta}} \end{bmatrix} = \begin{bmatrix} 0 & M^{-1}M_d & M^{-1}\mathcal{U} \\ -M_d M^{-1} & -R_d & \Lambda \\ -(M^{-1}\mathcal{U})^\top & -\Lambda^\top & -\Upsilon \end{bmatrix} \begin{bmatrix} \nabla_{x_q}\tilde{H} \\ \nabla_{x_p}\tilde{H} \\ \nabla_{x_{\tilde{\theta}}}\tilde{H} \end{bmatrix}. \tag{5.43}$$

*where* $\hat{\theta}$ *is the estimate of* $\theta$, $\tilde{\theta} = \hat{\theta} - \theta$ *is the estimation error,* $\Upsilon = \Upsilon^\top > 0$,

$$\begin{aligned} \Lambda &= F(q) - M_d M^{-1} F(q) - R_d M_d^{-1} \mathcal{U} \\ \Upsilon &= (M^{-1}\mathcal{U})^\top F(q) + \Lambda^\top M_d^{-1} \mathcal{U} \end{aligned} \tag{5.44}$$

*and*

$$\tilde{H}(q, p, \tilde{\theta}) = \frac{1}{2} x_p^\top M_d^{-1} x_p + \frac{1}{2}|\tilde{\theta}|^2 + V(x_q, \theta), \tag{5.45}$$

*is the desired Hamiltonian function. Then, the controller*

$$Gu = F(q)\hat{\theta} - M_d M^{-1} F(q)\hat{\theta} - M_d M^{-1} S(q) - R_d M_d^{-1} p + \mathcal{U}\dot{\hat{\theta}}, \tag{5.46}$$

*with the update law*

$$\dot{x}_{\hat{\theta}} = \dot{\hat{\theta}} = -M^{-1}\mathcal{U} F(q)\hat{\theta} - M^{-1}\mathcal{U} S(q) - \Lambda M_d^{-1} p, \tag{5.47}$$

***asymptotically*** *stabilizes the system at the equilibrium* $(q_e, 0, \theta)$. ■

**Remark 5.15.** The free matrix $\mathcal{U}$ is to be selected such that $\Upsilon$ is symmetric as to preserve the Hamiltonian structure. Note that in (5.44), substituting $\Lambda$ we obtain

$$\begin{aligned} \Upsilon &= (M^{-1}\mathcal{U})^\top F(q) + \Lambda^\top M_d^{-1}\mathcal{U} \\ &= (M^{-1}\mathcal{U})^\top F + (F - M_d M^{-1} F - R_d M_d^{-1}\mathcal{U})^\top M_d^{-1}\mathcal{U} \\ &= (M^{-1}\mathcal{U})^\top F + F M_d^{-1}\mathcal{U} - (M_d M^{-1} F)^\top M_d^{-1}\mathcal{U} - (R_d M_d^{-1}\mathcal{U})^\top M_d^{-1}\mathcal{U} \\ &= (M^{-1}\mathcal{U})^\top F - ((M^{-1}\mathcal{U})^\top F)^\top + F M_d^{-1}\mathcal{U} - (R_d M_d^{-1}\mathcal{U})^\top M_d^{-1}\mathcal{U} \\ &= F M_d^{-1}\mathcal{U} - (R_d M_d^{-1}\mathcal{U})^\top M_d^{-1}\mathcal{U}. \end{aligned} \tag{5.48}$$

For example, choosing $\mathcal{U} = M_d$ we obtain

$$\Upsilon = F M_d^{-1} M_d - (R_d M_d^{-1} M_d)^\top M_d^{-1} M_d = F - R_d.$$

Thus, $\Upsilon = \Upsilon^\top$ as both $F$ and $R_d$ are symmetric.

**Proof of Proposition 5.14:** The proof is established by (i) verifying the coincidence of the position and momenta states of system (3.1) with their corresponding states in (5.43). (ii) Showing that the expression of the update law $\dot{x}_{\hat{\theta}}$ doesn't depend on $\theta$. (iii) Showing that the proposed method achieves asymptotic stability.

(i) For the position states $q$, we have

$$\begin{aligned} \dot{q} &\equiv \dot{x}_q \\ M^{-1} p &\equiv M^{-1} M_d \nabla_{x_p} \tilde{H} + M^{-1}\mathcal{U}\nabla_{x_{\tilde{\theta}}} \tilde{H} = M^{-1} M_d M_d^{-1} x_p + M^{-1}\mathcal{U}\tilde{\theta} \\ &= M^{-1}(p - \mathcal{U}\tilde{\theta}) + M^{-1}\mathcal{U}\tilde{\theta}, \end{aligned}$$

and for the momenta $p$,

$$\begin{aligned}
\dot{p} &\equiv \dot{x}_p + \mathcal{U}\dot{\hat{\theta}} \quad (\dot{\tilde{\theta}} = \dot{\hat{\theta}} \text{ as } \theta \text{ is constant by definition}) \\
-\nabla_q H + Gu &= -M_d M^{-1}\nabla_{x_q}\tilde{H} - R_d\nabla_{x_p}\tilde{H} + \Lambda\nabla_{x_{\tilde{\theta}}}\tilde{H} + \mathcal{U}\dot{\hat{\theta}} \\
-F\theta + Gu &= -M_d M^{-1}(F\theta + S) - R_d M_d^{-1}(p - \mathcal{U}\tilde{\theta}) \\
&\quad + (F - M_d M^{-1}F - R_d M_d^{-1}\mathcal{U})\tilde{\theta} + \mathcal{U}\dot{\hat{\theta}}.
\end{aligned}$$

Using $(\tilde{\theta} = \hat{\theta} - \theta)$ and solving, we obtain (5.46).

(ii) The update law is given by

$$\begin{aligned}
\dot{x}_{\hat{\theta}} &= -M^{-1}\mathcal{U}\nabla_{x_q}\tilde{H} - \Lambda\nabla_{x_p}\tilde{H} - \Upsilon\nabla_{x_{\tilde{\theta}}}\tilde{H} \\
&= -M^{-1}\mathcal{U}(F\theta + S) - \Lambda M_d^{-1}(p - \mathcal{U}\tilde{\theta}) - (M^{-1}\mathcal{U}F + \Lambda M_d^{-1}\mathcal{U})\tilde{\theta} \\
&= -M^{-1}\mathcal{U}(F\theta + S) - \Lambda M_d^{-1}p + \Lambda M_d^{-1}\mathcal{U}\tilde{\theta} - M^{-1}\mathcal{U}F\tilde{\theta} - \Lambda M_d^{-1}\mathcal{U}\tilde{\theta} \\
&= -M^{-1}\mathcal{U}F\theta - M^{-1}\mathcal{U}S - \Lambda M_d^{-1}p - M^{-1}\mathcal{U}F\tilde{\theta}.
\end{aligned} \tag{5.49}$$

Substituting $(\tilde{\theta} = \hat{\theta} - \theta)$ in the last row in (5.49), yields

$$\dot{x}_{\hat{\theta}} = -M^{-1}\mathcal{U}F\theta - M^{-1}\mathcal{U}S - \Lambda M_d^{-1}p - M^{-1}\mathcal{U}F\hat{\theta} + M^{-1}\mathcal{U}F\theta.$$

Cancelling equal terms but with opposite signs, we obtain (5.47).

(iii) Consider the function (5.45), whose time-derivative along the trajectories of (5.43) along with (5.42) is

$$\begin{aligned}
\dot{\tilde{H}} &= (\nabla_{x_p}\tilde{H})^\top\dot{x}_p + (\nabla_{x_{\tilde{\theta}}}\tilde{H})^\top\dot{x}_{\hat{\theta}} + (\nabla_{x_q}\tilde{H})^\top\dot{x}_q \\
&= \nabla_{x_p}\tilde{H}^\top(-M_d M^{-1}\nabla_{x_q}\tilde{H} - R_d\nabla_{x_p}\tilde{H} + \Lambda\nabla_{x_{\tilde{\theta}}}\tilde{H}) \\
&\quad + \nabla_{x_{\tilde{\theta}}}\tilde{H}^\top(-M^{-1}\mathcal{U}\nabla_{x_q}\tilde{H} - \Lambda\nabla_{x_p}\tilde{H} - \Upsilon\nabla_{x_{\tilde{\theta}}}\tilde{H}) \\
&\quad + \nabla_{x_q}\tilde{H}^\top(M^{-1}M_d\nabla_{x_p}\tilde{H} + M^{-1}\mathcal{U}\nabla_{x_{\tilde{\theta}}}\tilde{H}) \\
&= -\nabla_{x_p}\tilde{H}^\top M_d M^{-1}\nabla_{x_q}\tilde{H} - \nabla_{x_p}\tilde{H}^\top R_d\nabla_{x_p}\tilde{H} + \nabla_{x_p}\tilde{H}^\top\Lambda\nabla_{x_{\tilde{\theta}}}\tilde{H} \\
&\quad - \nabla_{x_{\tilde{\theta}}}\tilde{H}^\top M^{-1}\mathcal{U}\nabla_{x_q}\tilde{H} - \nabla_{x_{\tilde{\theta}}}\tilde{H}^\top\Lambda\nabla_{x_p}\tilde{H} - \nabla_{x_{\tilde{\theta}}}\tilde{H}^\top\Upsilon\nabla_{x_{\tilde{\theta}}}\tilde{H} \\
&\quad + \nabla_{x_q}\tilde{H}^\top M^{-1}M_d\nabla_{x_p}\tilde{H} + \nabla_{x_q}\tilde{H}^\top M^{-1}\mathcal{U}\nabla_{x_{\tilde{\theta}}}\tilde{H}.
\end{aligned} \tag{5.50}$$

Taking the transpose of the terms $\nabla_{x_q}\tilde{H}^\top M^{-1}M_d\nabla_{x_p}\tilde{H}$, $\nabla_{x_{\tilde{\theta}}}\tilde{H}^\top\Lambda\nabla_{x_p}\tilde{H}$ and $\nabla_{x_q}\tilde{H}^\top M^{-1}\mathcal{U}\nabla_{x_{\tilde{\theta}}}\tilde{H}$ and rearranging, yields

$$\begin{aligned}\dot{\tilde{H}} &= -\nabla_{x_p}\tilde{H}^\top M_d M^{-1}\nabla_{x_q}\tilde{H} + (\nabla_{x_p}\tilde{H}^\top M_d M^{-1}\nabla_{x_q}\tilde{H})^\top - \nabla_{x_p}\tilde{H}^\top R_d\nabla_{x_p}\tilde{H}\\ &\quad + \nabla_{x_p}\tilde{H}^\top\Lambda\nabla_{x_{\tilde{\theta}}}\tilde{H} - (\nabla_{x_p}\tilde{H}^\top\Lambda\nabla_{x_{\tilde{\theta}}}\tilde{H})^\top - \nabla_{x_{\tilde{\theta}}}\tilde{H}^\top\Upsilon\nabla_{x_{\tilde{\theta}}}\tilde{H}\\ &\quad - \nabla_{x_{\tilde{\theta}}}\tilde{H}^\top M^{-1}\mathcal{U}\nabla_{x_q}\tilde{H} + (-\nabla_{x_{\tilde{\theta}}}\tilde{H}^\top M^{-1}\mathcal{U}\nabla_{x_q}\tilde{H})^\top\\ &= -\nabla_{x_p}\tilde{H}^\top R_d\nabla_{x_p}\tilde{H} - \nabla_{x_{\tilde{\theta}}}\tilde{H}^\top\Upsilon\nabla_{x_{\tilde{\theta}}}\tilde{H}\\ &\leq -|\nabla_{x_p}\tilde{H}|^2_{R_d} - |\nabla_{x_{\tilde{\theta}}}\tilde{H}|^2_{\Upsilon}.\end{aligned} \tag{5.51}$$

Thus, the system (5.43) has a stable equilibrium at $(q_e, 0, \theta)$ with $x_p, x_{\tilde{\theta}} \in \mathcal{L}_2 \cap \mathcal{L}_\infty$. The convergence of the states is established invoking the following practical corollary of Barbalat's lemma [7]:

**Corollary 5.16.** *Consider a function $\phi : \mathbb{R}_{\geq 0} \to \mathbb{R}$ and suppose that $\phi(t) \in \mathcal{L}_2 \cap \mathcal{L}_\infty$ and $\dot{\phi}(t) \in \mathcal{L}_\infty$. Then $\lim_{t\to\infty}\phi(t) = 0$.* ■

Applying Corollary 5.16, implies the convergence of states $x_p$ and $x_{\tilde{\theta}}$ to zero ($x_p, x_{\tilde{\theta}} \to 0$ as $t \to \infty$). Moreover, $\tilde{\theta} = 0 \implies \hat{\theta} = \theta$. Finally, the convergence of the states $x_q$ to their desired states is established as follows:

$x_p, x_{\tilde{\theta}} \equiv 0 \implies \dot{x}_p, \dot{\tilde{\theta}} \equiv 0$. Thus, under the dynamics of (5.43) yields:

$$\begin{aligned}\dot{x}_p &= -M_d M^{-1}\nabla_{x_q}\tilde{H} - R_d\nabla_{x_p}\tilde{H} + \Lambda\nabla_{x_{\tilde{\theta}}}\tilde{H} = 0\\ &= -M_d M^{-1}\nabla_{x_q}\tilde{H} - \underbrace{R_d M_d^{-1}x_p}_{=0} + \underbrace{\Lambda\tilde{\theta}}_{=0} = 0\\ &= -M_d M^{-1}\nabla_{x_q}\tilde{H} = 0.\end{aligned} \tag{5.52}$$

This implies $\nabla_{x_q}\tilde{H} = 0$. Invoking similar arguments to those in the proof of Proposition 5.4, we obtain

$$\nabla_{x_q}\tilde{H} \equiv 0 \implies x_q = q_e.$$

Since all trajectories converge to their desired values, we can conclude that the closed-loop system (5.43) has an *asymptotically* stable equilibrium at $(q_e, 0, \theta)$. ■

## 5.4 Robust Control of Non-separable Hamiltonian Systems

In this section, we extend our results in Section 5.3 to deal with non-separable PCH systems. In this case, as $M$ and $M_d$ are functions of $q$, their derivatives need to be taken into account in the construction of the control law. Fortunately, our approaches do not require significant changes in the interconnection matrices (thus the augmented closed-loop PCH models) which have been constructed from their separable counterparts (in [82] significant changes applied). As expected, more complicated control laws are obtained

as a consequence. Before we state the results, we show some necessary differentiations that are used throughout the proof of results. Similar to (5.6), we start by defining

$$\begin{aligned} x_p &= p + \mathcal{P} \\ \mathcal{P} &= M(x_q)Gx_v. \end{aligned} \tag{5.53}$$

The derivative is obviously

$$\dot{x}_p = \dot{p} + \dot{\mathcal{P}}, \tag{5.54}$$

while $\dot{x}_p$ and $\dot{p}$ are obtained directly from the PCH model. The term $\dot{\mathcal{P}}$ is calculated as

$$\begin{aligned} \dot{\mathcal{P}} &= \dot{M}Gx_v + MG\dot{x}_v, \\ \dot{M}Gx_v &= \sum_{i=1}^{n} (\nabla_{q_i} MGx_v)(e_i^\top \dot{x}_q). \end{aligned} \tag{5.55}$$

Second, given non-constant $M(x_q)$ and $M_d(x_q)$, the derivative of the Hamiltonian function

$$\tilde{H} = \frac{1}{2} x_p^\top M_d^{-1}(x_q) x_p + \frac{1}{2} x_v^\top K_i^{-1} x_v + V(x_q), \tag{5.56}$$

becomes

$$\begin{aligned} \dot{\tilde{H}} &= (\nabla_{x_p} \tilde{H})^\top \dot{x}_p + (\nabla_{x_v} \tilde{H})^\top \dot{x}_v + (\nabla_{x_q} \tilde{H})^\top \dot{x}_q \\ &= x_p^\top M_d^{-1} \dot{x}_p + x_v^\top K_i^{-1} \dot{x}_v + \left( \nabla_{x_q} V_x^\top + \frac{1}{2} \sum_{i=1}^{n} e_i x_p^\top \nabla_{q_i} M_d^{-1} x_p \right) \dot{x}_q, \end{aligned} \tag{5.57}$$

where the derivative of $M_d$ is now taken into account.

### 5.4.1 Integral IDA-PBC for non-separable PCH systems

**Proposition 5.17.** *Consider the non-separable PCH system (3.1). Assume a stabilizing IDA-PBC controller (3.3) has already been obtained with the desired (closed-loop) energy function (3.5) and the desired PCH dynamics take the form*

$$\begin{bmatrix} \dot{q} \\ \dot{p} \end{bmatrix} = \begin{bmatrix} 0 & M^{-1}(q) M_d(q) \\ -M_d(q) M^{-1}(q) & J_2 - R_d \end{bmatrix} \begin{bmatrix} \nabla_q H_d \\ \nabla_p H_d \end{bmatrix} + \begin{bmatrix} 0 \\ G \end{bmatrix} v. \tag{5.58}$$

*Defining the state transformation (5.6) to realize the augmented closed-loop PCH system*

$$\begin{bmatrix} \dot{x}_q \\ \dot{x}_p \\ \dot{x}_v \end{bmatrix} = \begin{bmatrix} 0 & M^{-1}(x_q) M_d(x_q) & -GK_i \\ -M_d(x_q) M^{-1}(x_q) & J_2 - R_d & 0 \\ K_i G^\top & 0 & 0 \end{bmatrix} \begin{bmatrix} \nabla_{x_q} \tilde{H} \\ \nabla_{x_p} \tilde{H} \\ \nabla_{x_v} \tilde{H} \end{bmatrix}, \tag{5.59}$$

*with the Hamiltonian function (5.56), asymptotic stability of the equilibrium point* $x_e = (x_{qe}, 0, 0) = (q_e, 0, 0)$ *is preserved with the integral control*

$$\begin{aligned} Gv = &-\frac{1}{2}M_d M^{-1}\sum_{i=1}^{n} e_i p^\top \nabla_{q_i} M_d^{-1} M G x_v - \frac{1}{2}M_d M^{-1}\sum_{i=1}^{n} e_i x_v^\top G M \nabla_{q_i} M_d^{-1} p \\ &- \frac{1}{2}M_d M^{-1}\sum_{i=1}^{n} e_i x_v^\top G M \nabla_{q_i} M_d^{-1} M G x_v + (J_2 - R_d) M_d^{-1} M G x_v \\ &- \sum_{i=1}^{n}\left(\frac{\partial M}{\partial x_{q_i}} G x_v\right)(e_i^\top \dot{x}_q) - M G \dot{x}_v \end{aligned} \tag{5.60}$$

*and* $\dot{x}_v = K_i G^\top \nabla_{x_q} \tilde{H}$. ■

**Proof of Proposition 5.17:** The proof can be established following the same procedures as in the proof of Proposition 5.4. The time derivative of the Hamiltonian function (5.56) along the trajectories of the system is

$$\begin{aligned} \dot{\tilde{H}} &= (\nabla_{x_p}\tilde{H})^\top \dot{x}_p + (\nabla_{x_v}\tilde{H})^\top \dot{x}_v + (\nabla_{x_q}\tilde{H})^\top \dot{x}_q \\ &= -(\nabla_{x_p}\tilde{H})^\top M_d M^{-1} \nabla_{x_q}\tilde{H} + (\nabla_{x_p}\tilde{H})^\top J_2 \nabla_{x_p}\tilde{H} - (\nabla_{x_p}\tilde{H})^\top R_d \nabla_{x_p}\tilde{H} \\ &\quad + (\nabla_{x_v}\tilde{H})^\top K_i G^\top \nabla_{x_q}\tilde{H} + (\nabla_{x_q}\tilde{H})^\top M^{-1} M_d \nabla_{x_p}\tilde{H} - (\nabla_{x_q}\tilde{H})^\top G K_i \nabla_{x_v}\tilde{H}. \end{aligned}$$

Taking a transpose of certain terms (to cancel out equal terms with different signs) and rearranging:

$$\begin{aligned} \dot{\tilde{H}} &= -(\nabla_{x_p}\tilde{H})^\top M_d M^{-1} \nabla_{x_q}\tilde{H} + \left((\nabla_{x_p}\tilde{H})^\top M_d M^{-1} \nabla_{x_q}\tilde{H}\right)^\top \\ &\quad + (\nabla_{x_v}\tilde{H})^\top K_i G^\top \nabla_{x_q}\tilde{H} - \left((\nabla_{x_v}\tilde{H})^\top K_i G^\top \nabla_{x_q}\tilde{H}\right)^\top \\ &\quad + (\nabla_{x_p}\tilde{H})^\top J_2 \nabla_{x_p}\tilde{H} - (\nabla_{x_p}\tilde{H})^\top R_d \nabla_{x_p}\tilde{H} \\ &= (\nabla_{x_p}\tilde{H})^\top J_2 \nabla_{x_p}\tilde{H} - (\nabla_{x_p}\tilde{H})^\top R_d \nabla_{x_p}\tilde{H} \\ &= -x_p^\top M_d^{-1} R_d M_d^{-1} x_p \leq 0. \end{aligned}$$

Note that because $J_2 = -J_2^\top$, the term $(\nabla_{x_p}\tilde{H})^\top J_2 \nabla_{x_p}\tilde{H}$ is equal to zero. Furthermore, asymptotic stability is concluded by applying LaSalle's invariance principle:

$$-x_p^\top M_d^{-1} R_d M_d^{-1} x_p = 0 \implies x_p \equiv 0 \implies \dot{x}_p \equiv 0 \implies M_d(x_q) M^{-1}(x_q) \nabla_{x_q}\tilde{H} = 0.$$

Given $M(x_q), M_d(x_q) > 0$, then we have $\nabla_{x_q}\tilde{H} = 0$ which is only true if the system converges to its equilibrium point $q_e$. Thus,

$$\nabla_{x_q}\tilde{H} \equiv 0 \implies x_q = q_e \text{ and } x_v = 0,$$

which proves that this equilibrium is *asymptotically* stable. The controller is obtained by matching the momenta of (5.58) and (5.59) along with the change of coordinates

(5.6) and its time derivative (5.54), we get

$$\begin{aligned}\dot{p} &= -M_d M^{-1}\nabla_q H_d + J_2\nabla_p H_d - R_d\nabla_p H_d + Gv \\ &\equiv \dot{x}_p - \dot{\mathcal{P}} \\ &= -M_d M^{-1}\nabla_{x_q}\tilde{H} + (J_2 - R_d)\nabla_{x_p}\tilde{H} - \dot{\mathcal{P}}.\end{aligned} \tag{5.61}$$

Rearranging the terms,

$$\begin{aligned}&-\frac{1}{2}M_d M^{-1}\sum_{i=1}^{n} e_i p^\top \nabla_{q_i} M_d^{-1} p - M_d M^{-1}\nabla_q V_d + (J_2 - R_d)M_d^{-1}p + Gv \\ &\equiv -\frac{1}{2}M_d M^{-1}\sum_{i=1}^{n} e_i x_p^\top \nabla_{q_i} M_d^{-1} x_p - M_d M^{-1}\nabla_q V_d + (J_2 - R_d)M_d^{-1}x_p - \dot{\mathcal{P}}.\end{aligned} \tag{5.62}$$

Now, substituting (5.53) and (5.55) in (5.62 ) and computing we obtain

$$\begin{aligned}&-\frac{1}{2}M_d M^{-1}\sum_{i=1}^{n} e_i p^\top \nabla_{q_i} M_d^{-1} p - M_d M^{-1}\nabla_q V_d + J_2 M_d^{-1}p - R_d M_d^{-1}p + Gv \\ &\equiv -\frac{1}{2}M_d M^{-1}(p^\top \nabla_q M_d^{-1} p) - \frac{1}{2}M_d M^{-1}\sum_{i=1}^{n} e_i p^\top (\nabla_{q_i} M_d^{-1})MGx_v \\ &\quad -\frac{1}{2}M_d M^{-1}\left(\sum_{i=1}^{n} e_i x_v^\top GM(\nabla_{q_i} M_d^{-1})p + \sum_{i=1}^{n} e_i x_v^\top GM(\nabla_{q_i} M_d^{-1})MGx_v\right) \\ &\quad - M_d M^{-1}\nabla_q V_d + (J_2 - R_d)M_d^{-1}p + (J_2 - R_d)M_d^{-1}MGx_v \\ &\quad -\sum_{i=1}^{n}\left(\frac{\partial M}{\partial x_{q_i}}Gx_v\right)(e_i^\top \dot{x}_q) - MG\dot{x}_v.\end{aligned} \tag{5.63}$$

Cancelling equal terms on the left-hand side and right-hand side of (5.63), we get the control law (5.60) and thus the proof is completed. ∎

### 5.4.2 Input-to-State-Stability for non-separable PCH systems using IDA-PBC method

#### A) iISS for time-varying matched disturbance

**Proposition 5.18.** *The PCH system (5.23) subject to matched disturbance $d_2$ only, is* naturally *iISS using the integral control proposed in Proposition 5.17 with the augmented PCH form (5.59) rewritten (to include the disturbance) as:*

$$\begin{bmatrix}\dot{x}_q \\ \dot{x}_p \\ \dot{x}_v\end{bmatrix} = \begin{bmatrix}0 & M^{-1}(x_q)M_d(x_q) & -GK_i \\ -M_d(x_q)M^{-1}(x_q) & J_2 - R_d & 0 \\ K_i G^\top & 0 & 0\end{bmatrix}\begin{bmatrix}\nabla_{x_q}\tilde{H} \\ \nabla_{x_p}\tilde{H} \\ \nabla_{x_v}\tilde{H}\end{bmatrix} + \begin{bmatrix}0 \\ d_2 \\ 0\end{bmatrix}, \tag{5.64}$$

*with the Hamiltonian function (5.56).* ∎

**Proof of Proposition 5.18:** This can be proved following similar procedures in Subsection (5.3.4) and Proposition 5.17. That is, by taking (5.56) as the candidate of the iISS-Lyapunov function, its derivative along the trajectories of (5.64) is computed as

$$\begin{aligned}
\dot{\tilde{H}} &= x_p^\top M_d^{-1}\dot{x}_p + x_v^\top K_i^{-1}\dot{x}_v + \left(\nabla_{x_q} V_x^\top + \frac{1}{2}\sum_{i=1}^{n} e_i x_p^\top \nabla_{q_i} M_d^{-1} x_p\right)\dot{x}_q \\
&= -x_p^\top M_d^{-1} R_d M_d^{-1} x_p + x_p^\top M_d^{-1} d_2 \leq -\lambda_{min}(R_d)|M_d^{-1}x_p|^2 + x_p^\top M_d^{-1} d_2 \\
\dot{\tilde{H}} &\leq -\frac{\lambda_{min}(R_d)}{2}|M_d^{-1}x_p|^2 + \frac{1}{2\lambda_{min}(R_d)}|d_2|^2 \\
&\leq -\alpha(|x_p|) + \sigma(|d_2|).
\end{aligned}$$

with $\alpha,\ \sigma \in \mathcal{K}_\infty$. This inequality proves that the system is smoothly dissipative. Furthermore, the system is zero-state detectable from the output $M_d^{-1}x_p$. This can be shown as follows, from (5.64) $d_2 \equiv 0$, $M_d^{-1}x_p \equiv 0 \implies x_p = x_q = x_v = 0$. Thus, all conditions of the iISS property [6] are satisfied, which proves that the closed-loop PCH system is iISS w.r.t the matched disturbances.

### B) ISS for time-varying matched and unmatched disturbances

**Proposition 5.19.** *Consider the non-separable PCH system (5.23) with time-varying bounded disturbances $d_1(t), d_2(t)$. Define the state transformation*

$$x_q = q - x_v; \qquad x_p = \frac{1}{2}p + x_v \tag{5.65}$$

*to realize the closed-loop system in the new variables $x := [x_q\ x_p\ x_v]$ as*

$$\begin{bmatrix}\dot{x}_q\\ \dot{x}_p\\ \dot{x}_v\end{bmatrix} = \begin{bmatrix} -M^{-1}(x_q) & M^{-1}M_d(x_q) & -M^{-1}(x_q)\\ -M_dM^{-1}(x_q) & J_2 - R_d & -M_dM^{-1}(x_q)\\ M^{-1}(x_q) & M^{-1}M_d(x_q) & -M^{-1}(x_q)\end{bmatrix}\begin{bmatrix}\nabla_{x_q}\tilde{H}\\ \nabla_{x_p}\tilde{H}\\ \nabla_{x_v}\tilde{H}\end{bmatrix} + \begin{bmatrix} d_1\\ \frac{d_2}{2}\\ 0\end{bmatrix}, \tag{5.66}$$

*with the desired Hamiltonian function*

$$\tilde{H} = \frac{1}{2}x_p^\top M_d^{-1}(x_q)x_p + \frac{1}{2}x_v^\top x_v + V(x_q), \tag{5.67}$$

*then the closed-loop system is ISS with respect to the disturbances $d_1$ and $d_2$ and the function (5.56) is the ISS-Lyapunov function for the system (5.66). Furthermore, the control law is obtained as*

$$\begin{aligned}
Gu &= \nabla_q H - 2(M^{-1} + M_dM^{-1})\nabla_{x_q}\tilde{H} + (J_2 - R_d)M_d^{-1}p - M^{-1}p \\
&\quad + 2(J_2 - R_d)M_d^{-1}x_v - 2M_dM^{-1}x_v - M^{-1}x_v \\
\dot{x}_v &= M^{-1}\nabla_{x_q}\tilde{H} + \frac{1}{2}M^{-1}p,
\end{aligned} \tag{5.68}$$

■

**Proof of Proposition 5.19:** Consider the desired Hamiltonian function (5.67) as a candidate ISS-Lyapunov function. Its time-derivative along the trajectories of (5.66) along with (5.65) is given by

$$\begin{aligned}
\dot{\tilde{H}} &= \nabla_{x_p}\tilde{H}^\top \dot{x}_p + x_v^\top \dot{x}_v + \nabla_{x_q}\tilde{H}(x_q)^\top \dot{x}_q \\
&= \nabla_{x_p}\tilde{H}^\top(-M_d M^{-1}\nabla_{x_q}\tilde{H}(J_2 - R_d)\nabla_{x_p}\tilde{H} - M_d M^{-1}\nabla_{x_v}\tilde{H} + d_2) \\
&\quad + \nabla_{x_v}\tilde{H}^\top(M^{-1}\nabla_{x_q}\tilde{H} + M^{-1}M_d\nabla_{x_p}\tilde{H} - M^{-1}\nabla_{x_v}\tilde{H}) \\
&\quad + \nabla_{x_q}\tilde{H}^\top(-M^{-1}\nabla_{x_q}\tilde{H} + M^{-1}M_d\nabla_{x_p}\tilde{H} - M^{-1}\nabla_{x_v}\tilde{H} + d_1) \\
&= \nabla_{x_p}\tilde{H}^\top J_2\nabla_{x_p}\tilde{H} - \nabla_{x_p}\tilde{H}^\top R_d\nabla_{x_p}\tilde{H} - \nabla_{x_v}\tilde{H}^\top M^{-1}\nabla_{x_v}\tilde{H} - \nabla_{x_q}\tilde{H}^\top M^{-1}\nabla_{x_q}\tilde{H} \\
&\quad + \nabla_{x_p}\tilde{H}^\top d_2 + \nabla_{x_q}\tilde{H}^\top d_1 \\
&= -x_p^\top M_d^{-1}R_d M_d^{-1}x_p - M^{-1}|\nabla_{x_q}\tilde{H}|^2 - M^{-1}|\nabla_{x_v}\tilde{H}|^2 + x_p^\top M_d^{-1}d_2 + \nabla_{x_q}\tilde{H}^\top d_1 \\
&\leq -\lambda_{min}(R_d)|M_d^{-1}x_p|^2 - \rho|\nabla_{x_q}\tilde{H}|^2 - \rho|\nabla_{x_v}\tilde{H}|^2 + x_p^\top M_d^{-1}d_2 + \nabla_{x_q}V^\top d_1,
\end{aligned}$$

where the constant $\rho$ is such that $\rho I_n \leq M^{-1}(q)$, and the term $\nabla_{x_p}\tilde{H}^\top J_2\nabla_{x_p}\tilde{H} = 0$ due to $J_2 = -J_2^\top$. Applying the Young's inequality, gives

$$\begin{aligned}
\dot{\tilde{H}} &\leq -\frac{\lambda_{min}(R_d)}{2}|M_d^{-1}x_p|^2 + \frac{1}{2\lambda_{min}(R_d)}|d_2|^2 - \frac{\rho}{2}|\nabla_{x_q}\tilde{H}|^2 + \frac{1}{2\rho}|d_1|^2 \\
&\quad - \frac{\rho}{2}|\nabla_{x_v}\tilde{H}|^2 \\
&\leq -\alpha(|x_q, x_p, x_v|) + \sigma(|d|),
\end{aligned} \tag{5.69}$$

Now, from (5.69) and the fact that $\tilde{H}$ function is positive definite, proper and has an isolated minimum (3.6) as a consequence of using IDA-PBC method, all conditions of the ISS property from Theorem 2.14 and Definition 2.16 are satisfied, which proves that the closed-loop PCH system is ISS with respect to the matched and unmatched disturbances.

### 5.4.3 Adaptive IDA-PBC control for non-separable PCH systems

#### A) Integral control on passive outputs

**Proposition 5.20.** *Consider the non-separable PCH system (3.1) which can be written on the form* $\dot{x} = f^*(x(t))$*, where* $f^*(x(t))$ *represents the ideal system,* $x = \begin{bmatrix} q \\ p \end{bmatrix}$*, and* $x_e = (q_e, 0)$ *is the equilibrium of the ideal system. Assume that the potential energy function* $V(q,\theta)$ *of the system contains uncertainties, hence its gradient can be represented as in (5.33). Define the augmented closed-loop PCH system as*

$$\begin{bmatrix} \dot{q} \\ \dot{p} \\ \dot{\hat{\theta}} \end{bmatrix} = \begin{bmatrix} 0 & M^{-1}(q)M_d(q) & 0 \\ -M_d(q)M^{-1}(q) & J_2 - R_d & Q(q)F(q) \\ 0 & -(Q(q)F(q))^\top & 0 \end{bmatrix} \begin{bmatrix} \nabla_q H_d \\ \nabla_p H_d \\ \nabla_{\tilde{\theta}} H_d \end{bmatrix}, \tag{5.70}$$

*where* $\hat{\theta}$ *is the estimate of* $\theta$, $\tilde{\theta} = \hat{\theta} - \theta$ *is the estimation error,*

$Q = (I_n - M_d M^{-1})$ *and*

$$H_d(q, p, \tilde{\theta}) = \frac{1}{2} p^\top M_d^{-1}(q) p + \frac{1}{2}|\tilde{\theta}|^2 + V_d(q, \theta) \tag{5.71}$$

*is the desired Hamiltonian function. Then, the controller*

$$\begin{aligned} Gu = {} & F\hat{\theta} + \frac{1}{2}\sum_{i=1}^{n} e_i p^\top \nabla_{q_i} M^{-1} p - M_d M^{-1} F\hat{\theta} - \frac{1}{2} M_d M^{-1} \sum_{i=1}^{n} e_i p^\top \nabla_{q_i} M_d^{-1} p \\ & - M_d M^{-1} S + (J_2 - R_d) M_d^{-1} p, \end{aligned} \tag{5.72}$$

*with the update law*

$$\dot{\hat{\theta}} = -(QF)^\top \nabla_p H_d, \tag{5.73}$$

*stabilizes the system at the equilibrium* $(q_e, 0, \theta)$. ■

**Proof of Proposition 5.20:** Consider the desired Hamiltonian function (5.71) as a candidate Lyapunov function. Its time derivative along the trajectories of (5.70) satisfies

$$\begin{aligned} \dot{H}_d &= p^\top M_d^{-1}(q)\dot{p} + \tilde{\theta}^\top \dot{\tilde{\theta}} + \nabla_q H_d^\top \dot{q} \\ &= p^\top M_d^{-1}(-M_d M^{-1}\nabla_q H_d + J_2 \nabla_p H_d - R_d \nabla_p H_d + QF\nabla_{\tilde{\theta}} H_d) - \tilde{\theta}^\top (F^\top Q^\top \nabla_p H_d) \\ &\quad + \nabla_q H_d^\top (M^{-1} M_d \nabla_p H_d) \\ &= -p^\top M^{-1}\nabla_q H_d + p^\top M_d^{-1} J_2 M_d^{-1} p - p^\top M_d^{-1} R_d M_d^{-1} p + p^\top M_d^{-1} QF\tilde{\theta} \\ &\quad - \tilde{\theta}^\top F^\top Q^\top M_d^{-1} p + \nabla_q H_d^\top M^{-1} p. \end{aligned}$$

Taking the transpose of certain terms and rearranging, yields

$$\begin{aligned} \dot{H}_d &= -p^\top M^{-1}\nabla_q H_d + (p^\top M^{-1}\nabla_q H_d)^\top + p^\top M_d^{-1} QF\tilde{\theta} - (p^\top M_d^{-1} QF\tilde{\theta})^\top \\ &\quad - p^\top M_d^{-1} R_d M_d^{-1} p \\ &= -p^\top M_d^{-1} R_d M_d^{-1} p \le -|M_d^{-1} p|^2_{R_d} \le 0. \end{aligned} \tag{5.74}$$

The stability proof can be established following the same procedures as in the proof of Proposition 5.13. The adaptive controller (5.72) is obtained by matching the momenta of (3.1) and (5.70), that is

$$\begin{aligned} & -\nabla_q H + Gu \equiv -M_d M^{-1}\nabla_q H_d + (J_2 - R_d)\nabla_p H_d + QF(q)\nabla_{\tilde{\theta}} H_d \\ & -F\theta - \frac{1}{2}\sum_{i=1}^{n} e_i p^\top \nabla_{q_i} M^{-1} p + Gu \equiv -M_d M^{-1}(F\theta + S(q)) + (J_2 - R_d) M_d^{-1} p \\ & \quad - \frac{1}{2} M_d M^{-1} \sum_{i=1}^{n} e_i p^\top \nabla_{q_i} M_d^{-1} p + (I_n - M_d M^{-1}) F(\hat{\theta} - \theta), \end{aligned}$$

Rearranging and using $\tilde{\theta} = \hat{\theta} - \theta$, yields

$$Gu \equiv -M_d M^{-1} F\theta - M_d M^{-1} S + \frac{1}{2}\sum_{i=1}^{n} e_i p^\top \nabla_{q_i} M^{-1} p + (J_2 - R_d) M_d^{-1} p + M_d M^{-1} F\theta$$
$$- M_d M^{-1} F\hat{\theta} + F\hat{\theta} - F\theta + F\theta - \frac{1}{2} M_d M^{-1} \sum_{i=1}^{n} e_i p^\top \nabla_{q_i} M_d^{-1} p.$$

Cancelling like terms but with opposite signs, we obtain the controller

$$Gu \equiv F\hat{\theta} + \frac{1}{2}\sum_{i=1}^{n} e_i p^\top \nabla_{q_i} M^{-1} p - M_d M^{-1} F\hat{\theta} - \frac{1}{2} M_d M^{-1} \sum_{i=1}^{n} e_i p^\top \nabla_{q_i} M_d^{-1} p$$
$$- M_d M^{-1} S + (J_2 - R_d) M_d^{-1} p.$$

Hence, it completes the proof. ∎

**B) Integral control on non-passive outputs**

**Proposition 5.21.** *Consider the nonseparable PCH system (3.1). Assume that the potential energy function $V(q,\theta)$ of the system contains uncertainties, hence its gradient can be represented as in (5.33). Define the state transformation*

$$\begin{aligned} x_q &= q \\ x_p &= p - \mathcal{U}\tilde{\theta} \\ x_{\tilde{\theta}} &= \tilde{\theta}, \end{aligned} \tag{5.75}$$

*to realize the augmented closed-loop PCH system*

$$\begin{bmatrix} \dot{x}_q \\ \dot{x}_p \\ \dot{x}_{\hat{\theta}} \end{bmatrix} = \begin{bmatrix} 0 & M^{-1}(x_q) M_d(x_q) & M^{-1}(x_q)\mathcal{U} \\ -M_d(x_q) M^{-1}(x_q) & J_2 - R_d & \Lambda \\ -(M^{-1}(x_q)\mathcal{U})^\top & -\Lambda^\top & -\Upsilon \end{bmatrix} \begin{bmatrix} \nabla_{x_q} \tilde{H} \\ \nabla_{x_p} \tilde{H} \\ \nabla_{x_{\tilde{\theta}}} \tilde{H} \end{bmatrix}. \tag{5.76}$$

*where $\hat{\theta}$ is the estimate of $\theta$, $\tilde{\theta} = \hat{\theta} - \theta$ is the estimation error, $\Upsilon = \Upsilon^\top > 0$,*

$$\Lambda = F(q) - M_d M^{-1} F(q) + (J_2 - R_d) M_d^{-1}\mathcal{U} - M_d M^{-1} \sum_{i=1}^{n} e_i p^\top \nabla_{q_i} M_d^{-1}\mathcal{U}$$
$$+ \frac{1}{2} M_d M^{-1} \sum_{i=1}^{n} e_i (\mathcal{U}\tilde{\theta})^\top \nabla_{q_i} M_d^{-1}\mathcal{U} \tag{5.77}$$
$$\Upsilon = (M^{-1}\mathcal{U})^\top F(q) + \Lambda^\top M_d^{-1}\mathcal{U} \tag{5.78}$$

*and*

$$\tilde{H}(q,p,\tilde{\theta}) = \frac{1}{2} x_p^\top M_d^{-1}(x_q) x_p + \frac{1}{2}|\tilde{\theta}|^2 + V(x_q,\theta), \tag{5.79}$$

*is the desired Hamiltonian function. Then, the controller*

$$\begin{aligned} Gu = {} & F(q)\hat{\theta} - M_d M^{-1}(F(q)\hat{\theta} + S(q)) + (J_2 - R_d)M_d^{-1}p + \frac{1}{2}\sum_{i=1}^{n} e_i p^\top \nabla_{q_i} M^{-1} p \\ & - \frac{1}{2} M_d M^{-1} \sum_{i=1}^{n} e_i p^\top \nabla_{q_i} M_d^{-1} p + \mathcal{U}\dot{\hat{\theta}}, \end{aligned} \tag{5.80}$$

*with the update law*

$$\dot{x}_{\hat{\theta}} = -M^{-1}\mathcal{U}(F(q)\hat{\theta} + S(q)) + (M^{-1} - M_d^{-1})F(q)p + \frac{1}{2}M^{-1}\mathcal{U}\sum_{i=1}^{n} e_i p^\top \nabla_{q_i} M_d^{-1} p, \tag{5.81}$$

***asymptotically*** *stabilizes the system at the equilibrium* $(q_e, 0, \theta)$. ■

**Proof of Proposition 5.21:**
Following the same procedures as in the proof of Proposition 5.14; the time derivative of the Hamiltonian function (5.79) along the trajectories of the system is obtained as

$$\begin{aligned} \dot{\tilde{H}} &= -\nabla_{x_p}\tilde{H}^\top (J_2 - R_d)\nabla_{x_p}\tilde{H} - \nabla_{x_{\tilde{\theta}}}\tilde{H}^\top \Upsilon \nabla_{x_{\tilde{\theta}}}\tilde{H} \\ &\leq -|\nabla_{x_p}\tilde{H}|^2_{R_d} - |\nabla_{x_{\tilde{\theta}}}\tilde{H}|^2_{\Upsilon}, \end{aligned}$$

where the term $(\nabla_{x_p}\tilde{H})^\top J_2 \nabla_{x_p}\tilde{H}$ is equal to zero because $J_2 = -J_2^\top$. Thus, the system (5.76) has a stable equilibrium at $(q_e, 0, \theta)$ with $x_p, x_{\tilde{\theta}} \in \mathcal{L}_2 \cap \mathcal{L}_\infty$. By applying Corollary 5.16, we can conclude the convergence of states $x_p$ and $x_{\tilde{\theta}}$ to zero ($x_p, x_{\tilde{\theta}} \to 0$ as $t \to \infty$). Moreover, $\tilde{\theta} = 0 \implies \hat{\theta} = \theta$.

The convergence of the states $x_q$ to their desired equilibrium is established as follows:

$$x_p, x_{\tilde{\theta}} \equiv 0 \implies \dot{x}_p, \dot{\hat{\theta}} \equiv 0.$$

Thus, under the dynamics of (5.76) yields:

$$\begin{aligned} \dot{x}_p &= -M_d M^{-1}\nabla_{x_q}\tilde{H} + (J_2 - R_d)\nabla_{x_p}\tilde{H} + \Lambda\nabla_{x_{\tilde{\theta}}}\tilde{H} = 0 \\ &= -M_d M^{-1}\left(\nabla_{x_q} V_x + \underbrace{\frac{1}{2}x_p^\top(\nabla_{x_q} M_d^{-1})x_p}_{=0}\right) + \underbrace{(J_2 - R_d)M_d^{-1}x_p}_{=0} + \underbrace{\Lambda\tilde{\theta}}_{=0} = 0 \\ &= -M_d M^{-1}\nabla_{x_q} V_x = 0. \end{aligned} \tag{5.81}$$

This implies $\nabla_{x_q} V_x = 0$. Invoking similar arguments to those in the proof of Proposition 5.4, we obtain

$$\nabla_{x_q} V_x \equiv 0 \implies x_q = q_e.$$

Since all trajectories converge to their desired values, we can conclude that the closed-loop system (5.43) has an *asymptotically* stable equilibrium at $(q_e, 0, \theta)$. The controller

is obtained by matching the momenta of (3.1) and (5.76), that is

$$\begin{aligned}
\dot{p} &\equiv \dot{x}_p + \mathcal{U}\dot{\hat{\theta}} \\
Gu - \nabla_q H &= -M_d M^{-1}\nabla_{x_q}\tilde{H} + (J_2 - R_d)\nabla_{x_p}\tilde{H} + \Lambda\nabla_{x_{\hat{\theta}}}\tilde{H} + \mathcal{U}\dot{\hat{\theta}} \\
Gu - F\theta - \frac{1}{2}\sum_{i=1}^{n} e_i p^\top \nabla_{q_i} M^{-1} p &= -M_d M^{-1}(F\theta + S) - \frac{1}{2} M_d M^{-1} \sum_{i=1}^{n} e_i x_p^\top \nabla_{q_i} M_d^{-1} x_p \\
&\quad + (J_2 - R_d) M_d^{-1} x_p + \Lambda\tilde{\theta} + \mathcal{U}\dot{\tilde{\theta}}. \qquad (5.82)
\end{aligned}$$

Substituting $x_p = p - \mathcal{U}\tilde{\theta}$ and (5.77) in (5.82) yields:

$$\begin{aligned}
Gu = {} & F\theta + \frac{1}{2}\sum_{i=1}^{n} e_i p^\top \nabla_{q_i} M^{-1} p - M_d M^{-1}(F\theta + S) - \frac{1}{2} M_d M^{-1} \sum_{i=1}^{n} e_i p^\top \nabla_{q_i} M_d^{-1} p \\
& + M_d M^{-1} \sum_{i=1}^{n} e_i p^\top \nabla_{q_i} M_d^{-1} \mathcal{U}\tilde{\theta} - \frac{1}{2} M_d M^{-1} \sum_{i=1}^{n} e_i \mathcal{U}\tilde{\theta}^\top \nabla_{q_i} M_d^{-1} \mathcal{U}\tilde{\theta} \\
& + \Bigg( F - M_d M^{-1} F + (J_2 - R_d) M_d^{-1}\mathcal{U} - M_d M^{-1} \sum_{i=1}^{n} e_i p^\top \nabla_{q_i} M_d^{-1}\mathcal{U} \\
& + \frac{1}{2} M_d M^{-1} \sum_{i=1}^{n} e_i \mathcal{U}\tilde{\theta}^\top \nabla_{q_i} M_d^{-1}\mathcal{U} \Bigg) \tilde{\theta} + (J_2 - R_d) M_d^{-1} p - (J_2 - R_d) M_d^{-1}\mathcal{U}\tilde{\theta} + \mathcal{U}\dot{\tilde{\theta}}.
\end{aligned}$$

Using $\tilde{\theta} = \hat{\theta} - \theta$ and cancelling like terms but with opposite signs, we obtain the controller (5.80). Finally, the update law is computed as:

$$\begin{aligned}
\dot{x}_{\hat{\theta}} &= -M^{-1}\mathcal{U}\nabla_{x_q}\tilde{H} - \Lambda\nabla_{x_p}\tilde{H} - \Upsilon\nabla_{x_{\hat{\theta}}}\tilde{H} \\
&= -M^{-1}\mathcal{U}(F\theta + S) - \frac{1}{2} M^{-1}\mathcal{U} \sum_{i=1}^{n} e_i x_p^\top \nabla_{q_i} M_d^{-1} x_p - \Lambda M_d^{-1} x_p - \Upsilon\tilde{\theta}. \qquad (5.83)
\end{aligned}$$

Substituting $x_p = p - \mathcal{U}\tilde{\theta}$, (5.77) and (5.78) in (5.83) yields:

$$\begin{aligned}
\dot{x}_{\hat{\theta}} = {} & -M^{-1}\mathcal{U}(F\theta + S) - \frac{1}{2} M^{-1}\mathcal{U} \sum_{i=1}^{n} e_i p^\top \nabla_{q_i} M_d^{-1} p + M^{-1}\mathcal{U} \sum_{i=1}^{n} e_i p^\top \nabla_{q_i} M_d^{-1}\mathcal{U}\tilde{\theta} \\
& - \frac{1}{2} M^{-1}\mathcal{U} \sum_{i=1}^{n} e_i \mathcal{U}\tilde{\theta}^\top \nabla_{q_i} M_d^{-1}\mathcal{U}\tilde{\theta} - \Big( F - M_d M^{-1} F + (J_2 - R_d) M_d^{-1}\mathcal{U} \\
& - M_d M^{-1} \sum_{i=1}^{n} e_i p^\top \nabla_{q_i} M_d^{-1}\mathcal{U} + \frac{1}{2} M_d M^{-1} \sum_{i=1}^{n} e_i \mathcal{U}\tilde{\theta}^\top \nabla_{q_i} M_d^{-1}\mathcal{U} \Big) M_d^{-1} p \\
& + \Bigg( F - M_d M^{-1} F + (J_2 - R_d) M_d^{-1}\mathcal{U} - M_d M^{-1} \sum_{i=1}^{n} e_i p^\top \nabla_{q_i} M_d^{-1}\mathcal{U} \\
& + \frac{1}{2} M_d M^{-1} \sum_{i=1}^{n} e_i \mathcal{U}\tilde{\theta}^\top \nabla_{q_i} M_d^{-1}\mathcal{U} \Bigg) M_d^{-1}\mathcal{U}\tilde{\theta} - \big( F M_d^{-1}\mathcal{U} - (J_2 - R_d)(M_d^{-1}\mathcal{U})^2 \\
& - \frac{1}{2} M^{-1}\mathcal{U} \sum_{i=1}^{n} e_i p^\top (\nabla_{q_i} M_d^{-1})\mathcal{U} \Bigg) \tilde{\theta}
\end{aligned}$$

Using $\tilde{\theta} = \hat{\theta} - \theta$ and cancelling like terms but with opposite signs, we obtain the update law (5.81). Hence, it completes the proof. ■

## 5.5 Application: the Inertia Wheel Pendulum

In this section, we use the Quanser IWP module (see [17]), as shown in Figure 3.1 together with the simplified free body diagram of its mechanical part, to illustrate in realistic simulations our results. The full description of the system was presented in Subsection 3.4.1. The dynamic equations of the IWP system can be written in a PCH form (3.1) with $n = 2$, $m = 1$ and

$$M = \begin{bmatrix} k_1 & k_2 \\ k_2 & k_2 \end{bmatrix}, \quad G = e_2 = \begin{bmatrix} 0 \\ 1 \end{bmatrix}, \text{ and} \tag{5.83}$$

$$V(q_1) = k_3 \left(1 + \cos(q_1)\right), \tag{5.84}$$

where the control input $u$ is the motor torque, $k_1 = m_p l_{c_1}^2 + m_w l^2 + I_p + I_w$, $k_2 = I_w$ and $k_3 = g(m_p l_{c_1} + m_w l)$. The complete parameters of the IWP are listed in Table 3.1.

### 5.5.1 IDA-PBC stabilizing controller

To start with, a stabilizing controller is obtained using IDA-PBC design procedures proposed in Subsection 3.4.2. The main objective is to provide a continuous control law to swing up the pendulum by spinning the wheel and to stabilize it at its upward position $q = (0, q_2)$ for any $q_2 \in [0,\ 2\pi]$.

By fixing $M_d$ to be a constant matrix of the form

$$M_d = \Delta \begin{bmatrix} m_1 & m_2 \\ m_2 & m_3 \end{bmatrix} = \Delta \begin{bmatrix} m_1 & \left(\frac{k_2}{k_1}\right) m_1 + \varepsilon \\ \left(\frac{k_2}{k_1}\right) m_1 + \varepsilon & m_3 \end{bmatrix}, \tag{5.85}$$

where $\varepsilon > 0$, $\Delta = k_1 k_2 - k_2^2$ and having $G^{\perp} = [1\ 0]$, the desired Hamiltonian (3.5) is obtained as

$$H_d = \frac{1}{2} p^{\top} M_d^{-1} p + V_d(q), \tag{5.86}$$

$$V_d(q) = -k_3 \gamma_1 \cos(q_1) + \frac{1}{2} K_p (\varepsilon k_1 \gamma_1 q_1 + q_2)^2, \tag{5.87}$$

with $\gamma_1 = \frac{1}{k_2(m_2 - m_1)}$ and $K_p > 0$ the gain of the energy shaping controller which is calculated as

$$u_{es} = \gamma_2 \sin(q_1) + K_p \gamma_3 (\varepsilon k_1 \gamma_1 q_1 + q_2), \tag{5.88}$$

with $\gamma_2 = -k_3\gamma_1(m_2k_2 - m_3k_2)$, $\gamma_3 = -\varepsilon k_1\gamma_1(m_2k_2 - m_3k_2) - (-m_2k_2 + m_3k_1)$. The damping injection controller is

$$u_{di} = -K_v\frac{\Delta}{\Delta_d}(-m_2p_1 + m_1p_2), \tag{5.89}$$

with $\Delta_d = \det(M_d) = \Delta^2(m_1m_3 - m_2^2)$ and $K_v > 0$ the damping injection controller gain. Thus, the IDA-PBC control law is of the form

$$u_{IDA} = u_{es} + u_{di}. \tag{5.90}$$

### 5.5.2 Integral action controller

We apply the procedure given in Proposition 5.9 to design the integral controller for the IWP system. Given $G = \begin{bmatrix}0 & 1\end{bmatrix}^\top$, then the matrix $\mathcal{G}$ is defined as

$$\mathcal{G} = \begin{bmatrix}0 & 0\\ 0 & 1\end{bmatrix}.$$

The integral controller on the non-passive output is then calculated as

$$\begin{aligned} v &= K_vK_i\frac{\Delta}{\Delta_d}(m_2k_1 - m_1k_2)x_v,\\ \dot{x}_v &= K_p(\varepsilon k_1\gamma_1q_1 + q_2)\end{aligned} \tag{5.91}$$

and the extra term $u_p = -K_ik_2K_p(\varepsilon k_1\gamma_1q_1 + q_2)$.

### 5.5.3 ISS controller

Following the ISS controller design presented in Subsection 5.3.4, in particular Proposition 5.10, the control input is obtained as

$$\begin{aligned} u = u_{IDA} &- \frac{\rho\Delta}{\Delta_d}\big(\beta_1(m_3p_1 - m_2p_2) - \beta_2(m_2p_1 - m_1p_2)\big)\\ &- \frac{\rho\Delta}{\Delta_d}\big(\beta_1(m_3k_2 - m_2k_2) - \beta_2(m_2k_2 - m_1k_2)\big)x_v\\ &- K_iK_vk_2\frac{\Delta}{\Delta_d}(m_2 + m_1)x_v - K_ik_2K_p(\varepsilon k_1\gamma_1q_1 + q_2),\end{aligned} \tag{5.92}$$

with

$$\dot{x}_v = K_iK_p(\varepsilon k_1\gamma_1q_1 + q_2) + \frac{1}{2}(k_1 - k_2)p_2, \tag{5.93}$$

and

$$\begin{aligned}\beta_1 &= K_p(\varepsilon k_1\gamma_1q_1 + q_2)\big(k_3\gamma_1\sin(q_1) + K_p\varepsilon k_1\gamma_1(\varepsilon k_1\gamma_1q_1 + q_2)\big)\\ \beta_2 &= K_p^2(\varepsilon k_1\gamma_1q_1 + q_2)^2.\end{aligned}$$

### 5.5.4 Adaptive controller

Following the discussion in Subsection 5.3.5, here we show the design of an adaptive controller to compensate for the uncertainty in the potential energy function $V(q)$.

Consider the potential energy function of IWP system (5.84), the gradient of this function is

$$\nabla_q V = -k_3 \sin(q_1), \tag{5.94}$$

which can be linearly parametrized as (5.33), with $F(q_1) = -\sin(q_1)$ and $\theta = k_3$ the uncertain term. Thus, the energy shaping controller (5.88) is rewritten as

$$u_{es} = -\theta\gamma_1(m_2k_2 - m_3k_2)\sin(q_1) + K_p\gamma_3(\varepsilon k_1\gamma_1 q_1 + q_2). \tag{5.95}$$

Now, applying Proposition 5.13, the overall adaptive-IDA control input (5.37) is obtained as

$$u = -\hat{\theta}\gamma_1(m_2k_2 - m_3k_2)\sin(q_1) + K_p\gamma_3(\varepsilon k_1\gamma_1 q_1 + q_2) - K_v\frac{\Delta}{\Delta_d}(-m_2p_1 + m_1p_2), \tag{5.96}$$

with the update law (5.38) takes the form

$$\dot{\hat{\theta}} = -\frac{\Delta}{\Delta_d}(k_2m_1 - k_2m_2 - 1)(-m_3p_1 + m_2p_2)\hat{\theta}\sin(q_1). \tag{5.97}$$

### 5.5.5 Simulation results

In this Subsection the integral, ISS and adaptive IDA-PBC controllers designed for the IWP system are implemented in a MATLAB/SIMULINK environment to evaluate the performance of the control system. The values of the model parameters are shown in Table 3.1. In all simulations, the initial condition $[q_0,\ p_0] = [\pi, 0, 0, 0]$ for the system is used.

#### A) Integral IDA-PBC simulations

Two sets of simulation set-up have been used to test the effectiveness of the proposed integral IDA-PBC controller.

The first set-up simulates a tracking control problem where the pendulum is required to track a sinusoidal reference signal $q_{1_r}$. A constant force disturbance of $1N$, which represents a constant force pushing the pendulum, is also injected into the dynamic of $q_1$. We implement the integral IDA-PBC controller with the parameters $m_1 = 0.4$, $m_3 = 5$, $\epsilon = 1$, $K_p = 0.5$, $K_v = 1 \times 10^{-5}$ and $K_i = 1.2$. The simulation results in Figure 5.1 show that without integral action, the system subject to external disturbance exhibits a large steady-state error, which can be observed particularly in the trajectory of $q_2$. With integral action, the trajectories track their desired references despite the

presence of the constant disturbance, bringing the trajectories to converge smoothly to their desired values. In Figure 5.2 we show the trajectory of $q_2$ comparing it to the case of no disturbance as the reference.

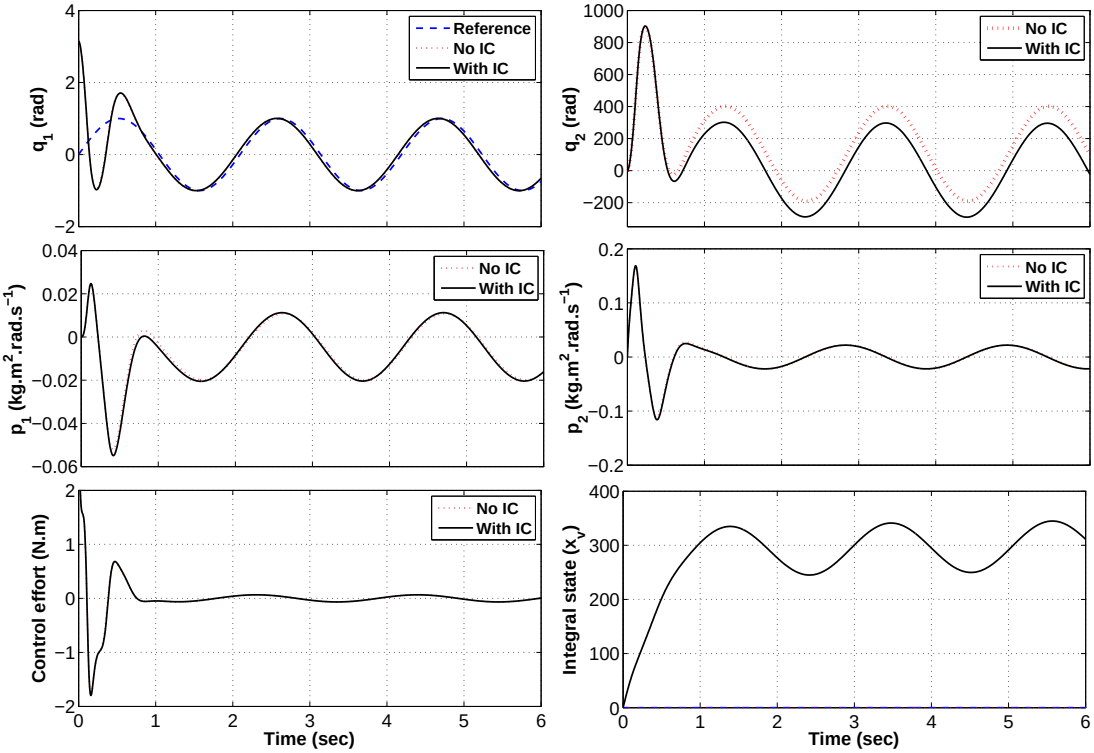


Figure 5.1: State histories and control input of the IWP system for the tracking and disturbance rejection control problem.

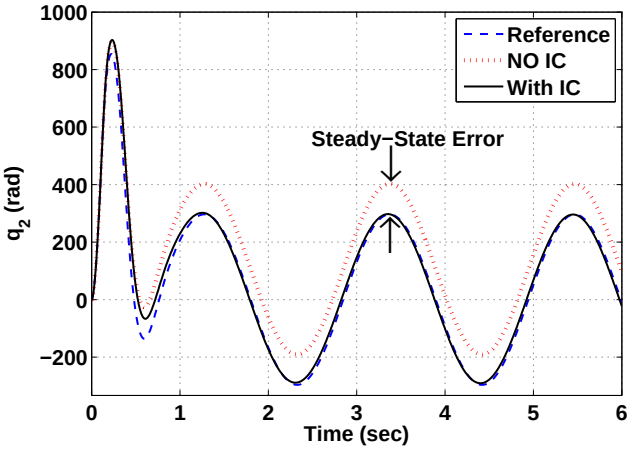


Figure 5.2: Angle of the wheel $q_2$ for the tracking and disturbance rejection control problem.

The second set-up illustrates the case of rejecting a constant torque disturbance of $1Nm$ injected into (pushing against) the dynamic of $q_2$, which represents a constant force pushing the pendulum, and highlights the effect of the integral gain. The controller

parameters for this set-up are $m_1 = 0.4$, $m_3 = 5$, $\epsilon = 1$, $K_p = 1.5$, $K_v = 5 \times 10^{-5}$. Figure 5.3 shows the response of the system at different integral gains: $K_i = 0$ (no integral action), $K_{i1} = 0.1$ and $K_{i2} = 1.0$. Figure 5.4 shows that steady-state errors induced by this disturbance appear when applying no integral action, while the integral action control eliminates these errors.

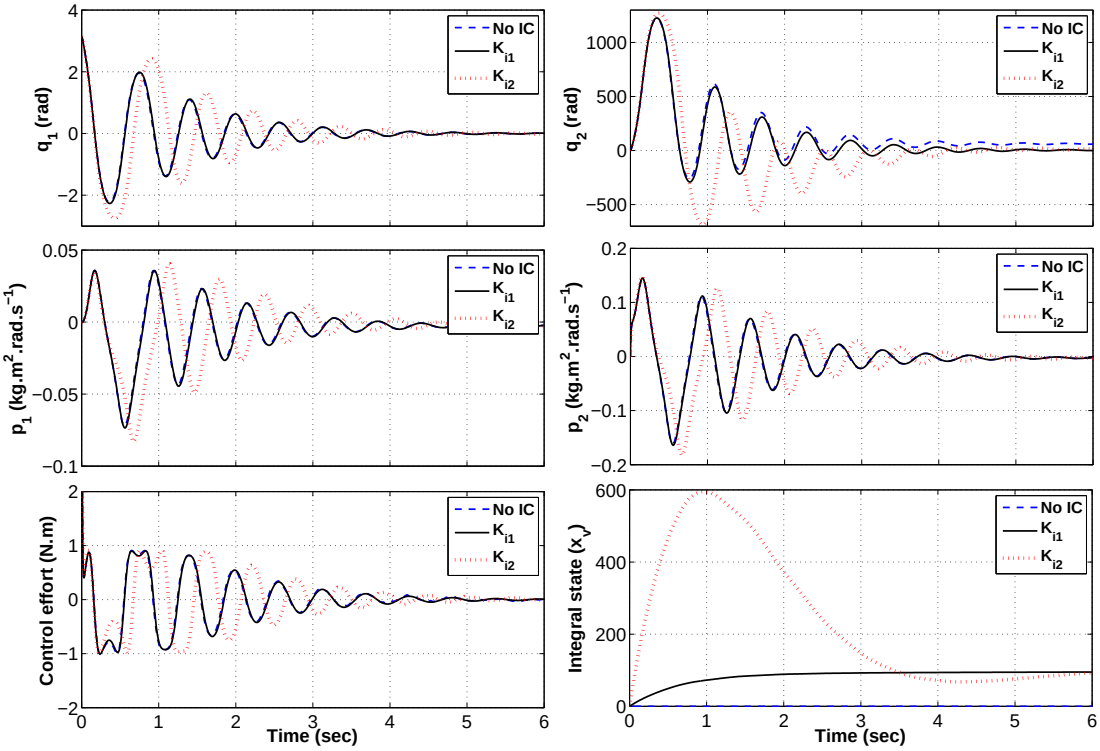


Figure 5.3: State histories and control input of the IWP system for the disturbance rejection control problem.

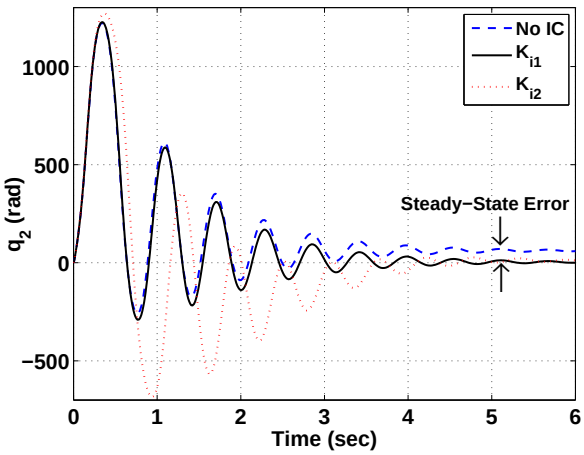


Figure 5.4: Angle of the wheel $q_2$ for the disturbance rejection control problem.

### B) ISS simulations

The ISS control law described above has been implemented on the IWP system for the case of both *matched* and *unmatched* disturbances with the design parameters $m_1 = 0.4$, $m_3 = 5$, $\epsilon = 1$, $K_p = 1.1$, and $K_v = 5.6 \times 10^{-5}$. The disturbance vector is selected as $d = \lambda \tanh(\dot{p})$, which represents a time varying bounded torque $d = \lambda \tanh(\dot{p})$ pushing against the arm and the pendulum for the case of matched and unmatched disturbances, respectively.

We first consider the robust control problem of the IWP system having *matched* disturbances. Figures 5.5 and 5.6 show the behaviour of the system subject to small ($\lambda = 0.5$) and large ($\lambda = 1$) disturbances where the **ISS** controller parameters have been chosen as $K_i = 1$ and $\rho = 0.1 \times 10^{-12}$. As expected, we can see that all states (signals) converge to their respective desired equilibrium values with excellent performance. Also, we have simulated the perturbed system when a non-robust controller is used (i.e. $K_i = \rho = 0$). Figure 5.7 shows that the system becomes unstable even with a small disturbance $\lambda = 0.5$.

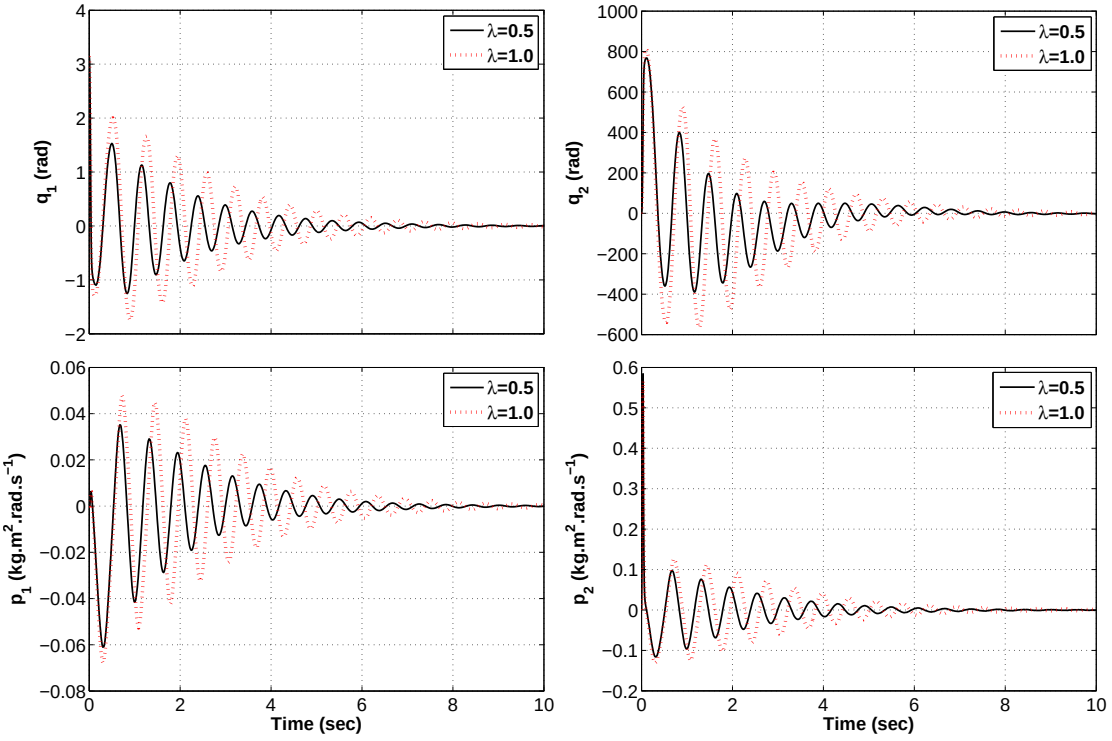


Figure 5.5: State histories of the IWP system for *matched* disturbance control problem using a *robust* IDA controller.

For the case of *unmatched* disturbances, we have selected two different sets of controller's parameters ($K_p = 1.1$, $K_v = 5.6 \times 10^{-5}$, $K_{i1} = 1.5$, $\rho_1 = 0.09 \times 10^{-12}$) and ($K_p = 0.4$, $K_v = 5.6 \times 10^{-5}$, $K_{i2} = 1.5$, $\rho_2 = 0.09 \times 10^{-11}$), in response to two different disturbance gains ($\lambda = 60$) and ($\lambda = 90$), respectively. The simulation results are shown in Figures 5.8 and 5.9. Again, we can see the convergence of all states to their

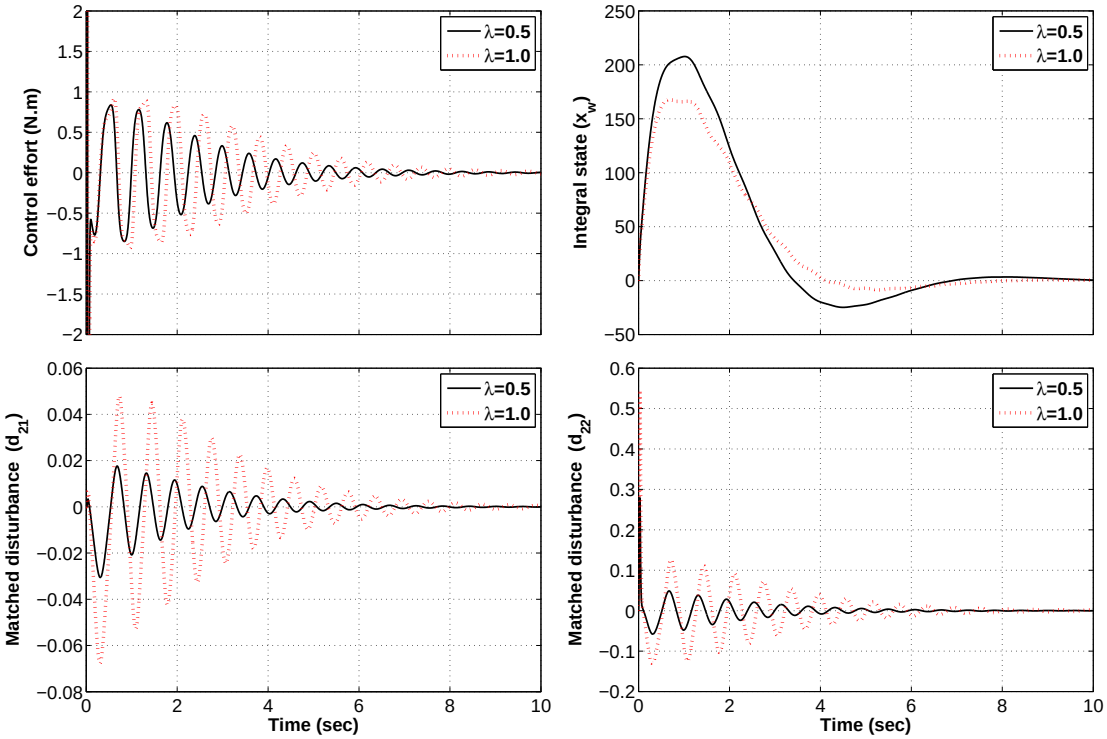


Figure 5.6: Control input, update law and disturbance inputs of the IWP for *matched* disturbance control problem using a *robust* IDA controller.

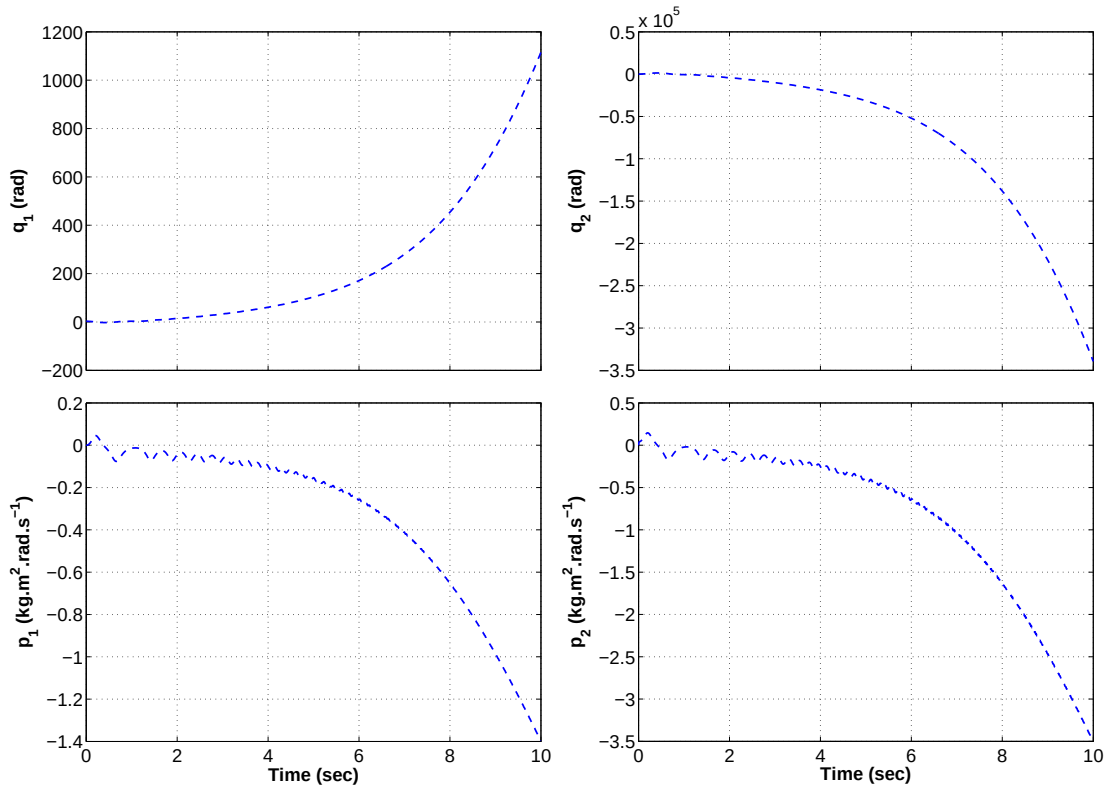


Figure 5.7: State histories of the IWP for *matched* disturbance control problem using a *non-robust* IDA controller ($\lambda = 0.5$).

desired values with reasonable transients. These figures also shows that for relatively high disturbances ($\lambda = 90$), we have selected a large value of $\rho_2$ to enlarge the domain of attraction and thus the system is ultimately bounded. This follows the proof of Proposition 5.10. Notice that we have also decreased the proportional gain $K_p$ to make sure that the maximum torque does not exceed the actuator limit. For comparison, the perturbed system is also simulated without using the robust controller as shown in Figure 5.10. It is apparent that in this case the system exhibits a significant steady-state error.

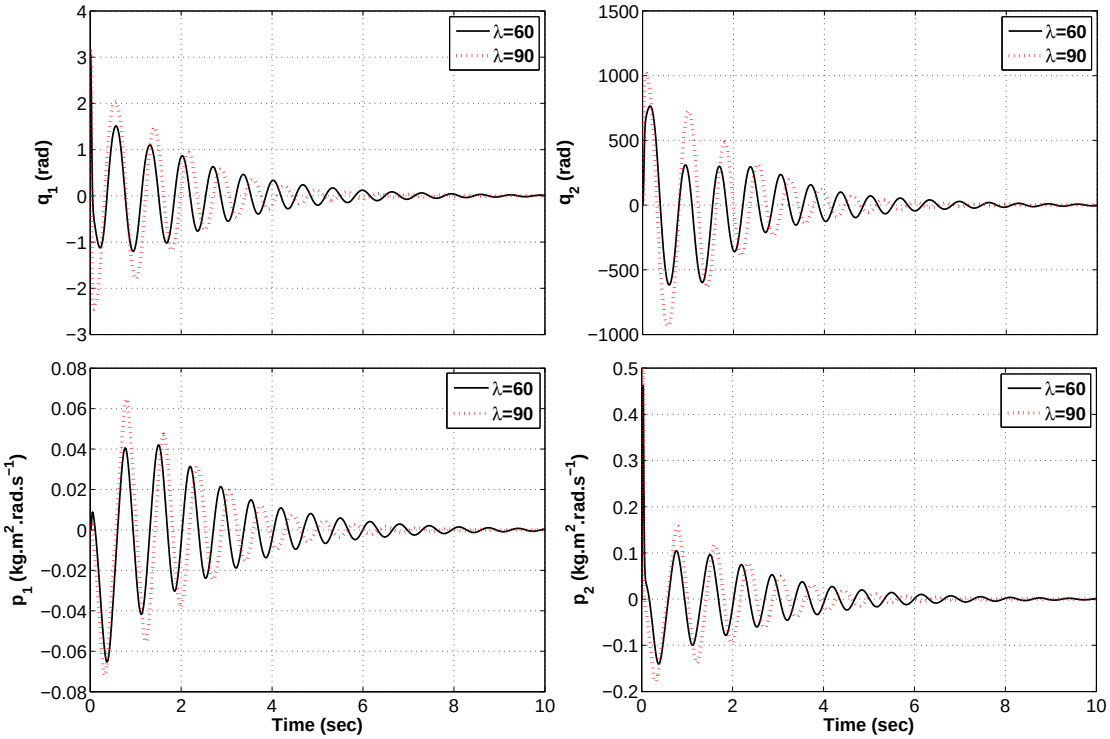


Figure 5.8: State histories of the IWP system for *unmatched* disturbance control problem using a *robust* IDA controller.

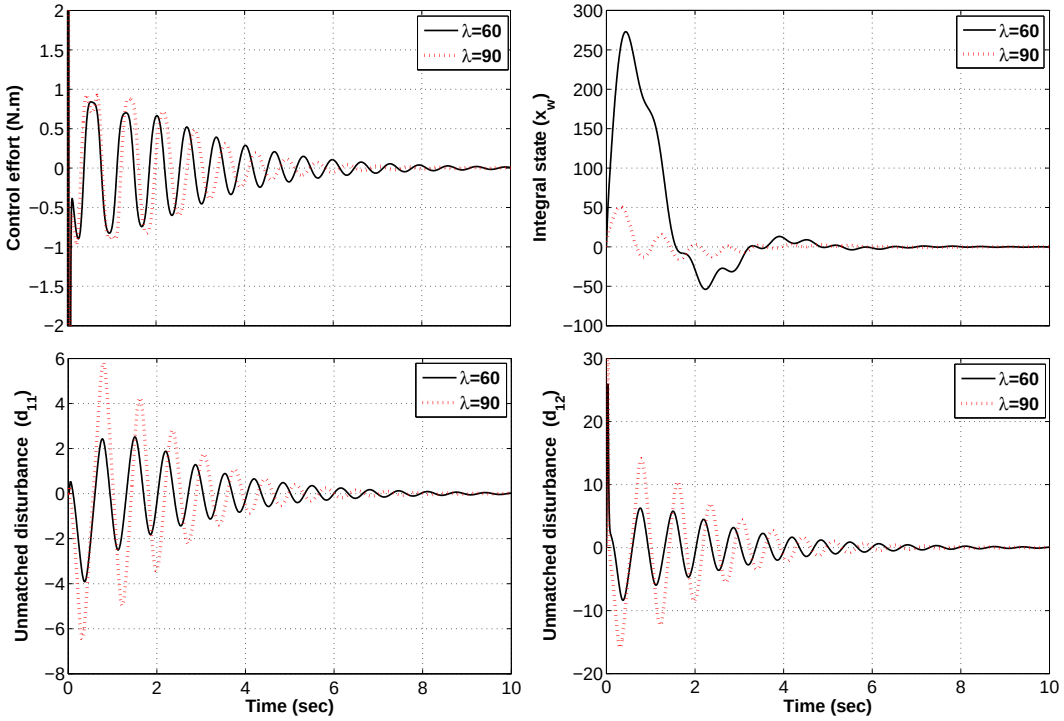


Figure 5.9: Control input, update law and disturbance input of the IWP for *unmatched* disturbance control problem using a *robust* IDA controller.

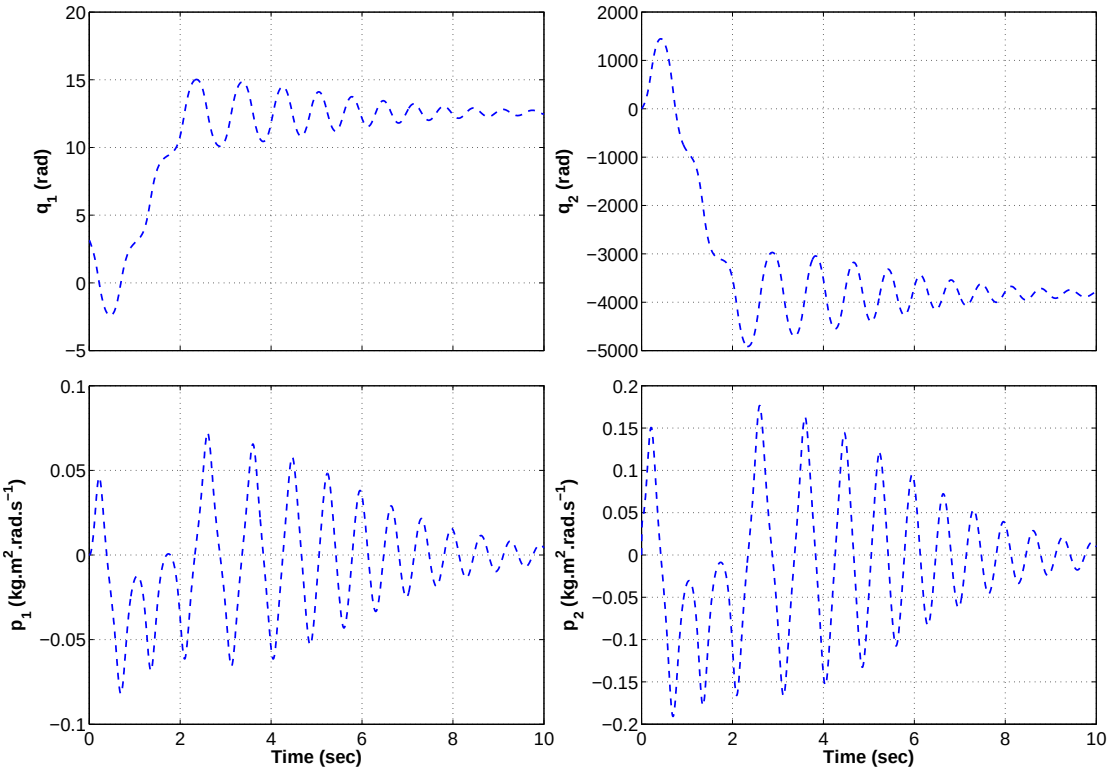


Figure 5.10: State histories of the IWP for *unmatched* disturbance control problem using a *non-robust* IDA controller ($\lambda = 60$).

### C) Adaptive IDA-PBC simulations

For the adaptive control method, we have selected the parameters and gains of the controller as $m_1 = 0.2$, $m_3 = 10$, $\epsilon = 1$, $K_p = 4.5$, and $K_v = 2.2 \times 10^{-4}$. Furthermore, we have adjusted the uncertain term $\theta = k_3$ as $\theta = \vartheta + \zeta$, with $\zeta$ is a fixed estimate. This enables us to compare this method with the non-adaptive one. Given the value of $\theta = g(m_p l_{c_1} + m_w l)$, we have selected $\zeta = \theta/2$ for this case.

Figures 5.11 and 5.12 show a comparative plot of the system's response with the adaptive IDA and the non-adaptive IDA-PBC controllers. As shown, without adaptation law the uncertainty in $V(q)$ results in a relatively large steady state error and unacceptable transients. In contrast, adding the proposed adaptive law, the trajectories of the IWP system converge to their desired states with excellent performance. Figure 5.12 shows the convergence of the estimate $\hat{\theta}$ to the true value $\theta$.

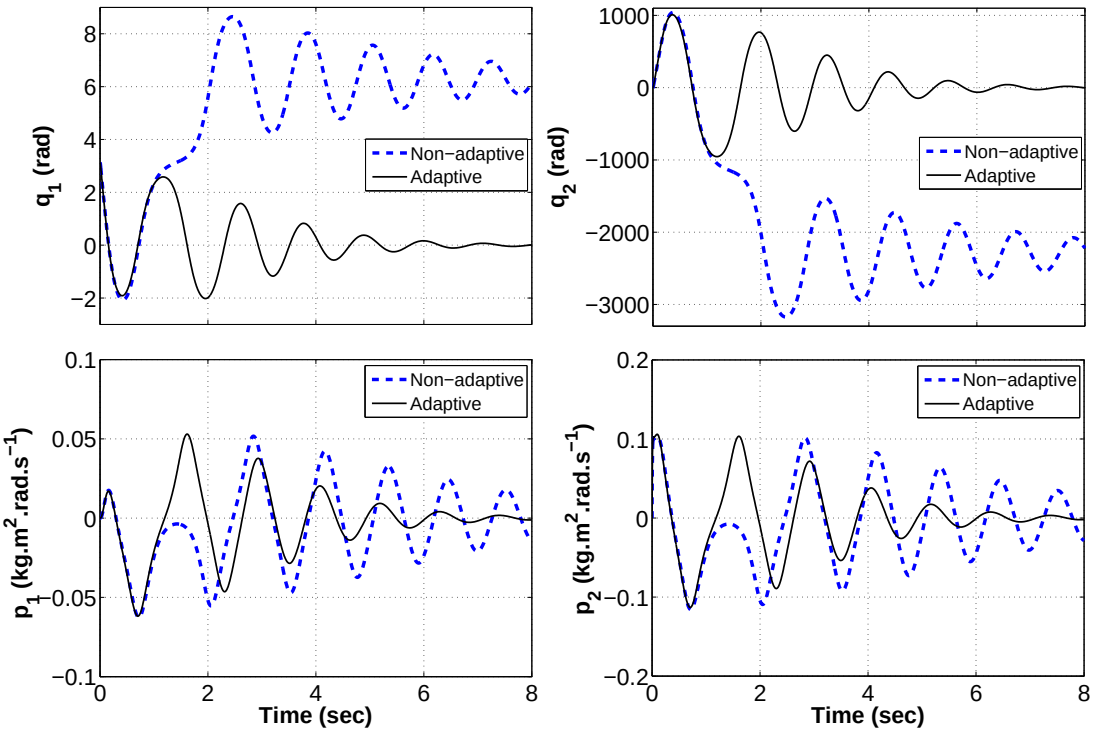


Figure 5.11: State histories of the IWP system for the adaptive control problem.

## 5.6 Conclusion

In this chapter, we have discussed the possibility of extending the IDA-PBC method by adopting a robustness perspective, with the aim of maintaining (asymptotic) stability of the system in the presence of uncertainty which could result from disturbances, noises, and modelling errors. The results extend some existing methods and provide a new

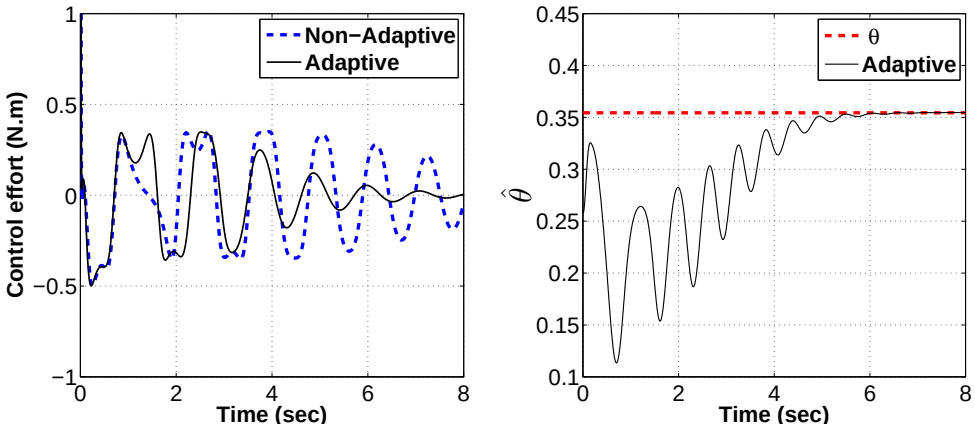


Figure 5.12: Control input and update law (estimate) of the IWP system for the adaptive control problem.

framework that allows the implementation of integral action control to underactuated PCH systems that are quite commonly found in practice.

First we have developed some robust control design methods to deal with the case of separable PCH mechanical systems. A crucial procedure of these designs is to use a change of coordinates which allows adding the integral action on the non-passive outputs which are the signals of interest. This has significantly enhanced the robustness of the closed loop PCH systems by eliminating the steady-state errors and rejecting disturbances, achieving stabilization in the ISS sense. Furthermore, An adaptive control scheme has been presented to deal with uncertainties in the potential energy function. Second, we have successfully extended the proposed control design methods to deal with the non-separable PCH systems. As expected, this has resulted in more complex designs as the derivative of the inertia matrices $M$ and $M_d$ are needed to be taken into account. Finally, Application to an inertia wheel pendulum which is an underactuated system has been presented, and the effectiveness of the proposed controllers has been shown through numerical simulations. The simulation results demonstrate that the system is robust with respect to different perturbations; preserving the PCH structure, and retaining the (asymptotic) stability with high performance.

# Chapter 6

# IDA-PBC of Microelectromechanical Systems

## 6.1 Introduction

In previous chapters we have discussed the IDA-PBC methodology for mechanical systems. In this chapter we focus on microelectromechanical systems (MEMSs). MEMSs are devices that are made using the techniques of microfabrication, integrating micrometer-sized mechanical structures (gears, levers, pistons, cantilevers, etc.) and electrical/electronic components [92]. MEMS devices are very small; their components are usually microscopic, generally range in size from few micrometers to a millimeter (see Figure 6.1). The highly integrated and interdisciplinary nature of MEMS with a strong and complex coupling between a wide range of energy domains, including mechanical, electrical, thermal, magnetic, all in miniaturized scale impose challenges on the design, fabrication and control of these devices.

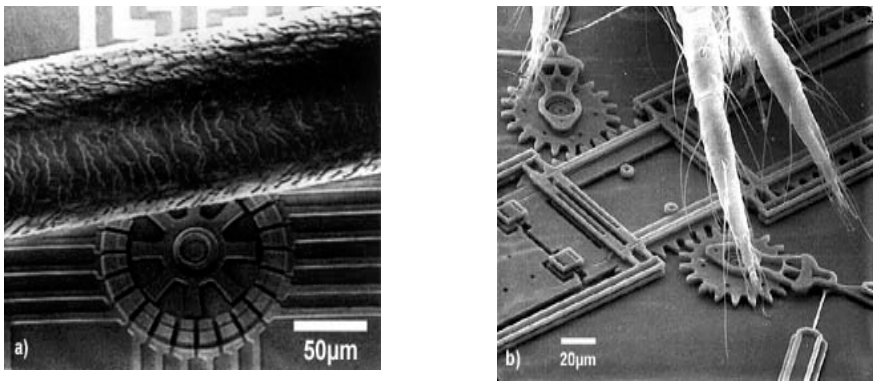


Figure 6.1: (a) A MEMS silicon motor together with a strand of human hair, and (b) the legs of a spider mite standing on gears from a micro-engine [76].

Due to its advantages of low cost through batch fabrication techniques, reduced size, reliability and lower power consumption, MEMS technology has been commercially and scientifically successful in various applications, and several interesting new products and applications are being developed. Automotive industry is among the major sectors where the success and reliability of MEMS have been proven. For example, inertia sensors such as accelerometers and gyroscopes, have now been in use for decades in airbag sensors, active suspension and anti-lock braking systems. Figure 6.2 shows an accelerometer MEMS which is in widespread use as an automotive airbag sensor.

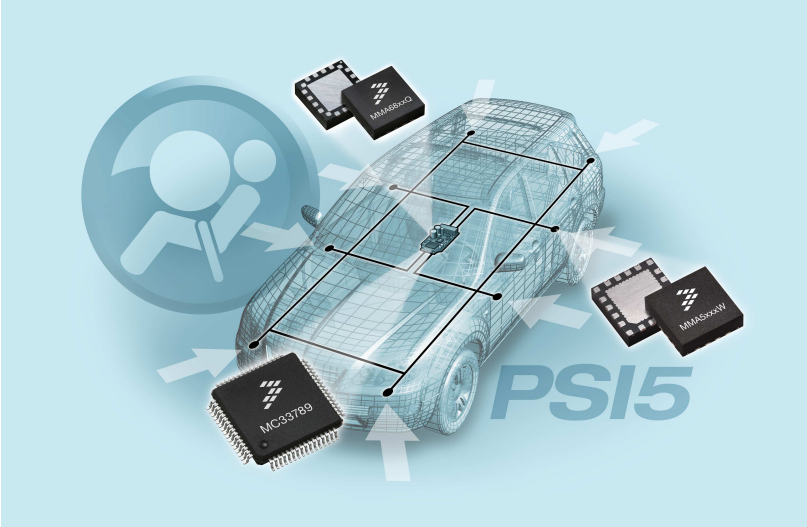


Figure 6.2: Modern day MEMS accelerometer [80].

A notable use of a MEMS inertia sensors is in motion sensing applications such as smartphones, digital audio players, and navigation control systems. For example, a three-axis accelerometer, three-axis gyroscope, and three-axis electronic compass are all employed to constitute much better and complete motion sensing, gaming and image stabilization. Figure 6.3 shows the MEMS sensors, introduced in the iPhone by Apple, to reorient the iPhone's screen [23].

The radio frequency (RF) MEMS is one of the fastest growing areas. The innovative RF MEMS elements, including switches, resonators, filters, and relays are extremely small, cheap, and require little power which make them suitable for mobile phones and wireless communication applications such as radar and global positioning systems. BioMEMS is another successful area where MEMS technology is becoming more popular for medical applications. Examples of BioMEMS are pressure sensors which are used to monitor blood pressure, a 'lab-on-a-chip' which performs one or several laboratory functions on a single chip utilising the advances in microfluidic systems and devices [76].

Among different actuation methods of MEMS, electrostatic actuation is the most popular one. In addition to the advantages of general MEMS, electrostatically actuated MEMS have advantages of simplicity of structure, versatility, flexibility in operation

Figure 6.3: Apple uses an accelerometer to change the iPhone's screen orientation when rotating the device [23].

and the fact that they can be easily fabricated from standard and well-understood materials [57]. The actuation principle behind them is the Coulombic attractive force between oppositely charged conductors. Electrostatically actuated MEMS devices can be split into two major configurations. The first is a comb drive type [78], in which an electrostatic force is generated when a voltage is applied between a set of 'interdigitated fingers'. The second configuration is a parallel plates type which consists of two parallel plates, one movable and one fixed. By applying a voltage across these plates an attractive electrostatic force is generated that drives the movable plate towards the fixed one. Electrostatically actuated MEMSs have been used in all the above mentioned applications but have been particularly successful to use in micro-mirrors, resonators, switches and accelerometers [41]. Figure 6.4 shows the electrostatically actuated mirrors which can be used in optical/photonic switches.

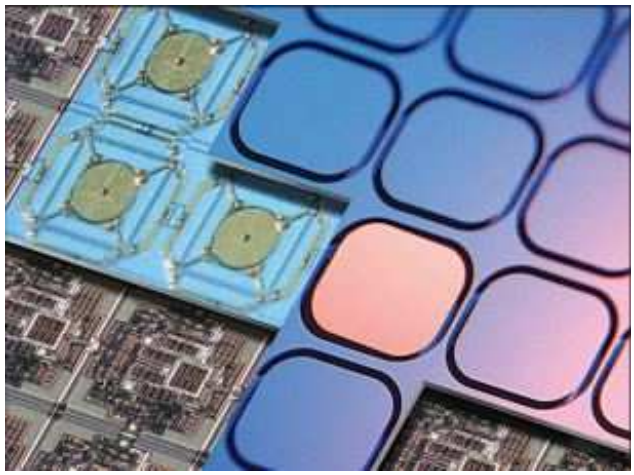

Figure 6.4: An electrostatically actuated micro-mirror array [18].

It is well known that the use of electrostatic actuated MEMS devices is significantly limited by their highly nonlinear dynamics leading to a saddle-node bifurcation known

as *snap-through* or *pull-in*. Pull-in instability limits the travel range of the movable plate to a third of its full gap. Over one-third of this gap the system becomes unstable and the movable plate collapses to the fixed one. Beside limiting the travel range or operation region of the MEMS, the repeated collapse may eventually damage the device [13]. To overcome this problem, with the aim of enhancing the functionality of MEMS to achieve a full operation range, fast responses and accurate positioning, several control methods have recently been developed. In [91], an approach that includes geometry or structure modification by adding additional circuitry (capacitor) in series with the actuator has been proposed. Static charge feedback method is introduced to control charge in the actuator by means of current driving [59]. Also, several nonlinear control techniques have been proposed including input-output linearization and passivity-based control using charge feedback [57], feedback linearization [75], sliding mode control [41], backstepping, flatness-based control and Control Lyapunov Function (CLF) synthesis [118].

However, beside solving the pull-in instability, two essential and challenging control issues for the MEMS need to be considered. First, while the position of the plate and charge of the device are available for measurement in practice by measuring the input current, capacitance and voltage across the plates [118], the velocity of the plate cannot be measured directly. Velocity observers have been constructed in some control schemes as in [118, 57]. The second important issue is that the above mentioned works require exact knowledge of the model parameters. However, modelling errors due to parametric uncertainties have not explicitly been taken into account in designing the controllers [106, 120]. These uncertainties may result from the difficulty on accurately identifying the model parameters in a miniaturized scale in practice, or parameter's variations due to inconsistencies in bulk micromachining. Other uncertainties may also exist due to measurement noise, environmental fluctuations and external disturbances that affect the stability and the performance of the system.

Few works have been reported in the literature to deal with uncertainties in the electrostatically actuated MEMS system. In [120], the adaptive backstepping state-feedback design along with an observer for unavailable velocity measurement have been constructed to control the MEMS system with parametric uncertainties. Furthermore, robustness of this method has been proved using input-to-state stabilization. Another adaptive backstepping design has been adopted in [106] to control the mechanical part of the bidirectionally driven electrostatic MEMS. Again, the backstepping adaptive observer has been used due to lack of velocity measurement. Adaptive tracking control problem has been developed in [104], and application of adaptive controller to electrostatically and electromagnitically actuated microrelays has been discussed in [13].

While most works in the literature have focused on solving the pull-in instability and control of MEMS in the presence of parametric uncertainties, still little is known about the robustness of these systems with respect to external disturbances due to noises

and environmental effects. Furthermore, in some works, only the mechanical dynamics of the system have been taken into account or the requirement of incorporating an observer to account for the lack of velocity measurements which makes the control system more complicated and difficult to implement practically. Motivated by this, we aim in this chapter to firstly solve the pull-in stability problem by designing an output-feedback controller that ensures that the system has global asymptotic stability equilibrium *without* the requirement of velocity measurement. Secondly, we propose a robust controller to counteract the external disturbances and other uncertainties in the system. These controllers are based on the passivity-based control approach, the IDA-PBC method in particular. While some PBC robust methods for PCH systems have been recently proposed to improve the robustness of mechanical systems (see Chapter 5 and [29, 82]), there has been relatively few works on robust control for electromechanical systems. The coupling between different energy domains in such systems complicates the design of such dynamic controller. In this chapter we show a framework to incorporate the integral control to improve the robustness of the MEMS described by PCH models. The main contributions of this chapter are:

- While most works have discussed the pull-in instability using a linearization of the model, we will show the stability analysis based on both the energy (Hamiltonian) and linearization methods.
- The design of an output-feedback controller based on the IDA-PBC method proposed in [66] while avoiding the velocity measurement which is difficult to do in practice.
- A control design framework to include the integral control action to electromechanical PCH systems. (Note: in earlier chapters only mechanical dynamic systems have been considered).
- A novel robust control scheme, based on ISS combined with the IDA-PBC, that preserves the stability of the MEMS in the face of external disturbances.

The organization of this chapter is as follows. Section 6.2 presents the model of the 1DOF electrostatically actuated MEMS. The analysis of the pull-in phenomena is investigated in Section 6.3. Main results are discussed in Sections 6.4 and 6.5, where the output-feedback and robust control designs are presented, respectively. In Section 6.6, some simulation results are provided, and in the last section conclusions are drawn.

## 6.2 Modelling of the Electrostatic MEMS

A simplified 1-DOF electrostatic micro-actuator model is schematically represented in Figure 6.5. The system is driven by controlling the voltage source $E$ which is modelled

as a constant input voltage connected in series with the resistance $R$. The mass, spring and dashpot represent the mechanical part of the actuator for which $m$, $k$ and $b$ are the mass of the moveable upper plate, the elastic constant, and the damping coefficient, respectively. $q$ is the position of the top plate relative to the bottom plate, and the zero voltage gap is denoted by $q_z$.

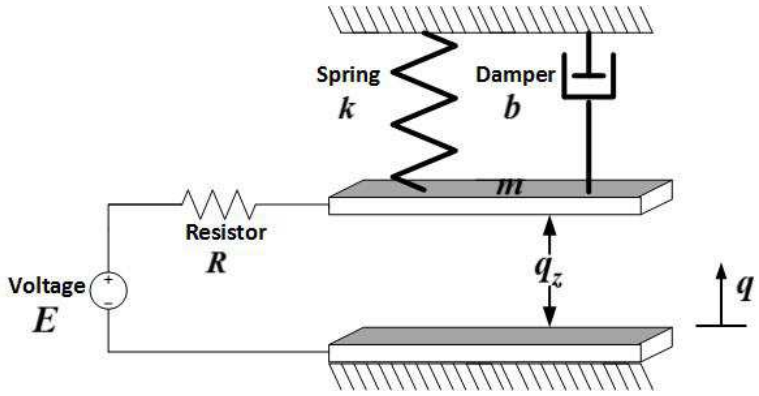


Figure 6.5: 1DOF model of parallel-plate electrostatic micro-actuator.

Applying Newton's law of motion in the mechanical domain and Kirchhoff's Current Law in the electrical domain, the equations of motion governing the behaviour of the actuator can be written as [57]

$$m\ddot{q}(t) + b\dot{q}(t) + k(q(t) - q_z) = -F(t), \tag{6.1}$$

and

$$\dot{Q}(t) = \frac{1}{R}\left(E(t) - \frac{Q(t)q(t)}{A\epsilon}\right), \tag{6.2}$$

where

$$F(t) = \frac{Q^2(t)}{2A\epsilon} = \frac{A\epsilon E^2(t)}{2q^2}, \tag{6.3}$$

is the attractive electrostatic force induced to the movable plate, $Q(t)$ is the charge of the device, $A$ is the plate area and $\epsilon$ is the permittivity in the gap. Rearranging, the system takes the following form of nonlinear dynamics [66]

$$\dot{q} = \frac{p}{m} \tag{6.4a}$$

$$\dot{p} = -k(q - q_z) - \frac{Q^2}{2A\epsilon} - \frac{b}{m}p \tag{6.4b}$$

$$\dot{Q} = -\frac{qQ}{RA\epsilon} + \frac{1}{R}u, \tag{6.4c}$$

where $p$ is the momentum. The nonlinearities mainly arise from the Coulomb electrostatic force. The total energy of the system, which is the sum of the elastic potential energy arising from a linear elastic force, the electrostatic potential energy of the capacitor subject to a voltage $E$, and the kinetic energy is given by the expression

$$H(q,p,Q) = \frac{1}{2}k(q-q_z)^2 + \frac{1}{2m}p^2 + \frac{q}{2A\epsilon}Q^2. \tag{6.5}$$

System (6.4) is defined on the state space

$$\mathcal{X} = \{(q,p,Q) \in \mathbb{R}^3 \mid 0 \leq q \leq q_z\}. \tag{6.6}$$

## 6.3 "Pull-in" Stability Analysis

At some critical voltage when a displacement of the top plate is equal to one-third of the zero-voltage gap, the system becomes unstable and this movable top plate rapidly snaps down to the fixed bottom plate, i.e. the gap collapses to zero. This phenomenon is called "snap-through" or "pull-in" and arises mainly from the tight and highly nonlinear electromechanical coupling. In this section we perform stability analysis of the MEMS device, and will show using energy (Hamiltonian) and linearization approaches why the equilibria of this system is only stable on one-third of the nominal gap.

The stability of this actuator is achieved from the balance between the elastic restoring force $k(q-q_z)$ and the electrostatic force (6.3), which must be equal at equilibrium position $q_{eq} \in (0, q_z)$

$$\begin{aligned} F_{spring} &= F_{electrostatic} \\ k(q_{eq}-q_z) &= \frac{Q_{eq}^2(t)}{2A\epsilon} = \frac{A\epsilon E_{eq}^2(t)}{2q_{eq}^2} \end{aligned} \tag{6.7}$$

### 6.3.1 Energy approach

As discussed in [74], also in Subsection 3.2, a Hamiltonian system is stable if the potential energy function $V(q)$ has an isolated minimum at the desired equilibrium point

$$q_{eq} = \arg\min V(q).$$

This is satisfied if both $\nabla_q V|_{q=q_{eq}} = 0$ and $\nabla_q^2 V|_{q=q_{eq}} > 0$ hold. The total potential energy $V$ of the system comprises the elastic potential of the linear spring and the electrostatic energy

$$V(q) = \frac{1}{2}k(q-q_z)^2 + \frac{A\epsilon E_{eq}^2}{2q}. \tag{6.8}$$

Substituting $E_{eq}^2$ from (6.7) in (6.8), we obtain

$$V(q) = \frac{1}{2}k(q-q_z)^2 + \frac{kq_{eq}^2(q_{eq}-q_z)}{q}. \tag{6.9}$$

Therefore,

$$\begin{aligned} \nabla_q V &= k(q - q_z) - \frac{k q_{eq}^2 (q_{eq} - q_z)}{q^2} \\ \nabla_q V|_{q=q_{eq}} &= k(q_{eq} - q_z) - \frac{k q_{eq}^2 (q_{eq} - q_z)}{q_{eq}^2} = 0, \end{aligned} \tag{6.10}$$

and

$$\begin{aligned} \nabla_q^2 V &= k + \frac{2k q_{eq}^2 (q_{eq} - q_z)}{q^3} \\ \nabla_q^2 V|_{q=q_{eq}} &= k\left(1 + \frac{2(q_{eq} - q_z)}{q_{eq}}\right) \\ &= k\left(3 - \frac{2q_z}{q_{eq}}\right) > 0 \implies q_{eq} > \frac{2}{3} q_z. \end{aligned} \tag{6.11}$$

From (6.11), the *Hessian* is only positive if $q_{eq} > \frac{2}{3} q_z$. Thus, the energy function has a local minimum and only stable at $q_{eq} > \frac{2}{3} q_z$ which is the upper one-third region of gap.

### 6.3.2 Linearization approach

In this section we perform the stability analysis of the MEMS device using linearization. The equilibrium points are determined by finding the solution so that the original state equations are zero, i.e. solving the following set of equations

$$\dot{q} = \frac{p}{m} = 0 \tag{6.12a}$$

$$\dot{p} = -k(q - q_z) - \frac{Q^2}{2A\epsilon} - \frac{b}{m} p = 0 \tag{6.12b}$$

$$\dot{Q} = -\frac{qQ}{RA\epsilon} + \frac{1}{R} u = 0. \tag{6.12c}$$

Thus, we obtain

$$p = 0, \tag{6.13a}$$

$$q = q_z - \frac{Q^2}{2kA\epsilon}, \tag{6.13b}$$

$$Q = \frac{u}{A\epsilon q}. \tag{6.13c}$$

Substituting (6.13c) into (6.13b) yields

$$q^3 - q_z q^2 + \frac{u^2}{c_0} = 0; \qquad c_0 = 2k(A\epsilon)^3. \tag{6.14}$$

There are three solutions for (6.14), one is negative for positive input voltages and can thus be ignored. The other two solutions are both positive. One of these equilibrium points is stable and the other is unstable. The stability of the system can also be

analyzed by applying Theorem 2.8 to the system (6.4), which gives

$$A = \begin{bmatrix} 0 & \frac{1}{m} & 0 \\ -k & -\frac{b}{m} & -\frac{Q}{A\epsilon} \\ -\frac{Q}{RA\epsilon} & 0 & -\frac{q}{RA\epsilon} \end{bmatrix}. \tag{6.15}$$

The eigenvalues of $A$ are obtained by solving $\det(\lambda I - A) = 0$. In this case

$$\begin{vmatrix} \lambda & -\frac{1}{m} & 0 \\ k & \lambda + \frac{b}{m} & \frac{Q}{A\epsilon} \\ \frac{Q}{RA\epsilon} & 0 & \lambda + \frac{q}{RA\epsilon} \end{vmatrix} = \lambda^3 + \left(\frac{q}{RA\epsilon} + \frac{b}{m}\right)\lambda^2 + \left(\frac{bq}{RA\epsilon m} + \frac{k}{m}\right)\lambda + \frac{kq}{RA\epsilon m} - \frac{Q^2}{R(A\epsilon)^2 m} = 0. \tag{6.16}$$

From (6.13b) we have $-Q^2 = 2kA\epsilon(q - q_z)$. Substituting this into (6.16), yields

$$\lambda^3 + \left(\frac{q}{RA\epsilon} + \frac{b}{m}\right)\lambda^2 + \left(\frac{bq}{RA\epsilon m} + \frac{k}{m}\right)\lambda + \frac{k}{RA\epsilon m}(3q - 2q_z) = 0. \tag{6.17}$$

As all terms are positive, it is clear from (6.17) that a condition for negative eigenvalues is that $3q - 2q_z > 0$, which implies

$$q_{eq} > \frac{2}{3}q_z,$$

i.e. the system is only stable in one third of its full gap and the region of stability is $q \in \left(\frac{2}{3}q_z, q_z\right]$.

The explanation of the 'pull-in' phenomenon is that the stability of the equilibrium is governed by two forces; the electrostatic force applied to the movable plate which pulls the plate down, and the elastic stiffness (spring force) which pulls the spring and thus the top plate up. Therefore, at equilibrium the relationship (6.7) is satisfied. From (6.7) with the spring force constant $k = 1$ and using (6.14), we can draw the relationship between the spring force linear (straight line) and the electrostatic force (curved line). Figure 6.6 plots the relationship between the spring force and the electrostatic force for various values of the input voltage $u$. As shown, there are two intersections, which means two equilibrium points, one is stable and one is unstable (saddle-node) [47]. When the upper plate's deflection is less than one-third of the zero voltage gap, and with small perturbation of the gap, the actuator returns to its equilibrium point as the increase in the restoring force of the linear spring is greater than the increase in the electrostatic force. As the displacement becomes greater than or equal to one-third of the zero voltage gap, any perturbation will result in the attractive electrostatic force being the dominant force and hence causes the top plate to collapse to the fixed plate. For voltage values above the pull-in limit, there are no equilibrium points (the curves never intersect).

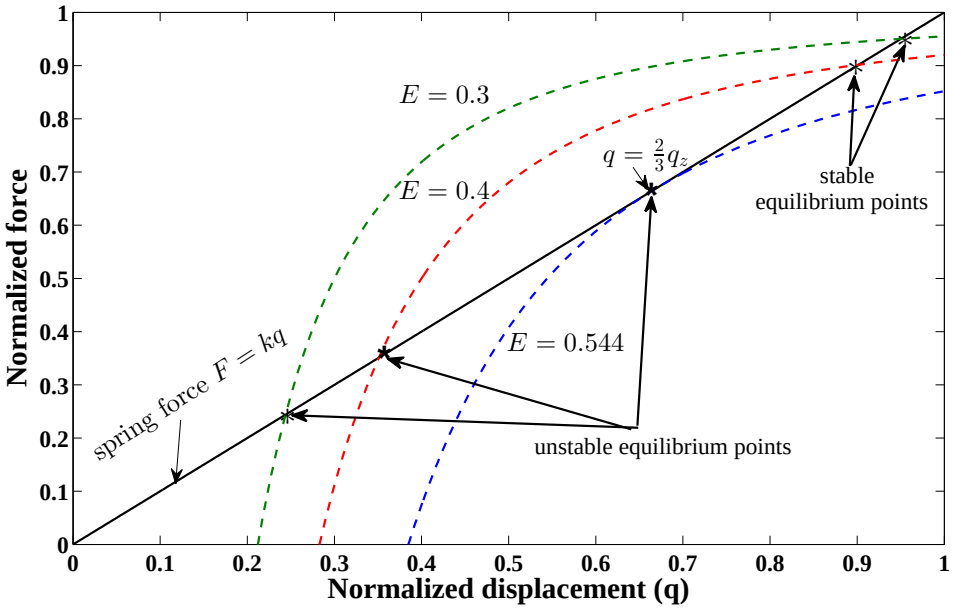


Figure 6.6: Pull-in displacement characteristic of the microactuator.

## 6.4 IDA-PBC Control Design

In this section we apply the IDA-PBC control method, suggested by [66], to design a suitable control law for the electrostatically actuated MEMS device. The objective is to control the gap between the two plates according to a given constant set-point. Consider the system (6.4) that can be written as PCH form (2.35) as

$$\begin{bmatrix} \dot{q} \\ \dot{p} \\ \dot{Q} \end{bmatrix} = \begin{bmatrix} 0 & 1 & 0 \\ -1 & -b & 0 \\ 0 & 0 & -\frac{1}{R} \end{bmatrix} \begin{bmatrix} \nabla_q H \\ \nabla_p H \\ \nabla_Q H \end{bmatrix} + \begin{bmatrix} 0 \\ 0 \\ \frac{1}{R} \end{bmatrix} u \qquad (6.18)$$
$$y = G^\top \nabla H$$

with the total energy function or the Hamiltonian function (6.5) and $G = \begin{bmatrix} 0 \\ 0 \\ \frac{1}{R} \end{bmatrix}$.

The idea here is to reshape the total energy function of the system, such that the system is stabilized over the entire gap. The controller design is concluded in the following proposition.

**Proposition 6.1.** *Consider the system (6.4) described by the open-loop PCH form (6.18) and the energy function (6.5). Assign the desired energy function as*

$$H_d(q,p,Q) = \frac{1}{2}k(q-q_z)^2 + \frac{1}{2m}p^2 + \frac{q}{2A\epsilon}Q^2 + \frac{1}{2}k_1Q^2, \qquad (6.19)$$

*and the desired PCH structure as*

$$\begin{bmatrix} \dot{q} \\ \dot{p} \\ \dot{Q} \end{bmatrix} = \begin{bmatrix} 0 & 1 & 0 \\ -1 & -b & 0 \\ 0 & 0 & -K_v \end{bmatrix} \begin{bmatrix} \nabla_q H_d \\ \nabla_p H_d \\ \nabla_Q H_d \end{bmatrix} \qquad y_d = G^\top \nabla H_d. \tag{6.20}$$

*Then, the output feedback controller*

$$u_{IDA} = (1 - RK_v)\frac{qQ}{A\epsilon} - RK_v k_1 Q, \tag{6.21}$$

*with $K_v, k_1 > 0$, asymptotically stabilizes the system over the full gap.* ■

**Proof of Proposition 6.1:** Consider the Hamiltonian function (6.19) as a candidate Lyapunov function for the system (6.20). Its derivative along the trajectories of the system is

$$\begin{aligned} \dot{H}_d &= \nabla_q H_d \dot{q} + \nabla_p H_d \dot{p} + \nabla_Q H_d \dot{Q} \\ &= \left( k(q - q_z) + \frac{Q^2}{2A\epsilon} \right) \nabla_p H_d - \nabla_p H_d \left( k(q - q_z) + \frac{Q^2}{2A\epsilon} + \frac{b}{m} p \right) \\ &\quad - \left( \frac{qQ}{A\epsilon} + k_1 Q \right) K_v \left( \frac{qQ}{A\epsilon} + k_1 Q \right) \\ &= -\frac{b}{m^2} p^2 - K_v \left( \frac{qQ}{A\epsilon} + k_1 Q \right)^2 < 0, \end{aligned}$$

which is negative definite. Thus, the desired equilibrium point $(q_e, 0, 0)$ is asymptotically stable. ■

**Remark 6.2.** The shaping of the total energy function includes the addition of the new *quadratic* term (last term in (6.19)). This implies adding more damping to the $Q$ coordinate represented by the last term in the controller (6.21). Consequently, the damping can only affect the electrical part of the system while the mechanical part is not significantly affected; limiting its application onto insufficiently damped MEMS devices, a problem that cannot be solved using a static feedback controller [57]. In Section 6.5, we propose a novel dynamic controller that enables adding damping in both electrical and mechanical coordinates of the MEMS which solves this problem on one hand, and improve the robustness of the system on the other hand.

**Remark 6.3.** In the MEMS applications, the velocity state is unmeasurable or even if possible the measurement is very expensive. The proposed controller is an output feedback control law that neither depends on the state $p$ nor requires constructing a velocity observer, which would clearly lead to a more complicated control law.

## 6.5 Robust IDA-PBC Control Design

The design method in Section 6.4 assumes an ideal system model. However, as discussed earlier in Section 6.1, in practice parametric uncertainty, external disturbances, and noise may exist as a result of parasitic capacitance, manufacturing deformations (tolerance) from bulk micromachining, states measurements and environmental fluctuations [120]. Consequently the reliability and performance of the MEMS are highly affected by the modelling errors and unmodelled dynamics. An obvious example is the accelerometers used in vehicle's airbag to sense the vehicle's acceleration. In such application, modelling errors may affect the estimation of the accelerometer's threshold (the point of maximum acceleration) and hence the decision whether to deploy the bag or not.

### 6.5.1 Problem formulation

One of the most popular approaches to counteract the effects of uncertainties, disturbances and noises on control systems is to add an integral action to the stabilization controller. For the PCH formulation, the inclusion of the integral action depends on how the inputs act on the states [29]. We call the states that receive direct action from the input as *passive* outputs, or *non-passive* otherwise. While the case of passive output can be applied directly on the MEMS using the method proposed in [66], the case of non-passive output is more complicated. In Chapter 5 (see also [29] and [82]), some constructive methods have been proposed to deal with the case of non-passive outputs for mechanical systems using a change of coordinates on the momenta. For electromechanical systems, or the MEMS in our case, since the control input is attainable from the charge $Q$ coordinates, then a change of coordinates can be applied to the state $Q$ to inject the integral control action to the dynamic of $p$. However, for the state $q$ (displacement), which are usually the states of interest, and given the complex coupling between different energy domains at micro-scale, the application of integral action becomes more complicated and requires change of coordinates in both $p$ and $Q$.

Consider the MEMS in PCH form

$$\begin{aligned}\begin{bmatrix}\dot{q}\\ \dot{p}\\ \dot{Q}\end{bmatrix} &= \begin{bmatrix}0 & 1 & 0\\ -1 & -b & 0\\ 0 & 0 & -\frac{1}{R}\end{bmatrix}\begin{bmatrix}\nabla_q H\\ \nabla_p H\\ \nabla_Q H\end{bmatrix} + \begin{bmatrix}0\\ 0\\ \frac{1}{R}\end{bmatrix} u + \begin{bmatrix}d_1\\ d_2\\ d_3\end{bmatrix},\\ y &= G^\top \nabla H\end{aligned} \tag{6.22}$$

with the Hamiltonian function

$$H(q,p,Q) = \frac{1}{2}k(q-q_z)^2 + \frac{1}{2m}p^2 + \frac{q}{2A\epsilon}Q^2, \tag{6.23}$$

where $d_1,\ d_2 \in R^1$ are unmatched disturbances and $d_3 \in R^1$ is the matched disturbance. The control objective is to find a dynamic feedback control law $u$ such that the stability of the closed-loop system is preserved despite the presence of uncertainties and/or disturbances. That is, we consider enhancing the IDA-PBC (6.21) by adding integral action such that the following are achieved:

- With no disturbances, the incorporation of the integral action on the passive and non-passive output improves the performance of the closed-loop system, such as eliminating the steady-state errors that may result from uncertainties.
- Preserving stability of the closed-loop system even in the presence of the matched and unmatched disturbances, ensuring the iISS and ISS with respect to matched and unmatched disturbances, respectively.

In the next subsections, we will discuss the inclusion of integral action for the MEMS starting from the simple case of passive output to the most complicated case of the non-passive output. Then, we investigate the design of a dynamic IDA-PBC controller for the disturbance rejection problem.

### 6.5.2 Integral control on passive output

From (6.22), the charge $Q$ is the passive output. Using the method proposed in [66], the integral action on the passive output can be added to the closed-loop PCH system (6.20) to form an augmented dynamical system

$$\begin{bmatrix} \dot{q} \\ \dot{p} \\ \dot{Q} \\ \dot{v} \end{bmatrix} = \begin{bmatrix} 0 & 1 & 0 & 0 \\ -1 & -b & 0 & 0 \\ 0 & 0 & -K_v & -K_i \\ 0 & 0 & K_i & 0 \end{bmatrix} \begin{bmatrix} \nabla_q H_d \\ \nabla_p H_d \\ \nabla_Q H_d \\ \nabla_v H_d \end{bmatrix} \tag{6.24}$$

with the integral control

$$v = -K_i \int y_d dt = -K_i G^\top \int \nabla_Q H_d dt, \tag{6.25}$$

and the integral gain $K_i = K_i^\top > 0$.

### 6.5.3 Integral control on non-passive output: the momentum state

**Proposition 6.4.** *Consider the open-loop MEMS (6.22) with $d = 0$. Define the state transformation*

$$x_q = q; \quad x_p = p; \quad x_Q^2 = Q^2 + 2A\epsilon x_v, \tag{6.26}$$

*to realize the augmented closed-loop PCH system*

$$\begin{bmatrix} \dot{x}_q \\ \dot{x}_p \\ \dot{x}_Q \\ \dot{x}_v \end{bmatrix} = \begin{bmatrix} 0 & 1 & 0 & 0 \\ -1 & -b & 0 & K_i \\ 0 & 0 & -K_v & 0 \\ 0 & -K_i & 0 & 0 \end{bmatrix} \begin{bmatrix} \nabla_{x_q}\tilde{H} \\ \nabla_{x_p}\tilde{H} \\ \nabla_{x_Q}\tilde{H} \\ \nabla_{x_v}\tilde{H} \end{bmatrix}, \tag{6.27}$$

*with the desired Hamiltonian function*

$$\tilde{H} = \frac{1}{2}k(x_q - q_z)^2 + \frac{1}{2m}x_p^2 + \frac{x_q}{2A\epsilon}x_Q^2 + \frac{1}{2}k_1 x_Q^2 + \frac{1}{2}K_i^{-1}x_v^2. \tag{6.28}$$

*Asymptotic stability of the equilibrium point* $x_e = (x_{qe}, 0, 0) = (q_e, 0, 0)$ *is preserved using the integral control*

$$\begin{aligned} v &= -\frac{2RK_v}{Q}(q + k_1 A\epsilon)x_v - \frac{1}{Q}RA\epsilon\dot{x}_v \\ \dot{x}_v &= -K_i\nabla_{x_p}\tilde{H}. \end{aligned} \tag{6.29}$$

*Furthermore, the total control input consisting of the IDA-PBC (6.21) with an integral action (6.29) takes the form*

$$u = u_{IDA} + v = (1 - RK_v)\frac{qQ}{A\epsilon} - RK_v k_1 Q - \frac{2RK_v}{Q}(q + k_1 A\epsilon)x_v - \frac{1}{Q}RA\epsilon\dot{x}_v. \tag{6.30}$$

■

**Proof of Proposition 6.4:** Consider the Hamiltonian function (6.28) as a candidate Lyapunov function for the system (6.27). Its derivative along the trajectories of the system and using (6.26) is

$$\begin{aligned} \dot{\tilde{H}} &= \nabla_{x_q}\tilde{H}\dot{x}_q + \nabla_{x_p}\tilde{H}\dot{x}_p + \nabla_{x_Q}\tilde{H}\dot{x}_Q + \nabla_{x_v}\tilde{H}\dot{x}_v \\ &= \nabla_{x_q}\tilde{H}\nabla_{x_p}\tilde{H} + \nabla_{x_p}\tilde{H}(-\nabla_{x_q}\tilde{H} - b\nabla_{x_p}\tilde{H} + K_i\nabla_{x_v}\tilde{H}) \\ &\quad + \nabla_{x_Q}\tilde{H}(-K_v\nabla_{x_Q}\tilde{H}) + \nabla_{x_v}\tilde{H}(-K_i\nabla_{x_p}\tilde{H}) \\ &= \nabla_{x_q}\tilde{H}\nabla_{x_p}\tilde{H} - \nabla_{x_p}\tilde{H}\nabla_{x_q}\tilde{H} + \nabla_{x_p}\tilde{H}K_i\nabla_{x_v}\tilde{H} - \nabla_{x_p}\tilde{H}K_i\nabla_{x_v}\tilde{H} \\ &\quad - b|\nabla_{x_p}\tilde{H}|^2 - K_v|\nabla_{x_Q}\tilde{H}|^2 \\ &= -b\left|\frac{1}{m}x_p\right|^2 - K_v\left|\frac{x_q x_Q}{A\epsilon} + k_1 x_Q\right|^2 \leq 0, \end{aligned} \tag{6.31}$$

which is negative semi-definite. Furthermore, asymptotic stability can be proven invoking detectability condition as in the proof of Proposition 6.7. The controller (6.30) is found by equating (6.22) and (6.27) and applying the coordinate transformation (6.26),

that is

$$\begin{aligned}
2Q\dot{Q} &\equiv 2x_Q\dot{x}_Q - 2A\epsilon\dot{x}_v \\
2Q\left(-\frac{1}{R}\nabla_Q H + \frac{1}{R}u\right) &= 2x_Q(-K_v\nabla_{x_Q}\tilde{H}) - 2A\epsilon\dot{x}_v \\
2Q\left(-\frac{qQ}{RA\epsilon} + \frac{1}{R}u\right) &= 2x_Q\left(-\frac{K_v}{A\epsilon}x_q x_Q - K_v k_1 x_Q\right) - 2A\epsilon\dot{x}_v \\
-\frac{2qQ^2}{RA\epsilon} + \frac{2Q}{R}u &= -\frac{2K_v}{A\epsilon}x_q x_Q^2 - 2K_v k_1 x_Q^2 - 2A\epsilon\dot{x}_v.
\end{aligned}$$

Substituting $x_q$ and $x_Q^2$ from (6.26) yields

$$\begin{aligned}
\frac{2Q}{R}u - \frac{2qQ^2}{RA\epsilon} &= -\frac{2K_v}{A\epsilon}q(Q^2 + 2A\epsilon x_v) - 2K_v k_1(Q^2 + 2A\epsilon x_v) - 2A\epsilon\dot{x}_v \\
\frac{2Q}{R}u &= \frac{2qQ^2}{RA\epsilon} - \frac{2K_v}{A\epsilon}qQ^2 - 2K_v k_1 Q^2 - 4K_v q x_v - 4K_v k_1 A\epsilon x_v - 2A\epsilon\dot{x}_v.
\end{aligned}$$

Multiplying both sides with $\frac{R}{2Q}$, we obtain the control law (6.30). ■

**Remark 6.5.** Note that the denominator of the control law (6.30) is equal to zero if $Q = 0$. However, by definition, zero charge is corresponding to zero voltage which means the system is at rest or at the equilibrium. Thus, we can ensure that the denominator of the control law is never be zero for $Q \neq 0$, i.e. there are no singularities.

### 6.5.4 Integral control on non-passive output: the position state

The state $q$ is the signal of interest in this application. The inclusion of the integral action in the position state is more complicated. This is due to the coupling between the position and momentum states in the interconnection matrix in one side, and the coupling between the position and the charge in the energy function, particularly the term $\frac{q}{2A\epsilon}Q^2$. Consequently, the incorporation of integral action requires a change of coordinates on both $p$ and $Q$ states, as constructed in the following proposition.

**Proposition 6.6.** *Consider the the open-loop MEMS (6.22) with* $d = \begin{bmatrix} d_1 & d_2 & d_3 \end{bmatrix}^\top = 0$. *Define the state transformation*

$$\begin{aligned}
x_q &= q \\
x_p &= p + mx_v \\
x_Q^2 &= Q^2 + 2A\epsilon(bx_v + m\dot{x}_v),
\end{aligned} \tag{6.32}$$

*to realize the augmented closed-loop PCH system*

$$\begin{bmatrix} \dot{x}_q \\ \dot{x}_p \\ \dot{x}_Q \\ \dot{x}_v \end{bmatrix} = \begin{bmatrix} 0 & 1 & 0 & K_i \\ -1 & -b & 0 & 0 \\ 0 & 0 & -K_v & 0 \\ -K_i & 0 & 0 & 0 \end{bmatrix} \begin{bmatrix} \nabla_{x_q}\tilde{H} \\ \nabla_{x_p}\tilde{H} \\ \nabla_{x_Q}\tilde{H} \\ \nabla_{x_v}\tilde{H} \end{bmatrix}, \tag{6.33}$$

*with the desired Hamiltonian function*

$$\tilde{H} = \frac{1}{2}k(x_q - q_z)^2 + \frac{1}{2m}x_p^2 + \frac{x_q}{2A\epsilon}x_Q^2 + \frac{1}{2}k_1 x_Q^2 + \frac{1}{2}K_i^{-1}x_v^2. \tag{6.34}$$

*Asymptotic stability of the equilibrium point* $x_e = (x_{qe}, 0, 0) = (q_e, 0, 0)$ *is preserved with the integral control*

$$\begin{aligned} v &= -\frac{2RK_v b}{Q}(q + k_1 A\epsilon)x_v - \frac{2R}{Q}(K_v mq + K_v k_1 A\epsilon m + A\epsilon b)\dot{x}_v - \frac{2R}{Q}A\epsilon m\ddot{x}_v \\ \dot{x}_v &= -K_i \nabla_{x_q}\tilde{H}. \end{aligned} \tag{6.35}$$

*Furthermore, the total control input consisting of the IDA-PBC (6.21) with integral action (6.35) takes the form*

$$\begin{aligned} u = u_{IDA} + v = (1 - RK_v)\frac{qQ}{A\epsilon} - RK_v k_1 Q - \frac{2RK_v b}{Q}(q + k_1 A\epsilon)x_v \\ - \frac{2R}{Q}(K_v mq + K_v k_1 A\epsilon m + A\epsilon b)\dot{x}_v - \frac{2R}{Q}A\epsilon m\ddot{x}_v. \end{aligned} \tag{6.36}$$

■

**Proof of Proposition 6.6:** Consider the Hamiltonian function (6.34) as a candidate Lyapunov function for the system (6.33). Its derivative along the trajectories of the system is

$$\begin{aligned} \dot{\tilde{H}} &= \nabla_{x_q}\tilde{H}\dot{x}_q + \nabla_{x_p}\tilde{H}\dot{x}_p + \nabla_{x_Q}\tilde{H}\dot{x}_Q + \nabla_{x_v}\tilde{H}\dot{x}_v \\ &= \nabla_{x_q}\tilde{H}(\nabla_{x_p}\tilde{H} + K_i\nabla_{x_v}\tilde{H}) + \nabla_{x_p}\tilde{H}(-\nabla_{x_q}\tilde{H} - b\nabla_{x_p}\tilde{H}) \\ &\quad + \nabla_{x_Q}\tilde{H}(-K_v\nabla_{x_Q}\tilde{H}) + \nabla_{x_v}\tilde{H}(-K_i\nabla_{x_q}\tilde{H}) \\ &= \nabla_{x_q}\tilde{H}\nabla_{x_p}\tilde{H} - \nabla_{x_p}\tilde{H}\nabla_{x_q}\tilde{H} + \nabla_{x_q}\tilde{H}K_i\nabla_{x_v}\tilde{H} - \nabla_{x_q}\tilde{H}K_i\nabla_{x_v}\tilde{H} \\ &\quad - b|\nabla_{x_p}\tilde{H}|^2 - K_v|\nabla_{x_Q}\tilde{H}|^2 \\ &= -b\left|\frac{1}{m}x_p\right|^2 - K_v\left|\frac{x_q x_Q}{A\epsilon} + k_1 x_Q\right|^2 \leq 0, \end{aligned} \tag{6.37}$$

which is negative semi-definite. Furthermore, asymptotic stability can be proven invoking detectability condition as in the proof of Proposition 6.7. We complete the proof by showing that the system (6.22) with the controller (6.36) coincide with the desired PCH system (6.33). Applying the change of coordinates (6.32) for the state $q$, we have

$$\begin{aligned} \dot{q} &= \frac{p}{m} \\ &\equiv \dot{x}_q \\ &= \nabla_{x_p}\tilde{H} + K_i\nabla_{x_v}\tilde{H} = \frac{1}{m}(p - mx_v) + K_i K_i^{-1}x_v, \end{aligned}$$

and for the state $p$ we have

$$\begin{aligned}\dot{p} &= -\nabla_q H - b\nabla_p H = k(q - q_z) - \frac{Q^2}{2A\epsilon} - \frac{b}{m}p \\ &\equiv \dot{x}_p + m\dot{x}_v \\ &= -\nabla_{x_q}\tilde{H} - b\nabla_{x_p}\tilde{H} + m\dot{x}_v = k(x_q - q_z) - \frac{x_Q^2}{2A\epsilon} - \frac{b}{m}x_p + m\dot{x}_v.\end{aligned}$$

Finally for the state $Q$, we have

$$\begin{aligned}2Q\dot{Q} &\equiv 2x_Q\dot{x}_Q - 2A\epsilon b\dot{x}_v - 2A\epsilon m\ddot{x}_v \\ 2Q\left(-\frac{1}{R}\nabla_Q H + \frac{1}{R}u\right) &= 2x_Q(-K_v\nabla_{x_Q}\tilde{H}) - 2A\epsilon b\dot{x}_v - 2A\epsilon m\ddot{x}_v \\ 2Q\left(-\frac{qQ}{RA\epsilon} + \frac{1}{R}u\right) &= 2x_Q\left(-\frac{K_v}{A\epsilon}x_q x_Q - K_v k_1 x_Q\right) - 2A\epsilon b\dot{x}_v - 2A\epsilon m\ddot{x}_v \\ -\frac{2qQ^2}{RA\epsilon} + \frac{2Q}{R}u &= -\frac{2K_v}{A\epsilon}x_q x_Q^2 - 2K_v k_1 x_Q^2 - 2A\epsilon b\dot{x}_v - 2A\epsilon m\ddot{x}_v.\end{aligned} \tag{6.38}$$

Substituting $x_q$, $x_p$ and $x_Q^2$ from (6.32) yields

$$\begin{aligned}\frac{2Q}{R}u - \frac{2qQ^2}{RA\epsilon} &= -\frac{2K_v}{A\epsilon}q(Q^2 + 2A\epsilon(bx_v + m\dot{x}_v)) - 2A\epsilon b\dot{x}_v - 2A\epsilon m\ddot{x}_v \\ &\quad - 2K_v k_1(Q^2 + 2A\epsilon(bx_v + m\dot{x}_v)) \\ \frac{2Q}{R}u &= \frac{2qQ^2}{RA\epsilon} - \frac{2K_v}{A\epsilon}qQ^2 - 2K_v k_1 Q^2 - 4K_v b(q + k_1 A\epsilon)x_v \\ &\quad - (4K_v m + 4K_v k_1 A\epsilon m + 2A\epsilon b)\dot{x}_v - 2A\epsilon m\ddot{x}_v.\end{aligned} \tag{6.39}$$

Multiplying both sides of (6.39) by $\frac{R}{2Q}$ yields the control law (6.36). ∎

### 6.5.5 iISS and ISS for time-varying matched and unmatched disturbances

In previous subsections, we have introduced the integral action for both passive and non-passive outputs assuming no disturbances. In this subsection, we propose new control design approaches that ensure robustness of the system in the presence of disturbances. Particularly, we are interested in designing controllers that ensure the integral input-to-state and input-to-state properties with respect to matched and unmatched disturbances, respectively, for the MEMS system.

Interestingly, the system (6.22) subject to *matched* disturbance $d_3$ only ($d_1 = d_2 = 0$), is *naturally* iISS using the integral control on passive outputs as in Subsection 6.5.2 and following the same procedures as in Subsection 5.3.4. The case of *unmatched* disturbances $d_1, d_2$ requires a change of coordinates on the position, momentum and charge states to establish the ISS property. The whole procedure is concluded in the following proposition.

**Proposition 6.7.** *Consider the open-loop MEMS (6.22) with time-varying bounded unmatched $d_1, d_2$ disturbances. Define the state transformation*

$$\begin{aligned} x_q &= q - x_v \\ x_p &= p + x_v \\ x_Q^2 &= Q^2 + \mathcal{C}x_v, \quad \left(\mathcal{C} = 2A\epsilon\left(k - \frac{b}{m}\right)\right) \end{aligned} \tag{6.40}$$

*to realize the closed-loop system in the new variables $x := [x_q\ x_p\ x_v]$ as*

$$\begin{bmatrix} \dot{x}_q \\ \dot{x}_p \\ \dot{x}_Q \\ \dot{x}_v \end{bmatrix} = \begin{bmatrix} -\frac{1}{2} & \frac{1}{2} & 0 & -\frac{1}{2} \\ -\frac{1}{2} & -b & 0 & -\frac{1}{2} \\ 0 & 0 & -K_v & 0 \\ \frac{1}{2} & \frac{1}{2} & 0 & -\frac{1}{2} \end{bmatrix} \begin{bmatrix} \nabla_{x_q}\tilde{H} \\ \nabla_{x_p}\tilde{H} \\ \nabla_{x_Q}\tilde{H} \\ \nabla_{x_v}\tilde{H} \end{bmatrix} + \begin{bmatrix} d_1 \\ d_2 \\ 0 \\ 0 \end{bmatrix}, \tag{6.41}$$

*with the desired Hamiltonian function*

$$\tilde{H} = \frac{1}{2}k(x_q - q_z)^2 + \frac{1}{2m}x_p^2 + \frac{x_q}{2A\epsilon}x_Q^2 + \frac{1}{2}k_1x_Q^2 + \frac{1}{2m}x_v^2. \tag{6.42}$$

*Then the closed-loop system is ISS with respect to the disturbances $d_1$ and $d_2$ and the function (6.42) is the ISS-Lyapunov function for the system (6.41). Furthermore, the control law is obtained as*

$$\begin{aligned} u = \frac{R}{2Q}\Bigg(&\frac{2Q^2}{A\epsilon}\left(\frac{q}{R} - k_vq + k_vx_v\right) - \frac{2k_v\mathcal{C}}{A\epsilon}qx_v + \frac{2k_v\mathcal{C}}{A\epsilon}x_v^2 - 2k_vk_1Q^2 \\ &-2k_vk_1\mathcal{C}x_v - \mathcal{C}\dot{x}_v\Bigg) \\ \dot{x}_v = \frac{1}{2}\nabla_{x_q}\tilde{H} &+ \frac{1}{2}\nabla_{x_p}\tilde{H} - \frac{1}{2}\nabla_{x_v}\tilde{H}. \end{aligned} \tag{6.43}$$

■

**Proof of Proposition 6.7:** Consider the desired Hamiltonian function (6.42) as a candidate ISS-Lyapunov function. Its time-derivative along the trajectories of (6.41) along with (6.40) is given by

$$\begin{aligned} \dot{\tilde{H}} &= \nabla_{x_q}\tilde{H}\dot{x}_q + \nabla_{x_p}\tilde{H}\dot{x}_p + \nabla_{x_Q}\tilde{H}\dot{x}_Q + \nabla_{x_v}\tilde{H}\dot{x}_v \\ &= \nabla_{x_q}\tilde{H}(-\frac{1}{2}\nabla_{x_q}\tilde{H} + \frac{1}{2}\nabla_{x_p}\tilde{H} - \frac{1}{2}\nabla_{x_v}\tilde{H} + d_1) \\ &\quad + \nabla_{x_p}\tilde{H}(-\frac{1}{2}\nabla_{x_q}\tilde{H} - b\nabla_{x_p}\tilde{H} - \frac{1}{2}\nabla_{x_v}\tilde{H} + d_2) \\ &\quad + \nabla_{x_Q}\tilde{H}(-K_v\nabla_{x_Q}\tilde{H}) + \nabla_{x_v}\tilde{H}(\frac{1}{2}\nabla_{x_q}\tilde{H} + \frac{1}{2}\nabla_{x_p}\tilde{H} - \frac{1}{2}\nabla_{x_v}\tilde{H}) \\ &= -\frac{1}{2}|\nabla_{x_q}\tilde{H}|^2 + \nabla_{x_q}\tilde{H}d_1 - b|\nabla_{x_p}\tilde{H}|^2 + \nabla_{x_p}\tilde{H}d_2 - k_v|\nabla_{x_Q}\tilde{H}|^2 \\ &\quad - \frac{1}{2}|\nabla_{x_v}\tilde{H}|^2. \end{aligned} \tag{6.44}$$

Applying Young's inequality, yields

$$\begin{aligned}\dot{\tilde{H}} &\leq -\frac{1}{4}|\nabla_{x_q}\tilde{H}|^2 + |d_1|^2 - \frac{b}{2}|\nabla_{x_p}\tilde{H}|^2 + \frac{1}{2b}|d_2|^2 - k_v|\nabla_{x_Q}\tilde{H}|^2 - \frac{1}{2}|\nabla_{x_v}\tilde{H}|^2 \\ &\leq -\alpha(|x_q, x_p, x_Q, x_v|) + \sigma(|d|),\end{aligned} \tag{6.45}$$

with $\alpha,\ \sigma \in \mathcal{K}_\infty$. Now, from (6.45) and the fact that $\tilde{H}$ is positive definite and proper, all conditions of the ISS property from Theorem 2.14 and Definition 2.16 are satisfied, which proves that the closed-loop PCH system is ISS with respect to the unmatched disturbances. ■

## 6.6 Simulation Results

To make the system analysis and control design easier and to avoid numerical problems in simulation, we transform the system (6.1)-(6.2) through normalized coordinates by using scaling of $t = \sigma\hat{t}$, where $\sigma$ is the attenuation. The normalization is performed as follows [57]:

Let $v = \sigma R\beta$, $\alpha = \epsilon\sigma AR$, $\beta = \epsilon\sigma A\sqrt{\sigma mR}$ and the state vector $x = \left[\frac{q}{\alpha}, \frac{\dot{q}}{\alpha}, \frac{Q}{\beta}\right]$. The system parameters are defined as

$$w_n^2 = \frac{k}{m},$$
$$2\zeta w_n = \frac{b}{m},$$
$$w = \frac{w_n}{\sigma},$$

where $w_n$ and $\zeta$ are the natural frequency and the damping ratio of the system, respectively. Through this normalization, the system takes the following form of nonlinear dynamics

$$\dot{x}_1 = x_2 \tag{6.46a}$$
$$\dot{x}_2 = -w^2(x_1 - q_z) - 2\zeta w x_2 - \frac{x_3^2}{2} \tag{6.46b}$$
$$\dot{x}_3 = -x_1 x_3 + u, \tag{6.46c}$$

with the normalized energy function

$$H(x_1, x_2, x_3) = \frac{1}{2}(x_1 - g_0)^2 + \frac{1}{2}x_1 x_3^2 + \frac{1}{2}x_2^2. \tag{6.47}$$

This model is defined on the state space $\mathcal{X} = \{(x_1, x_2, x_3) \in \mathbb{R}^3 \mid 0 \leq x_1 \leq 1\}$.

Simulations have been carried out using MATLAB/SIMULINK. A pulse voltage with a width of 0.2 seconds and amplitude of 2 volts is applied to steer the operation. The actuator is supposed to be driven by a voltage source, whose amplitude is limited to $\pm 3$

volts. The IDA-PBC design is applied to the normalized nonlinear electrostatic actuator model. The considered task is a set point regulation where the responses of the control system are observed, to test and validate the and the performance of MEMS using the proposed control algorithm.

The positions of the movable plate at different set-points $10\%, 50\%$, and $90\%$ deflections corresponding to 0.9, 0.5 and 0.1 gap positions, respectively using IDA-BPC proposed controller (6.21) with controller parameters $K_v = 2, k_1 = 1, w = 1,$ and $\zeta = 1$ are shown in Figure 6.7. The results show that the proposed controller ensures a stable full gap operation.

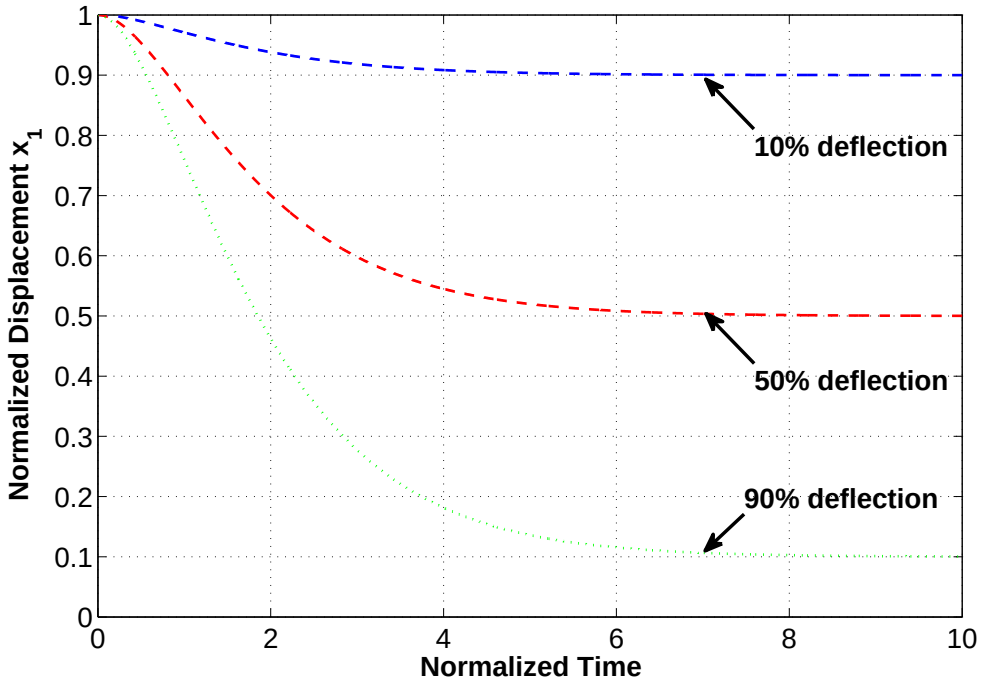


Figure 6.7: Stabilization of 0.1, 0.5 and 0.9 gap positions.

The positions of the movable plate and the control effort corresponding to 40% deflection (0.6 gap position) with varied $K_v$ are shown in Figure 6.8 and Figure 6.9, respectively. It can be seen that, values of $K_v < 1$ result in a large steady-state error. Furthermore in (6.21), $K_v = \frac{1}{R}$, the first term on the right-hand side becomes zero and we obtain the simple linear feedback controller which is directly proportional to charge $Q$ [57]. We note also that the amplitude of the control input is high at the initial stage, this is due to a significantly law charge and hence excessive control signal is required to charge the capacitor [119]. However, as demonstrated in Figure 6.9 the control signal becomes quite smooth afterwards.

The system is also simulated at various values of the damping ratio $\zeta$. As shown in Figure 6.10, when $\zeta = 0$ , the response becomes oscillatory. An increase in $\zeta$ $(0 < \zeta < 1)$

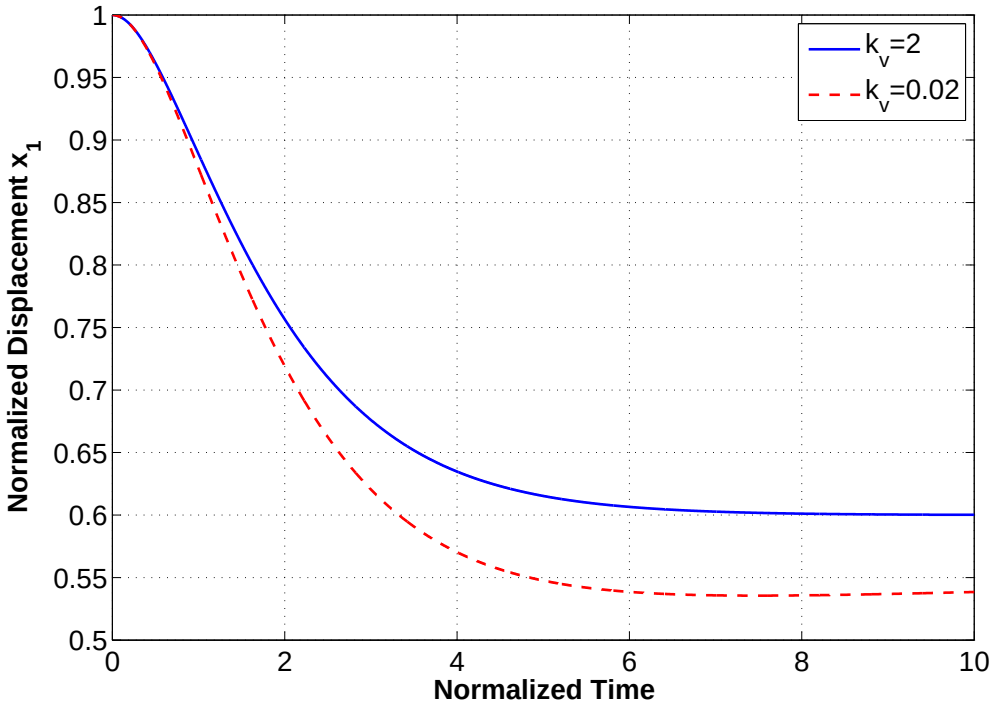


Figure 6.8: Stabilization of 0.4 gap position at different values of $K_v$.

reduces the oscillations and shorten the settling time, with $\zeta = 1$ brings the fastest response. An overdamped system with $\zeta > 1$ responds more slowly to any inputs. The variations in $\zeta$ give rise to an important issue related to the uncertainty in dynamical systems. Bulk micromachining of MEMS may cause manufacturing inconsistencies in MEMS devices [118]. This results in uncertain MEMS devices, and parameters such as damping ratio $\zeta$, is difficult to be accurately identified, especially when dealing with systems in micro scale, where a very tiny error may bring significant effects to system's functionality. Hence, robust control techniques is very useful to apply to control MEMS devices.

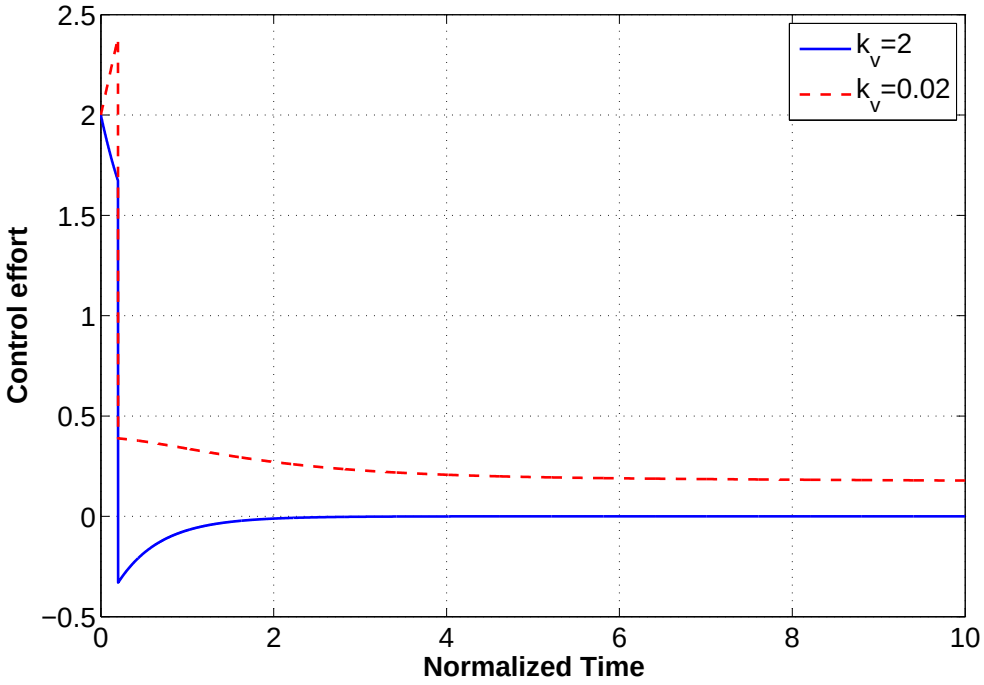


Figure 6.9: Control effort for stabilization of 0.4 gap position at different values of $K_v$.

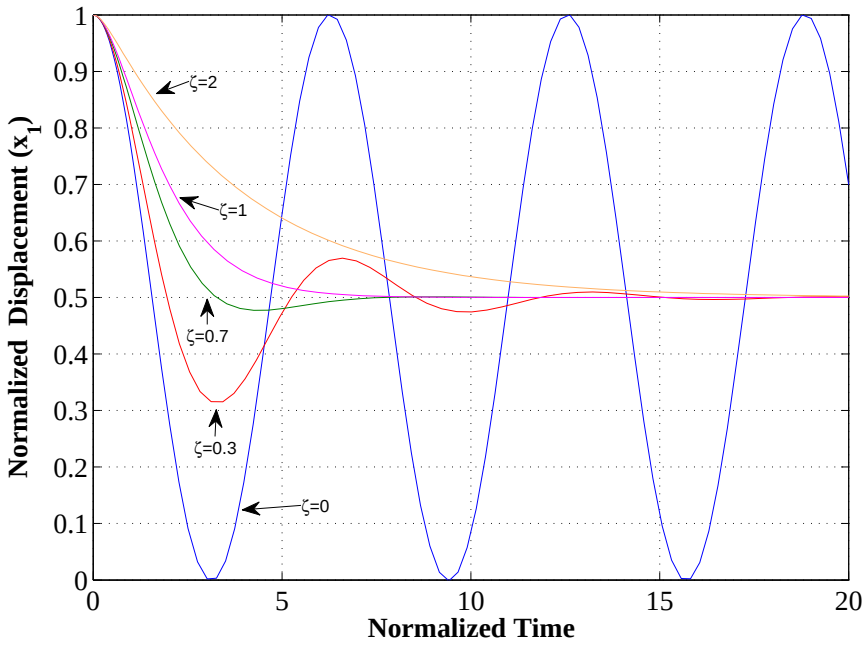


Figure 6.10: Stabilization of 0.5 gap position at different values of $\zeta$.

## 6.7 Conclusion

Electrostatically actuated MEMS devices exhibit an inherently nonlinear operational instability phenomena called pull-in which is associated with the interaction between the electrostatic and elastic restoring forces. We have investigated this phenomenon from the energy-based and linearization perspectives, and we have proposed an output-feedback IDA-PBC design that can successfully extend the stable operational range of these systems. This method ensures global asymptotic stability without the need to construct an observer for the velocity, thus reducing the complexity of the control law.

We have also presented some results to include the integral action for both passive and non-passive outputs in the IDA-PBC construction, to improve the robustness of the MEMS. This inclusion of integral action has been achieved by exploiting a change of coordinates, which is more complicated for electromechanical systems than for mechanical systems, due to the coupling between different energy domains. The robust control scheme presented in this chapter ensures that the stability of the MEMS is maintained in a robust sense, under the effect of external disturbances. This is proved by demonstrating that by using this robust controller the closed-loop MEMS subject to matched and unmatched disturbances satisfies the ISS property.

# Chapter 7

# Experimental Results

## 7.1 Introduction

In Chapter 3 we have proposed novel results to simplify the PDEs associated with the IDA-PBC methodology for underactuated mechanical systems. The results significantly simplify the IDA-PBC design and expand the class of systems that can be stabilized using this method. In Chapter 4 we have applied the results to design a controller to stabilize the rotary inverted pendulum. In that chapter, we have proved theoretically by stability analysis the 'almost' global asymptotic stability of the closed-loop system at its equilibrium point. The theoretical results have been illustrated through numerical simulations which have also shown good performance of the rotary inverted pendulum. These simulations are based on a model which cannot exactly capture the real behaviour of the system. For example in the modeling procedure of this system we have ignored the effect of friction. Thus, the results are experimentally validated by implementing the proposed controller on a laboratory setup of rotary inverted pendulum.

## 7.2 Experimental Setup

Experiments are performed with the Quanser QUBE-Servo rotary pendulum. The hardware comprises an 18V brushed DC motor contained in a solid aluminium frame and attached to the arm using magnets. Two single-ended optical shaft encoders are used to measure the angular positions of the pendulum, $q_1$, and arm, $q_2$. The hardware is connected to a PC through the QUBE-Servo USB interface. This interface has its own built-in PWM voltage-controlled power amplifier and data acquisition device. The output voltage range to the load is between $\pm$10V. The interaction between the PC and the hardware is interfaced using QUARC real-time control software integrated with Matlab/Simulink to drive the DC motor and read the angular positions $q_1$ and $q_2$. The sampling time of the control is 0.002 second.

**Remark 7.1.** The motor dynamics are omitted as it is much faster than the dynamics of the mechanical part of the system. From the equations of motions of the rotary inverted pendulum (4.36-4.37), the control input $u$ for the mechanical system is the motor torque $\tau$. This applied torque at the base of the rotary arm generated by the servo motor is described by the equation:

$$\tau = \frac{k_m(V_m - k_m\dot{\theta}}{R_m}).$$

This equation represents the relationship between the voltage and the torque and was implemented on the SIMULINK model.

## 7.3 Non-Conservative Forces Compensation

Note that the PCH modeling framework neglects some components of the dynamics to comply with the underlying concept of energy conservation in this modelling approach. For the inverted pendulum, the PCH model used in Chapter 4 and throughout this thesis does not consider non-conservative forces (e.g. friction) [1]. Thus, applying the controller (4.79), (4.81) alone is not enough to stabilize the pendulum in the hardware implementation, due to the effects of friction which are not taken into account in the controller design. Friction is present in almost every mechanical system and is a crucial aspect of many control systems. It can be highly nonlinear and may lead to steady-state errors, tracking errors, limit cycles and other undesirable behaviour [65]. Friction compensation is a common approach to deal with such effects and to achieve improved performance.

In general, friction compensation models can be divided into two groups: static and dynamic models [65]. The static friction models are described by a static relation between velocity and applied external forces. The classical examples are *Coulomb friction* and *viscous friction*. Coulomb friction can be described as

$$F_r = k_f sign(v), \tag{7.1}$$

where $F_r$ is the friction force, $v$ is the velocity, and $k_f$ is the friction coefficient. Viscous friction is given by

$$F_r = bv, \tag{7.2}$$

where $b$ is the viscous damping coefficient. The viscous friction is often combined with Coulomb friction as shown in Figure 7.1. This model has been widely used for friction compensation in many control systems applications (see [3, 102, 89]). However, in some situations such as at very low or zero velocities, stiction or bristles effects, friction forces can be more accurately described by dynamic models [24]. Some dynamic friction compensation models has been developed such as Dahl model and LuGre model [24] (see also [65] for a survey of friction models and friction compensation). While dynamic friction

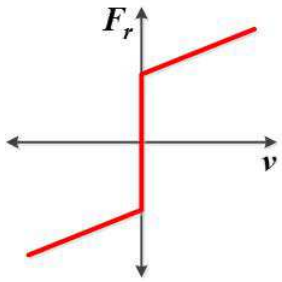


Figure 7.1: Static friction model.

models provide more adequate and precise description of the friction behaviour, they depend on a number of parameters which need to be identified. Identifying/estimating and tuning these parameters are not straightforward as they depend on the availability of measuring devices and often affected by noise. This also imposes higher demands on hardware and software [25].

We have chosen to use the static model of friction, the Coulomb and viscous friction models that capture the essential behaviour of the friction, as well as to avoid any complications resulting from applying the dynamic friction model.

**Friction compensation for the rotary inverted pendulum**

For a rotary inverted pendulum, the friction phenomenon appears on both joints; the pendulum joint and the arm joint. The friction in the pendulum joint can be modelled by a viscous/damping coefficient which has a relatively small value and, in most cases, can be neglected [1]. The friction on the arm joint is the main source of friction in the system. Initial experiments have shown that the friction parameters provided by [79] do not adequately describe the friction that influence the rotary system. This is because it does not take into account the unmodelled dynamics introduced by the encoder cable as shown in Figure 4.1. Hence, we have taken these parameters as first estimates and we have tuned them manually in several experiments at different input voltages and angular velocities to obtain more accurate friction model and parameters. The friction compensation term is:

$$u_f = b(\dot{q}_2 - \dot{q}_1) + k_f sign(\dot{q}_2 - \dot{q}_1), \tag{7.3}$$

where $k_f$ is the Coulomb friction coefficient and $b$ is the viscous damping coefficient of the link. This is added to the IDA-PBC controller (4.79), (4.81) in order to overcome/compensate friction, thus enhances the performance of the closed-loop system. Considering the friction in the joints and taking into account the unmodelled dynamics introduced by the encoder cable as shown in Figure 4.1, the best friction model's parameters are estimated as $k_f = 0.5755$ and $b = 0.005755$. Thus, the total control law applied to the hardware is of the form

$$u = u_{es} + u_{di} + u_f. \tag{7.4}$$

## 7.4 States Measurement

The two optical shaft encoders that measure the angular positions of the pendulum and the arm have the resolution of 2048 counts per revolution in quadrature mode (512 lines per revolution). The momenta $p_1$ and $p_2$ are obtained from the relation $p = M\dot{q}$, where the angular velocities $\dot{q}_1$ and $\dot{q}_2$ of the pendulum and arm are obtained by differentiating their corresponding measured angular positions. A low-pass filter has been added to the output of each differentiator to remove some high-frequency components (noise) which appears as a result of quantization due to the encoder measurement. The low-pass filters have been set as $50/(s+50)$, with the cutoff frequency $w_f = 50$ rad/sec or $w_f = 50/(2\pi) = 7.96$ Hz. This is constructed in Matlab/Simulink as shown in Figure 7.2.

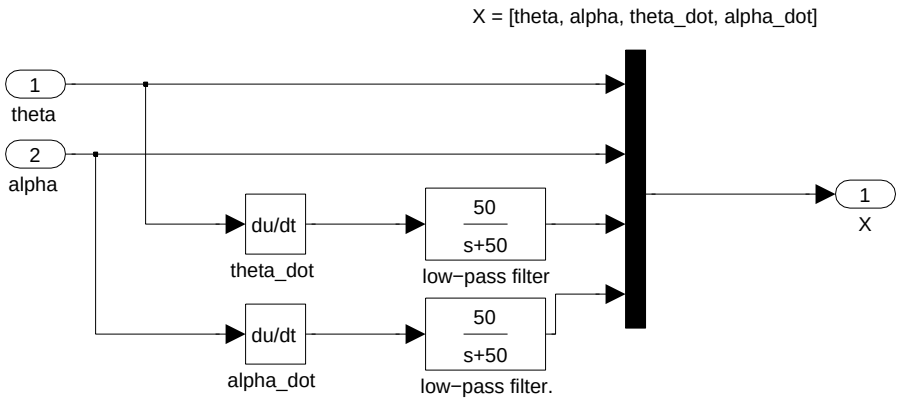


Figure 7.2: Obtaining velocity from position measurement.

## 7.5 Experimental Results

In this section, we present the results of our experiments on the QUBE- rotary pendulum system. The total control law (7.4) has been applied to stabilize the pendulum at its upward position. The initial condition for the position of the pendulum was $q_{1_0} = 45°$. We will discuss later in this chapter the limiting factors from achieving a larger DoA. However, this DoA is still much larger than what was obtained using some linear controllers (the maximum achieved using a linear controller given in [79] was $q_{1_0} = 20°$).

In the experiment, the pendulum was set to start from a downward position. A swing-up controller based on the strategy developed in [11] has been applied to drive the pendulum up to the initial angle ($q_{1_0}$). Once the pendulum reaches this angle, the controller switches to the IDA-PBC stabilizing controller. The controller parameters used in the experiment were $m_3 = 67$, $K_p = 8.0 \times 10^{-4}$, $K_v = 6 \times 10^{-6}$ and $\epsilon = 1$. Note that while in simulation we can set the initial value of every state, this is not the case

for the experiment. The only state for which the initial value can be set directly is the pendulum angle $q_{1_0}$, as the other states depend on the swing-up movement.

Figures 7.3 and 7.4 show the experimental results when applying the hybrid controller (i.e. swing-up and stabilizing) to the inverted pendulum. In order to clearly show the effect of our proposed controller, we have magnified the parts of these figures starting from the instant of commutation ($t = 6.16$ sec), i.e. the instant in which the switching to IDA-PBC stabilizing controller takes place as shown in Figures 7.5 and 7.6. We can observe from Figure 7.5, which depicts the time histories of the angular positions and velocities of the pendulum and the arm, that all states converge to their desired equilibrium point, thus achieving *asymptotic* stabilization of the closed-loop system with the controller (7.4). Furthermore, this figure shows the smooth and fast convergence of the states while the pendulum and arm exhibit slight oscillatory behaviour ($< 1.5$ degrees). The profile of the control input is shown in Figure 7.6. We can observe the smooth control effort, with a more demanding effort to balance the pendulum at its vertical upward position.

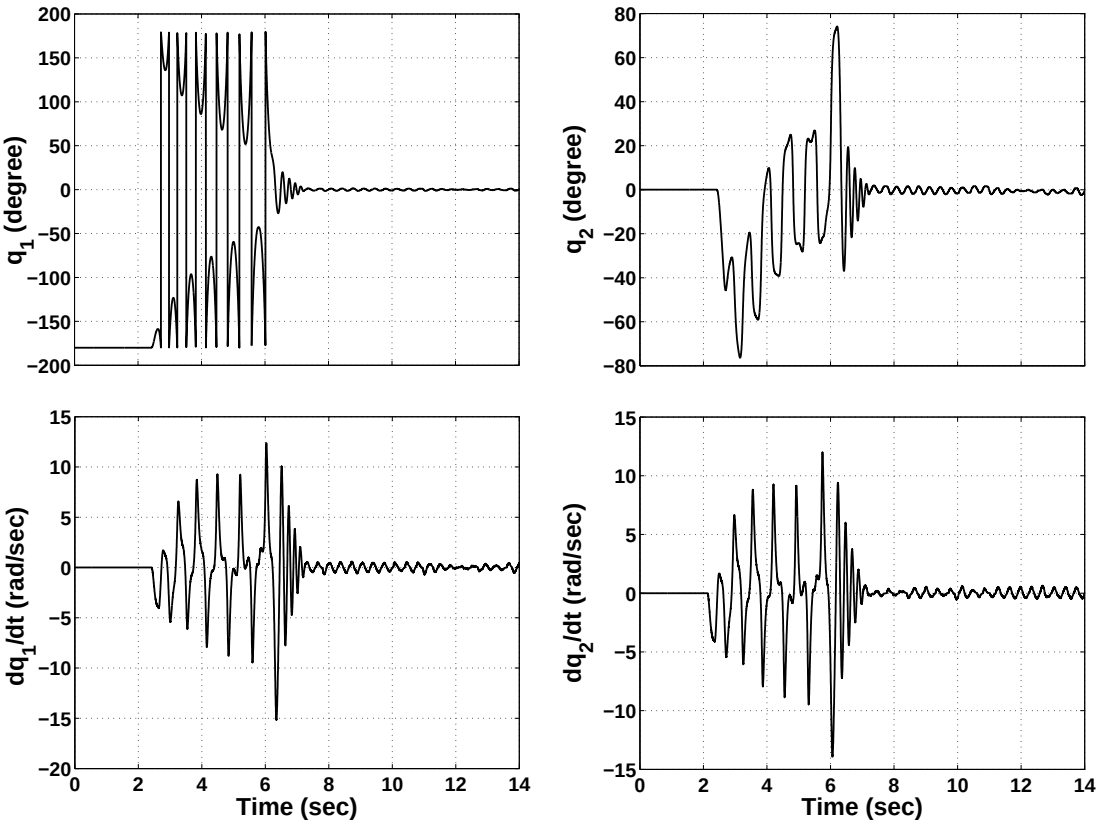


Figure 7.3: Experimental results (swing-up and stabilization): state histories of the rotary inverted pendulum system.

**Remark 7.2.** Comparing the results obtained from the simulations (see Section 4.6) and the experiments, we can observe that in the experimental results the system exhibits more oscillations and longer settling times. These differences could be due to 1) a friction compensator is added to the control input in the experiments while it is not considered

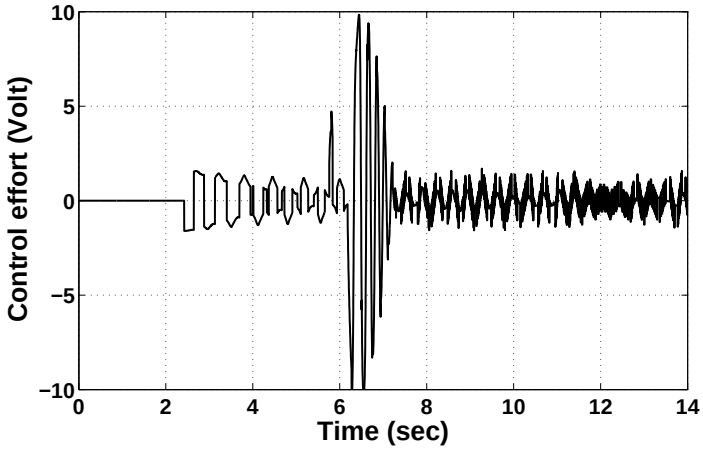


Figure 7.4: Experimental results (swing-up and stabilization): control input.

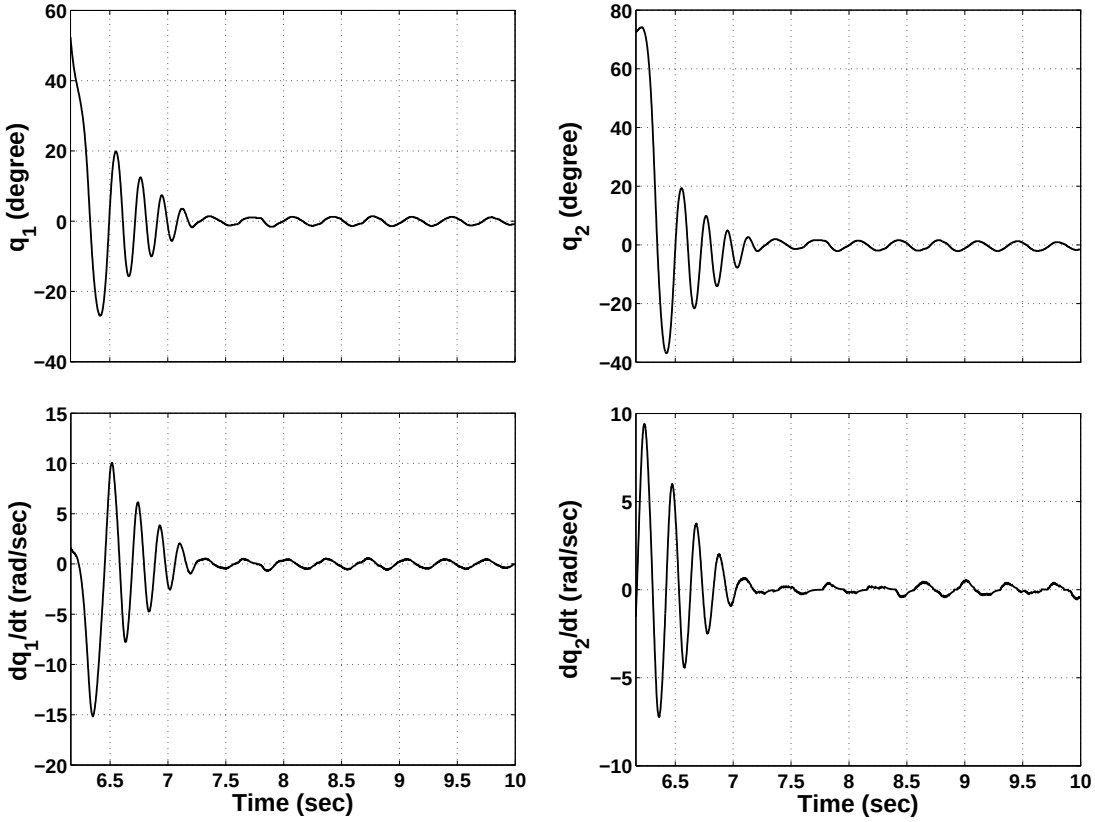


Figure 7.5: Experimental results (stabilization): state histories of the rotary inverted pendulum system.

in the simulations. 2) modelling errors and actuator dynamics not being taken into account. 3) high-frequency noises which appear as a result of quantization due to the velocity measurement using a differentiator.

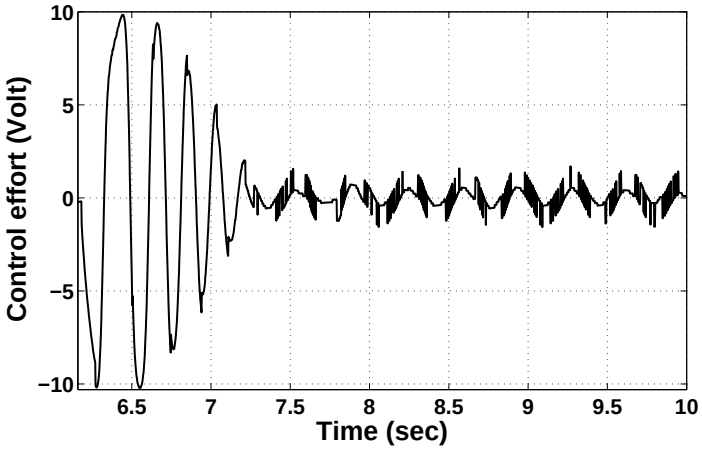


Figure 7.6: Experimental results (stabilization): control input.

## 7.6 Robustness of the Proposed IDA-PBC

In order to show the robustness of the proposed controller, the pendulum was perturbed, by slight push to it, at $t = 14.5$ sec. The experimental results are shown in Figures 7.7 and 7.8. As we can observe, the states recover from the injected disturbance, converging fast and smoothly to their desired values. While the trajectories of the states $q_1$, $\dot{q}_1$ and $\dot{q}_2$ converge to their exact desired values, the arm position, $q_2$, converges to another position. This is expected as each position of the arm is a stable equilibrium. Furthermore, Figure 7.8 shows that the control effort in response to the perturbation is smooth and remains within the acceptable voltage range. It is evident from these graphs that, the closed-loop system is robust with respect to disturbances on the pendulum.

## 7.7 Discussion and Conclusion

The experimental results presented in this chapter show the effectiveness of the proposed controller for the stabilization of the rotary inverted pendulum at its unstable vertical upward position. The smooth behaviour and fast response of the closed-loop system, as well as its robustness against perturbations have been observed. In the following, we will analyze the general performance of the closed-loop systems and the factors that limit achieving 'almost' global stabilization as expected by the theory.

- The closed-loop system exhibits oscillatory behaviour: Although of small magnitude ($< 1.5$ degrees), the oscillation in the system was unavoidable. The main reasons are that the oscillatory behaviour is typical of systems with low inertia [89], and also the friction in the arm and pendulum has not perfectly compensated for. Finally, the noise and additional delays imposed by measurements and the differentiator as well as the filter used to obtain the velocities of the arm and pendulum [35]. These factors also affect the transient performance of the system.

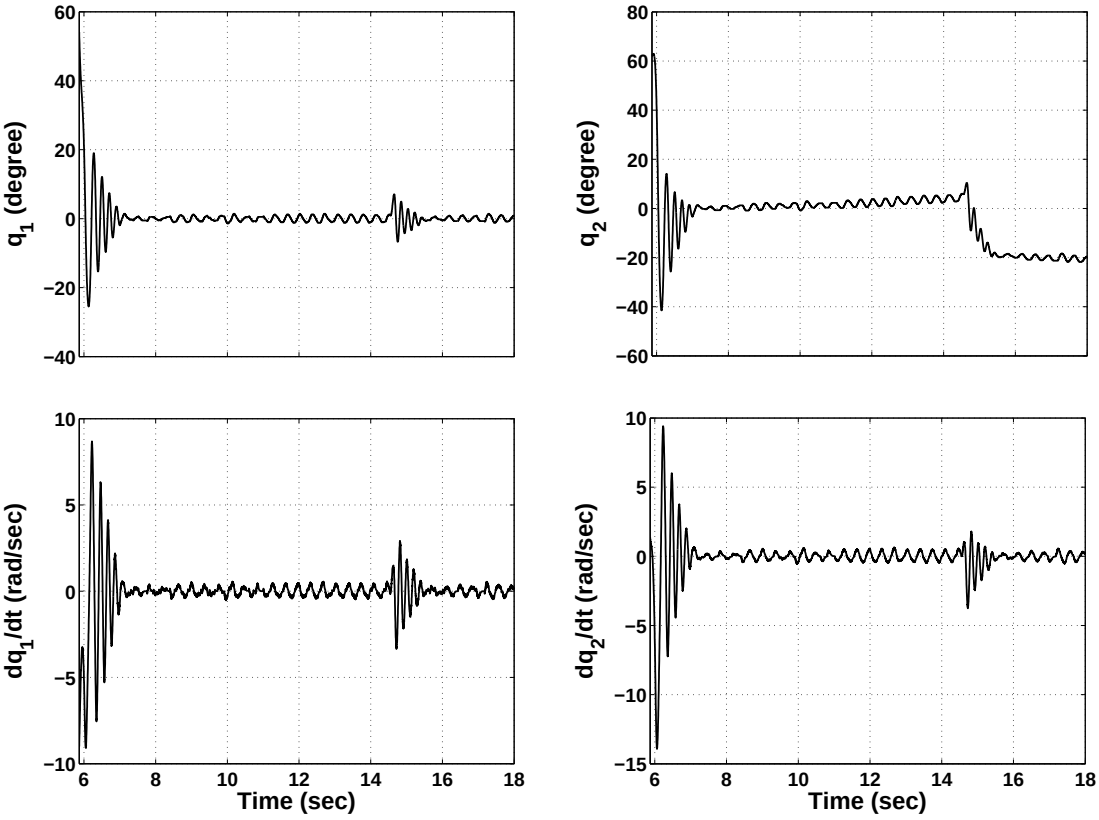


Figure 7.7: Experimental results (robustness): state histories of the rotary inverted pendulum system.

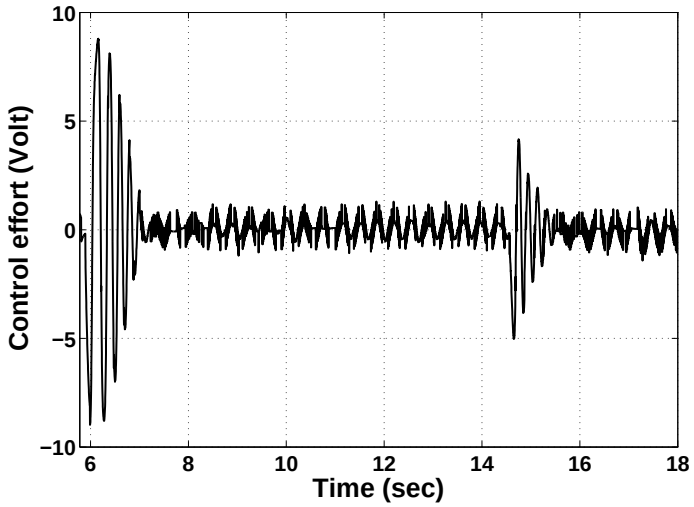


Figure 7.8: Experimental results (robustness): control input.

- Although in theory, as also shown in simulation in Chapter 4, 'almost' global asymptotic stabilization can be achieved, the maximum experimental value of the pendulum angle achieved was $q_{1_0} = 45°$. This can be attributed mainly to hardware limitations: 1) Saturation of the control input; the motor is relatively small and provides insufficient torque to enlarge the initial pendulum angle, thus the domain of attraction. As shown in Figure 7.6, the control signal reaching $\pm 10V$,

which is the maximum amplifier voltage range to the load, was required already to stabilize the system starting from $q_{1_0} = 45°$. 2) The arm does not rotate a full 360° by design: the encoder cable is attached from the pendulum module encoder to the Encoder 1 connector on the top panel of the QUBE-Servo, hence a stopper is used to avoid any contact between the pendulum and the cable as shown in Figure 7.9(a). The QUBE-Servo with the attached pendulum and connected cable is pictured in Figure 7.9(b).

- While the closed-loop system has exhibited a reasonable robustness margin, oscillations, steady-state errors (especially in the arm position), and uncertainty in the parameters are still important issues that need to be considered to enhance the performance of this system. One option to deal with this is to add an integral control. We have discussed in Chapter 5 a framework to add the integral action control to the underactuted mechanical system. Moreover, we have introduced the adaptive control procedure to deal with parametric uncertainties.

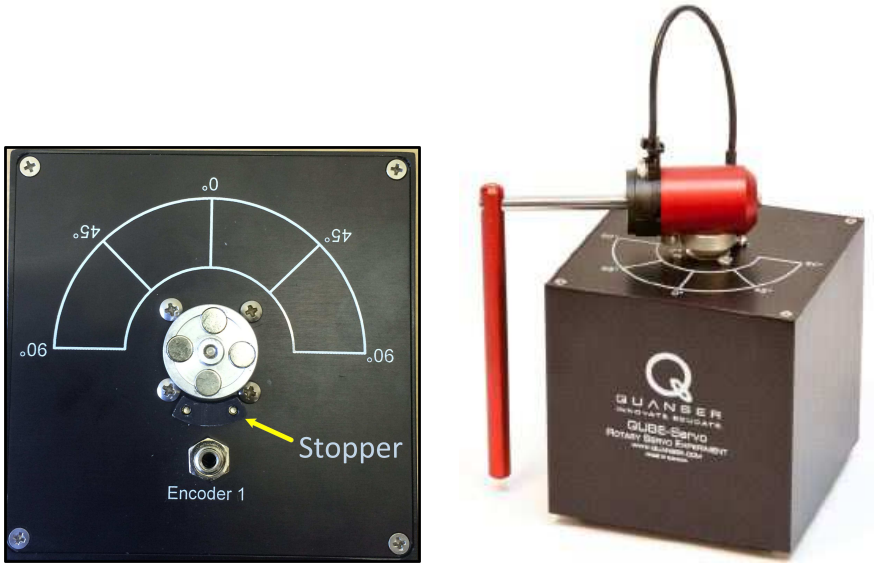


(a) QUBE-Servo top view (b) QUBE-Servo with pendulum module

Figure 7.9: QUBE-Servo components.

# Chapter 8

# Conclusions and Future Research

## 8.1 Conclusion

In this thesis, we have investigated important issues on the design and analysis of nonlinear control systems, with a focus on electromechanical and underactuated mechanical systems. We have developed methodologies for controlling systems with a specific physical structure, the port-controlled Hamiltonian systems which have several advantages and are suitable modelling framework for the application of passivity-based control approaches. These methods have provided solutions to the main important challenges in controller design for real systems; nonlinearity and uncertainty.

In this work, we have improved the IDA-PBC method for underactuated mechanical systems. This improvement is achieved via a particular simplification of the matching PDEs. Solving these PDEs is the main difficulty in application of this method. We have developed a novel general procedure to reparametrize the inertia matrix, which is then used to simplify and solve the potential energy PDEs, achieving total energy shaping which is essential for stabilization of the underactuated mechanical systems. The result has been successfully applied to solve a global stabilization control design for an inertia wheel pendulum and a rotary inverted pendulum which belong to two groups of PCH systems, the separable and non-separable systems, respectively. The proposed method has significantly simplified the design computation and also yields a simpler form of the controller for both systems. It has also been shown by realistic simulations that this design results in a very high closed-loop performance of these systems in their full nonlinear dynamics.

We have also extended our results to several control designs to deal with various robustness related issues within PCH framework. In particular, IDA-PBC method along with a dynamic state-feedback controller that involves integral action is used to improve the robustness of the closed-loop system. First, we have presented several results

on integral control for a class of PCH systems, extending the results of [29, 82]. Second, we have provided a general framework that allows the use of integral action for under-actuated mechanical systems. This work is the first of its kind that discusses the incorporation of integral control for under-actuated mechanical system within PCH framework. The matched and unmatched disturbance rejection problems are solved using the integral action controller with a particular change of coordinates that involves adding some damping terms such that the well know iISS and ISS properties are satisfied. A novel adaptive IDA-BPC framework to deal with parametric uncertainties in PCH models, particularly uncertainties in the potential energy function, has been also proposed, for both separable and non-separable PCH systems. Application to an inertia wheel pendulum which is an underactuated system has been presented, and the effectiveness of the proposed controllers has been demonstrated through numerical simulations. The simulation results demonstrate that the system is robust with respect to different perturbations; preserving the PCH structure and retaining the (asymptotic) stability without much degradation.

We have also presented results on MEMS control design. The electrostatically actuated type of MEMS suffers from a limitation in its operational range known as *pull-in*, a nonlinear structural instability phenomenon that results from the interaction between the electrostatic and elastic forces. After an in-depth analysis of this phenomenon, we have employed the IDA-PBC design, proposed in [66] to solve the stabilization problem for this device. The proposed method has successfully extended the range of operation of these actuators, achieving global asymptotic stability. Another advantage of this method is that it is an output-feedback control design that avoids the unmeasurable velocity state and the need to construct observer to account for the lack of velocity measurements which makes the control system more complicated and difficult to implement practically. In addition, we have considered in this thesis improving the robustness of the MEMS devices in the presence of uncertainties. First, we have introduced a framework to incorporate the integral action in the PCH model for electromechanical systems which exhibit a strong coupling between different energy domains. Similar to the case of underactuated mechanical systems, this incorporation requires a change of coordinates but involves more states due to the coupling in the energy and interconnection matrix. Finally, the integral action is combined with the IDA-PBC controller to asymptotically stabilize the MEMS subject to external matched and unmatched disturbances. In this case the robustification objective has been achieved ensuring the satisfaction of the ISS property.

Finally, we have successfully experimentally implemented our simplified IDA-PBC controller to the rotary inverted pendulum hardware. The results have proved the effectiveness of the controller and its robustness with respect to disturbances. The theoretical results presented in this thesis and the experimental results can be used as the motivation to apply this method in other real engineering applications.

## 8.2 Future Research

This thesis has presented a comprehensive investigation of underactuated mechanical and electromechanical systems in the field of nonlinear control. A number of nonlinear and robust control methods has been developed based on the passivity-based control approach by adopting the port-controlled Hamiltonian framework. However, new open problems and further potential areas of research have been revealed, which can be summerized as follows:

- In this thesis we have presented a framework to simplify the PDEs considering underactuated systems with $n = 2$ and $m = 1$ which are the most popular systems in literature. It is possible to extend our results to a more general case of systems with underactuation degree 1, with the challenge of more complicated formalism as it will require the inverse operation for a matrix with dimension higher than $2 \times 2$.

- The control laws proposed in this thesis for underactuted mechanical systems are state-feedback controllers that assume measurement availability of all states. As the velocities are usually difficult or unavailable for direct measurement in practice, it would be interesting to design a speed observer. In an interesting paper [9], an observer has been constructed using the I&I methodology for mechanical systems within the PCH framework. This design has been recently combined with a new static state-feedback passivity-based controller (PBC) in [83] to design a globally exponentially stable tracking controller for mechanical systems. It is possible to start from these results to propose an observer that facilitates the IDA-PBC methodology in particular.

- We have developed an adaptive scheme to deal with uncertainties in the potential energy function $V$ for underactuated mechanical systems. It will be very useful to develop a general scheme which takes into account uncertainties in other functions and structures. At the same time, particularly important and troublesome is the uncertainties in the inertia matrix $M$. This is because not all its elements are attainable from the control input (only the passive outputs) due to the underactuation nature of such systems. However, with the change of coordinates proposed in this research, it should be possible to develop a general adaptive controller.

- In this thesis, the robust control methods which are based on the inclusion of integral action are applied only for the MEMS device. It is very important to broaden the class of electromechanical systems that can be robustly controlled.

- Another area of future research is to link the results in this thesis with the immersion and invariance (I&I) methodology introduce in [8]. The reasons for adopting I&I are twofold:

1. Equivalence of I&I and IDA-PBC. Some relationships between the two methods have been shown in [89, 50]. For example, the relationships have been utilized in the Acrobot application to design I&I controller from the structural knowledge of the IDA-PBC approach. Hence, we may exploit these relationships to develop constructive results in both directions.
2. The I&I is a successful approach for the stabilization of nonlinear systems with established adaptive scheme that has been developed and applied to many classes of dynamical systems. Although, there has been no adaptive control design method for underactuated mechanical systems within PCH framework using this method, a constructive I&I stabilization method for a class of underactuated mechanical systems with constant inertia matrix has been recently presented [89]. Therefore, one may extend these results to the case of non-constant inertia matrix and then develop an adaptive scheme.

- There has been a lot of interest on the PID control of robotic manipulators since the 1980s and 1990s of the last century led by a pioneering work of [105]. The fact that the dynamics of these manipulators are highly nonlinear with strongly coupled joints, this limits the application of the linear control theory. Exploiting the physical structure of these manipulators and their energy and passivity properties, a number of nonlinear PID control designs has been proposed in literature, among them are [105, 46, 68], see [116] for outlook. The drawbacks of these methods are that some of these proposed designs can only ensure local stability, or lack robustness against uncertainties, or impose constraints on the controller parameters [116]. It is of great interest to investigate the PID-like control design developed in this thesis more extensively. This may provide solutions to these problems in a unified scheme leading to improved performance of the manipulators.

- Finally, implementation of the proposed schemes to various hardware setups is still another interesting challenge.

# References


[1] Acosta, J. A. (2010). Furuta's pendulum: A conservative nonlinear model for theory and practise. *Mathematical Problems in Engineering*, 2010:29.

[2] Acosta, J. A., Ortega, R., Astolfi, A., and Mahindrakar, A. (2005). Interconnection and damping assignment passivity based control of mechanical systems with underactuation degree one. *IEEE Transactions on Automatic Control*, 50:1936–1955.

[3] Akesson, J. and Aström, K. J. (2001). Safe manual control of the Furuta pendulum. In *Proceedings of the IEEE International Conference on Control Applications*, pages 890–895.

[4] Akhtaruzzaman, M. and Shafie, A. A. (2010). Modeling and control of a rotary inverted pendulum using various methods, comparative assessment and result analysis. In *Proceedings of the International Conference on Mechatronics and Automation (ICMA)*, pages 1342–1347.

[5] Angeli, D. (2001). Almost global stabilization of the inverted pendulum via continuous state feedback. *Automatica*, 37:1103–1108.

[6] Angeli, D., Sontag, E., and Wang, Y. (2000). A characterization of integral input-to-state stability. *IEEE Transactions on Automatic Control*, 45(6):1082–1097.

[7] Astolfi, A., Karagiannis, D., and Ortega, R. (2007). *Nonlinear and adaptive control design and applications*. Springer-Verlag, London.

[8] Astolfi, A. and Ortega, R. (2003). Immersion and invariance: a new tool for stabilization and adaptive control of nonlinear systems. *IEEE Transactions on Automatic Control*, 48(4):590–606.

[9] Astolfi, A., Ortega, R., and Venkatraman, A. (2010). A globally exponentially convergent immersion and invariance speed observer for mechanical systems with nonholonomic constraints. *Automatica*, 46(1):182–189.

[10] Aström, K. J., Aracil, J., and Gordillo, F. (2008). A family of smooth controllers for swinging up a pendulum. *Automatica*, 44:1841–1848.

[11] Aström, K. J. and Furuta, K. (2000). Swing up a pendulum by energy control. *Automatica*, 36:287–295.

[12] Auckly, D. and Kapitanski, L. (2002). On the $\lambda-$equations for matching control laws. *SIAM Journal on Control and Optimization*, 41:1372–1388.

[13] Bastani, Y. and de Queiroz, M. S. (2008). Lyapunov-based stabilization of MEMS relays. *Journal of Dynamic Systems, Measurement, and Control*, 131(1):9.

[14] Blankenstein, G., Ortega, R., and van der Schaft, A. J. (2002). The matching conditions of controlled Lagrangians and IDA-passivity based control. *International Journal of Control*, 75:645–665.

[15] Bloch, A., Leonard, N., and Marsden, J. (1999). Stabilization of the pendulum on a rotor arm by the method of controlled Lagrangians. In *Proceedings of IEEE International Conference on Robotics and Automation*, volume 1, pages 500–505.

[16] Bloch, A., Leonard, N., and Marsden, J. (2000). Controlled Lagrangians and the stabilization of mechanical systems. I. The first matching theorem. *IEEE Transactions on Automatic Control*, 45(12):2253–2270.

[17] Block, D. J., Aström, K. J., and Spong, M. W. (2007). *The Reaction Wheel Pendulum*. Morgan & Claypool Publishers.

[18] Bryzek, J., Flannery, A., and Skurnik, D. (2004). Integrating microelectromechanical systems with integrated circuits. *IEEE Instrumentation Measurement Magazine*, 7(2):51–59.

[19] Byrnes, C. I., Isidori, A., and Willems, J. C. (1991). Passivity, feedback equivalence, and the global stabilization of minimum phase nonlinear systems. *IEEE Transactions on Automatic Control*, 36(11):1228–1240.

[20] Cazzolato, B. and Primeo, Z. (2011). On the dynamics of the Furuta pendulum. *Journal of Control Science and Engineering*, 2011(6):8.

[21] Chang, D. E. and McLenaghan, R. (2013). Geometric criteria for the quasi-linearization of the equations of motion of mechanical systems. *IEEE Transactions on Automatic Control*, 58(4):1046–1050.

[22] Craig, J. J. (2005). *Introduction to Robotics-Mechanics and Control*. Pearson Prentice Hall, Upper Saddle River, NJ, USA, 3rd edition.

[23] Crothers, B. (2009). Device made popular in iphone catching on. http://www.cnet.com/news/device-made-popular-in-iphone-catching-on/. [Online; accessed 12-April-2013].

[24] De Wit, C., Olsson, H., Aström, K. J., and Lischinsky, P. (1995). A new model for control of systems with friction. *IEEE Transactions on Automatic Control*, 40(3):419–425.

[25] Dietz, T. (2006). Model-based friction compensation for the the Furuta pendulum using the LuGre model. Master's thesis, Department of Automatic Control, Lund University.

[26] Dirksz, D. A. and Scherpen, J. M. (2010). Adaptive tracking control of fully actuated port- Hamiltonian mechanical systems. In *Proceedings of the IEEE International Conference on Control Applications (CCA)*, pages 1678–1683.

[27] Dirksz, D. A. and Scherpen, J. M. (2012a). Power-based control: Canonical coordinate transformations, integral and adaptive control. *Automatica*, 48(6):1045–1056.

[28] Dirksz, D. A. and Scherpen, J. M. (2012b). Structure preserving adaptive control of port-Hamiltonian systems. *IEEE Transactions on Automatic Control*, 57(11):2880–2885.

[29] Donaire, A. and Junco, S. (2009). On the addition of integral action to port-controlled Hamiltonian systems. *Automatica*, 45(8):1910–1916.

[30] Dorf, R. C. and Bishop, R. (2007). *Modern Control Systems*. Prentice-Hall, Inc., Upper Saddle River, NJ, USA, 11th edition.

[31] Duindam, V., Macchelli, A., Stramigioli, S., and Bruyninckx, H. (2009). *Modeling and Control of Complex Physical Systems: The Port-Hamiltonian Approach*. Springer.

[32] Evans, S. (2013). 1812 miles in three 2013 Honda Accords. http://www.motortrend.com/features/travel/1301_1812_miles_in_three_2013_honda_accords/photo_03.html. [Online; accessed 2-March-2013].

[33] Fantoni, I. and Lozano, R. (2002a). *Nonlinear Control for Underactuated Mechanical Systems*. Springer.

[34] Fantoni, I. and Lozano, R. (2002b). Stabilization of the Furuta pendulum around its homoclinic orbit. *International Journal of Control*, 75(6):390–398.

[35] Freidovich, L., Shiriaev, A., and Manchester, I. (2007). Experimental implementation of stable oscillations of the Furuta pendulum around the upward equilibrium. In *Proceedings of the IEEE/RSJ International Conference on Intelligent Robots and Systems*, pages 171–176.

[36] Fujimoto, K., Sakurama, K., and Sugie, T. (2003). Trajectory tracking control of port-controlled Hamiltonian systems via generalized canonical transformations. *Automatica*, 39(12):2059–2069.

[37] Fujimoto, K. and Sugie, T. (2001). Stabilization of Hamiltonian systems with nonholonomic constraints based on time-varying generalized canonical transformations. *Systems & Control Letters*, 44(4):309–319.

[38] Galaz, M., Ortega, R., Bazanella, A. S., and Stankovic, A. M. (2003). An energy-shaping approach to the design of excitation control of synchronous generators. *Automatica*, 39(1):111–119.

[39] Gomez-Estern, F., Ortega, R., Rubio, F., and Aracil, J. (2001). Stabilization of a class of underactuated mechanical systems via total energy shaping. In *Proceedings of the 40th IEEE Conference on Decision and Control*, volume 2, pages 1137–1143.

[40] Gomez-Estern, F. and van der Schaft, A. J. (2004). Physical damping in IDA-PBC controlled underactuated mechanical systems. *European Journal of Control*, 10(5):451–468.

[41] Gronle, M., Zhu, G., and Saydy, L. (2010). Sliding mode tracking control of an electrostatic parallel-plate MEMS. In *Proceedings of the IEEE/ASME International Conference on Advanced Intelligent Mechatronics (AIM)*, pages 999–1004.

[42] Hill, D. and Moylan, P. (1976). The stability of nonlinear dissipative systems. *IEEE Transactions on Automatic Control*, 21(5):708–711.

[43] Hill, D. and Moylan, P. (1980). Dissipative dynamical systems: Basic input-output and state properties. *Journal of the Franklin Institute*, 309(5):327–357.

[44] Isidori, A. (1995). *Nonlinear Control Systems*. Springer-Verlag, London, UK, 3rd edition.

[45] Isidori, A. (1999). *Nonlinear Control Systems II*. Springer-Verlag, London, UK.

[46] Kelly, R. and Carelli, R. (1996). A class of nonlinear PD-type controllers for robot manipulators. *Journal of Robotic Systems*, 13(12):793–802.

[47] Khalil, H. (2002). *Nonlinear Systems*. Prentice Hall, NJ, USA, 3rd edition.

[48] Kokotović, P. and Arcak, M. (2001). Constructive nonlinear control: a historical perspective. *Automatica*, 37(5):637–662.

[49] Kotyczka, P. (2013). Local linear dynamics assignment in IDA-PBC. *Automatica*, 49(4):1037–1044.

[50] Kotyczka, P. and Sarras, I. (2013). On the equivalence of two nonlinear control approaches: Immersion and Invariance and IDA-PBC. *European Journal of Control*, 19(6):445 – 453.

[51] Krstić, M., Kanellakopoulos, I., and Kokotović, P. (1995). *Nonlinear and Adaptive Control Design*. John Wiley & Sons, Inc., New York, NY, USA.

[52] Laila, D. S. and Astolfi, A. (2005). Discrete-time IDA-PBC design for separable Hamiltonian system. In *Proceedings of the 16th IFAC World Congress*, pages 838–843.

[53] Laila, D. S. and Astolfi, A. (2006). Discrete-time IDA-PBC design for underactuated Hamiltonian control systems. In *Proceedings of the American Control Conference*, pages 6 pp.–.

[54] Lewis, A. (2006). Potential energy shaping after kinetic energy shaping. In *Proceedings of 45th IEEE Conference on Decision and Control*, pages 3339–3344.

[55] Liu, Y. and Yu, H. (2013). A survey of underactuated mechanical systems. *Control Theory Applications, IET*, 7(7):921–935.

[56] Mahindrakar, A. D., Astolfi, A., Ortega, R., and Viola, G. (2006). Further constructive results on interconnection and damping assignment control of mechanical systems: the Acrobot example. *International Journal of Robust and Nonlinear Control*, 16:671–685.

[57] Maithripala, D. H. S., Berg, J. M., and Dayawansa, W. P. (2005). Control of an electrostatic microelectromechanical system using static and dynamic output feedback. *Journal of Dynamic Systems, Measurement, and Control*, 127:443–450.

[58] Murray, R. (2003). Future directions in control, dynamics, and systems: Overview, grand challenges, and new courses. *European Journal of Control*, 9(23):144–158.

[59] Nadal-Guardia, R., Dehe, A., Aigner, R., and Castaner, L. M. (2002). Current drive methods to extend the range of travel of electrostatic microactuators beyond the voltage pull-in point. *Journal of Microelectromechanical Systems*, 11(3):255–263.

[60] Nair, S. and Leonard, N. (2002). A normal form for energy shaping: application to the Furuta pendulum. In *Proceedings of the 41st IEEE Conference on Decision and Control*, volume 1, pages 516–521.

[61] Nise, N. (2008). *Control Systems Engineering.* John Wiley & Sons, Inc., New York, NY, USA, 5th edition.

[62] Ogata, K. (2005). *Modern Control Engineering, 5th Ed.* Prentice Hall, Saddle River, NJ, USA, 5th edition.

[63] Olfati-Saber, R. (2001). *Nonlinear control of underactuated mechanical systems with application to robotics and aerospace vehicles.* PhD thesis, MIT, Dept. of EECS.

[64] Olfati-Saber, R. (2002). Normal forms for underactuated mechanical systems with symmetry. *IEEE Transactions on Automatic Control*, 47(2):305–308.

[65] Olsson, H., Aström, K., de Wit, C. C., Gäfvert, M., and Lischinsky, P. (1998). Friction models and friction compensation. *European Journal of Control*, 4(3):176–195.

[66] Ortega, R. and Garcia-Canseco, E. (2004). Interconnection and damping assignment passivity-based control: A survey. *European Journal of Control*, 10:432–450.

[67] Ortega, R., Liu, Z., and Su, H. (2012). Control via interconnection and damping assignment of linear time-invariant systems: a tutorial. *International Journal of Control*, 85(5):603–611.

[68] Ortega, R., Loria, A., and Kelly, R. (1995). A semiglobally stable output feedback $PI^2D$ regulator for robot manipulators. *IEEE Transactions on Automatic Control*, 40(8):1432–1436.

[69] Ortega, R., Loria, A., Nicklasson, P., and Sira-Ramirez, H. (1998). *Passivity-based Control of Euler-Lagrange Systems*. Springer-Verlag, London, UK.

[70] Ortega, R. and Romero, J. G. (2012). Robust integral control of port-Hamiltonian systems: The case of non-passive outputs with unmatched disturbances. *Systems & Control Letters*, 61(1):11–17.

[71] Ortega, R., Spong, M. W., Gomez-Estern, F., and Blankenstein, G. (2002a). Stabilization of a class of underactuated mechanical systems via interconnection and damping assignment. *IEEE Transactions on Automatic Control*, 47:1218–1233.

[72] Ortega, R., van der Schaft, A. J., Mareels, I., and Maschke, B. (2001). Putting energy back in control. *Control Systems, IEEE*, 21(2):18–33.

[73] Ortega, R., van der Schaft, A. J., Maschke, B., and Escobar, G. (1999). Energy-shaping of port-controlled Hamiltonian systems by interconnection. In *Proceedings of the 38th IEEE Conference on Decision and Control*, volume 2, pages 1646–1651 vol.2.

[74] Ortega, R., van der Schaft, A. J., Maschke, B., and Escobar, G. (2002b). Interconnection & damping assignment passivity-based control of port-controlled Hamiltonian systems. *Automatica*, 38:585–596.

[75] Owusu, K. O. and Lewis, F. L. (2007). Solving the "Pull-in" instability problem of electrostatic microactuators using nonlinear control techniques. In *Proceedings of the 2nd IEEE International Conference on Nano/Micro Engineered and Molecular Systems (NEMS '07)*, pages 1190–1195.

[76] Partnership, P. F. (2002). An introduction to MEMS (Micro-electromechanical Systems). http://http://www.lboro.ac.uk/microsites/mechman/researc/ipm-ktn/pdf/Technology_review/an-introduction-to-mems.pdf. [Online; accessed 22-June-2012].

[77] Petrovic, V., Ortega, R., and Stankovic, A. (2001). Interconnection and damping assignment approach to control of PM synchronous motors. *IEEE Transactions on Control Systems Technology*, 9(6):811–820.

[78] Piyabongkarn, D., Sun, Y., Rajamani, R., Sezen, A., and Nelson, B. (2005). Travel range extension of a MEMS electrostatic microactuator. *IEEE Transactions on Control Systems Technology*, 13(1):138–145.

[79] Quanser Inc. (2014). QUBE-servo rotary pendulum user manual and workbook.

[80] Reze, M. (2011). MEMS accelerometer to tackle vehicle safety issues. http://automotive-eetimes.com/en/mems-accelerometer-to-tackle-vehicle-safety. [Online; accessed 10-Feb-2015].

[81] Rodriguez, H. and Ortega, R. (2003). Stabilization of electromechanical systems via interconnection and damping assignment. *International Journal of Robust and Nonlinear Control*, 13(12):1095–1111.

[82] Romero, J. G., Donaire, A., and Ortega, R. (2013). Robust energy shaping control of mechanical systems. *Systems & Control Letters*, 62(9):770–780.

[83] Romero, J. G., Ortega, R., and Sarras, I. (2015). A globally exponentially stable tracking controller for mechanical systems using position feedback. *IEEE Transactions on Automatic Control*, 60(3):818–823.

[84] Ryalat, M. and Laila, D. S. (2013). IDA-PBC for a class of underactuated mechanical systems with application to a rotary inverted pendulum. In *Proceedings of the 52nd IEEE Conference on Decision and Control*, pages 5240–5245.

[85] Ryalat, M. and Laila, D. S. (2015). A simplified IDA-PBC design for underactuated mechanical systems with applications. *European Journal of Control, submitted*.

[86] Ryalat, M., Laila, D. S., and Torbati, M. (2014). Robust IDA-PBC and PID-like control for port-controlled Hamiltonian systems. *IEEE Transactions on Automatic Control, submitted*.

[87] Ryalat, M., Laila, D. S., and Torbati, M. (2015). Integral IDA-PBC and PID-like control for port-controlled Hamiltonian systems. In *Proceedings of the 2015 American Control Conference*.

[88] Sandoval, J., Ortega, R., and Kelly, R. (2008). Interconnection and damping assignment passivity-based control of the Pendubot. In *Proceedings of the 17th IFAC World Congress*, pages 7700–7704.

[89] Sarras, I., Acosta, A. J., Ortega, R., and Mahindrakar, A. D. (2013). Constructive immersion and invariance stabilization for a class of underactuated mechanical systems. *Automatica*, 49(5):1442–1448.

[90] Sarras, I., Ortega, R., and van der Schaft, A. J. (2012). On the modeling, linearization and energy shaping control of mechanical systems. In *Proceedings of the 4th IFAC Workshop on Lagrangian and Hamiltonian Methods for Non Linear Control*, pages 161–166.

[91] Seeger, J. I. and Crary, S. B. (1997). Stabilization of electrostatically actuated mechanical devices. In *Proceedings of the 1997 International Conference on Solid State Sensors and Actuators*, volume 2, pages 1133–1136.

[92] Senturia, S. (2001). *Microsystem Design*. Kluwer Academic Publishers, Norwell, MA, USA.

[93] Sepulchre, R., Jankovic, M., and Kokotović, P. (1997). *Constructive Nonlinear Control*. Springer-Verlag.

[94] Siciliano, B., Sciavicco, L., Villani, L., and Oriolo, G. (2008). *Robotics: Modelling, Planning and Control*. Springer Publishing Company.

[95] Slotine, J. J. and Li, W. (1991). *Applied nonlinear control*. Prantice-Hall, Englewood Cliffs, NJ, USA.

[96] Sontag, E. (1989). Smooth stabilization implies coprime factorization. *IEEE Transactions on Automatic Control*, 34(4):435–443.

[97] Sontag, E. (2008). Input to state stability: Basic concepts and results. In Nistri, P. and Stefani, G., editors, *Nonlinear and Optimal Control Theory*, pages 163–220. Springer Berlin Heidelberg.

[98] Sontag, E. and Wang, Y. (1995). On characterizations of the input-to-state stability property. *Systems & Control Letters*, 24(5):351–359.

[99] Sontag, E. and Wang, Y. (1996). New characterizations of input-to-state stability. *IEEE Transactions on Automatic Control*, 41(9):1283–1294.

[100] Spong, M. W. (1994). Partial feedback linearization of underactuated mechanical systems. In *Proceedings of the IEEE/RSJ/GI International Conference on Intelligent Robots and Systems. 'Advanced Robotic Systems and the Real World'*, volume 1, pages 314–321.

[101] Spong, M. W. (1996). Energy based control of a class of underactuated mechanical systems. In *Proceedings of the IFAC World Congress*, pages 431–435.

[102] Spong, M. W., Block, D., and Aström, K. J. (2001). The mechatronics control kit for education and research. In *Proceedings of the IEEE International Conference on Control Applications*, pages 105–110.

[103] Spong, M. W., Corke, P., and Lozano, R. (1999). Nonlinear control of the inertia wheel pendulum. *Automatica*, 37:1845–1851.

[104] Sun, W., Yeow, J., and Sun, Z. (2012). Robust adaptive control of a one degree of freedom electrostatic microelectromechanical systems model with output-error-constrained tracking. *Control Theory Applications, IET*, 6(1):111–119.

[105] Takegaki, M. and Arimoto, S. (1981). A new feedback method for dynamic control of manipulators. *The ASME Journal of Dynamic Systems, Measurement and Control*, 103(2):119–125.

[106] Tee, K. P., Ge, S., and Tay, F. (2009). Adaptive control of electrostatic microactuators with bidirectional drive. *IEEE Transactions on Control Systems Technology*, 17(2):340–352.

[107] van der Burg, J., Ortega, R., Scherpen, J., Acosta, J., and Siguerdidjane, H. (2007). An experimental application of total energy shaping control: Stabilization of the inverted pendulum on a cart in the presence of friction. In *Proceedings of the European Control Conference*, pages 1990–1996.

[108] van der Schaft, A. J. (1986). Stabilization of Hamiltonian systems. *Nonlinear Analysis: Theory, Methods & Applications*, 10(10):1021–1035.

[109] van der Schaft, A. J. (2000). *L2-Gain and Passivity Techniques in Nonlinear Control*. Springer, Berlin Heidelberg.

[110] Venkatraman, A., Ortega, R., Sarras, I., and van der Schaft, A. J. (2010). Speed observation and position feedback stabilization of partially linearizable mechanical systems. *IEEE Transactions on Automatic Control*, 55(5):1059–1074.

[111] Viola, G., Ortega, R., Banavar, R., Acosta, J. A., and Astolfi, A. (2007). Total energy shaping control of mechanical systems: Simplifying the matching equations via coordinate changes. *IEEE Transactions on Automatic Control*, 52(6):1093–1099.

[112] Wikipedia (2013). Mars rover. http://en.wikipedia.org/wiki/Mars_rover. [Online; accessed 2-March-2013].

[113] Willems, J. C. (1972a). Dissipative dynamical systems part I: General theory. *Archive for Rational Mechanics and Analysis*, 45(5):321–351.

[114] Willems, J. C. (1972b). Dissipative dynamical systems part II: Linear systems with quadratic supply rates. *Archive for Rational Mechanics and Analysis*, 45(5):352–393.

[115] Willems, J. C. (2007). Dissipative dynamical systems. *European Journal of Control*, 13(23):134 – 151.

[116] Xu, J. and Qiao, L. (2013). Robust adaptive PID control of robot manipulator with bounded disturbances. *Mathematical Problems in Engineering*, 2013:13 pages.

[117] Zhou, K. and Doyle, J. C. (1998). *Essential of Robust Control*. Prentice Hall, New Jersey.

[118] Zhu, G., Levine, J., and Praly, L. (2005). Improving the performance of an electrostatically actuated MEMS by nonlinear control: Some advances and comparisons. In *Proceedings of the 44th IEEE Conference on Decision and Control and 2005 European Control Conference (CDC-ECC '05)*, pages 7534–7539.

[119] Zhu, G., Levine, J., and Praly, L. (2007). Stabilization of an electrostatic MEMS including uncontrollable linearization. In *Proceedings of the 46th IEEE Conference on Decision and Control*, pages 2433–2438.

[120] Zhu, G., Saydy, L., Hosseini, M., Chianetta, J.-F., and Peter, Y.-A. (2008). A robustness approach for handling modeling errors in parallel-plate electrostatic MEMS control. *Journal of Microelectromechanical Systems*, 17(6):1302–1314.